The ecology and pathology of ash dieback disease

A thesis submitted to Cardiff University for the degree of Doctor of Philosophy

by

Matthew James Combes

July 2022

Funders: Defra, Woodland Trust, Network Rail

Supervisors: Professor Lynne Boddy and Dr Joan Webber

Statement of contributions

Chapter 2: Local volunteer groups collected *H. fraxineus* infected rachises and posted the material to Forest Research throughout summer 2018 and 2019.

Chapter 3: Local volunteer groups operated spore traps and posted the material to Forest Research throughout summer 2018 and 2019. Simon Scott-Brown assisted in the design of FRAXTRAP spore traps.

Chapter 6: Ruth Chitty conducted the DNA extraction, PCR, DNA clean-up and posted samples for sequencing.

Summary

Ash dieback disease, caused by the ascomycete *Hymenoscyphus fraxineus*, emerged in Poland in the early 1990s and is currently causing mortality of *Fraxinus excelsior* throughout Europe. *H. fraxineus* is dependent on its sexual cycle for dispersal and host infection, but little is known about how environmental conditions affect these processes. Through laboratory and field experiments this thesis aims to understand the environmental effects on pathogen apothecia development on rachises (including the petiole) in the litter layer, ascospore ejection and germination, and subsequent host colonisation of rachises in the litter layer and its relationship to disease severity.

Field studies revealed that temperature positively affected apothecia development, and this effect was greater at higher relative humidity and under sheltered litter layers, such as under vegetation, also associated with more open canopies. Laboratory studies uncovered the threshold for apothecia development was around 10°C and higher overwintering temperature increased the rate of subsequent apothecia development, but decreased the probability that they would develop.

Ascospores were more likely to be ejected with increasing relative humidity and temperature, although the increase in ejection with increasing temperature was greater in areas with exposed litter layers. A greater density of ascospores was related to increased rachis colonisation by *H. fraxineus*, which was related to greater disease severity. Ascospores could germinate under a range of temperatures (5°C-30°C), but did not germinate at 35°C or -4.01 MPa (adjusted with KCl), and germination was greater in field collected rather than laboratory produced apothecia.

A preliminary survey of *F. excelsior* trunk basal lesions detected both *Armillaria gallica* and *Armillaria mellea*, but trees with basal necrosis did not have more severe crown symptoms. Nascent management suggestions involve reduction of apothecia development and ascospore ejection by minimising moisture retention at tree bases, and prioritising surveys in sites with higher moisture in the litter layer.

Contents

List of Figures

List of Tables

Chapter 1: Introduction

1.1 Background

Ash dieback disease is caused by the invasive Asian ascomycete *Hymenoscyphus fraxineus* (Class: Leotiomycete; Order: Helotiales; Family: Helotiaceae) (Baral et al., 2014) and is leading to mortality of *Fraxinus spp.* throughout much of Europe (Coker et al., 2019). The disease was first noted in Poland in the early 1990s in the form of intensive crown dieback of *F. excelsior* (Kowalski, 2006), and has since spread at a rate of approximately 30-70 km per year (Enderle et al., 2019). The disease is currently present as far west as Ireland (McCracken et al., 2017), as far east as Moscow (Musolin et al., 2017), as far north as Finland (Rytkönen et al., 2011) and as far south as Montenegro (Milenković et al., 2017). The disease was first recorded in the UK in 2012, however qPCR detection of *H. fraxineus* from cankers combined with growth ring counts detected the pathogen on *F. excelsior* that died as early as 2004/5 (Wylder et al., 2018). The delayed detection of the pathogen is consistent with examination of mycological herbaria samples from Estonia which date *H. fraxineus* back to at least 1997, despite first detection of disease symptoms being in 2003 (Drenkhan et al., 2016). The pathogen was not identified until 2006 as *Chalara fraxinea* based on the anamorph (Kowalski, 2006), which was then mistakenly identified based on the teleomorph as *Hymenoscyphus albidus* in 2009 (Kowalski and Holdenrieder, 2009), a non-pathogenic cryptic species native to Europe. The pathogen was subsequently identified as a separate species, *Hymenoscyphus pseudoalbidus*, in 2011 based on DNA sequence differences in the ITS, calmodulin, translation elongation factor 1-α loci, and inter-simple sequence repeat anchored PCR (ISSR-PCR) fingerprinting (Queloz et al., 2011). Additionally, in contrast to *H. fraxineus*, *H. albidus* does not possess an anamorphic stage (Kirisits et al., 2013), and lacks croziers at the ascus base (Baral and Bemmann, 2014). The pathogen was then named based on the holomorph in 2014 as *Hymenoscyphus fraxineus* (Baral et al., 2014). Together, this highlights the delay between disease establishment and research directed towards understanding and management of the disease.

Current research has mainly focused on the epidemiology and the genetics of both the pathogen and the host. However, further understanding of the pathogen ecology and disease pathology is required to understand both current and future disease impacts. The project aims to fill these gaps in our knowledge to allow more accurate advice for disease management.

1.2 The primary host: *Fraxinus excelsior*

Three species of *Fraxinus* are native to Europe; *F. excelsior*, *F. angustifolia* and *F. ornus* (Wallander, 2008). *F. pallisiae*, which is present but rare, in steppe areas of South East Europe, has also been named as a native species (Chira et al., 2017), but is considered synonymous with *F. angustifolia* by other studies (Wallander, 2008; Hinsinger et al., 2013). *F. excelsior* is the most widely distributed and the only native *Fraxinus* spp. to the British Isles, whereas *F. angustifolia* and *F. ornus* are largely restricted to southern Europe (FRAXIGEN, 2005).

F. excelsior ranges from Norway in the north to Italy in the South, and Ireland in the west to approaching the Volga river in the East (FRAXIGEN, 2005). This exemplifies the wide range of conditions *F. excelsior* can tolerate. Indeed, *F. excelsior* grows best under a 'warm' climate, yet can withstand conditions of -15°C (Dobrowolska et al., 2011). The wide distribution range of the species, its fast growth, and the strong and flexible properties of the wood mean it has been an important natural resource for thousands of years. For example, the material has been used in the construction of Roman Army single-felloe cartwheels and WW2 aircraft (Pratt, 2017). In addition to the economic and cultural value of the species, *F. excelsior* is an important component of ecosystems. A total of 953 species have been identified as associated with *F. excelsior* in the UK. Of these, 11 species of fungi (likely a huge underestimate), 29 invertebrates and 4 lichens were classified as obligately associated with *F. excelsior* (Mitchell et al., 2014). Additionally, estimates from Sweden identified 483 species associated with *F. excelsior*, with 11% exclusive to *F. excelsior* (Hultberg et al., 2020) and the ecosystem effects of crown dieback caused by ash dieback have been associated with four trophic levels (Michalko et al., 2021). Importantly, no species or species mixture has been identified which replaces the ecosystem function or conservation value of *F. excelsior* (Mitchell et al., 2016). The costs of ash dieback in Great Britain have been estimated at £14.8 billion by accounting for both ecosystem service loss and disease management (Hill et al., 2019). However, current *F. excelsior* mortality estimates vary between studies and range from 69.4% after 15 years of disease presence to 30% after 13 years of disease presence. Future projections of mortality are highly uncertain, with 95% confidence interval ranging between around 40% after 30 years of pathogen arrival to 100% after 15 years of pathogen arrival (Coker et al., 2019). Together, this highlights the need for better understanding of disease processes to effectively manage and mitigate the impacts of the disease.

1.3 The pathogen: *Hymenoscyphus fraxineus*

The sudden emergence and spread of the pathogen from East to West through Europe, combined with the lower virulence on *F. ornus* suggested an Asian origin for the pathogen because *F. ornus* is more closely related to Asian ash species (Queloz et al., 2011). Accordingly, *H. fraxineus* occurs on the foliage of *F. mandshurica* and *F. rhynchophylla* in Japan, China, far East Russia and Korea in the absence of crown dieback (Zhao et al., 2012; Han et al., 2014; Zheng and Zhuang, 2014; Cleary et al., 2016).

H. fraxineus in Europe has low allelic richness, and European populations have lower genetic variation than populations from Asia (Zhao et al., 2012; Han et al., 2014; Zheng and Zhuang, 2014; Cleary et al., 2016; McMullan et al., 2018). Furthermore, European *H. fraxineus* could be grouped into two divergent haplotypes, thus suggesting European populations were founded by two genetically divergent individuals (McMullan et al., 2018). Concurring with these findings, other studies have noted that European *H. fraxineus* isolates are biallelic (Gross, Hosoya et al., 2014; Meyn et al., 2019). This highlights the importance of preventing further introductions of the pathogen to Europe, with associated genetic diversity, that could result in higher virulence of the pathogen, or greater environmental tolerances that could allow the pathogen to adapt to future climatic changes, which are expected to alleviate ash dieback disease pressure in certain regions (Goberville et al., 2016). It is not known how the pathogen was introduced to Europe, although it has been hypothesised that it could have been introduced via exotic plantings of *F. mandshurica* (Drenkhan et al., 2014). Indeed, *Fraxinus* spp. introduced to New Zealand from Europe are associated with several European fungi which had not been reported in New Zealand (Power et al., 2017). The evidence that the disease outbreak in Europe was started by two haploid individuals emphasises the importance of preventing the movement of plant material from *Fraxinus* spp. from Asia to Europe. Furthermore, tested *H. fraxineus* isolates from Japan can cause significantly longer bark lesions on *F. excelsior* compared with strains of the pathogen currently found in Europe (Gross and Sieber, 2015). Importantly, current evidence demonstrates there is no selection pressure on the aggressiveness of *H. fraxineus* individuals (Lygis et al., 2016; Kosawang et al., 2020).

However, despite the low allelic richness, populations of *H. fraxineus* in Europe display high genotypic diversity (Gross, Grünig et al., 2012; Kraj et al., 2012; Gross, Hosoya et al., 2014; Burokiene et al., 2015). Variations of pathogen growth rate *in vivo* and *in vitro* at different temperatures (Kowalski and Bartnik, 2010), combined with different exoenzyme profiles (Nave et al., 2017) of individuals and the high rates of vegetative incompatibility (Brasier and Webber, 2013) also exemplify high phenotypic diversity in *H. fraxineus*. Together, this indicates that outcrossing sexual reproduction is dominant in *H.*

fraxineus. Indeed, *MAT1-1* and *MAT1-2* genotypes have been identified in *H. fraxineus* at a 1:1 ratio from examined populations in Poland and Switzerland, and only the crossing of individuals with different *MAT* genes, which is further facilitated by asexual spores acting as conidia, leads to the production of apothecia (Gross, Zaffarano et al., 2012). Additionally, segregation distortion has been detected, thereby indicating that more than two nuclei can be involved in mating (Wey et al., 2016). Therefore, *H. fraxineus* maintains high genotypic and phenotypic diversity via a dependence on heterothallic sexual reproduction and has adapted to maximise outcrossing, which makes the species more resilient to environmental changes. Furthermore, the higher transposable element content of *H. fraxineus* genome compared to its homothallic native European competitor *H. albidus* exemplifies a greater ability to adapt to environmental changes (Elfstrand et al., 2021). Accordingly, *H. fraxineus* has outcompeted its native saprotrophic relative, which occupies the same niche on ash rachises (collectively referring to the rachis and petiole in this thesis), to such a degree that it has been assumed extinct (McKinney et al., 2012) and *H. albidus* ascospores were no longer detected in an initially asymptomatic Norwegian woodland 3 years after the study commencement (Hietala et al., 2018).

Little genetic differentiation is present between populations in continental Europe (Gross, Hosoya et al., 2014; Burokiene et al., 2015), and between populations in continental Europe and the UK, with UK subpopulations not showing a founder effect (Orton et al., 2017). This demonstrates an interconnectivity of populations throughout Europe, which combined with the dependence on sexual reproduction, highlights that the pathogen produces a large quantity of sexual spores that can disperse over large distances. This means local eradication of the pathogen will not be possible unless conducted across the whole continent and emphasises the importance of continent-wide control measures to prevent the introduction of further *H. fraxineus* individuals. Thus, as local eradication of the disease is not possible, understanding host resistance and the ecology and pathology of *H. fraxineus* are important for management of the disease in the landscape. The dependence of *H. fraxineus* on its sexual cycle for dispersal and infection of the host makes this an essential process to understand. The pathogen infects host foliage via aerially dispersed ascospores (Cleary et al., 2013) that are actively ejected (Hietala et al., 2013) from apothecia formed primarily on the rachises in the litter layer from the previous seasons (Kirisits, 2015) (Figure 1.1). The role of ascospores as the primary infectious agent of *H.fraxineus* is further emphasised by the low conidial germination rate of 6.3% after 24 h (Fones et al., 2016).

1.3.1 Sexual Lifecyle

1.3.1.1 Apothecia Development

H. fraxineus forms a pseudosclerotial plate on infected rachises in the litter layer, which is resistant to biotic and abiotic degradation (Gross and Holdenrieder, 2013). For example, of 202 petioles, only fruit bodies from one other species (*Cyathicula coronata*) was detected on one rachis on the *H. fraxineus* pseudosclerotial plates (Kowalski and Bilański, 2021). The pathogen can be present on rachises for up to 2 years before apothecia are formed (Gross and Holdenreider, 2013), and rachises can continue producing apothecia for up to 5 years (Kirisits, 2015). Therefore, this could lead to 'wave years' which allow the persistence of the pathogen in sites where conditions may not be favourable for apothecia production every year (Kirisits, 2015). Concurring with these findings, in 2010 in East Ukraine *H. fraxineus* was detected from symptomatic *F. excelsior* shoots, but was not detected on petioles, which indicates the pathogen was present during previous seasons but did not sporulate and produce ascospores to infect petioles during the study period. Importantly, the growing season prior to the study involved temperatures of up to 50°C with limited precipitation (Davydenko et al., 2013).

The flood risk index of a site was positively correlated with the density of apothecia (Grosdidier, Ioos, Marçais et al., 2018), and this pattern is consistent with the distribution in Japan where more apothecia were observed in areas classified as shady and humid compared to areas classified as dry and sunny (Inoue et al., 2019). Furthermore, apothecia production is greater under areas of vegetation cover compared to areas of exposed litter cover (Gross and Holdenrieder, 2013; Mansfield et al., 2018). Notably, the peak period for apothecia production occurs during summer in both Europe (Mansfield et al., 2018) and Japan (Inoue et al., 2019), which suggests an important role for temperature in apothecia formation. The timing of the maximum apothecia development is likely different between sites because the first observed date of apothecia varies between studies, ranging from the end of May (Mansfield et al., 2018) to the beginning of July (Hietala et al., 2013). Within site differences have also been noted, with apothecia detection occurring 2 weeks earlier under vegetation cover compared to on open ground (Mansfield et al., 2018). Together, these results highlight the environmental sensitivity of *H. fraxineus* apothecia development, and emphasise the importance of understanding this process in greater detail to guide management practices and accurately project impacts of ash dieback both within and between woodlands.

The number of apothecia is also related to the proportion of *H. fraxineus* infected rachises in a woodland, which suggests that the frequency of mating partners can limit the subsequent apothecia development in the field (Grosdidier, Ioos, Marçais et al., 2018). Indeed, up to eight *H. fraxineus* genotypes were present on a *F. excelsior* petiole,

although on 6/10 only one genotype was detected (Gross, Zaffarano et al., 2012). A separate study also found up to eight genotypes present on a petiole and, in a total of 79 petioles assessed, 150 genotypes were present, but the authors acknowledged that the microsatellite markers used may have limited discriminatory power (Haňáčková et al., 2017). However, the high density of apothecia in heavily infested *F. excelsior* woodlands, which can be as great as 2000 m^{-2} (Kowalski et al., 2013), indicates that the frequency of

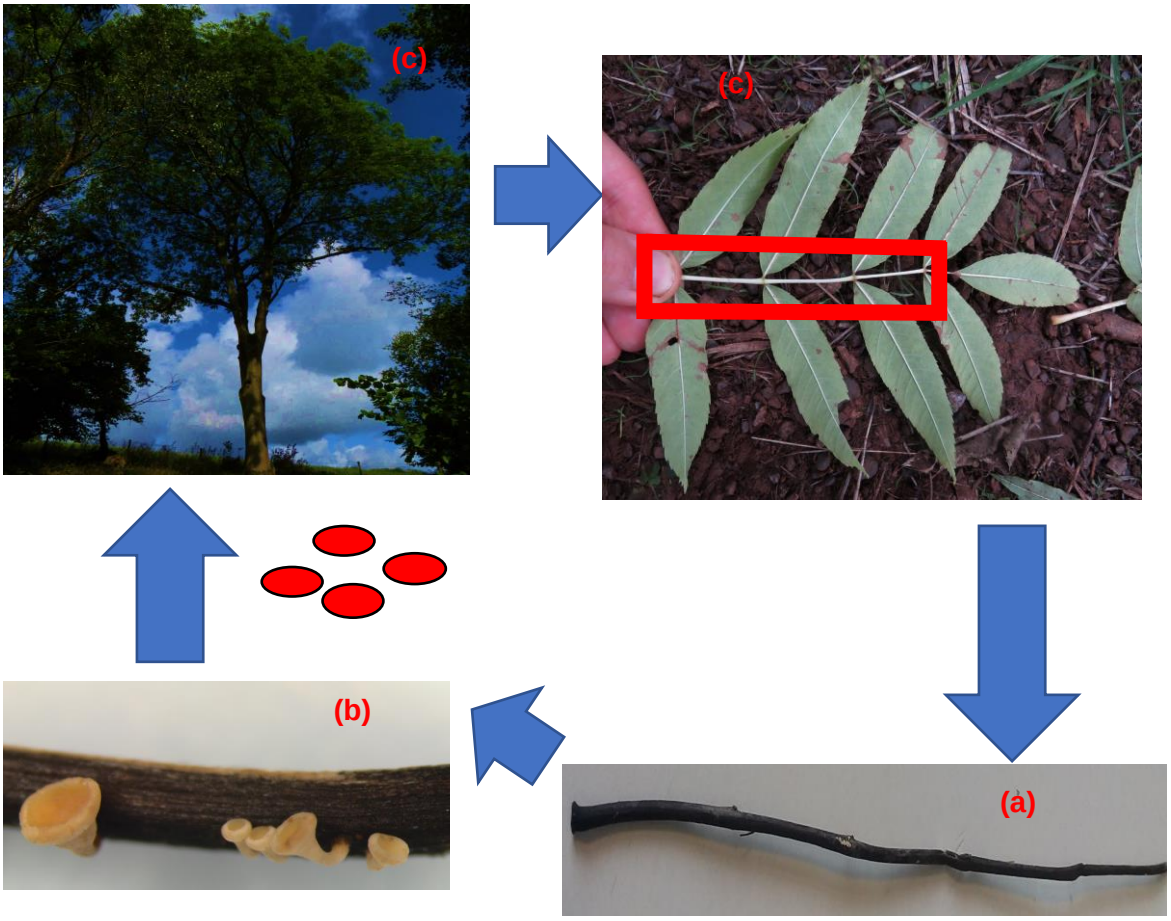

Figure 1.1 Simplification of the lifecycle of *H. fraxineus*. **(a)** *F. excelsior* rachis in the litter layer colonised by *H. fraxineus*, as indicated by the presence of a black pseudosclerotial layer covering the rachis (Kowalski and Bilański 2021). The pseudosclerotial layer is resistant to biotic and abiotic degradation, which allows the pathogen to survive in the litter layer and produce apothecia over multiple seasons (Kirisits, 2015). **(b)** Following mating with a compatible partner with different *MAT* genes, which can be facilitated by asexual spores acting as spermatia, (Gross, Zaffarano et al., 2012), *H. fraxineus* produces apothecia typically during the summer months when conditions are appropriate (Gross and Holdenrieder, 2013; Mansfield et al., 2018). Apothecia actively eject ascospores (Hietala et al., 2013; Mansfield et al., 2018) and **(c)** infect *F. excelsior* foliage (Cleary et al., 2013). Upon leaf shed, *H. fraxineus* continues to colonise the foliage and will subsequently form a pseudosclerotial layer on the rachis (highlighted in the red box) for continuation of the lifecycle (Gross and Holdenrieder, 2013). Damage to the host occurs via reducing photosynthesis (Klesse, von Arx et al., 2021), and growth of the pathogen from the foliage into the branches via the petiole-shoot junction (Haňáčková et al., 2017) can kill shoots, lead to crown dieback, and girdle the host (Bengtsson et al., 2014). H. fraxineus can also infect via lenticels (Nemesio-Gorriz et al., 2019), and infection of the roots and root collar is associated with subsequent colonisation by *Armillaria* spp. (Chandelier et al., 2016; Marçais et al., 2016) which accelerates the decline of trees (Enderle et al., 2017).

mating partners should not be a limiting factor when *F. excelsior* is dense and heavily colonised by *H. fraxineus*. Accordingly, the severity of crown dieback seems to be positively associated with greater density of *H. fraxineus* apothecia on rachises (Marçais et al., 2016). The biotic and abiotic conditions that affect mating in *H. fraxineus* have not been investigated, although it has been demonstrated that UV light is necessary for mature apothecia development (Gross, Zaffarano et al., 2012). Additionally, incubation of field collected rachises from Japan demonstrated that after 4 weeks of incubation in the laboratory, rachises are able to develop apothecia (Inoue et al., 2019). This indicates the possibility of more than one infection cycle per season.

The quantity of *F. excelsior* litter is positively related to the density of apothecia (Marçais et al., 2016). Therefore, understanding the conditions that accelerate the decomposition of *F. excelsior* litter could be important to limiting *H. fraxineus* apothecia development. The species litter mixture significantly affected the quantity of ash litter in the soil (Bartha et al., 2017), and soil pH negatively affects the quantity of *F. excelsior* litter (Marçais et al., 2016). Furthermore, a decrease in the quantity of apothecia on rachises with the number of years over which apothecia are produced on rachises (Kirisits, 2015) demonstrates that the process of litter decomposition affects the ability of *H. fraxineus* to form apothecia. Recent research has demonstrated the utility of composting to treat *H. fraxineus* infected litter, with 1 day of large-scale composting at 40°C sufficient to prevent subsequent apothecia development (Noble et al., 2019). Additionally, 92 days was the longest period that *F. excelsior* rachises with pseudosclerotial plates could be kept at 20°C and 20-40% relative humidity in the laboratory and *H. fraxineus* successfully isolated (Gross and Holdenrieder, 2013). Together, this knowledge could be utilised to dispose of *F. excelsior* litter whilst maintaining biosecurity.

1.3.1.2 Ascospore Release

As previously mentioned, ascospores are actively ejected from the apothecia. When incubated in the laboratory, ascospores can be ejected from apothecia to a height of 0.5 cm (Mansfield et al., 2018). In the field there was a logarithmic decrease in ascospore density by 0.5 to 3 m height above ground (Chandelier et al., 2014). The mean dispersal distance of *H. fraxineus* was estimated at either 1.4 km or 2.6 km (Grosdidier, Ioos, Husson et al., 2018). However, the approximate rate of spread of the disease front at 30-70 km/ year (Enderle et al., 2019) suggests that ascospores are capable of long-distance dispersal, although most spores are dispersed within 50 m of an infected stand (Chandelier et al., 2014; Grosdidier, Ioos, Husson et al., 2018).

The triggers for ascospore ejection have not been directly studied for *H. fraxineus*, however aerial ascospore density is highest in the early hours of the morning in woodlands roughly between 4h30 and 8h30 (Hietala et al., 2013). Laboratory observations also revealed the peak timing of ascospore release between 06h00 (am) and 12h00 (pm) (Mansfield et al., 2018). This indicates the presence of a circadian clock in *H. fraxineus* that leads to early morning spore ejection. However, field experiments demonstrate that the time of the spore peak depends on the environmental conditions. The net radiation within 2 hours either side of the spore trapping and 2-24 h prior to trapping had the largest effect on delaying the timing of spore release (Burns et al., 2022). Furthermore, rainfall (mm h^{-1}) 2 hours either side of spore trapping appears to delay spore release slightly, however the relationship is very weak (Burns et al., 2022). Together, these results indicate the diurnal pattern of ascospore ejection is affected by environmental conditions, thereby varying both within and between sites, and likely affecting disease progression.

The conditions that affect aerial ascospore density have not been separated from the conditions that affect apothecia development. However, aerial ascospore density is positively associated with sites classified as wet (Čermáková et al., 2017), relative humidity, leaf wetness (Dvorak et al., 2015) and leaf moisture (Burns et al., 2022). Aerial ascospore density is also positively associated with temperature, both during the trapping period (Chandelier et al., 2014) and accumulated over the year as growing degree days (Hietala et al., 2018). A positive effect of soil temperature peaked at approximately 16°C and then became negative (Burns et al., 2022), although this could be due to drying of the litter layer at warmer soil temperatures, or that soil temperature was not measured on site in the latter study. Furthermore, there is a positive effect of growing degree days the previous year, up to the end of the infection period, on the ascospore quantity the next season (Hietala et al., 2018). Higher spore density the previous season can be expected to increase the number of successful mating events.

The ascospore density varies within sites, between sites and between sampling years (Chandelier et al., 2014; Hietala et al., 2018). The timing of maximum ascospore density also varies between sites and study years, ranging from end of June (Grosdidier, Ioos, Husson et al., 2018) to end of August (Hietala et al., 2018). Together, this highlights the need for studies across multiple sites and multiple locations within a site whilst accounting for apothecia development to quantify accurately the effect of environmental variables on aerial ascospore density.

1.3.1.3 Host Colonisation

Once on the foliage, *H. fraxineus* must germinate to colonise the host, but there is little understanding of the conditions that may affect this. The percentage of ascospore

germination is high in the presence of water, yielding 26-40% germination within 24 h and 84-93% germination within 48 h. This drops to between 5.7% and 11.7% after 48 h following 7 days of drying in the laboratory (Mansfield et al., 2018). This indicates that ascospores will still be capable of infecting *F. excelsior* following long distance dispersal of ascospores. Other research also demonstrates a high *in vitro* germination rate of *H. fraxineus* reaching 91% on water agar after 68 h at 20°C (Brühwiler and Sieber, 2020) and between 84.8% and 96% on malt extract agar after 67 h at 20°C (Schlegel et al., 2016). Interestingly, *Fraxinus* leaf endophytes can inhibit *in vitro* germination of *H. fraxineus*, although this did not translate into preventing disease progression in seedlings that were inoculated with endophytes and exposed to *H. fraxineus* in the field (Schlegel et al., 2016).

On *F. excelsior* foliage, *H. fraxineus* ascospores germinate and form an appressorium, which appears to help *H. fraxineus* adhere to the foliage and lead to enzymatic degradation of the cuticle (Cleary et al., 2013). However, up to 80% of ascospores penetrating the foliar surface did not form germ tubes prior to appressorium formation (Mansfield et al., 2018). Epidermal cells are mechanically penetrated by *H. fraxineus*, and hyphae appressed to the cuticle can enter the host via the stomata (Cleary et al., 2013), although there was no common pattern to hyphal growth (Cleary et al., 2013) and a separate study found no hyphal growth on the leaf surface nor stomatal targeting (Agan et al., 2020). Once the epidermal cell wall is penetrated, the cell membrane is invaginated and intracellular hyphae subsequently penetrate neighbouring cells (Mansfield et al., 2018). *H. fraxineus* behaves initially as a biotroph, before switching to necrotrophy (Mansfield et al., 2018). Droplet inoculation of detached *F. excelsior* compound leaves revealed no more than three cells were colonised when cell death occurred (Mansfield et al., 2018). This indicates that *H. fraxineus* does not colonise host foliage extensively without necrotrophy. Field experiments relate a large increase in *H. fraxineus* DNA in *F. excelsior* foliage (Hietala et al., 2013; Cross et al., 2017) and change in fungal community structure to the presence of necrosis (Cross et al., 2017). This suggests that *H. fraxineus* has an extended quiescent phase before reaching a threshold density that can trigger a switch to a more aggressive lifestyle (Cross et al., 2017).

The effect of spore density on disease progression has not been investigated despite the differential symptom development following *H. fraxineus* infection. For example, the appearance of leaf necroses in the field were observed at a site in Norway approximately 1 month after the first qPCR detection of *H. fraxineus* on foliage in 2011. However, leaf necroses were reported to increase rapidly after approximately 1 week of the first qPCR detection of *H. fraxineus* in 2012 (Cross et al., 2017) and leaf necrosis were first observed 7 days after droplet inoculation on detached compound leaves with *H. fraxineus* ascospore suspensions at a concentration of 5×10^4 ml^{-1} (Mansfield et al., 2018). Furthermore, chlorosis and mottling of some leaves followed by browning and

abscission after exposure to *H. fraxineus* (Cleary et al., 2013), and the presence of foliar symptoms such as ‘leaf drop’ and ‘pre-top dead’ symptom in the absence of necrosis (Orton et al., 2019), demonstrates the variety of interactions the *H. fraxineus* hemi-biotroph has with host foliage.

Substantial numbers of hyphae grow in the vascular bundle of *Fraxinus* spp. petioles (Cleary et al., 2013), and the ability of *H. fraxineus* to colonise leaflet midribs, veins and petioles has been associated with its ability to produce apothecia on these species (Nielsen, McKinney, Hietala et al., 2017). High sporulation of *H. fraxineus* and its rapid (considerable) colonisation of *F. excelsior* foliage comparatively early in the season means that *H. fraxineus* has a competitive advantage over foliar endophytes (Cross et al., 2017). However, although multiple studies have identified endophytes that inhibit *H. fraxineus* growth *in vitro* (Haňáčková et al., 2017; Becker et al., 2020; Ulrich et al., 2020), there is currently no *in vivo* evidence.

Multiple studies found that *F. excelsior* foliar fungal (Schlegel et al., 2018; Agan et al., 2020; Becker et al., 2020) and bacterial (Ulrich et al., 2020) community structure does not significantly differ between trees with different health status, although particular bacteria (Ulrich et al., 2020) and fungi (Becker et al., 2020) were noted on tolerant trees. *H. fraxineus* DNA increase and foliar necrosis was associated with a large increase in total fungal biomass. This included saprotrophic epiphytes and endophytes with pathogenic potential, likely due to *H. fraxineus* associated host weakening (Cross et al., 2017). Additionally, a separate study revealed positive correlation between fungal alpha diversity and foliar DNA quantity of *H. fraxineus* (Griffiths et al., 2019).

Following foliar colonisation, *H. fraxineus* can enter the branches of *F. excelsior* via the petiole-shoot junction (Haňáčková et al., 2017), and colonisation of the woody tissue of host trees can lead to girdling and subsequent death (Bengtsson et al., 2014). The pathogen causes a reduction in growth of *F. excelsior* regardless of susceptibility, and basal area increment prior to disease arrival is negatively related to disease susceptibility (Klesse, von Arx et al., 2021). This indicates a positive feedback and demonstrates that expression of host defence responses, utilisation of *F. excelsior* nutrients by *H. fraxineus* and early leaf shed negatively impact *F. excelsior*.

H. fraxineus can colonise the woody tissue of host trees and leads to necrosis that is greater in sapwood tissue compared to the external bark (Bengtsson et al., 2014), which suggests spread through the host occurs quickest via vessels and paratracheal parenchyma (Schumacher et al., 2010). A separate study found strong colonisation of phloem, axial paratracheal parenchyma and ray parenchyma, with xylem vessels and tracheids less colonised by *H. fraxineus* than parenchyma cells (Montecchio et al., 2012). Accordingly, most *H. fraxineus* biomass accumulated in sapwood parenchyma, although

perimedullary pith was of particular importance for the spread of *H. fraxineus* (Matsiakh et al., 2015). Regardless, *H. fraxineus* appears to be able to spread in all woody tissues in all directions (Schumacher et al., 2010), although lesions following inoculation have greater length than depth (Montecchio et al., 2012), and lesions spread significantly more downward than upward (Bengtsson et al., 2014). Spread between cells appears to occur via shared pits and there are few cases of fungal colonisation of cells being inhibited (Mansfield et al., 2019). Indeed, *H. fraxineus* even induces stem necrosis on *F. mandshurica* following wound inoculation, albeit to a lesser extent than in *F. excelsior* (Gross and Holdenrieder, 2015).

Roughly a quarter of lesions monitored across four sites in Sweden on *F. excelsior* became inactive. This most commonly occurred at a branch-stem base or intersection of multiple shoots, but the reasons for this were not known. However, lesions were not examined below the bark, thus some lesions classified as dormant may have been growing below the bark (Bengtsson et al., 2014). Additionally, 71 fungal taxa, some of which are potentially pathogenic, were detected from 720 sampled necrotic lesions on *F. excelsior* stem and twigs (Kowalski et al., 2016; Kowalski et al., 2017), thus suggesting a possible role in disease development.

The pathogen largely produces apothecia on *F. excelsior* foliage, therefore infection of this tissue is beneficial for the pathogen. However, infection of *F. excelsior* via shoot lenticels means that the pathogen can colonise host tissue without the need for foliar infection (Nemesio-Gorriz et al., 2019). In fact, infection via lenticels is presumably responsible for *H. fraxineus* lesions at the trunk base of *F. excelsior* and in the root system (Husson et al., 2012; Chandelier et al., 2016; Meyn et al., 2019). Collar lesions in *F. excelsior* have been associated with *Armillaria* spp., and their presence is associated with collar lesions of greater severity (Marçais et al., 2016; Enderle et al., 2017). *Armillaria gallica* is the most common *Armillaria* spp. associated with these lesions in Germany, France and Belgium (Enderle et al., 2013; Marçais et al., 2016; Chandelier et al., 2016), although *Armillaria cepistipes* is most dominant in Lithuania (Lygis et al., 2005; Bakys et al., 2011). *H. fraxineus* was detected in 98% of 103 lesions from 12 stands, and *Armillaria* spp. in 41%, with *H. fraxineus* detected in 95% of these (Chandelier et al., 2016). This is consistent with *H. fraxineus* primarily initiating the lesions, and secondary colonisation by *Armillaria* spp. significantly worsening lesions and reducing the health status of the trees.

1.4 Factors affecting disease progression

1.4.1 Genetic and epigenetic factors

Numerous studies have reported that a small proportion of *F. excelsior* possess genetically based resistance (also referred to as tolerance) to *H. fraxineus* (McKinney et al., 2011; Stener, 2013; Enderle et al., 2014; Lobo et al., 2015; Havrdová et al., 2016; Stocks et al., 2017). Associative transcriptomics have identified one cDNA-based SNP and two gene expression markers associated with heightened resistance to *H. fraxineus* from Danish resistance trials (Harper et al., 2016). Further analysis of these data identified 20 gene expression markers associated with disease symptoms. The top five of these markers were then examined for their ability to predict disease severity for 58 Danish ash accessions. Importantly, trees with predicted damage of less than 50% demonstrated fewer symptoms. Moreover, the same markers predict as many as 25% of British trees will have less than 25% canopy damage, in comparison with 9% of the Danish ash population (Sollars et al., 2016). However, the percentage of 'healthy' trees with minimal damage from a British Isles provenance trial was still between 0.3 and 7.6% (Stocks et al., 2017), which is consistent with estimates from continental Europe between 1-5% (McKinney et al., 2014). The complete sequencing of 12500 trees and subsequent genome wide association study identified 3149 SNPs associated with disease resistance. Additionally, genomic prediction models correctly categorised 67% of trees as either high or low susceptibility using 150 individuals as a training dataset. Furthermore, when the top 20% of genomic estimated breeding values were analysed (i.e. those estimated as least susceptible), 200 SNPs could correctly categorise susceptibility with more than 90% accuracy. This study further demonstrates the utility of these SNPs at selecting resistant individuals as the training dataset were trees from a different seed source population (Stocks et al., 2019). Additionally, Fourier-transform infrared spectroscopy of uninfected bark can be utilised as a cost-effective method to screen populations for resistance (Villari et al., 2018).

Importantly, identified tolerant and susceptible Swedish genotypes exhibited low genetic differentiation (Chaudhary et al., 2020). Combined, with the quantitative nature of resistance, this indicates ash dieback disease resistance can be obtained via natural selection and breeding programmes (Stocks et al., 2019) whilst retaining genetic diversity to maximise resilience of *F. excelsior* populations to future threats such as emerald ash borer, which is now present in Ukraine (Orlova-Bienkowskaja et al., 2020). Indeed, trees with lower susceptibility to the disease were more likely to reproduce (Semizer-Cuming et al., 2019; Semizer-Cuming et al., 2021).

A significant interaction between the genotype and environment on disease severity was noted following artificial spring frost and summer drought treatments (Pliura

et al., 2015). Contrary to findings from field trials (Lobo et al., 2015), the absence of correlation of disease severity between offspring and parent from two natural woodlands in Austria (Wohlmuth et al., 2018) further highlights the complexity of understanding disease resistance under natural woodland conditions. Indeed, the identification of 1683 significantly differentially methylated regions dependent on disease severity, and variation in methylation within genotypes (Sollars et al., 2018) highlights the role of environmental regulation of disease resistance.

The mechanisms underlying disease resistance have not been fully elucidated. However, 61 SNPs that differed between 'healthy' and damaged individuals from 192 most significant SNPs were associated with genes whose homologues are associated with plant pathogen interactions (Stocks et al., 2019). Additionally, gene expression analysis from symptomatic tissues and asymptomatic tissues from bark of susceptible and resistant genotypes revealed the role of the abscisic acid and Jasmonate signalling pathways in response to the pathogen (Sahraei et al., 2020). Furthermore, application of *N*-methyl-*N*-methoxyamide-7-carboxybenzo(1.2.3)thiadiazole (BTWHA) to saplings inhibited lesion development following wound inoculation with *H. fraxineus*, thereby demonstrating the utility of defence responses affected by BTWHA application in resisting the pathogen (Turczański et al., 2021). Previous research found that BTHWA application to tobacco plants enhanced expression of genes associated with jasmonic acid, ethylene and salicylic acid signalling pathways (Frąckowiak et al., 2019).

Metabolites also differ between high and low susceptibility *F. excelsior* which have not been exposed to *H. fraxineus*. Of the 64 differing between susceptibility categories, 39 were more abundant in low susceptibility genotypes. Furthermore, two metabolites of the coumarin chemical family inhibited *H. fraxineus in vitro* at estimated physiological concentrations, and methanolic bark extracts from low susceptibility individuals inhibited the growth of *H. fraxineus*, thereby demonstrating the presence of constitutive defence responses effective against *H. fraxineus* (Nemesio-Gorriz et al., 2020).

1.4.2 Other factors

The age of a tree is an important determinant of disease progression. Trees with a greater diameter at breast height (measured 1.3 m above ground level) (dbh) and greater height above the ground are less affected by the disease (Havrdová et al., 2017; Grosdidier et al., 2020; Klesse, Abegg et al., 2021). Surveys from France and Belgium estimate annual mortality of *F. excelsior* between 5-25 cm dbh is 11% in comparison to 3.2% annual mortality in trees with dbh greater than 25 cm 9 years after pathogen arrival (Marçais et al., 2017). This effect is presumably because mature trees have a higher canopy thus will likely be exposed to fewer *H. fraxineus* ascospores, and in older trees the

pathogen requires more growth to colonise branches and ultimately girdle the host. Earlier flushing (Bakys et al., 2013) and leaf senescence (McKinney et al., 2011) are also associated with reduced disease susceptibility. Smaller lesions were present on *F. excelsior* seedlings which had flushed prior to wound inoculation with *H. fraxineus* (Nielsen, Mckinney, Kjaer et al., 2017), which suggests a role of age-related resistance (Hu and Yang, 2019).

Density of *F. excelsior* has been shown to positively affect disease severity (Grosdidier et al., 2020). A greater density of *F. excelsior* will be associated with a greater density of *F. excelsior* rachises in the litter layer from which *H. fraxineus* can complete its sexual cycle. The negative relationship between altitude and disease severity (Havrdová et al., 2017) has been hypothesised to result from decreased abundance of *F. excelsior* at higher altitudes (Klesse, Abegg et al., 2021). However, this relationship may also be explained by increased disease resistance from provenances originating from higher altitudes (Havrdová et al., 2016).

Mean annual temperature is positively correlated with disease severity (Havrdová et al., 2017), although mean maximum daily temperature is negatively associated with disease severity (Grosdidier, Ioos, Marçais et al., 2018). This may be due to its positive effects on *H. fraxineus* aerial ascospore density (Hietala et al., 2018) and *H. fraxineus* growth rates, which peak at approximately 20°C *in vitro* (Kowalski and Bartnik, 2010; Hauptman et al., 2013) with only 10% isolates growing at 30°C in one study (Kowalski and Bartnik, 2010). Indeed, heat treatment of saplings reduced *H. fraxineus* isolation from 100% in the control, to 30% after 5 hours at 36°C, to 5% after 5 hours at 40°C, with no isolation after 5 hours at 44°C (Hauptman et al., 2013).

Moisture is positively related to disease severity via indicators such as Landolt's indicator value (humidity estimate via the vegetation) (Marçais et al., 2016), the presence and width of a watercourse (Havrdová et al., 2017), precipitation (Chumanová et al., 2019; Klesse, Abegg et al., 2021), distance to a river (Grosdidier et al., 2020) and forest types classified as wet (Erfmeier et al., 2019; Klesse, Abegg et al., 2021). This could be due to the positive association between moisture, apothecia abundance (Grosdidier et al., 2018) and aerial ascospore density (Dvorak et al., 2015; Čermáková et al., 2017; Burns et al., 2022). The microclimate will be highly variable under field conditions, with a negative effect of tree cover fragmentation (Grosdidier et al., 2020) and positive effect of vertical terrain heterogeneity (Havrdová et al., 2017).

Furthermore, species admixture (Havrdová et al., 2017), soil pH and organic matter content (Turczański et al., 2020) are associated with disease severity. This could be due to effects on the decomposition of *F. excelsior* litter which reduce the spore load of

the pathogen, as both species litter mixture and soil pH affect the rate of *F. excelsior* litter breakdown (Marçais et al., 2016; Bartha et al., 2017).

Together, the impact of environmental factors and stand characteristics on disease progression highlight the necessity of further understanding *H. fraxineus* sexual cycle and host colonisation to provide more accurate disease prognosis and develop more effective management strategies.

1.5 Aims and Objectives

As detailed above, the pathogen is dependent on aerial dispersal of ascospores for host infection (Cleary et al., 2013). These ascospores are actively ejected (Hietala et al., 2013) from apothecia which form on infected rachises from previous seasons (Kirisits, 2015) but many questions remain about their production and germination. The aims of the thesis, therefore, were to understand better the ecology of sexual spores in the disease. This is required for more accurate disease modelling and management. A second aim was to begin to understand the development of collar necrosis in the UK and their associated species, which is also required to effectively manage the risk to the public.

Therefore, the objective of the thesis are to:

(1) Determine the environmental effects on *H. fraxineus* apothecia formation and subsequent ascospore release.

(2) Investigate the effect of solute potential and temperature on ascospore germination.

(3) Establish the consequences of *H. fraxineus* ascospore density on host colonisation.

(4) Identify the *Armillaria* spp. associated with collar necrosis on *F. excelsior* from UK hedgerows, woodlands and urban environments.

Hypotheses

It is expected that:

(1) there will be considerable within site variation in *H. fraxineus* apothecia formation and spore density. However, temperature relative humidity and vegetation cover are expected to positively affect ascospore density and apothecia development.

(2) solute potential will negatively affect ascospore germination, but temperature will positively affect ascospore germination up to 20°C.

(3) areas with higher spore densities will be positively related to *H. fraxineus* colonisation of rachises in the litter layer, which will be positively related to crown dieback severity.

(4) collar necrosis will be most prevalent in woodland environments and predominantly associated with *Armillaria gallica.*

Chapter 2: Environmental effects on *Hymenoscyphus fraxineus* apothecia development: Field Study

2.1 Introduction

Hymenoscyphus fraxineus disperses through aerial ejection of ascospores from apothecia formed in the leaf litter layer under infected trees (Timmermann et al., 2011). The ascospores then infect either via enzymatic degradation of leaf epidermal cells, or via lenticels on shoots or at the root collar (Cleary et al., 2013; Husson et al., 2012; Nemesion-Gorriz et al., 2019). If *H. fraxineus* colonises the leaf tissue, it forms a 'pseudosclerotial plate' on the infected leaf rachises the winter following leaf shed (Baral and Bemmann, 2014). This psuedosclerotial plate is highly resistant to degradation and allows *H. fraxineus* to survive and form apothecia for at least 5 years following infection (Kirisits, 2015). The dependence of the infection process on apothecia formation and subsequent ascospore release makes understanding this process essential for understanding the epidemiology of ash dieback disease.

Variation in levels of symptom severity in ash dieback disease have been linked with variables such as temperature, elevation, incline, site moisture and edaphic series (Marçais et al., 2016; Havrdová et al., 2017; Enderle et al., 2018). These findings therefore either indicate a role of the environment in host susceptibility, fungal development, or a combination of both. However, our current knowledge of the ecology of *H. fraxineus*, and the conditions affecting the pathogen life-cycle, are inadequate to distinguish between these possibilities. In addition, previous research into the conditions affecting inoculum production has produced contrasting results. Čermáková et al. (2017) noted higher aerial ascospore density in sites classified as wet, whereas Chandelier et al. (2014) and Hietala et al. (2018) found a significant relationship between aerial ascospore density and temperature. The inconsistency and variation in these studies means it is not yet possible to produce an accurate predictive model of the inoculum quantity throughout a season and indicates that potentially complex interacting factors are involved.

Furthermore, it is important to note that these studies only measured the aerial ascospore density and did not monitor the development of the apothecia or consider the relationship between apothecia development and ascospore numbers. This means that two potentially separate processes which contribute to the variation in aerial ascospore density were conflated. Therefore, the goal of this study is to examine the environmental conditions which affect the development of apothecia throughout the spring and summer under field conditions. This was achieved by monitoring the apothecia development at

seven sites covering a range of different climates prior to and during the fruiting season (May until September). A range of environmental variables (temperature, canopy closure, ground cover, relative humidity) were recorded. It was hypothesised that temperature, relative humidity, canopy closure and ground cover all significantly affect apothecia formation, however their effect would be dependent on the other variables.

2.2 Materials and Methods

2.2.1 Site Selection

Seven *H. fraxineus* infected *F. excelsior* woodlands were selected to capture a gradient of long term (1960-2014) temperature and precipitation from May until the end of September at a 5 km^2 resolution (Met Office, 2017). Availability of local volunteer groups to conduct sample collection was another selection factor. Apothecia development was monitored at six of the sites during 2018, and all seven sites in 2019 (Table 2.1).

2.2.2 Apothecia sample collection

Four quadrats were established at least 20 m apart at each of the seven study sites. Quadrat locations were chosen to maximise volunteer accessibility, minimise the risk of public vandalism and to capture variations in ground cover. Each quadrat consisted of 13 grids (25 x 25 cm). Twenty-five separate infected ash (*F. excelsior*) rachises collected from the immediate vicinity of each quadrat location (no more than 100 m^2 area with the quadrat as the focal point) were placed in each of the 13 grids of a quadrat. Rachises were identified as infected by the presence of a pseudosclerotial plate, which is characteristic of *H. fraxineus* colonisation (Kowalski and Bilański, 2021) and molecular verification (detailed below). Sampling was conducted by local volunteer groups on 12 separate occasions throughout the spring/summer (Supplementary Table 2.1). Sampling involved the collection of 25 infected rachises from one randomly selected grid per quadrat. The rachis samples from each quadrat were then placed in sealed cardboard A4 mailing tubes and posted in sealed jiffy bags to the laboratory, arriving within 2 days of collection.

Table 2.1 Experimental sites where *H. fraxineus* apothecia development was monitored at 1-2 week intervals (Supplementary Table 2.1) from May-September 2018 and 2019, with the mean May-September precipitation and temperature (1960-2014) at a 5km resolution (Met Office, 2017). Date and locations of canopy photography for gap fraction calculation is provided (Section 2.2.5).

Site	Grid ref.	Mean May-Sept precip. (mm)	Mean May-Sept temp. (°C)	Years studied	Canopy photography
County Durham (Hedley Hall Woods)	NZ218559	57.48	13.60	2018, 2019	A, B, C, D (07/08/20)
Shropshire (The Highfields)	SJ688275	60.64	13.99	2018, 2019	A, B, C, D (13/08/20)
Devon (Penstave Copse)	SX691611	128.33	13.39	2018, 2019	A, B, C, D (31/07/20)
Wiltshire (Colerne Park and Monks Wood)	ST837723	66.34	14.33	2018, 2019	A, B (17/08/20); C, D (16/08/20)
Hampshire (Alice Holt Forest)*	SU802401	63.27	15.34	2018, 2019	A, D (28/08/18); B, C (18/08/20)
Carmarthenshire (National Botanic Gardens of Wales)	SN518179	96.73	14.58	2018, 2019	A, B, C, D (11/08/20)
Northumberland (Nunsbrough Wood)	NY950595	62.83	12.90	2019	A, B, C, D (03/08/20)

*Mean May-September precipitation and temperature values for Alice Holt Forest at 5 km resolution were for a site 16.9 km away (Garbett's wood).

Figure 2.1 Locations of experimental sites used to monitor *H. fraxineus* apothecia development during summer 2018 and/or 2019 (Table 2.1; Supplementary Table 2.1). Site locations are indicated by numbered red markers (1 = Devon; 2 = Hampshire; 3 = Wiltshire; 4 = Carmarthenshire; 5 = Shropshire; 6 = County Durham; 7 = Northumberland).

2.2.3 Apothecia Sample Measurements

Upon arrival at the laboratory, the proportion of all 25 rachises per quadrat with apothecia was recorded. Eight infected rachises were then blindly selected from each quadrat sample and apothecia were removed from the lower 6 cm segment of the rachises (1 cm above the rachis base) and placed 'cup down' (see Figure 5.1 for image of apothecium) onto a thin layer of Vaseline on Petri dish bases to keep apothecia fixed in position for photography at either x1, x2, x3, x4, x5, or x6.3 magnification, depending on the size of the apothecia, using the Olympus SC100 Camera (Olympus, Tokyo, Japan) attached to the NIKON SMZ800 (Nikon, Tokyo, Japan) stereomicroscope. The mean diameter of apothecia were measured (two perpendicular measurements) to the nearest

10 µm either using microscope imaging software cellSens Dimension (Olympus, Version 1.7.1) or ImageJ software (Schneider et al., 2012).

2.2.4 Apothecia Identification

In addition to the morphological identification of apothecia on rachises, real-time PCR diagnosis was used to test for *H. fraxineus* presence using methods already developed for *H. fraxineus* by Ioos, Kowalski et al. (2009). Four infected rachises were selected per site, plus a further separate eight apothecia (taken from separate rachises on 13/08/18) per site. This was conducted for all sites except Northumberland, where *H. fraxineus* presence was tested via real-time PCR amplification of spore trap samples (Section 3.2). The surface of rachises were cleaned by wiping with 70% methylated spirit to remove any *H. fraxineus* ascospores. A thin segment of pseudosclerotial plate was removed with a scalpel and DNA extracted using the DNeasy PowerSoil Kit (Qiagen, Hilden, Germany). Small segments of apothecia were removed and DNA extracted using the Extract-N-AMP Plant Tissue PCR kit (Sigma-Aldrich, St. Louis, MO, USA).

Real-time PCR reactions consisted of Takyon No Rox Probe 2X MasterMix Blue dTTP (Eurogentec, Seraing, Belgium), Cfrax-F/-R/-P (Table 2.2), 18S uni-F/-R/-P (Table 2.2), 1 µl sample and molecular grade water to make a final reaction volume of 20 µl. Cfrax-F/- R/-P is specific to *H. fraxineus* (Ioos, Kowalski et a., 2009) and 18S uni-F/-R/-P (Ioos, Fourier et al., 2009) acts as a control for DNA extraction by detecting a range of plant and fungal DNA. Cfrax-F/- R/-P has been tested for specificity in multiplex with 18S uni-F/-R/-P (Ioos, Kowalski et al., 2009). Each real-time PCR was run on Rotor-Gene Q (Qiagen, Hilden, Germany) and cycling parameters were 95°C for 3 minutes followed by 40 cycles of 95°C for 10 seconds and 60°C for 60 seconds. C_q was determined using quantitation analysis (Rotor-Gene Q series software, Version 2.3.1), manually setting the threshold above background noise and early in the exponential phase.

2.2.5 Site Characteristics

Data loggers (Tinytag Plus 2, Gemini Data Loggers UK) were positioned 40 cm above ground level in two locations at each site. The loggers recorded temperature and relative humidity every 10 minutes. Dominant ground cover of quadrats was classified as either Moss, Vegetation, Litter or Soil. Areas classified as vegetation cover were dominated by a range of herbaceous plants (e.g. dog's mercury (*Mercurialis perennis*) and grasses) that shielded the litter layer below, whereas the ground was mainly covered in either mixed broadleaf litter ((except for Carmarthenshire D, which was also covered by bamboo (Bambusoideae) litter), moss, or bare soil with limited other leaf litter or plant

Table 2.2 Primers/ Probes used in the multiplex real-time PCR reaction for detection of *H. fraxineus*, with a DNA extraction control to detect the presence of plant/ fungal DNA. Primers/probes have already been developed and tested for specificity ([a]Ioos, Kowalski et al., 2009; [b]Ioos, Fourier et al., 2009).

Primer/ Probe	Sequence (5'-3')	Reaction concentration (µM)	Species target
Cfrax-F	ATTATATTGTTGCTTTAGCAGGTC	0.5	*H. fraxineus*[a]
Cfrax-R	TCCTCTAGCAGGCACAGTC	0.5	
Cfrax-P	6FAM-CTCTGGGCGTCGGCCTCG-BHQ1	0.05	
18S uni-F	GCAAGGCTGAAACTTAAAGGAA	0.5	Non-specific plant/ fungi[b]
18S uni-R	CCACCACCCATAGAATCAAGA	0.5	
18S uni-P	6JOEN-ACGGAAGGGCACCACCAGGAGT-BHQ1	0.05	

growth, in areas that were classified as either litter, moss or soil cover respectively. Hemispherical photographs were taken of the canopy using a Canon EOS 50D camera with Sigma 4.5 mm f/2.8 EX DC HSM fisheye lens attached and mounted on SLM9 self-levelling mount (Delta-T Devices, Cambridge) during July and August 2020 at all locations except Hampshire location A and D (Table 2.1). These locations were not photographed in 2020 because of tree felling in these sampling areas during autumn 2019. Photographs were taken at 1.3 m above each quadrat during summer 2020 and gap fraction, a measure of canopy closure, calculated using HemiView software version 2.1 (Delta-T devices, 1999).

2.2.6 Statistical Analysis

Only apothecia > 200 µm diameter were used in the analysis, as smaller apothecia could not be sampled reliably. The data were analysed using R software version 4.1.1 stats (R Core Team, 2021), lme4 (Bates et al., 2015), lmerTest (Kuznetsova et al., 2017), MuMIn (Barton, 2020), qpcR (Spiess et al., 2018), car (Fox and Weisburg, 2019), emmeans (Length, 2021), merTools (Knowles and Frederick, 2020), DHARMa (Hartig, 2021), ggplot2 (Wickham, 2016) packages. The total apothecia area (approximated using πr^2) from a quadrat on a given sampling date was used as the response variable in statistical models. Nested linear mixed effects models were fitted with site, quadrat and sampling year all defined as random effects, and with quadrats nested within sites. This

allows the examination of both site and quadrat level variables, whilst controlling for unaccounted variance between sites, quadrats and sampling years. The square root of the total apothecia area was taken in order to meet the linear response assumption of the model. The $\log_{10}$ of the square root of the total apothecia area (mm^2) was used as the response variable and zero values were removed to meet model assumptions of a normal distribution of residuals.

Maximal nested linear mixed effects models were constructed for mean temperature interacting with mean relative humidity and ground cover. Models were also constructed replacing ground cover with gap fraction, which were modelled separately due to variable correlation. Mean relative humidity and temperature were measured from 7 to 42 days prior to collection at 7 day intervals. Fewer sampling weeks were assessed at some sites because of late set-up of data loggers (Supplementary Table 2.1).

All continuous explanatory variables were scaled by subtracting the mean and dividing the standard deviation from a given value, which allowed the modelling of variables on different scales.

The maximal nested linear mixed effects models, fitted using REML (restricted/ residual maximum likelihood), were subject to stepwise model reduction of non-significant effects using Kenward-Roger approximation for denominator degrees of freedom (Luke, 2017), and 0.01 as a threshold value for significance. The reduced models containing significant variables were then fitted with ML (maximum likelihood), and AICc (second-order Akaike Information Criterion) values calculated, which provide a relative measure of model performance based on Kullback-Leibler information (Hurvich and Tsai, 1989). Models were compared using ΔAICc values, which provide a figure of information loss of models relative to the most supported model. Models with ΔAICc values of less than 7 can be considered plausible (Burnham et al., 2011).

Data could not be analysed with site as a random effect for models that included gap fraction due to insufficient spread of gap fraction values between sites. Therefore, site was included in these models as a fixed effect to account for between site variation. Likelihood ratio tests of models (fitted using ML) with site as a random effect and ΔAICc less than 7 were used to test the effect of removing site as a random effect. If site could be removed as a random effect without significantly affecting models, then these models could be compared with gap fraction models where fitting of site as a random effect was not possible.

Most supported models (ΔAICc values less than 7) were fitted using REML to describe model features. The interactions in models were examined by calculating the estimated marginal mean of the $\log_{10}(\sqrt{(\text{total apothecia area})})$ within measured ranges of the explanatory variables, using Kenward-Roger approximation for denominator degrees

of freedom. The variance explained by fixed effects in these models was represented using marginal R^2 values, and the variance explained by both fixed effects and random effects was represented using conditional R^2 values (Nakagawa and Schielzeith, 2013).

2.3 Results

2.3.1 Site characteristics and apothecia size and identification

Real-time PCR tests ascribed apothecia and pseudosclerotial plates to *H. fraxineus.* There was considerable variation in the apothecia area both within and between sites throughout the sampling period (Figure 2.2). The maximum apothecia area was mostly greater in 2019 (at 17/24 sampling locations). Within sites, there was some indication that locations with vegetation cover had higher maximum apothecia area, whereas locations with litter cover had lower maximum apothecia area, but within site variability was high. The high intra-site variation made site level inferences from the raw data difficult.

Mean daily temperature varied considerably, but peaked during July in both 2018 and 2019, although the precise dates varied between sites and sampling years (Figure 2.3). In 2018, the period of peak temperatures was longer on the more easterly sites (Hampshire and County Durham), as well as in the Shropshire site corresponding with achieving maximum apothecia area slightly later on these sites in 2018 (Figure 2.2; Figure 2.3). However, the period of peak mean daily temperature was slightly longer in 2019 than in 2018 for the sites in Devon, Carmarthenshire and Wiltshire, but this did not correlate with the dates when maximum apothecia area were achieved. Overall, mean daily temperatures were cooler in 2019 than in 2018, although the median temperature at sites in August were similar across both sampling years (Figure 2.3).

The mean daily relative humidity varied throughout both sampling seasons (Figure 2.4) A drop in relative humidity was present on all sites at the end of June 2018. There was also a drop in relative humidity at the end of June 2019 in Devon, Wiltshire and Hampshire, although this was smaller than in 2018. The median relative humidity was greater at all sites in June and July 2019 than in 2018 (Figure 2.4).

Gap fraction was related to ground cover type (Figure 2.5). Vegetation cover typically had the greatest gap fraction, followed by litter cover, and then soil and moss cover. Variability in gap fraction was low within most sites (Figure 2.5).

(a)

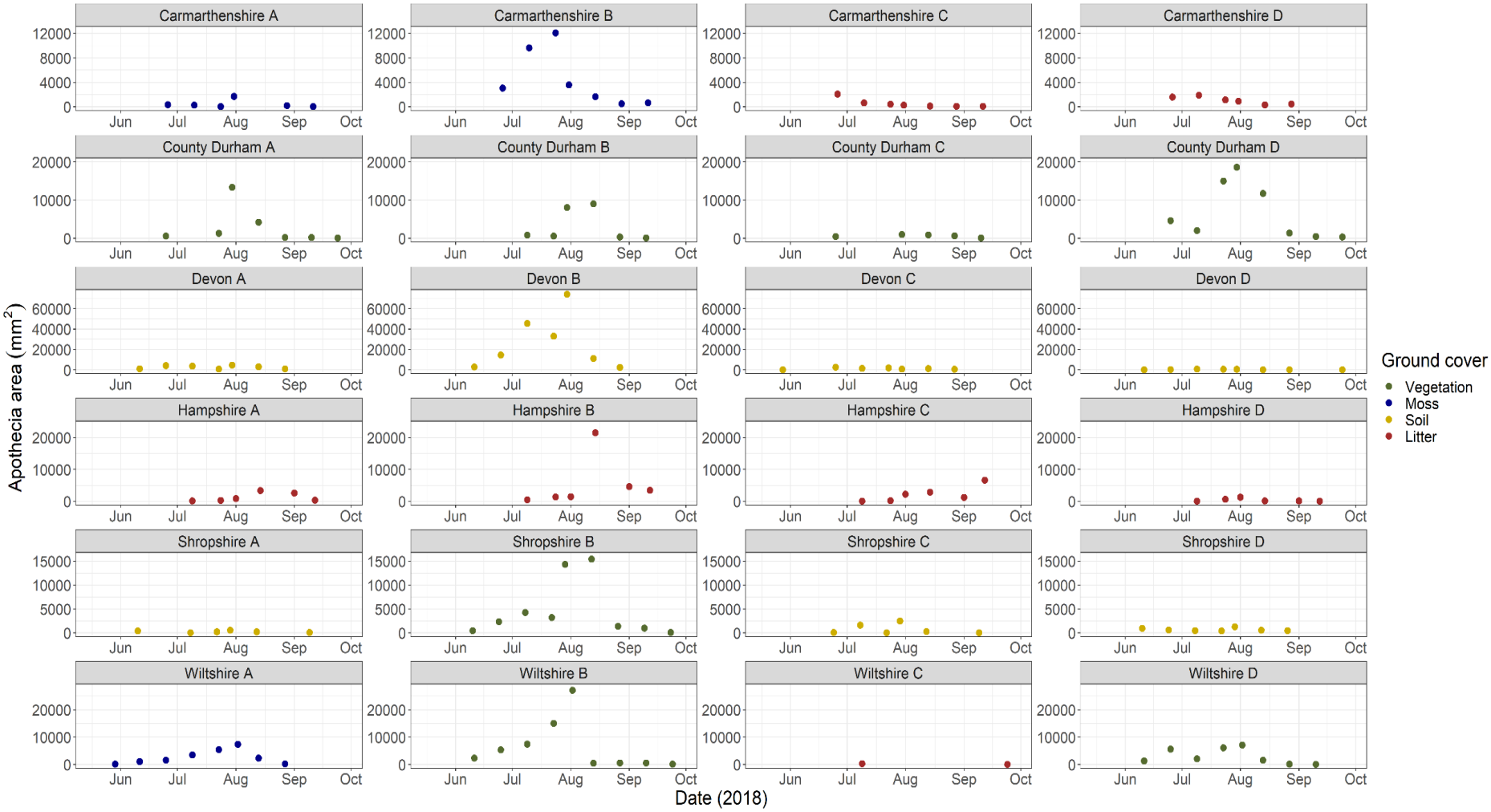
Carmarthenshire A
Carmarthenshire B
Carmarthenshire C
Carmarthenshire D
County Durham A
County Durham B
County Durham C
County Durham D
Devon A
Devon B
Devon C
Devon D
Hampshire A
Hampshire B
Hampshire C
Hampshire D
Shropshire A
Shropshire B
Shropshire C
Shropshire D
Wiltshire A
Wiltshire B
Wiltshire C
Wiltshire D
Jun
Jul
Aug
Sep
Oct
Apothecia area (mm^2)
Date (2018)
Ground cover
Vegetation
Moss
Soil
Litter

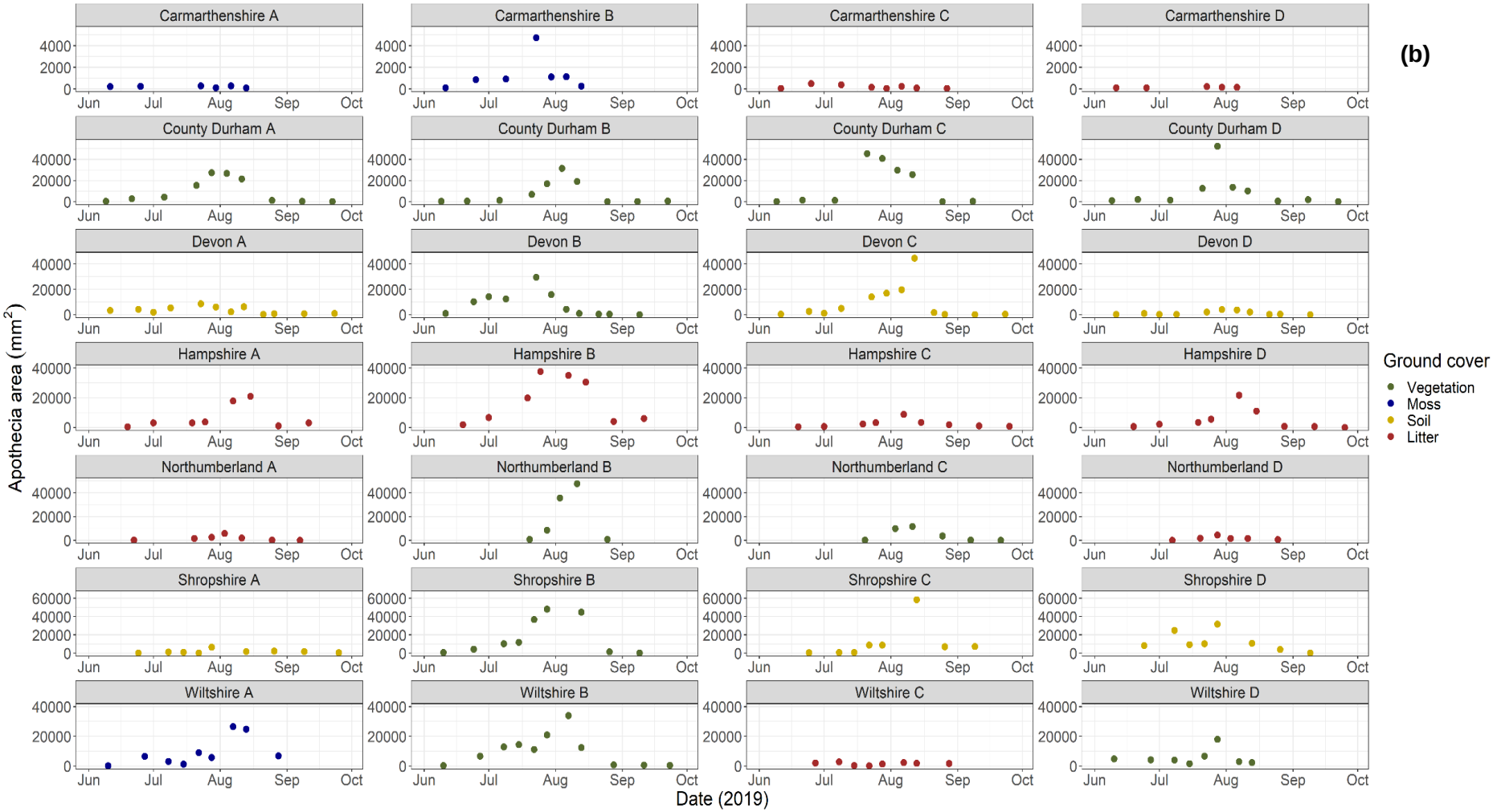

Figure 2.2 (a) *Hymenoscyphus fraxineus* apothecia area (mm^2) from four replicate locations (A, B, C, D) across six sites (Carmarthenshire, Count Durham, Devon, Hampshire, Shropshire, Wiltshire) from July – September 2018 (Figure 2.1; Table 2.1; Supplementary Table 2.1) (b) and from locations (A, B, C, D) across seven sites (Carmarthenshire, Count Durham, Devon, Hampshire, Northumberland, Shropshire, Wiltshire) from June – September 2019 (Supplementary Table 2.1). Apothecia area (mm^2) was calculated from the sum of the measured area ($\sum\prod r^2$) from 6 cm segments from eight randomly selected *H. fraxineus* infected rachises that were collected from sampling locations (Section 2.2).

(a)

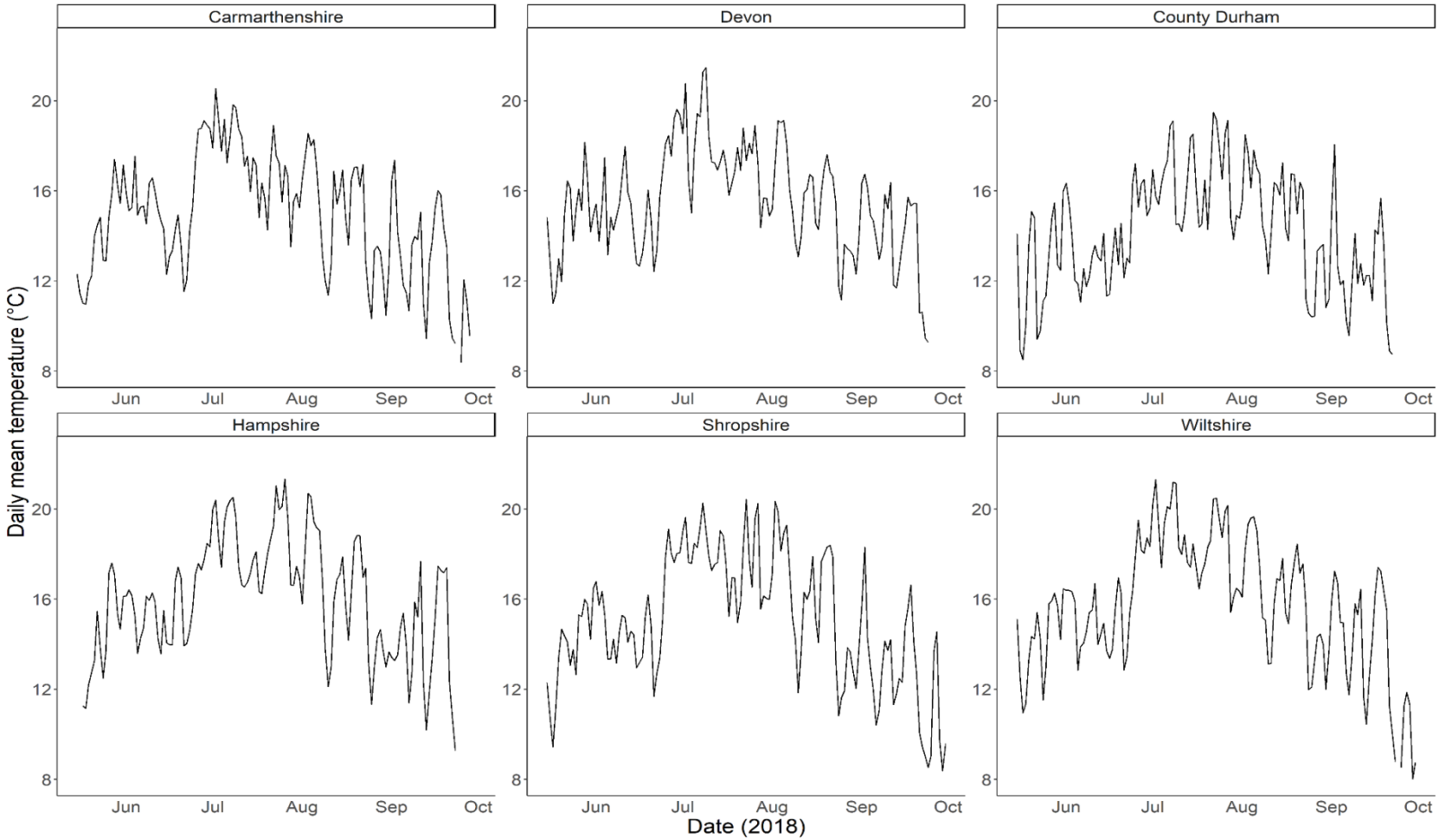
Carmarthenshire
Devon
County Durham
Hampshire
Shropshire
Wiltshire
Daily mean temperature (°C)
8
12
16
20
Jun
Jul
Aug
Sep
Oct
Date (2018)

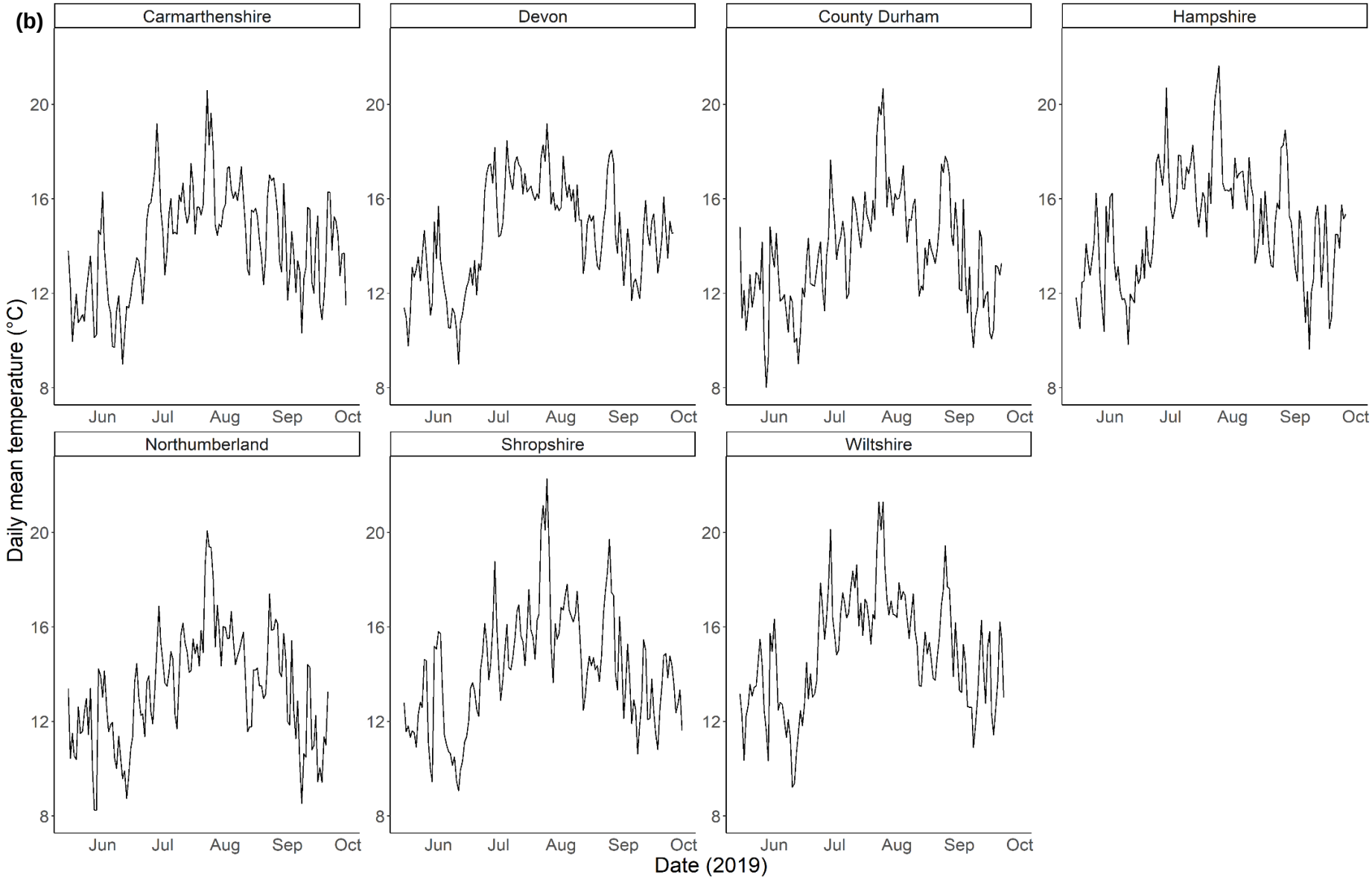
(b)
Carmarthenshire
Devon
County Durham
Hampshire
Northumberland
Shropshire
Wiltshire
Daily mean temperature (°C)
8
12
16
20
Jun
Jul
Aug
Sep
Oct
Date (2019)

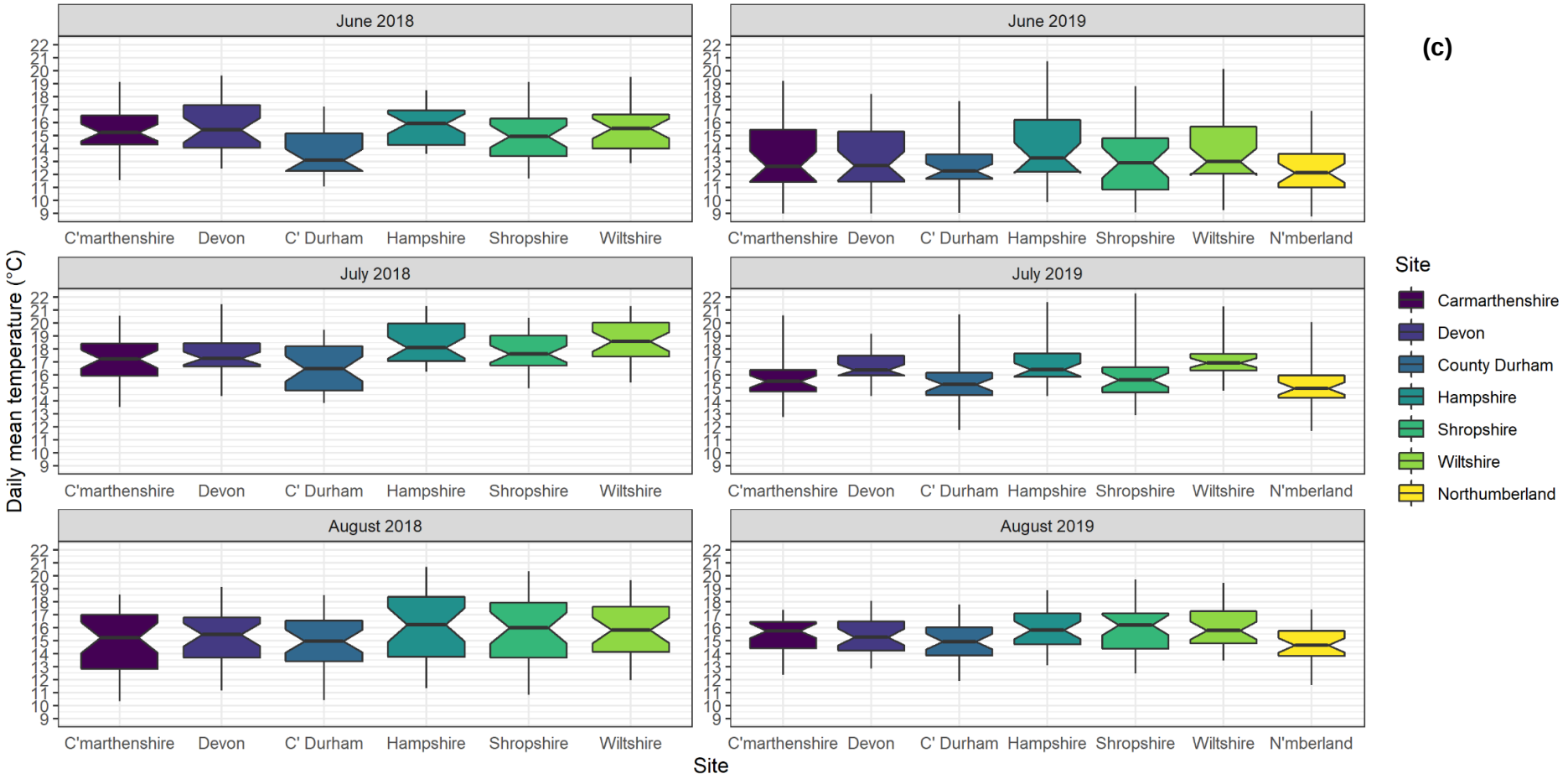

Figure 2.3 Daily mean temperature (°C) during **(a)** May – September 2018 at six sites (Carmarthenshire, Devon, County Durham, Hampshire, Shropshire, Wiltshire) where *Hymenoscyphus fraxineus* apothecia area (mm^2) measured at 1-2 week intervals from April – September 2018 (Section 2.2) **(b)** May – September 2019 at seven sites (Carmarthenshire, Devon, County Durham, Hampshire, Shropshire, Wiltshire, Northumberland) where *H. fraxineus* apothecia area (mm^2) was measured at 1-2 week intervals from April – September 2019 (Section 2.2; Supplementary Table 2.1). **(c)** Boxplot of daily mean temperature (°C) during June – August 2018 and 2019 at sites where *H. fraxineus* apothecia area (mm^2) was measured during April – September 2018 and/ or 2019 (Section 2.2; Supplementary Table 2.1). The median is represented by the central line in the boxplot, the whiskers represent the maximum and minimum recorded values, and the notches represent 1.58 * interquartile range / √ (no. of observations).

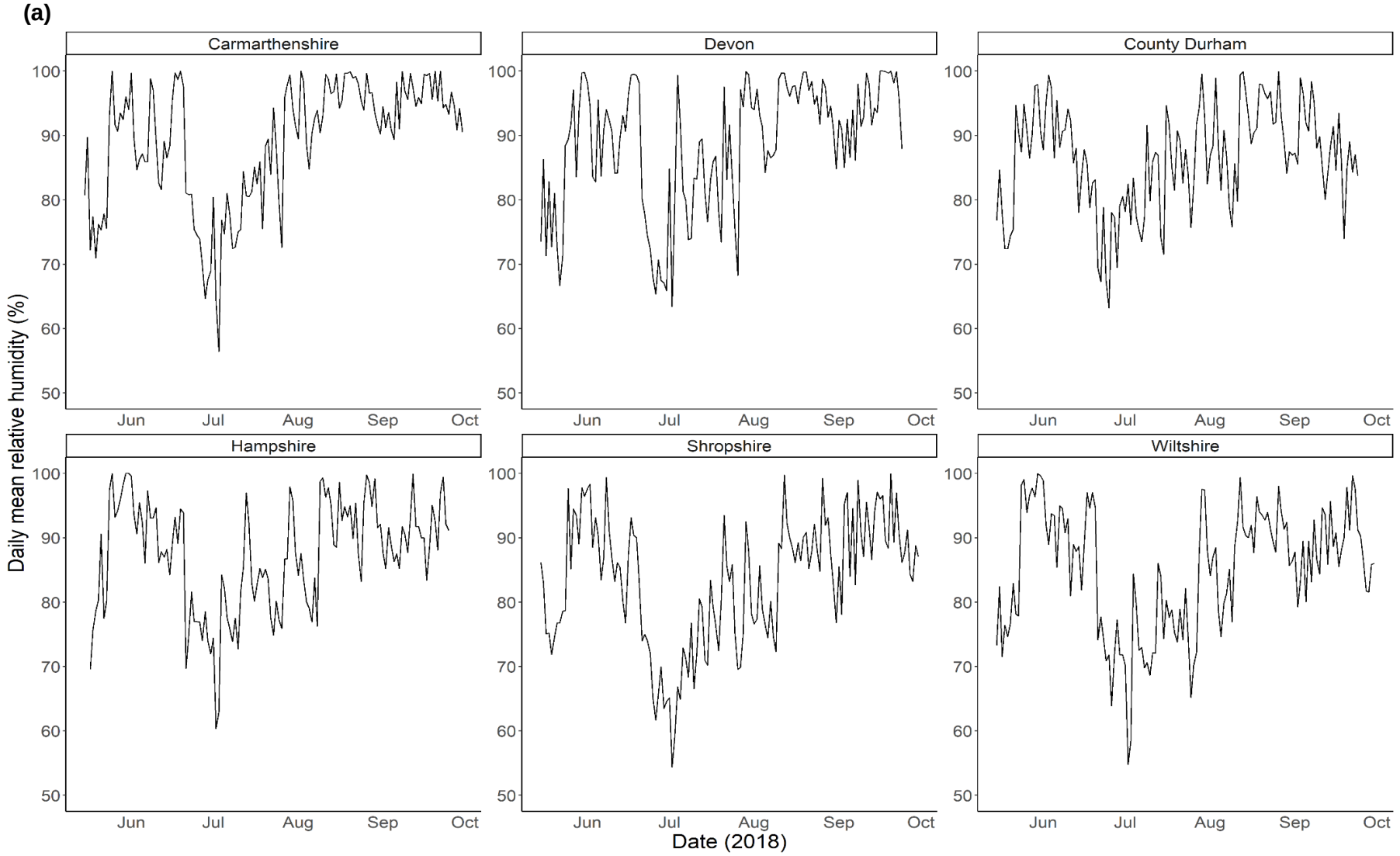
(a)
Carmarthenshire
Devon
County Durham
Hampshire
Shropshire
Wiltshire
Daily mean relative humidity (%)
100
90
80
70
60
50
Jun
Jul
Aug
Sep
Oct
Date (2018)

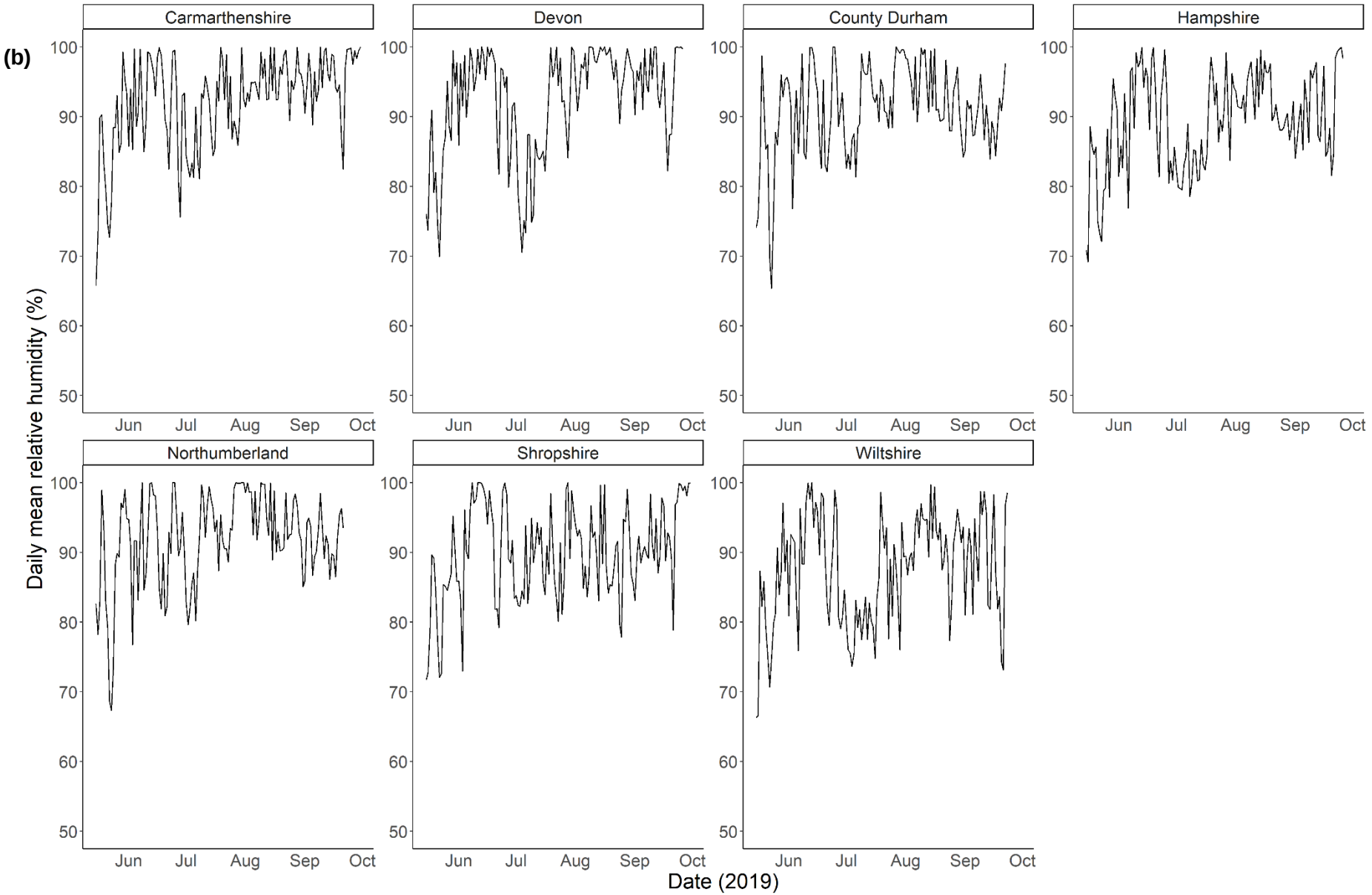
(b)
Carmarthenshire
Devon
County Durham
Hampshire
Northumberland
Shropshire
Wiltshire
Daily mean relative humidity (%)
100
90
80
70
60
50
Jun
Jul
Aug
Sep
Oct
Date (2019)

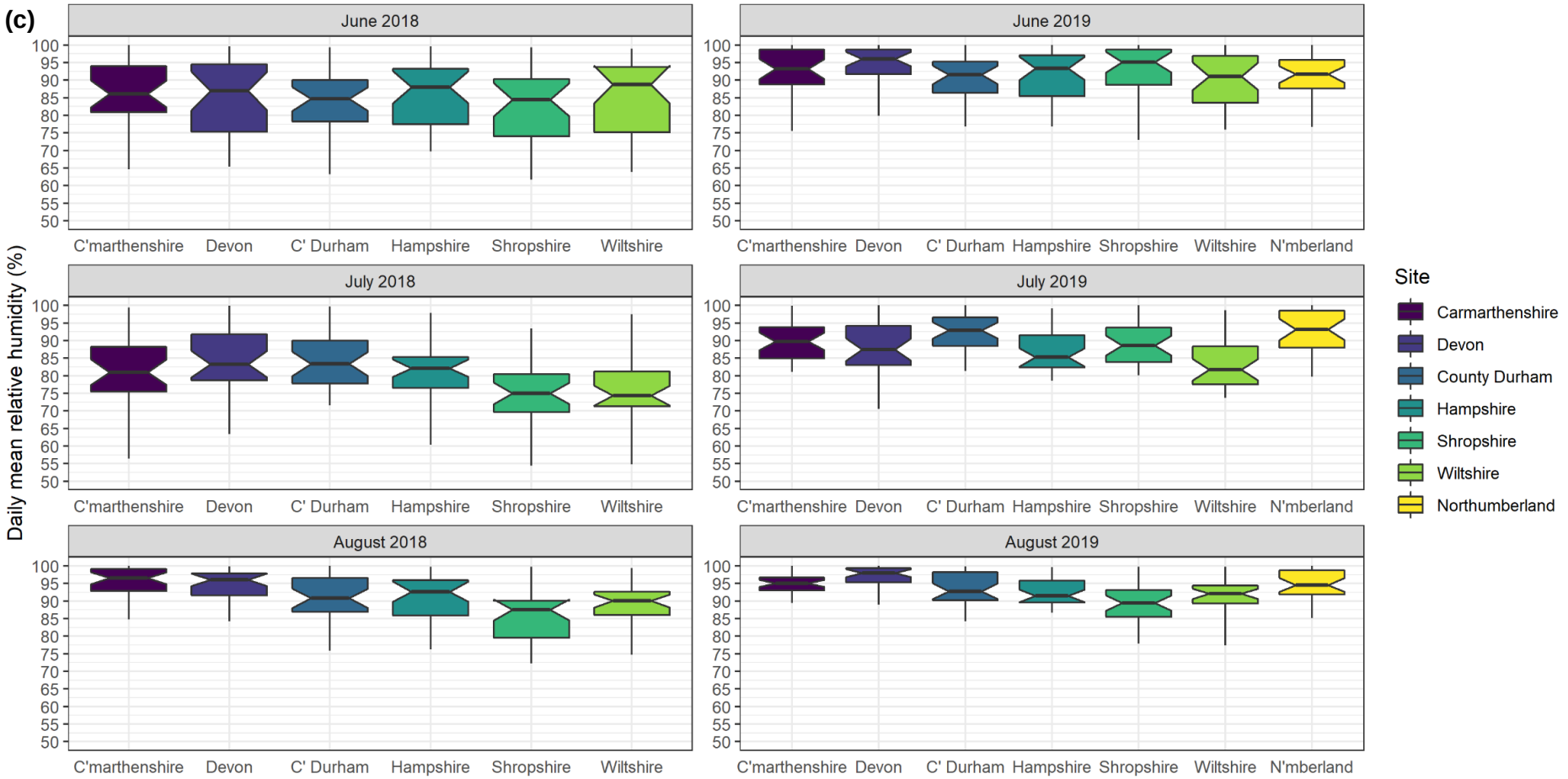

Figure 2.4 Daily mean relative humidity (%) **(a)** May – September 2018 at six sites (Carmarthenshire, Devon, County Durham, Hampshire, Shropshire, Wiltshire) where *Hymenoscyphus fraxineus* apothecia area (mm^2) was measured at 1-2 week intervals from April – September 2018 (Section 2.2) **(b)** May – September 2019 at seven sites (Carmarthenshire, Devon, County Durham, Hampshire, Shropshire, Wiltshire, Northumberland) where *H. fraxineus* apothecia area (mm^2) was measured at 1-2 week intervals from April – September 2019 (Section 2.2; Supplementary Table 2.1). **(c)** Boxplot of daily mean relative humidity (%) June – August 2018 and 2019 at sites where *H. fraxineus* apothecia area (mm^2) was measured April – September 2018 and/ or 2019 (Section 2.2; Supplementary Table 2.1). The median is represented by the central line in the boxplot, the whiskers represent the maximum and minimum recorded values, and the notches = 1.58*interquartile range / √ (no. of observations).

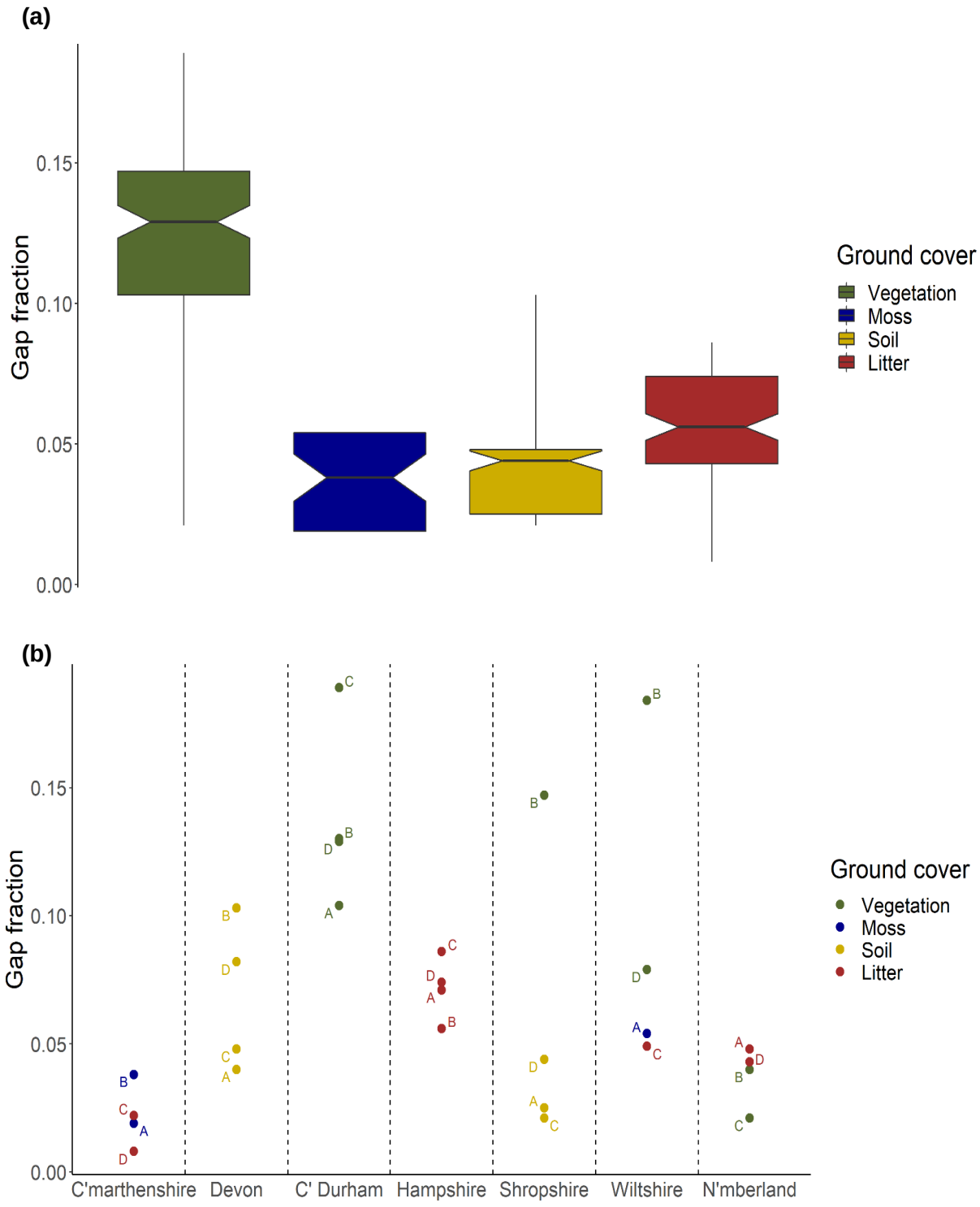

Figure 2.5 (a) Gap fraction (a measure of canopy openness) (Section 2.2.5) above sampling locations (A, B, C, D) where *H. fraxineus* apothecia area (mm^2) was measured at 1-2 week intervals from April – September 2018 at six sites (Carmarthenshire, Devon, County Durham, Hampshire, Shropshire, Wiltshire) and May – September 2019 at seven sites (Carmarthenshire, Devon, County Durham, Hampshire, Shropshire, Wiltshire, Northumberland) (Section 2.2). **(b)** Boxplot of the gap fraction above sampling locations with different ground cover. The median is represented by the central line in the boxplot, the whiskers represent the maximum and minimum recorded values, and the notches represent 1.58 * interquartile range / √ (no. of observations).

2.3.2 Model construction and ranking

Three models were identified with a ΔAICc value less than 7 (Table 2.3) based on the following: removal of site as a random effect did not significantly affect tested models and site was not retained as a significant fixed effect in models that included gap fraction. Therefore, ΔAICc values of models including gap fraction and vegetation were calculated without site as a random effect to allow more accurate comparison of the fixed effects. However, where possible, the final models presented were fitted with site as a random effect as it still accounted for a small amount of model variance.

2.3.2.1 Apothecia model 1 (Figure 2.6)

Apothecia Model 1 <- Log_{10}(√H. fraxineus apothecia area) ~ scale(mean relative humidity previous 7 days) + scale(mean temperature previous 14 days) + Ground Cover + (1 | Site/Quadrat) + (1 | Year) + scale(mean relative humidity previous 7 days):scale(mean temperature previous 14 days) + scale(mean temperature previous 14 days):Ground Cover

Apothecia model 1 had significant two-way interaction between mean temperature over the previous 14 days and mean relative humidity over the previous 7 days (ddf = 369.5, $p < 0.001$). As temperature increased the effect of relative humidity became positive (Figure 2.7). For example, the estimated marginal mean of the change in $\log_{10}$(√total apothecia area(mm^2)) per unit relative humidity increased from -0.0115 (se = 0.0040, df = 370) at mean temperature 14˚C over the previous 14 days, to 0.0050 (se = 0.0028, df = 370) at mean temperature 16.5˚C over the previous 14 days.

In addition to the significant interaction between mean temperature over the previous 14 days and mean relative humidity over the previous 7 days (ddf = 369.5, $p < 0.001$), the mean temperature over the previous 14 days also significantly interacted with the ground cover (ddf = 371.32, $p < 0.001$) (Figure 2.8). At a lower relative humidity (80%), the estimated marginal mean of the change in $\log_{10}$(√total apothecia area(mm^2)) per unit temperature was greatest under vegetation (0.0997, se = 0.0166, df = 371), then moss (0.0631, se = 0.0262, df = 369), soil (0.0307, se = 0.0204, df = 366) and litter cover (-0.0004, se = 0.0191, df = 373). At a higher relative humidity (95%), the estimated marginal mean of the change in $\log_{10}$(√total apothecia area(mm^2)) per unit temperature increased by 0.0991 (se = 0.0178, df = 368) on all ground cover types (Vegetation = 0.1988, se = 0.0154, df = 371; Soil = 0.1298, se = 0.0184, df = 367; Moss = 0.1622, se = 0.0262, df = 370; Litter = 0.0987, se = 0.0169, df = 368).

At a cooler mean temperature (14°C) over the previous 14 days and a lower mean relative humidity (80%) over the previous 7 days (Figure 2.8), the estimated marginal mean of $\log_{10}(\sqrt{\text{total apothecia area}(mm^2)})$ was largest at soil ground cover (1.67, se = 0.15, df = 3.07) compared to vegetation (1.51, se = 0.14, df = 2.38), moss (1.46, se = 0.18, df = 5.75) or litter ground cover (1.43, se = 0.15, df = 2.95). When relative humidity increased to 95%, the estimated marginal means of $\log_{10}(\sqrt{\text{total apothecia area}(mm^2)})$ decreased by 0.17 (se = 0.06, df = 370.2) on all ground cover types (Soil = 1.50, se = 0.15, df = 2.68; Vegetation = 1.34, se = 0.14, df = 2.08; Moss = 1.29, se = 0.18, df = 5.16; Litter = 1.26, se = 0.15, df = 2.45).

At a warmer mean temperature (16.5°C) over the previous 14 days and a lower mean relative humidity (80%) over the previous 7 days (Figure 2.8), the estimated marginal mean of $\log_{10}(\sqrt{\text{total apothecia area}(mm^2)})$ was greatest for vegetation (1.76, se = 0.14, df = 2.16 and soil (1.74, se = 0.15, df = 2.53), followed by moss (1.62, se = 0.18, df = 4.79), and then litter cover (1.43, se = 0.14, df = 2.41). When relative humidity was increased to 95%, the estimated marginal means of $\log_{10}(\sqrt{\text{total apothecia area}(mm^2)})$ increased by 0.075 (se = 0.041, df = 370.2) on all ground cover types (Vegetation = 1.83, se = 0.14, df = 2.09; Soil = 1.82, se = 0.15, df = 2.56; Moss = 1.69, se = 0.18, df = 4.76; Litter = 1.51, se = 0.14, df = 2.35).

2.3.2.2 Apothecia model 2 (Figure 2.9)

Apothecia Model 2 <- $Log_{10}(\sqrt{H.\ fraxineus\ apothecia\ area})$ ~ scale(mean relative humidity previous 7 days) + scale(mean temperature previous 14 days) + scale(Gap Fraction) + (1 | Site:Quadrat) + (1 | Year) + scale(mean relative humidity previous 7 days):scale(mean temperature previous 14 days) + scale(mean temperature previous 14 days):scale(Gap Fraction)

Apothecia model 2 had a significant two-way interaction between mean relative humidity over the previous 7 days and mean temperature over the previous 14 days (ddf = 371.49, $p < 0.001$). As the temperature increased, the effect of increasing mean relative humidity became positive (Figure 2.10). For example, the estimated marginal mean of the change in $\log_{10}(\sqrt{\text{total apothecia area}(mm^2)})$ per unit relative humidity increased from -0.0102 (se = 0.0040, df = 380) at mean temperature 14˚C over the previous 14 days, to 0.0056 (se = 0.0027, df = 384) at mean temperature 16.5˚C over the previous 14 days.

The mean temperature over the previous 14 days also significantly interacted with the gap fraction (ddf = 377.1, $p < 0.001$). As the temperature increased, the effect of gap

fraction became more positive (Figure 2.11). At a cooler mean temperature (14°C) the estimated marginal mean of the change in $\log_{10}(\sqrt{\text{total apothecia area}(mm^2)})$ per 0.1 gap fraction was 0.1417 (se = 0.0720, df = 29.6), which increased to 0.3028 (se = 0.0721, df = 29.5) at a warmer mean temperature (16.5°C).

The effect of mean temperature over the previous 14 days on $\log_{10}(\sqrt{\text{total apothecia area}(mm^2)})$ was greater as both gap fraction and mean relative humidity over the previous 14 days increased (Figure 2.11). For example, at a lower relative humidity (80%), the estimated marginal mean of the change in $\log_{10}(\sqrt{\text{total apothecia area}(mm^2)})$ per unit temperature (°C) was greater at a higher gap fraction (0.15) (0.1003, se = 0.0125, df = 371), compared to a lower gap fraction (0.05) (0.0358, se = 0.0146, df = 376). At a higher mean relative humidity (95%) over the previous 7 days, the estimated marginal mean of the change in $\log_{10}(\sqrt{\text{total apothecia area}(mm^2)})$ per unit temperature (°C) increased by 0.09454 (se = 0.01791, df = 371) (0.15 gap fraction = 0.1948, se = 0.0161, df = 374; 0.05 gap fraction = 0.1304, se = 0.0125, df = 371).

At a lower mean temperature (14°C) over the previous 14 days and a lower mean relative humidity (80%) over the previous 7 days (Figure 2.11), the estimated marginal mean of $\log_{10}(\sqrt{\text{total apothecia area}(mm^2)})$ was greater at a higher gap fraction (0.15) (1.61, se = 0.14, df = 2.02) compared to a lower gap fraction (0.05) (1.47, se = 0.13, df = 1.57) gap fraction. When relative humidity was increased to 95%, the estimated marginal mean of $\log_{10}(\sqrt{\text{total apothecia area}(mm^2)})$ decreased by 0.15 (se = 0.02, df = 371) regardless of the gap fraction (0.15 gap fraction = 1.46, se = 0.132, df = 1.82; 0.05 gap fraction = 1.32, se = 0.12, df = 1.26)

At a warmer mean temperature (16.5°C) over the previous 14 days (Figure 2.11), the estimated marginal mean of $\log_{10}(\sqrt{\text{total apothecia area}(mm^2)})$ at a lower relative humidity (80%) over the previous 7 days was greater at a higher gap fraction (0.15) (1.86, se = 0.13, df = 1.83) compared to a lower gap fraction (0.05) (1.56, se = 0.12, df = 1.27). As relative humidity was increased to 95%, the estimated marginal mean of $\log_{10}(\sqrt{\text{total apothecia area}(mm^2)})$ increased by 0.08 (se = 0.04, df = 384.4) irrespective of gap fraction (0.15 gap fraction = 1.94, se = 0.132, df = 1.82; 0.05 gap fraction = 1.64, se = 0.120, df = 1.26).

2.3.2.3 Apothecia model 3 (Figure 2.12)

*Apothecia Model 3 <- Log_{10}(√H. fraxineus apothecia area) ~ scale(mean relative humidity previous 42 days) * scale(mean temperature previous 14 days) * Ground Cover + (1 | Site/Quadrat) + (1 | Year)*

Apothecia model 3 had a significant three-way interaction effect between ground cover, the mean temperature 14 days prior to collection and the mean humidity 42 days prior to collection (ddf = 362.6, $p < 0.01$) (Figure 2.13). The effect of increasing temperature on $\log_{10}$(√total apothecia area(mm^2)) became more positive as relative humidity increased on all ground cover types except moss cover, where the effect of increasing temperature became less positive. For example, at a lower relative humidity (85%) over the previous 42 days, the estimated marginal mean of the change in $\log_{10}$(√total apothecia area(mm^2)) per unit temperature increase was greatest under vegetation cover (0.1235, se = 0.0153, df = 363), then moss (0.0944, se = 0.0262, df = 358), soil (0.0550, se = 0.0208, df = 359) and litter cover (0.0322, se = 0.0201, df = 363). As relative humidity was increased to 92%, the effect of temperature was greatest under vegetation cover (0.1953, se = 0.0196, df = 364), then soil (0.1660, se = 0.0260, df = 360), litter (0.1007, se = 0.0279, df = 360) and moss (0.0140, se = 0.0464, df = 360).

The estimated marginal mean of the change in $\log_{10}$(√total apothecia area(mm^2)) per unit relative humidity increase was negative on all ground cover types at lower temperatures (14˚C) (Litter = -0.0246, se = 0.0133, df = 372; Soil = -0.0291, se = 0.0107, df = 363; Vegetation = -0.0317, se = 0.0087, df = 376), except for moss cover where the effect was slightly positive (0.0049, se = 0.0155, df = 366). As temperature increased, the effect of relative humidity became more positive on all ground cover types, except moss where the inverse was true. Indeed, at warmer temperatures (16.5˚C) the effect of increasing humidity was slightly positive on soil ground cover (0.0105, se = 0.0069, df = 368), neutral under litter ground cover (0.0001, se = 0.0090, df = 372), but negative under vegetation (-0.0061, se = 0.0067, df = 376) and on moss cover (-0.0238, se = 0.0117, df = 366).

At a cooler temperature (14˚C) and lower humidity (85%), the estimated marginal mean of $\log_{10}$(√total apothecia area(mm^2)) was greater for soil (1.68, se = 0.17, df = 2.68) compared to vegetation (1.52, se = 0.16, df = 2.04), litter (1.39, se = 0.17, df = 2.85) and moss cover (1.37, se = 0.20, df = 4.53).

At a cooler temperature (14˚C) and higher humidity (92%), the estimated marginal mean of $\log_{10}$(√total apothecia area(mm^2)) was greater for soil (1.48, se = 0.17, df = 2.42) and moss (1.40, se = 0.20, df = 5.02) compared to vegetation (1.30, se = 0.16, df = 1.89) and litter cover (1.22, se = 0.16, df = 2.29).

At a warmer temperature (16.5˚C) and lower humidity (85%), the estimated marginal mean of $\log_{10}(\sqrt{\text{total apothecia area}(mm^2)})$ was greater for vegetation (1.83, se = 0.15, df = 1.87) and soil (1.82, se = 0.16, df = 2.21), compared to moss (1.60, se = 0.19, df = 3.85) and litter cover (1.47, se = 0.16, df = 2.18).

At a warmer temperature (16.5˚C) and higher humidity (92%), the estimated marginal mean of $\log_{10}(\sqrt{\text{total apothecia area}(mm^2)})$ was greatest for soil (1.89, se = 0.17, df = 2.51) and vegetation (1.79, se = 0.16, df = 2.02) compared to litter (1.47, se = 0.17, df = 2.42) and moss (1.44, se = 0.21, df = 5.32).

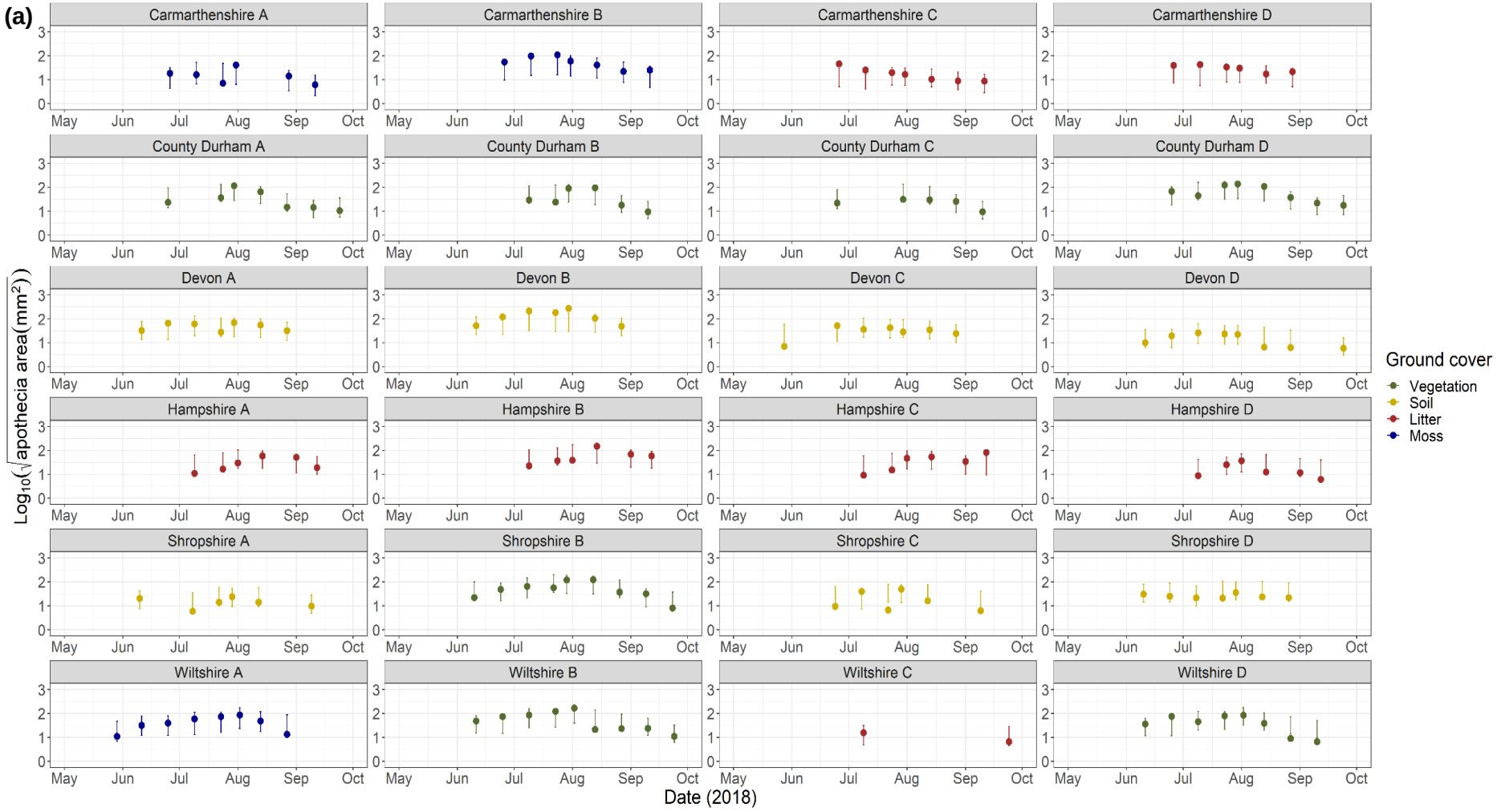
(a)
Carmarthenshire A
Carmarthenshire B
Carmarthenshire C
Carmarthenshire D
County Durham A
County Durham B
County Durham C
County Durham D
Devon A
Devon B
Devon C
Devon D
Hampshire A
Hampshire B
Hampshire C
Hampshire D
Shropshire A
Shropshire B
Shropshire C
Shropshire D
Wiltshire A
Wiltshire B
Wiltshire C
Wiltshire D
May
Jun
Jul
Aug
Sep
Oct
0
1
2
3
Log10(√apothecia area(mm2))
Date (2018)
Ground cover
Vegetation
Soil
Litter
Moss

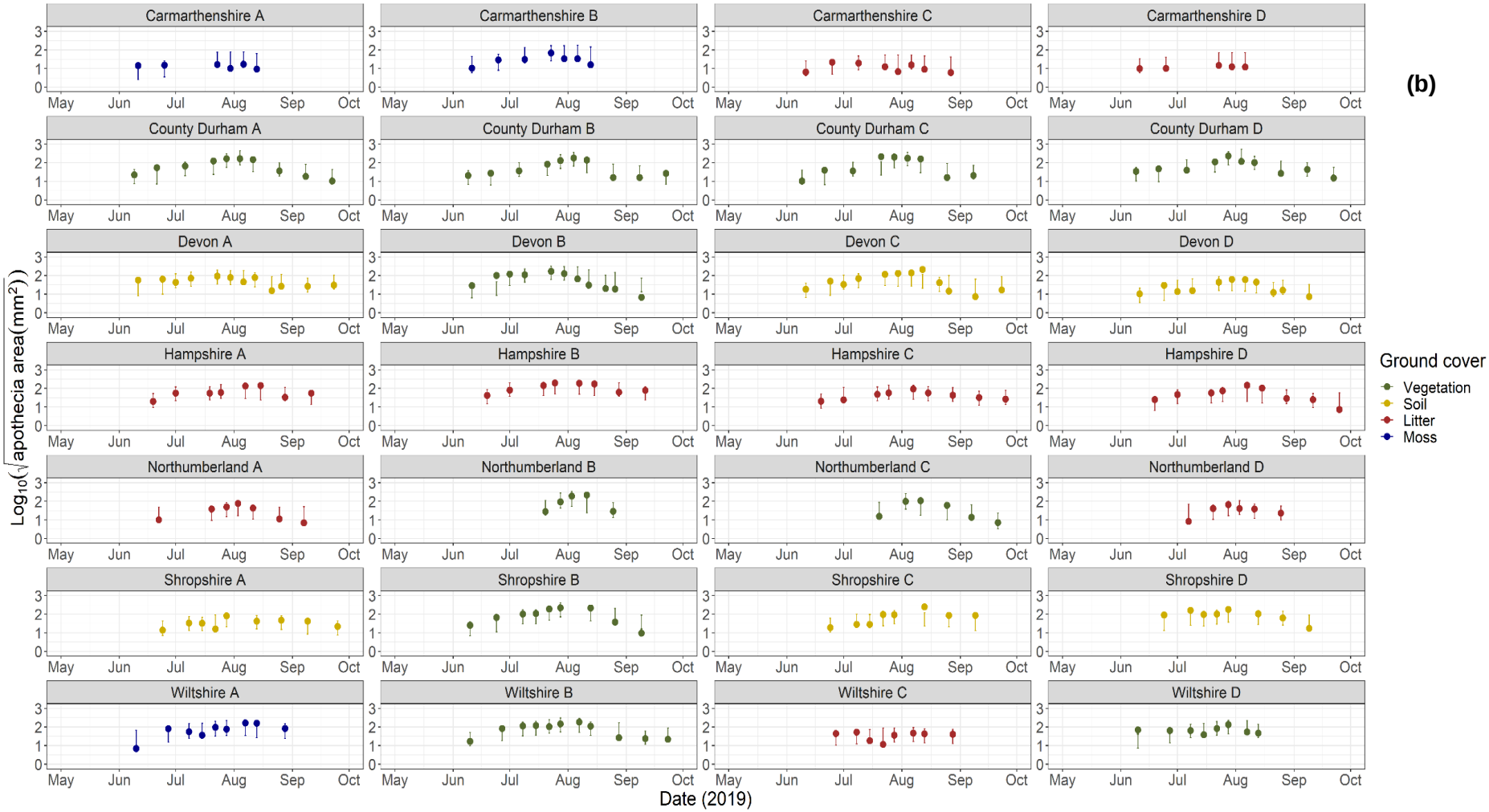

Figure 2.6 (a) $Log_{10}(\sqrt{}$*H. fraxineus* apothecia area (mm^2)) from locations (A, B, C, D) within six sites (Carmarthenshire, County Durham, Devon, Hampshire, Shropshire, Wiltshire) from May – September 2018 (Section 2.2; Figure 2.1; Table 2.1; Supplementary Table 2.1) **(b)** and from locations (A, B, C, D) across seven sites (Carmarthenshire, County Durham, Devon, Hampshire, Northumberland, Shropshire, Wiltshire) from May – September 2019 (Section 2.2) with the most supported linear mixed effects model (apothecia model 1; ΔAICc = 0; marginal R2 = 0.29; conditional R2 = 0.61) fitted to the datapoints with corresponding 95% confidence intervals. The model accounted for unexplained variation between sites, sampling locations and sampling years by specifying these variables as random effects and that sampling locations were nested within sites. Fixed effects (explanatory variables) included in the model were

mean temperature (°C) over the 14 days prior to sample collection, mean relative humidity (%) over the 7 days prior to sample collection and dominant ground cover (vegetation, soil, litter or moss) at the sampling location. An interaction was present between mean temperature (°C) over the 14 days prior to sample collection and dominant ground cover, and between mean temperature (°C) over the 14 days prior to sample collection and mean relative humidity (%) over the 7 days prior to sample collection (Section 2.2.6; Section 2.3.2.1).

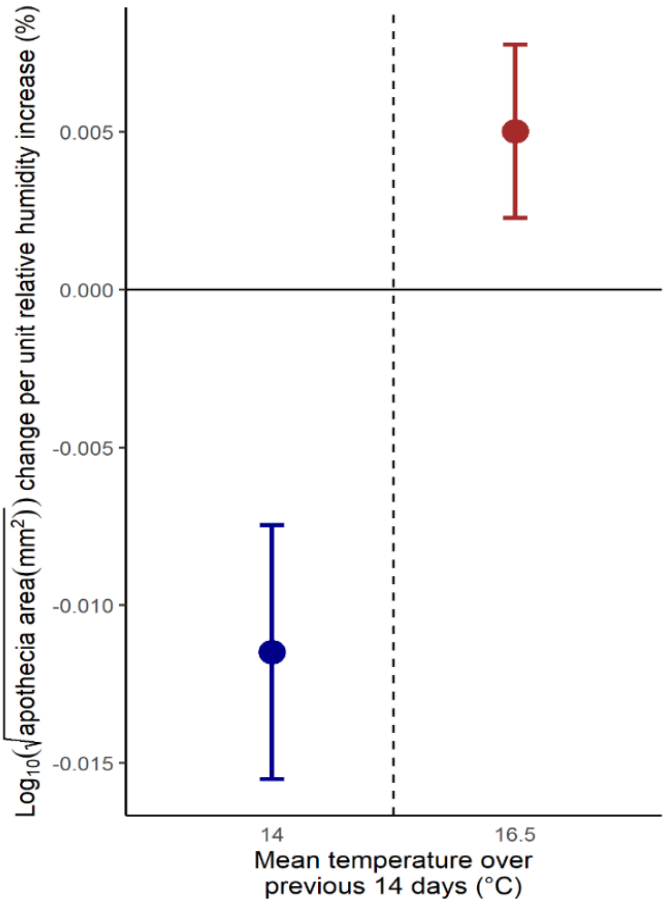

Figure 2.7 The significant interactive effect on $\log_{10}(\sqrt{}$*H. fraxineus* apothecia area (mm^2)) in apothecia model 1 (Section 2.3.2.1) between mean temperature (°C) over the 14 days prior to sample collection and the mean relative humidity over the 7 days prior to sample collection (ddf =369.5, $p < 0.001$). The change in the estimated marginal mean (from apothecia model 1) of $\log_{10}(\sqrt{}$*H. fraxineus* apothecia area (mm^2)) and standard error per unit increase of the mean relative humidity (%) over the 7 days prior to sample collection at a cooler (14°C) and warmer (16.5°C) mean temperature over the previous 14 days.

(a)

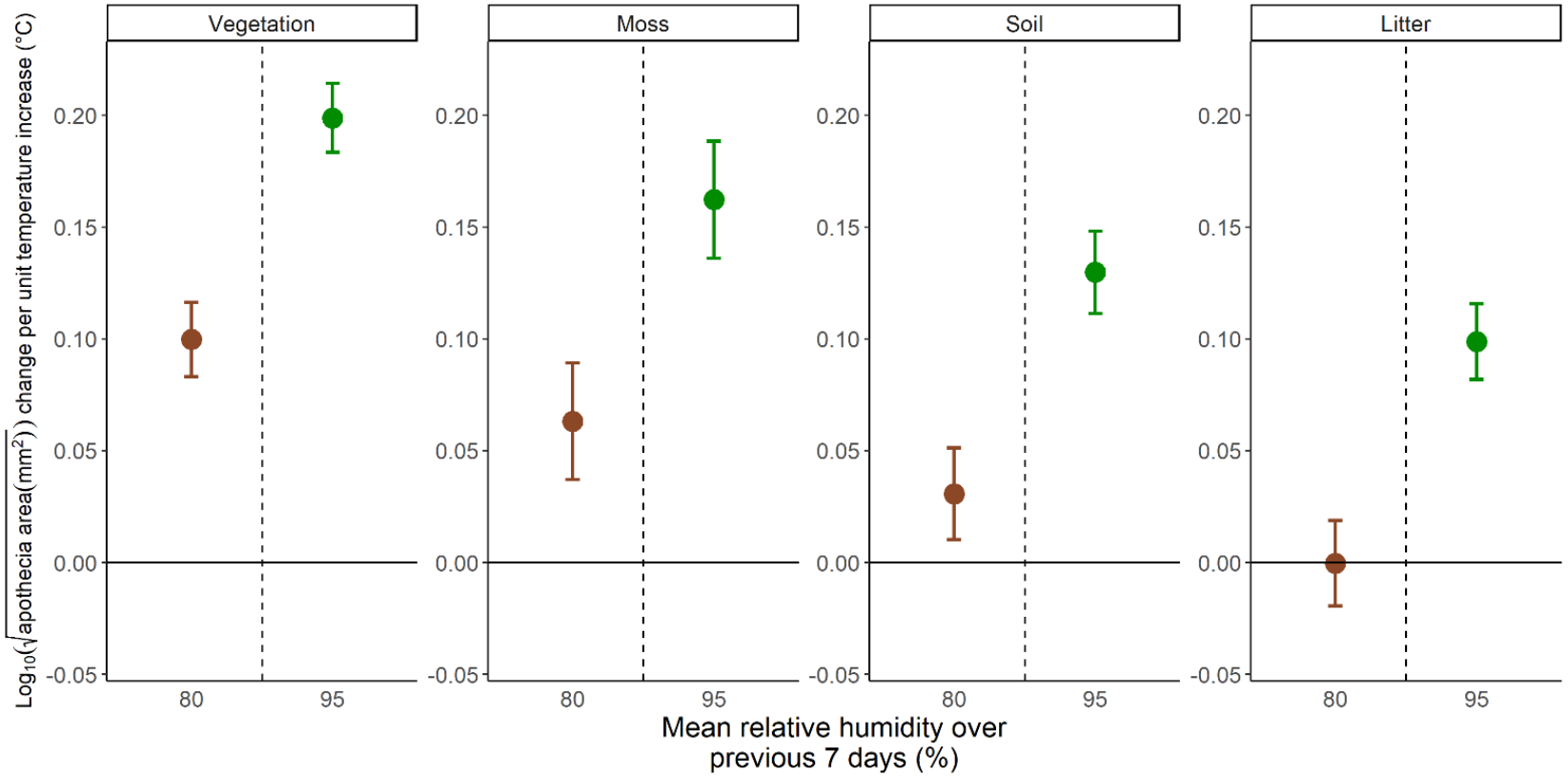
Vegetation
Moss
Soil
Litter
0.20
0.15
0.10
0.05
0.00
-0.05
80
95
Log10(√apothecia area(mm2)) change per unit temperature increase (°C)
Mean relative humidity over previous 7 days (%)

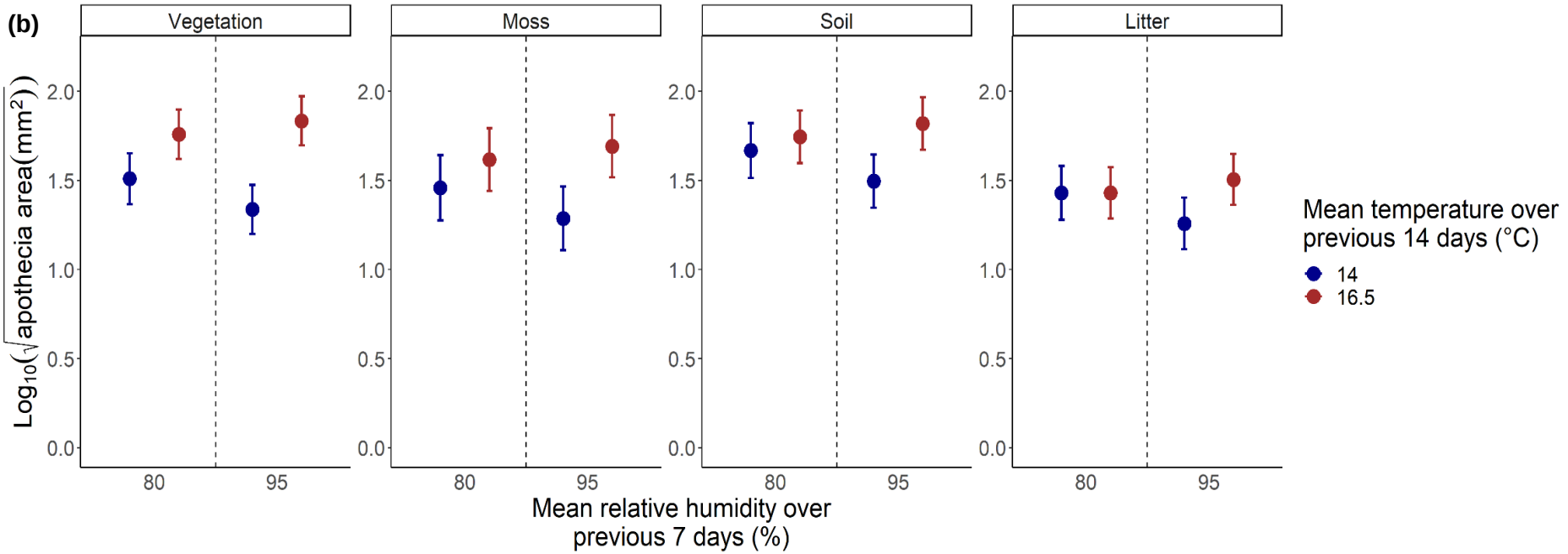

Figure 2.8 The significant interactive effects on $\log_{10}(\sqrt{}$*H. fraxineus* apothecia area (mm^2)) in apothecia model 1 (Section 2.3.2.1) between mean temperature (°C) over the 14 days prior to sample collection and the mean relative humidity (%) over the 7 days prior to sample collection (ddf =369.5, $p < 0.001$) as well as the mean temperature (°C) over the 14 days prior to sample collection and the ground cover (vegetation, moss, soil or litter) at the sampling location (ddf = 371.32, $p < 0.001$). **(a)** The change in the estimated marginal mean (from apothecia model 1) of $\log_{10}(\sqrt{}$*H. fraxineus* apothecia area (mm^2)) and standard error per unit increase of the mean temperature (°C) over the 14 days prior to sample collection in areas with predominantly vegetation, moss, soil or litter ground cover at a lower (80%) and higher (95%) mean relative humidity over the previous 7 days. **(b)** The estimated marginal mean of $\log_{10}(\sqrt{}$*H. fraxineus* apothecia area (mm^2)) and standard error estimated from apothecia model 1 in areas with predominantly vegetation, soil, moss or litter ground cover at a cooler (14°C) and warmer (16.5°C) mean temperature over the previous 14 days at a lower (80%) and a higher (95%) mean relative humidity over the previous 7 days.

(a)

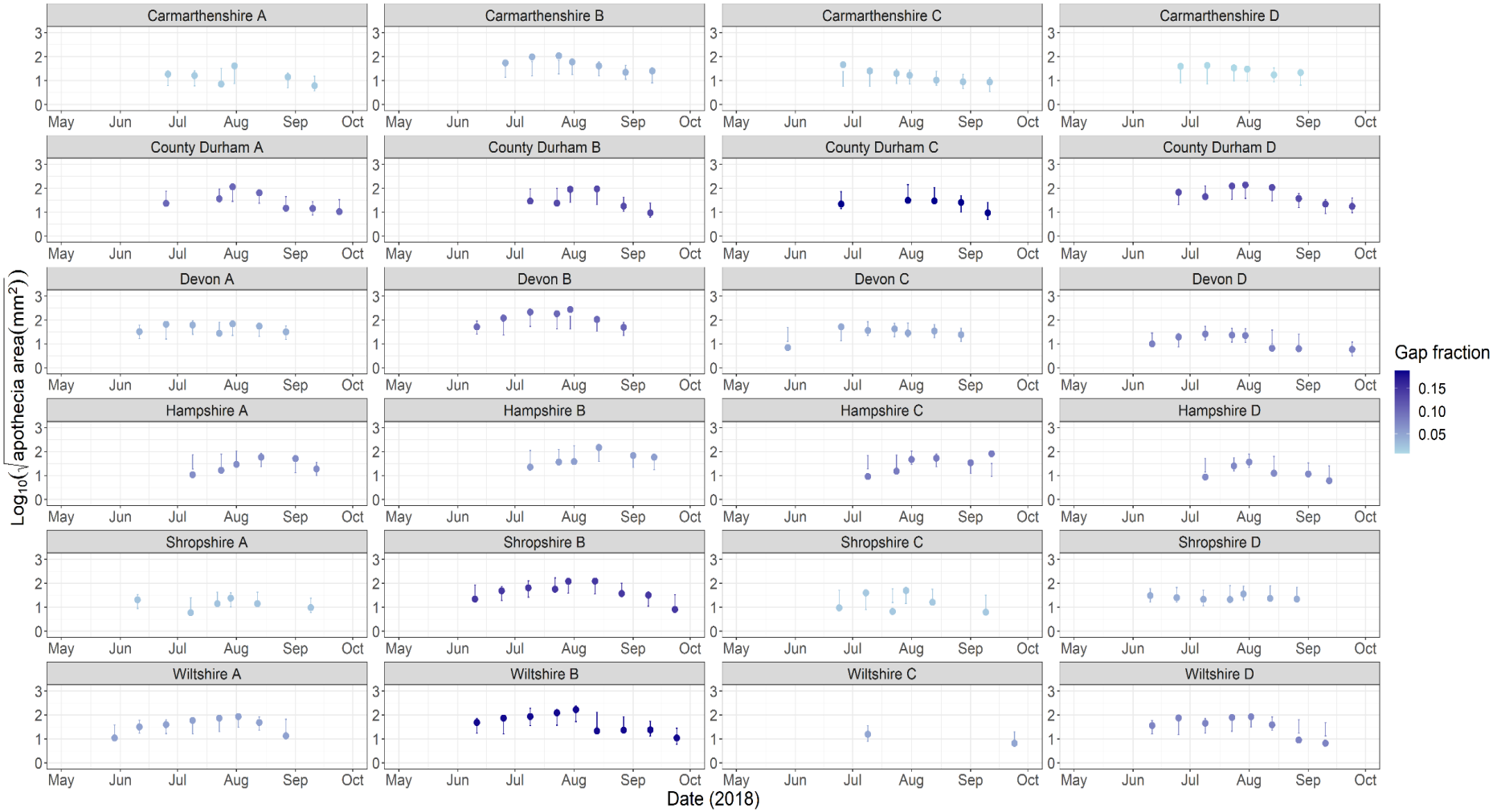
Carmarthenshire A
Carmarthenshire B
Carmarthenshire C
Carmarthenshire D
County Durham A
County Durham B
County Durham C
County Durham D
Devon A
Devon B
Devon C
Devon D
Hampshire A
Hampshire B
Hampshire C
Hampshire D
Shropshire A
Shropshire B
Shropshire C
Shropshire D
Wiltshire A
Wiltshire B
Wiltshire C
Wiltshire D
May
Jun
Jul
Aug
Sep
Oct
0
1
2
3
Log10(√apothecia area(mm2))
Date (2018)
Gap fraction
0.15
0.10
0.05

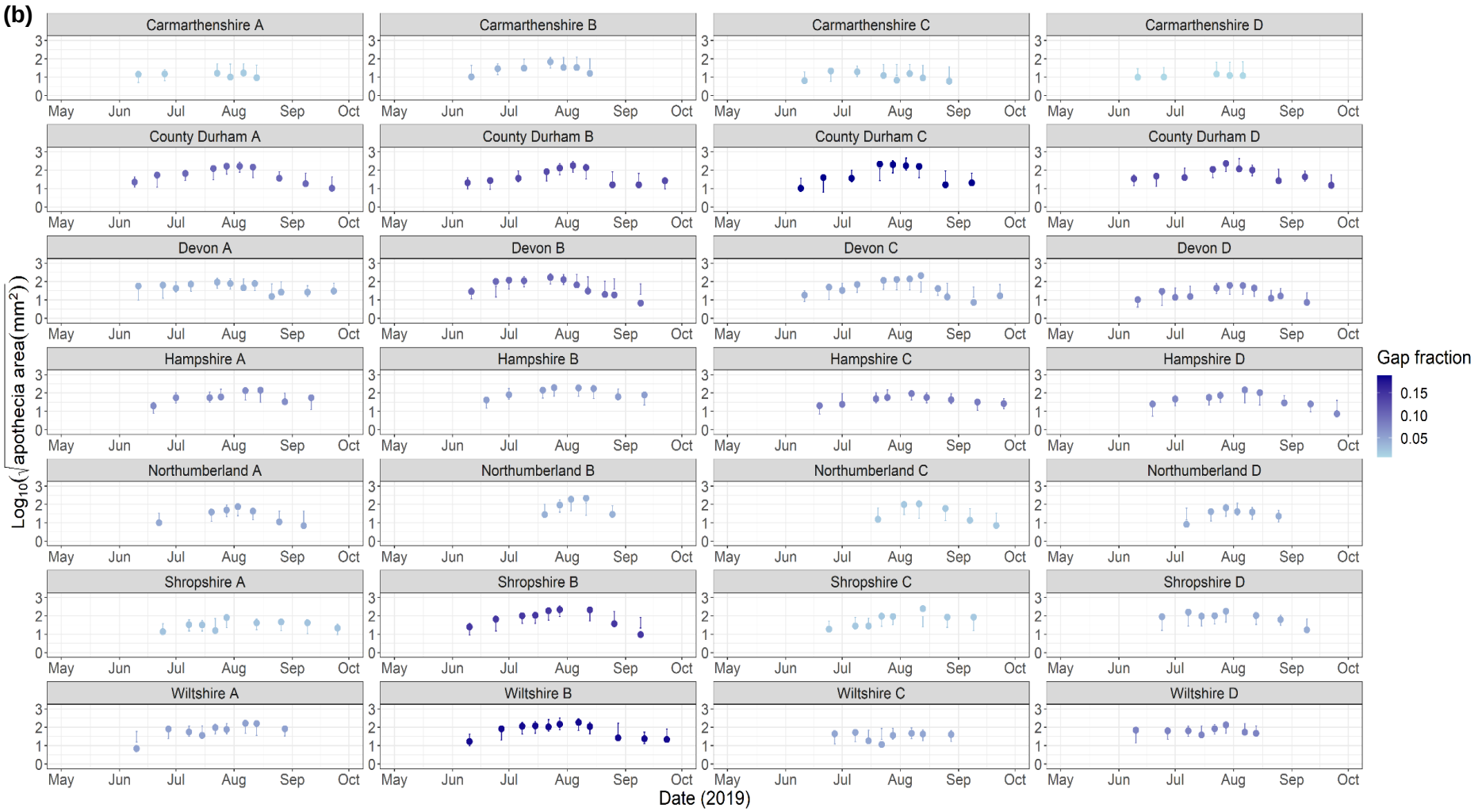

Figure 2.9 (a) $Log_{10}(\sqrt{}$*H. fraxineus* apothecia area (mm^2)) from locations (A, B, C, D) within six sites (Carmarthenshire, County Durham, Devon, Hampshire, Shropshire, Wiltshire) from May – September 2018 (Section 2.2) (b) and from locations (A, B, C, D) across seven sites (Carmarthenshire, County Durham, Devon, Hampshire, Northumberland, Shropshire, Wiltshire) from May – September 2019 (Section 2.2) with the second most supported linear mixed effects model (apothecia model 2; ΔAICc = 0.04; marginal R2 = 0.30; conditional R^2 = 0.57) fitted to the datapoints with corresponding 95% confidence intervals. The

model accounted for unexplained variation between sites, sampling locations and sampling years by specifying these variables as random effects and that sampling locations were nested within sites. Fixed effects (explanatory variables) included in the model were mean temperature (°C) over the 14 days prior to sample collection, mean relative humidity (%) over the 7 days prior to sample collection and gap fraction at the sampling location. An interaction was present between mean temperature (°C) over the 14 days prior to sample collection and gap fraction, and between mean temperature (°C) over the 14 days prior to sample collection and mean relative humidity (%) over the 7 days prior to sample collection (Section 2.2.6; Section 2.3.2.2).

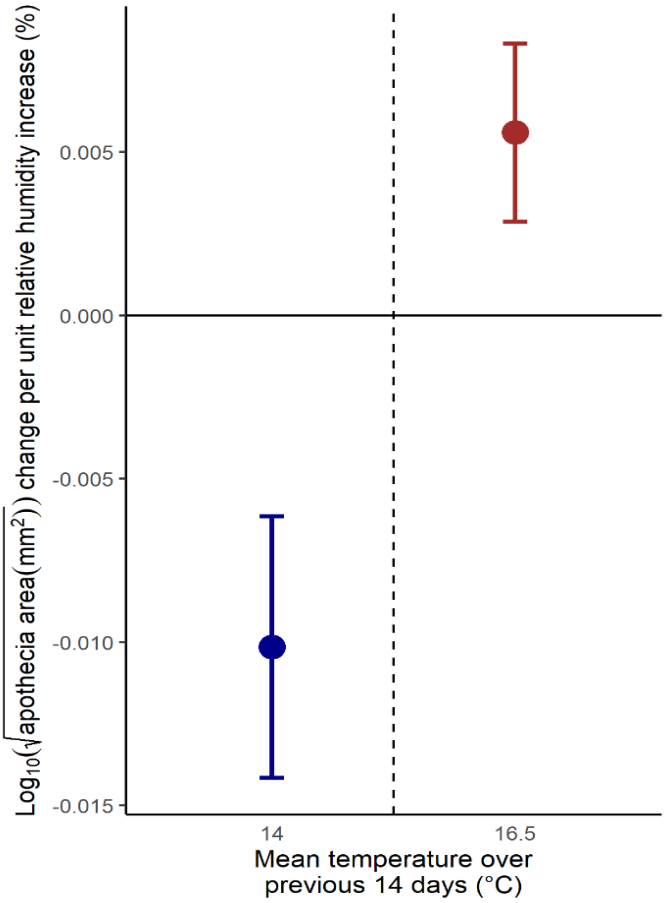

Figure 2.10 The significant interactive effect on $\log_{10}(\sqrt{}$*H. fraxineus* apothecia area (mm^2)) in apothecia model 2 (2.3.2.2) between mean temperature (°C) over the 14 days prior to sample collection and the mean relative humidity over the 7 days prior to sample collection (ddf = 371.49, $p < 0.001$). The change in the estimated marginal mean (from apothecia model 2) of $\log_{10}(\sqrt{}$*H. fraxineus* apothecia area (mm^2)) and standard error per unit increase of the mean relative humidity (%) over the 7 days prior to sample collection at a cooler (14°C) and warmer (16.5°C) mean temperature over the previous 14 days.

(a)

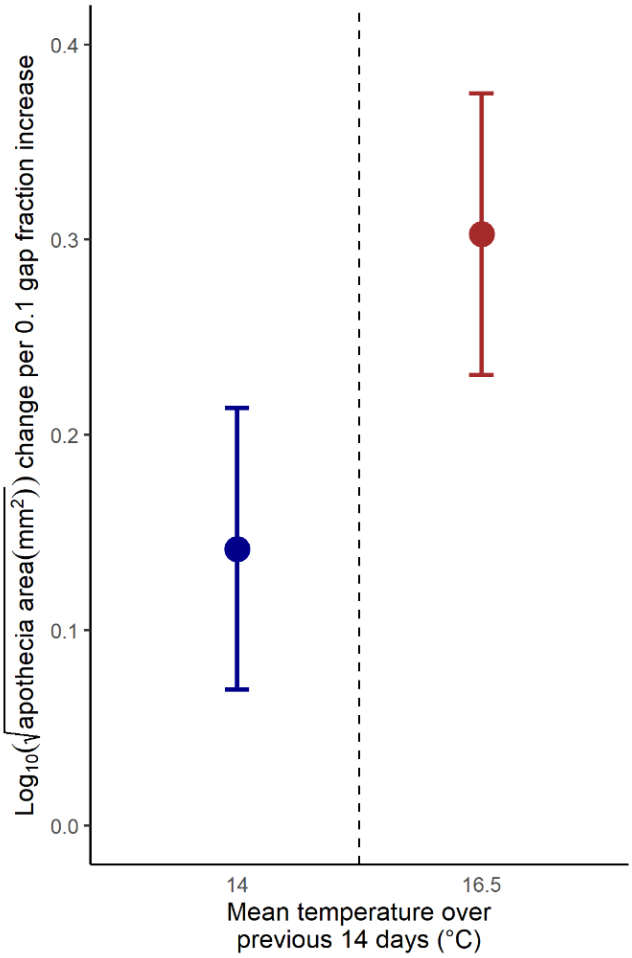
0.4
0.3
0.2
0.1
0.0
$Log_{10}(\sqrt{apothecia\ area(mm^2)})$ change per 0.1 gap fraction increase
14
16.5
Mean temperature over previous 14 days (°C)

(b)

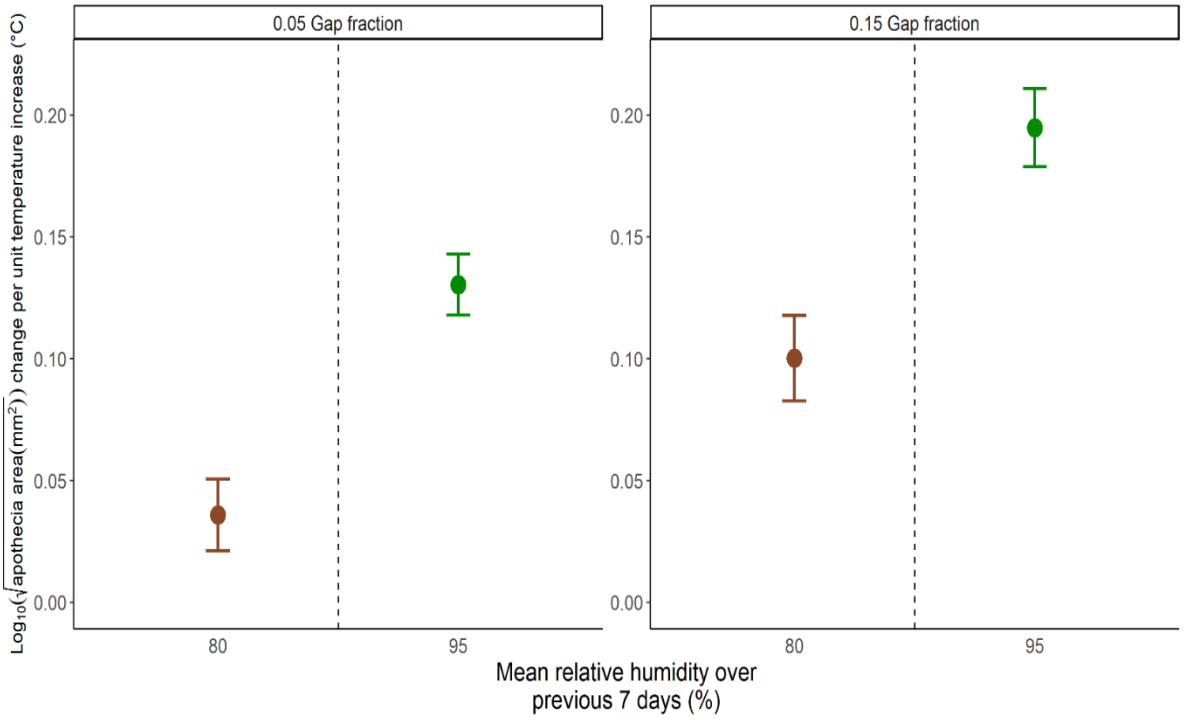
0.05 Gap fraction
0.15 Gap fraction
0.20
0.15
0.10
0.05
0.00
$Log_{10}(\sqrt{apothecia\ area(mm^2)})$ change per unit temperature increase (°C)
80
95
Mean relative humidity over previous 7 days (%)

(c)

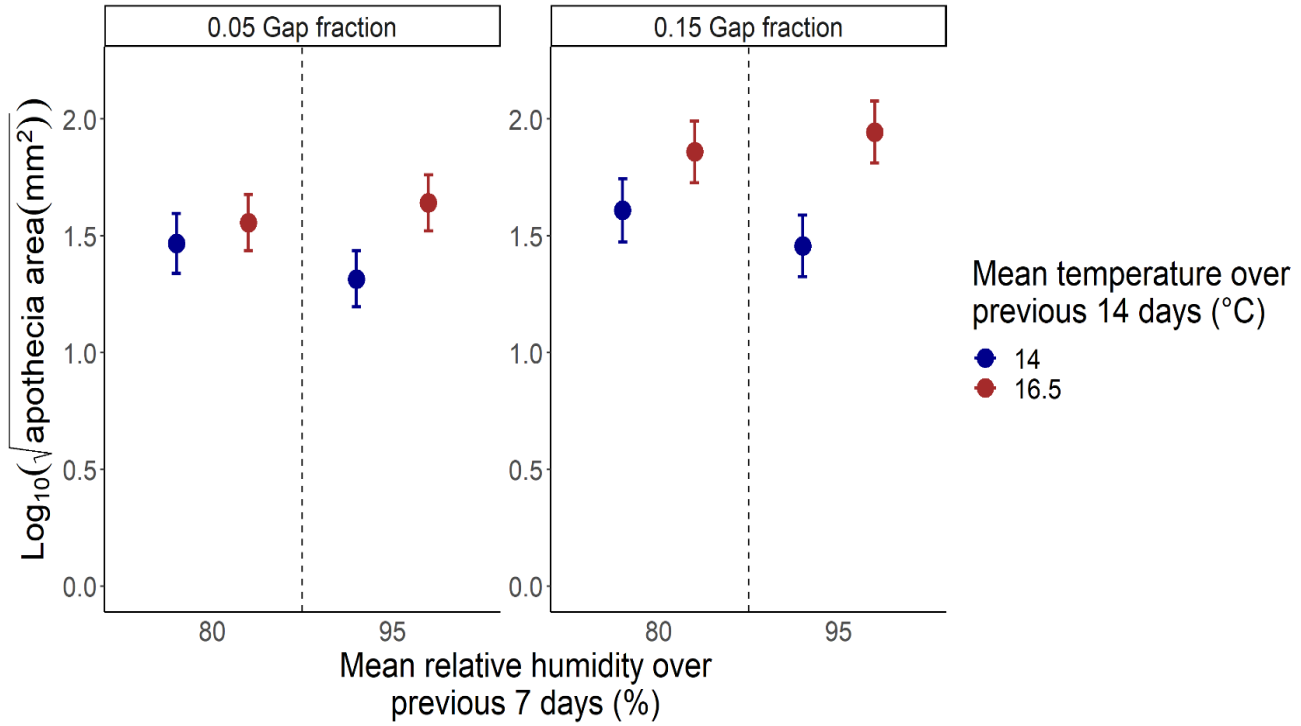

Figure 2.11 The significant interactive effect on $\log_{10}(\sqrt{}$*H. fraxineus* apothecia area (mm^2)) in apothecia model 2 (2.3.2.2) between mean temperature (°C) over the 14 days prior to sample collection and gap fraction at the sampling location (ddf = 377.1, $p < 0.001$). **(a)** The change in the estimated marginal mean (from apothecia model 2) of $\log_{10}(\sqrt{}$*H. fraxineus* apothecia area (mm^2)) and standard error per 0.1 increase of the gap fraction at a cooler (14°C) and warmer (16.5°C) mean temperature over the previous 14 days. **(b)** The change in the estimated marginal mean (from apothecia model 2) of $\log_{10}(\sqrt{}$*H. fraxineus* apothecia area (mm^2)) and standard error per unit increase of the mean temperature over the previous 14 days at a lower (80%) and higher (95%) mean relative humidity over the previous 7 days, at a lower (0.05) and higher (0.15) gap fraction. **(c)** The estimated marginal mean (from apothecia model 2) of $\log_{10}(\sqrt{}$*H. fraxineus* apothecia area (mm^2)) and standard error at a cooler (14°C) and warmer (16.5°C) mean temperature over the previous 14 days, at a lower (80%) and higher (95%) mean relative humidity over the previous 7 days, at a lower (0.05) and higher (0.15) gap fraction.

(a)

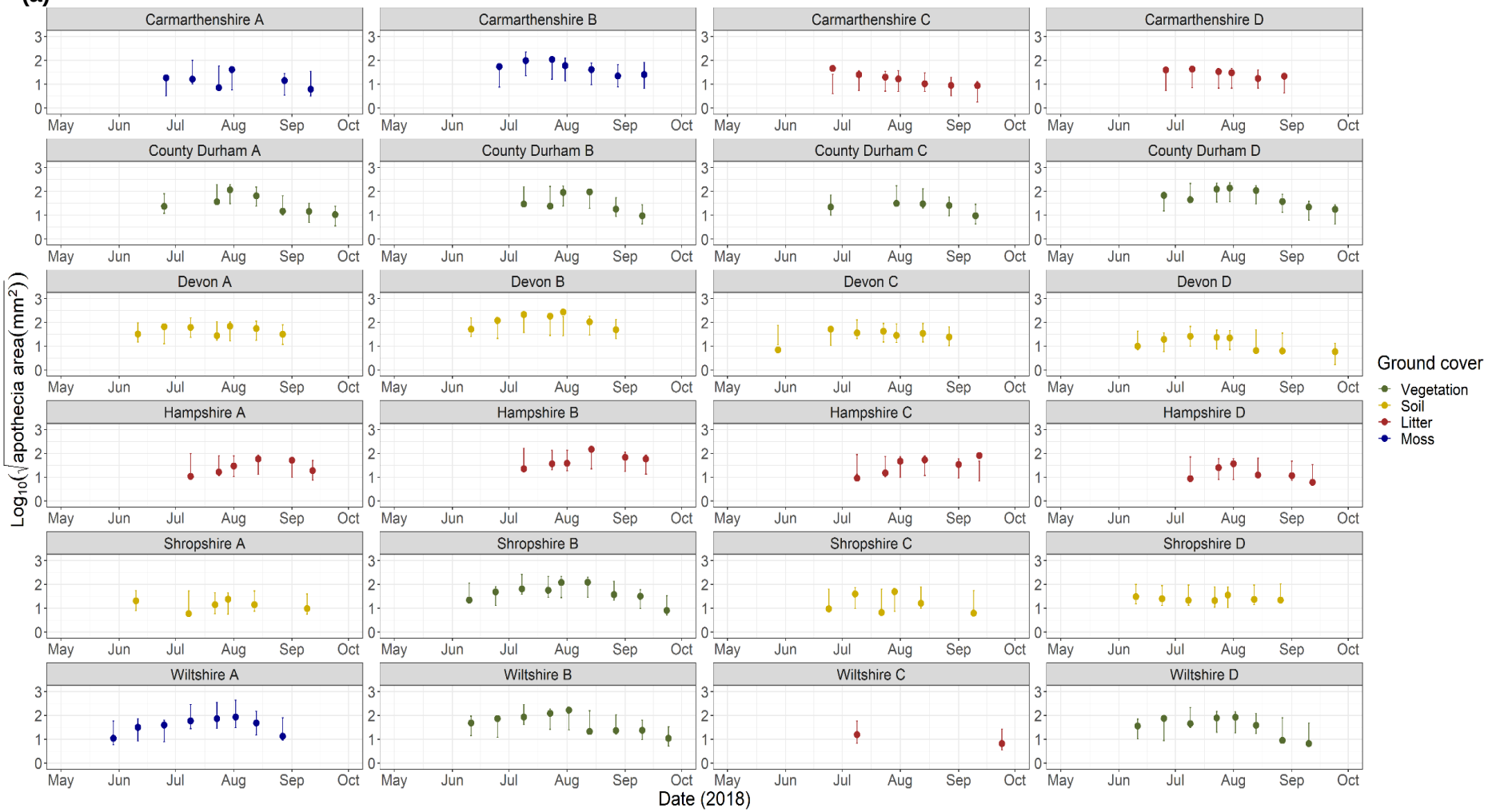
Carmarthenshire A
Carmarthenshire B
Carmarthenshire C
Carmarthenshire D
County Durham A
County Durham B
County Durham C
County Durham D
Devon A
Devon B
Devon C
Devon D
Hampshire A
Hampshire B
Hampshire C
Hampshire D
Shropshire A
Shropshire B
Shropshire C
Shropshire D
Wiltshire A
Wiltshire B
Wiltshire C
Wiltshire D
May
Jun
Jul
Aug
Sep
Oct
0
1
2
3
Log10(√apothecia area(mm2))
Date (2018)
Ground cover
Vegetation
Soil
Litter
Moss

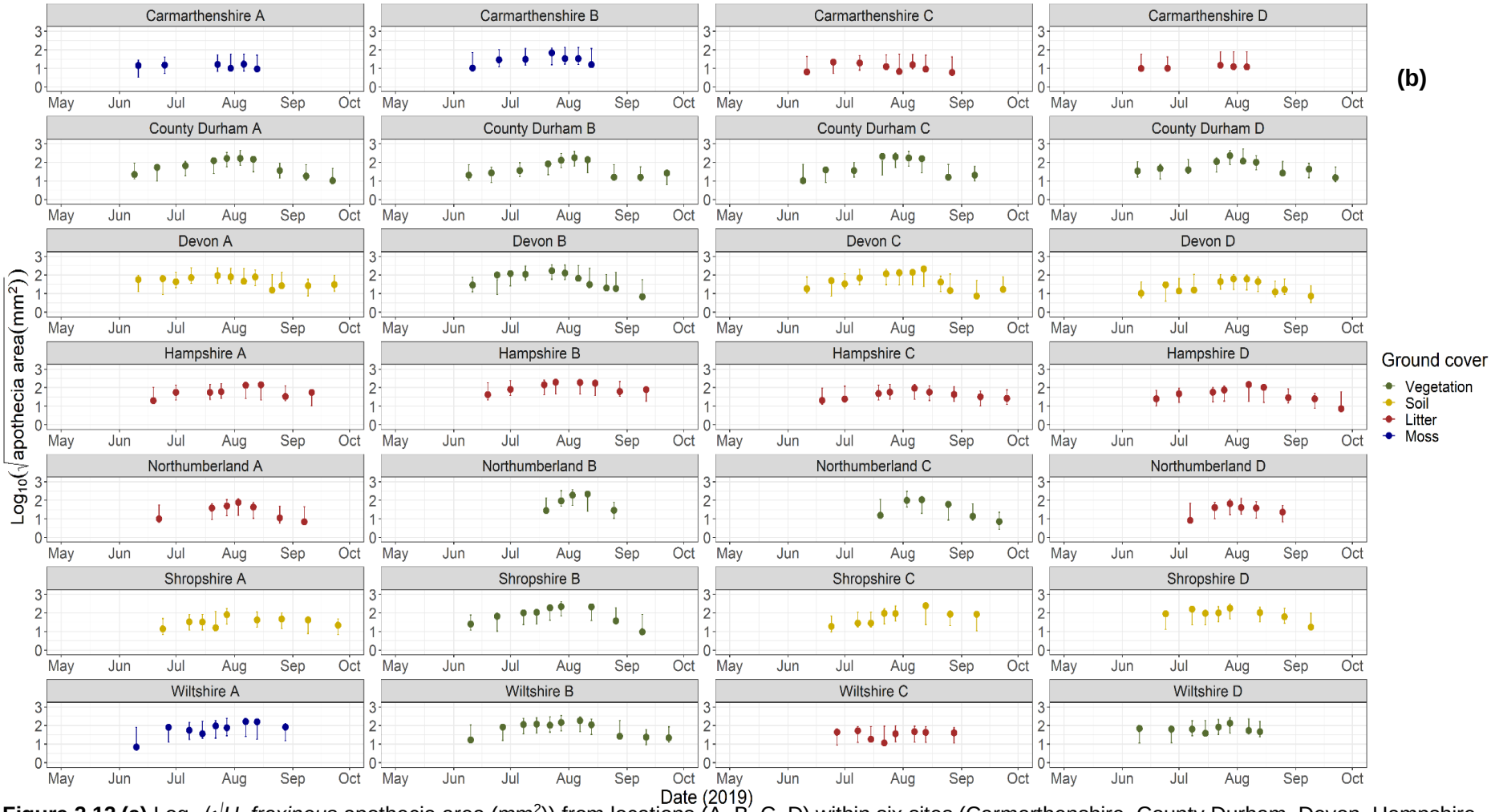

Figure 2.12 (a) $Log_{10}(\sqrt{}$*H. fraxineus* apothecia area (mm^2)) from locations (A, B, C, D) within six sites (Carmarthenshire, County Durham, Devon, Hampshire, Shropshire, Wiltshire) from May – September 2018 (Section 2.2) **(b)** and from locations (A, B, C, D) across seven sites (Carmarthenshire, County Durham, Devon, Hampshire, Northumberland, Shropshire, Wiltshire) from May – September 2019 (Section 2.2) with the third most supported linear mixed effects model (apothecia model 3; ΔAICc = 3.27; marginal R^2 = 0.30; conditional R^2 = 0.65) fitted to the datapoints with corresponding 95% confidence intervals. The model accounted for unexplained variation between sites, sampling locations and sampling years by specifying these variables as random effects and that sampling locations were nested within sites. Fixed effects (explanatory variables) included in the model were mean temperature (°C) over the 14 days prior to

sample collection, mean relative humidity (%) over the 42 days prior to sample collection and dominant ground cover (vegetation, soil, litter or moss) at the sampling location. A three-way interaction was present between mean temperature (°C) over the 14 days prior to sample collection, mean relative humidity (%) over the 42 days prior to sample collection and the dominant ground cover (Section 2.2.6; Section 2.3.2.3).

(a)

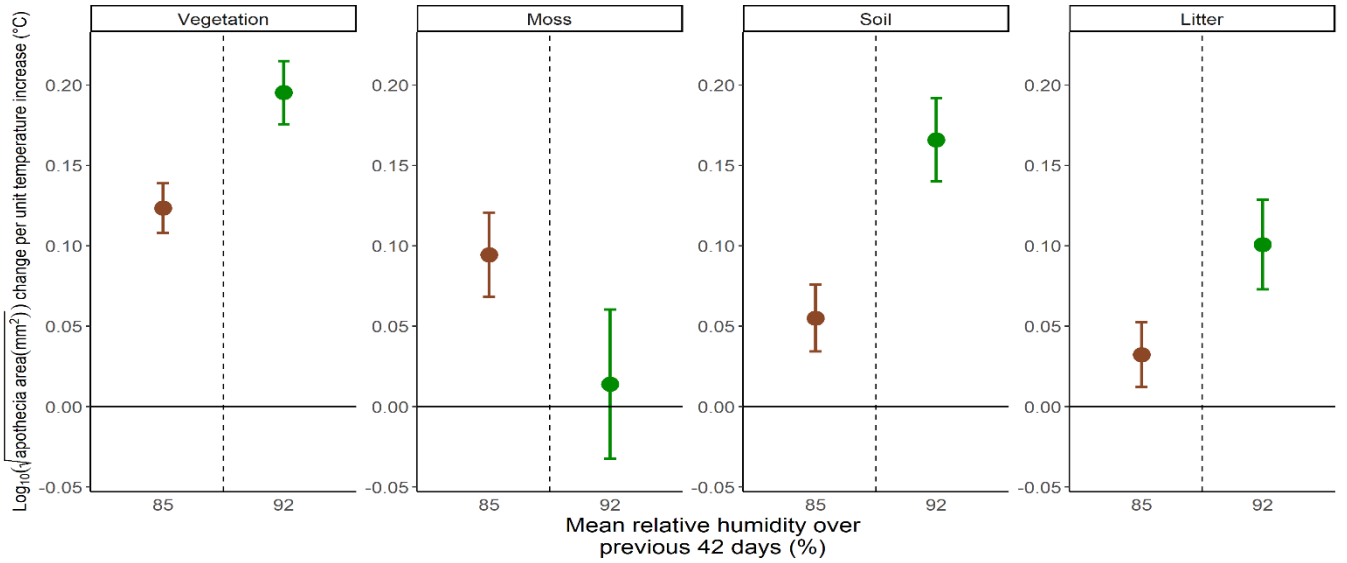
Vegetation
Moss
Soil
Litter
0.20
0.15
0.10
0.05
0.00
-0.05
85
92
Log10(√(apothecia area(mm²))) change per unit temperature increase (°C)
Mean relative humidity over previous 42 days (%)

(b)

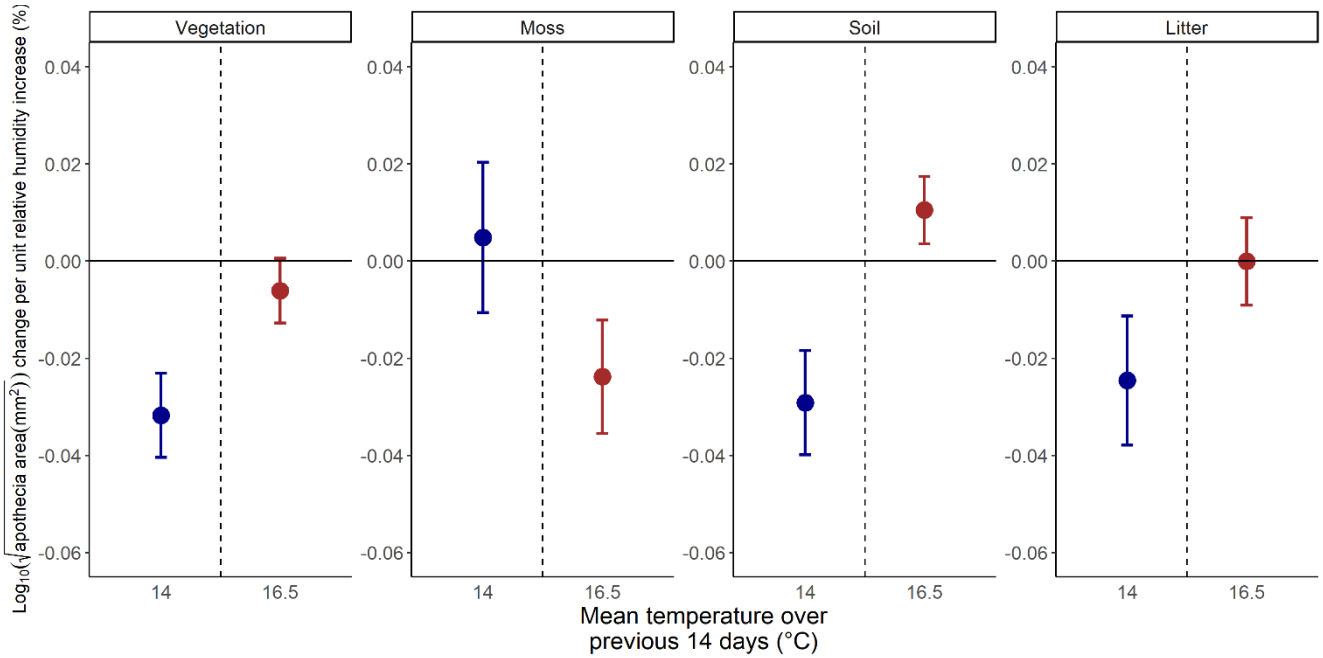
Vegetation
Moss
Soil
Litter
0.04
0.02
0.00
-0.02
-0.04
-0.06
14
16.5
Log10(√(apothecia area(mm²))) change per unit relative humidity increase (%)
Mean temperature over previous 14 days (°C)

(c)

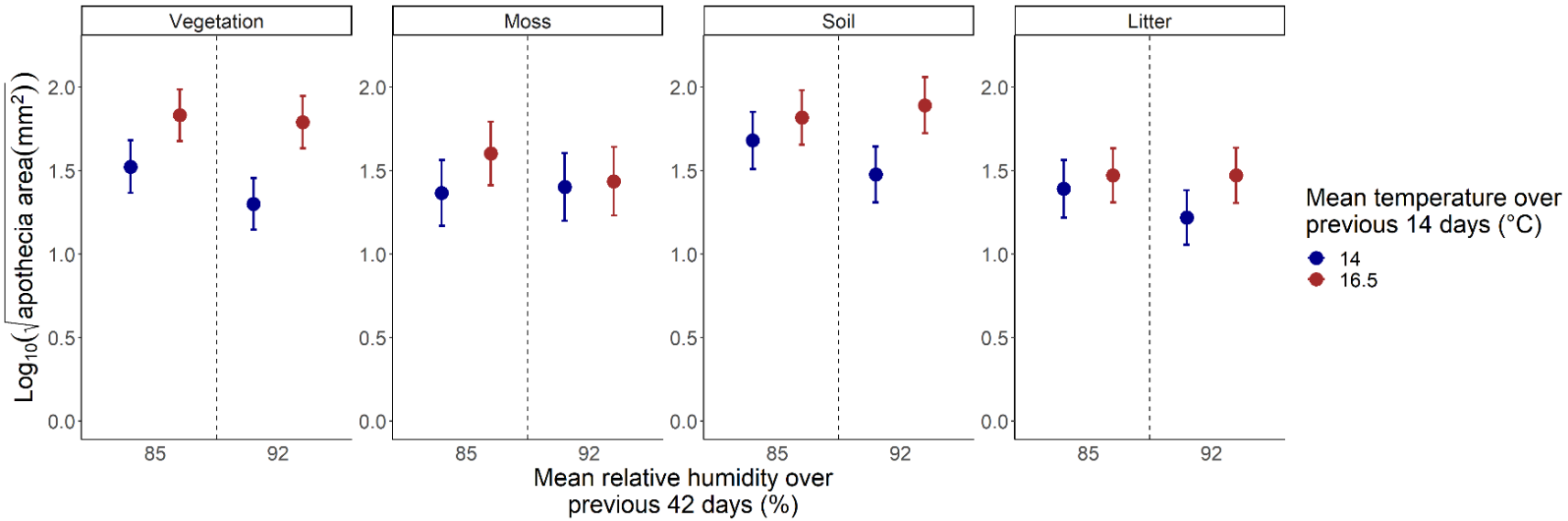

Figure 2.13 The significant interactive effect on $\log_{10}(\sqrt{}$*H. fraxineus* apothecia area (mm^2)) in apothecia model 3 (2.3.2.3) between mean temperature (°C) over the 14 days prior to sample collection, mean relative humidity (%) over the 42 days prior to sample collection and the ground cover (vegetation, moss, soil or litter) at the sampling location (ddf = 362.61, $p < 0.01$). **(a)** The change in the estimated marginal mean (from apothecia model 3) of $\log_{10}(\sqrt{}$*H. fraxineus* apothecia area (mm^2)) and standard error per unit increase of the mean temperature (°C) over the 14 days prior to sample collection at a lower (85%) and higher (92%) mean relative humidity over the previous 42 days in areas with predominantly vegetation, moss, soil or litter ground cover. **(b)** The change in the estimated marginal mean (from apothecia model 3) of $\log_{10}(\sqrt{}$*H. fraxineus* apothecia area (mm^2)) and standard error per unit increase of the mean relative humidity (%) over the 42 days prior to sample collection at a cooler (14°C) and warmer (16.5°C) mean temperature over the previous 14 days in areas with predominantly vegetation, moss, soil or litter ground cover. **(c)** The estimated marginal mean (from apothecia model 3) of $\log_{10}(\sqrt{}$*H. fraxineus* apothecia area (mm^2)) and standard error estimated from apothecia model 1 in areas with predominantly vegetation, soil, moss or litter ground cover at a cooler (14°C) and warmer (16.5°C) mean temperature over the previous 14 days, at a lower (85%) and higher (92%) mean relative humidity over the previous 42 days.

Table 2.3 Plausible linear mixed effects models for *H. fraxineus* apothecia development ($log_{10}(\sqrt{}$apothecia area (mm^2)) that had ΔAICc (Δ second-order Akaike Information Criterion) < 7 (Section 2.2.6; Section 2.3.2). Fixed effects are listed at their highest interaction (: denotes an interaction) and p values were calculated using Kenward-Roger approximation for denominator degrees of freedom (ddf). The variance of random effects denotes the variability in site, quadrat and sampling year in the model. AICc and ΔAICc values were calculated not including site as a random effect to allow for comparison of fixed effects of models.

Model	Fixed Effects	p (ddf)	Random Effects	Variance (Std. Dev)	AICc (excluding site)	ΔAICc (excluding site)	Marginal R^2/ Conditional R^2
Apothecia model 1	14 day mean temperature (˚C): 7 day mean relative humidity (%)	< 0.001 (369.50)	Site	0.0104 (0.1017)	192.30	0	0.29/ 0.61
	14 day mean temperature (˚C): Ground cover	< 0.001 (371.32)	Quadrat	0.0284 (0.1686)			
			Year	0.02469 (0.1571)			
Apothecia model 2	14 day mean temperature (˚C): 7 day mean relative humidity (%)	< 0.001 (371.49)	Quadrat	0.02498 (0.1581)	192.34	0.04	0.30/ 0.57
	14 day mean temperature (˚C): Gap fraction	< 0.001 (377.10)	Year	0.02531 (0.1591)			
Apothecia model 3	14 day mean temperature (˚C): Ground cover: 42 day mean relative humidity (%)	<0.01 (360.36)	Site	0.01400 (0.1183)	195.57	3.27	0.30/ 0.65
			Quadrat	0.02863 (0.1692)			
			Year	0.03300 (0.01817)			

2.4 Discussion

This study has revealed the significant effects of temperature, relative humidity, ground cover and gap fraction (a measure of canopy openness) on *H. fraxineus* apothecia development. Unexplained variation remained within models and is exemplified by the large variation in the apothecia development at the same ground cover conditions within sites on the same sampling year (Figure 2.2). Nonetheless, three plausible models were identified (with ΔAICc value less than 7). Where ground cover was moss results were different to those for other ground types, and were difficult to explain. This may be due to a smaller sample size in areas of moss cover compared to other ground cover types.

The absence of apothecia throughout winter months indicates that low temperatures are not conducive for apothecia development. Accepting that apothecia development and ascospore numbers are linked, higher annual temperatures (measured as degree days) were positively correlated with the maximum quantity of ascospores at a site in Norway (Hietala et al., 2018). Furthermore, variations in the duration of spore release between sites and seasons has been suggested to be associated with temperature differences (Chandelier et al., 2014). In accordance, my findings demonstrate that temperature significantly affects the development of apothecia. Importantly, growth rates of *H. fraxineus* appear to reach a maximum around 22°C, whilst fungal survivability is limited above 36°C (Hauptman et al., 2013). In my study, the maximum mean daily temperature recorded at 40 cm above ground level was 22.79˚C. This included unseasonably warm periods during both study years and indicates that even in UK 'heatwave' conditions, temperatures on the forest floor should not constrain apothecia development of *H. fraxineus*.

The period of maximum mean daily temperature on sites (July-August) corresponded with the timing of maximum apothecia development, and longer periods of maximum mean daily temperature in 2018 corresponded with slightly later maximum apothecia development. This is probably because a longer period of warmer temperatures provides *H. fraxineus* with more time for continued development. This pattern was not present in 2019 for sites that had a slightly longer period of maximum mean daily temperature in comparison to 2018, and absolute temperature differences between sites and sampling years did not correspond with differences in apothecia development. This was probably because other environmental factors also influence the apothecia development. For example, the sampling period was warmer in 2018 than in 2019, but this did not correspond with greater apothecia development in 2018, which could be because the sampling period in 2019 was more humid.

My results show that the effect of increasing temperature on apothecia development was dependent on relative humidity, ground cover and the gap fraction.

Apothecia model 3 (Section 2.3.2.3) found a 3-way interactive effect between the effect of temperature, relative humidity and ground cover on apothecia development. However, this was likely due to the less positive impact of increasing temperature on apothecia development for rachises on moss ground cover at high humidity (92%). The positive effect of temperature on apothecia development increased with relative humidity and gap fraction, and increasing temperature had a greater positive effect on apothecia development for rachises under vegetation than on soil or mixed with litter. Importantly, the less positive effect of temperature for rachises on soil compared to under vegetation cover does not mean that less apothecia development occurred. In fact, apothecia development was greater for rachises on areas of bare soil compared to under vegetation at a cooler temperature (14°C), but was similar at a warmer temperature (16.5°C). The greater apothecia development at a cooler temperature in areas of soil cover could be explained by less canopy openness in comparison to areas of ground vegetation and litter cover. More canopy openness could result in more heat loss at lower site temperatures, therefore rachises could be exposed to lower minimum temperatures that will be more likely to be detrimental to apothecia development. Contrastingly, the less positive effect of increasing temperature on apothecia development for rachises mixed with litter was associated with less apothecia development at both a cooler (14°C) and a warmer (16.5°C) temperature, and can also probably be explained by microclimatic differences at the litter layer. Relative humidity will be higher underneath vegetation because of reduced air flow at the ground level, and protection of the ground from evaporation. Similarly, areas of bare soil, that are typically associated with low canopy openness, will be sheltered from solar radiation, which will reduce evaporation from the ground. However, due to more exposure of the rachises, areas of litter cover will probably be subject to greater evaporation and more air flow that acts to lower the humidity surrounding the rachises. As higher relative humidity increases the positive effect of temperature on rachises, the lower relative humidity surrounding rachises in areas of litter cover can be expected to impact apothecia development negatively. My results suggest that higher mean daily temperatures, up to 22°C, and particularly with high moisture, increase the apothecia development of *H. fraxineus* and thereby probably the infection pressure on host trees. This will be limited in areas of woodland with predominantly litter ground cover in comparison to areas of vegetation ground cover, or well shaded areas of bare soil. Comparatively lower relative humidity in areas of litter cover will make apothecia development less robust to drops in humidity.

In concurrence with my findings, the effect of ground cover on apothecia production has previously been described and associated with moisture availability. No apothecia were found at an exposed site observed over a single season, yet numerous apothecia formed when rachises were incubated under humid conditions in the laboratory

(Gross and Holdenrieder, 2013). Furthermore, a reduced number of apothecia was found on open ground compared to under vegetation within a UK woodland (Mansfield et al., 2018). My results support the hypothesis that microclimatic effects of ground cover influence apothecia development.

Increasing relative light intensity in the understorey has been associated with greater *H. fraxineus* infection on juvenile ash trees, although the reasons for this were not known (Erfmeier et al., 2019). My research demonstrates greater apothecia development and a greater positive effect of temperature as gap fraction increased. Additionally, as temperature increased, the effect of increasing gap fraction on apothecia development became more positive. This is probably because canopy openness is associated with vegetation cover on the ground, which as discussed previously retains higher humidity, which, because humidity is then not a limiting factor, means apothecia development is more responsive to increases in temperature. Importantly, these results indicate a potential positive feedback loop of *H. fraxineus* infection. As the crowns of affected ash trees decline, this causes greater gaps in the canopy, which in turn can lead to greater *H. fraxineus* apothecia development and therefore possibly greater infection pressure.

Moisture has consistently been identified as an important factor in explaining the development of ash dieback in woodlands (Marçais et al., 2016; Havrdová et al., 2017; Grosdidier et al., 2020; Klesse, Abegg et al., 2021), although this could be due to multiple factors other than *H. fraxineus* apothecia development. However, the number of apothecia on a site have been associated with its flood risk index (Grosdidier, Ioos, Marçais et al., 2018), and higher *H. fraxineus* spore numbers have been detected at sites described as wet (Čermáková et al., 2017). Additionally, to produce apothecia in the laboratory, rachises must be incubated under humid conditions. My research further supports a small, but significant effect of relative humidity on apothecia development, and this relationship depends on both the temperature and the ground cover. As temperature increases, the effect of increasing relative humidity transitions from slightly negative at cooler temperatures (such as 14°C) to slightly positive at warmer temperatures (such as 16.5°C). Surprisingly, these results indicate that at cooler temperatures, higher humidity decreases fruit body development. This could be because at suboptimal temperatures for apothecia, their degradation occurs quicker under higher moisture.

Both temperature and humidity vary within woodlands, particularly in the maximum and minimum recorded values, and is likely the reason unexplained variation remained in models. Fluctuations in environmental variables, as well as minimum or maximum values can be used as predictors of biological processes rather than mean values (van de Pol et al., 2016). However, it was not appropriate to use fluctuations or minimum and maximum values of temperature and humidity as site level variables in the present study because of

the within site variation of these variables. Additionally, temperature and precipitation preceding the summer sampling period that can affect the microclimate during the spring or summer by influencing factors such as soil moisture or degree of vegetation cover. Future studies should focus on examining the microclimatic effects on *H. fraxineus* apothecia development in more detail.

The number of infected rachises from the previous season has been associated with the number of apothecia present on a rachis (Grosdidier, Ioos, Marçais et al., 2018). This indicates that the availability of mating partners can limit the production of apothecia in a forest environment. It is possible that overwinter conditions also could influence the mating success of *H. fraxineus*. For example, growth of *H. fraxineus* is limited in culture at lower temperatures and the fungus does not grow at 0.5˚C (Bengtsson et al., 2014). Lower winter temperatures could thereby limit the mating success of *H. fraxineus*. However, the mating process of *H. fraxineus* and its environmental regulators are poorly understood.

2.5 Conclusions

H. fraxineus is dependent on its sexual cycle for dispersal and host infection (Gross, Holdenrieder et al., 2014). However, relatively little is known about the conditions which affect the formation of the apothecia prior to the infection process. This study has focused on this lack of information, using field data collected at regular intervals to produce a model of apothecia development related to environmental factors.

My results suggest that apothecia development can be regulated by changes in woodland composition that impact on temperature or humidity. Indeed, disease progression has previously been linked to indicators of moisture, temperature and woodland composition (Havrdová et al., 2017; Erfmeier et al., 2019; Klesse, Abegg et al., 2021). My study demonstrates that these factors interact to affect apothecia development, and therefore the potential inoculum production of *H. fraxineus.* The effects of inoculum production on disease progression are poorly understood and are investigated in Chapter 4. Unexplained variation should be identified through further studies and temperature and moisture thresholds identified, in order to produce predictive models of apothecia development for site managers.

Chapter 3: Environmental effects on *Hymenoscyphus fraxineus* ascospore release

3.1 Introduction

Hymenoscyphus fraxineus produces both conidia and ascospores following mating between sexual compatibility types (Kowalski, 2006; Kowalski and Holdenrieder 2009; Gross, Zaffarano et al., 2012). The high genotypic diversity of *H. fraxineus*, 1:1 ratio of sexually compatible types and many vegetative compatibility groups demonstrate that sexual reproduction is dominant in the population (Gross, Zaffarano et al., 2012; Brasier and Webber, 2013). The apothecia which produce and release ascospores are common during the summer months in the litter layer under infected ash trees (Timmermann et al., 2011), and conidia are believed to play an important role in the process of sexual reproduction by acting as spermatia (Gross, Zaffarano et al., 2012). For successful continuation of the life-cycle, ascospores released from apothecia must spread to the foliage of host trees. The logarithmic decrease of ascospore density with increasing height highlights the logistical challenges of this process (Chandelier et al., 2014).

The observation of spore jets from apothecia and peaks in ascospore density between roughly 04h30 and 08h30 (Hietala et al., 2013) indicate that spores are actively ejected in a regulated process. A recent study found that increased net radiation within two hours of the daily spore peak delays the timing of this peak. However, further studies are necessary because only 60 data points from a single site were used for analysis (Burns et al., 2022). Research on other ascomycetes demonstrates that temperature and moisture controls for ascospore release play a critical role in the process, although the optimal conditions vary between species (Clarkson et al., 2003; Mondal et al., 2003; Rossi et al., 2010; Manstretta and Rossi, 2015).

Knowledge of conditions which affect spore release in plant pathogens can be used to guide disease management. For example, knowledge of the conditions affecting ascospore release of the causal agents of powdery mildew of grapevine, *Erysiphe necator,* and apple scab disease, *Venturia inaequalis*, have been used to generate models that guide both symptom assessment and coordination of fungicide treatment (Rossi et al., 2007; Caffi et al., 2011). Currently, no commercially available effective treatment exists that can be applied to *H. fraxineus* infected trees, although recent findings highlight antagonistic species that can limit *H. fraxineus*, as well as chemical inducers of resistance such as *N*-methyl-*N*-methoxyamide-7-carboxybenzo(1.2.3)thiadiazole (BTHWA) and ammonium phosphite (Keča et al., 2018; Becker et al., 2020; Turczański et al., 2021). In the current absence of available chemical treatments for disease control, knowledge of the factors which reduce apothecia

production (see Chapter 2) and limit ascospore ejection could provide land managers with a more detailed understanding of where infection pressures may be highest and when this is likely to occur. Such understanding would give managers the tools to prioritise disease surveys and structure woodlands to limit *H. fraxineus* infection pressure. Furthermore, this knowledge could allow future targeted application of treatments which may become commercially available.

Therefore, the goal of this study was to understand the conditions affecting *H. fraxineus* ascospore release in the natural environment. To achieve this, rotating arm spore traps were used to collect ascospore samples of *H. fraxineus* which were quantified using real-time PCR. Study sites were set up within four woodlands in 2018 and six woodlands in 2019 and relied on locally trained volunteer groups to collect samples from each site. In addition to collecting spore samples, temperature and relative humidity were monitored at each site, and at each trapping location the ground cover was classified, and apothecia development estimated from the model produced in Chapter 2. The hypothesis was that temperature and relative humidity would positively affect ascospore release, but the effect of these variables would be dependent on the microclimatic influences of ground cover. As apothecia development was expected to positively affect the ascospore density it was included in the models as a controlled effect to enable this study to investigate the factors affecting *H. fraxineus* ascospore release.

3.2 Methods

3.2.1 Site Selection

Seven *H. fraxineus* infected *F. excelsior* woodlands were selected to capture a gradient of long term (1960-2014) temperature and precipitation values from May until the end of September at a 5 km^2 resolution (Met Office, 2017). Sites were also selected based on the availability of local volunteer groups to conduct sample collection. Spore density was measured at four of the sites during 2018, and six sites in 2019 (Table 3.1; Figure 3.1).

Table 3.1 Experimental sites used to monitor *H. fraxineus* ascospore density during summer 2018 and 2019 (Supplementary Table 3.1), with the mean May-September precipitation and temperature (1960-2014) at a 5 km resolution (Met Office, 2017), the year of study and the type of spore trap used. R denotes ROTTRAP 120, and F denotes FRAXTRAP (Section 3.2.3).

Site	Grid ref.	Mean May-Sept precip (mm)	Mean May-Sept temp (°C)	Years studied (Trap used)
Devon (Penstave Copse)	SX691611	128.33	13.39	2018 (R), 2019 (F)
Hampshire (Alice Holt Forest)*	SU802401	63.27	15.34	2019 (F)
Wiltshire (Colerne Park and Monks Wood)	ST837723	66.34	14.33	2019 (F)
Carmarthenshire (National Botanic Gardens of Wales)	SN518179	96.73	14.58	2018 (R), 2019 (F)
Shropshire (The Highfields)	SJ688275	60.64	13.99	2018 (F), 2019 (F)
County Durham (Hedley Hall Woods)	NZ218559	57.48	13.60	2018 (R)
Northumberland (Nunsbrough Wood)	NY950595	62.83	12.90	2019 (F)

*Mean May-September precipitation and temperature values for Alice Holt Forest at 5 km resolution were for a site 16.9 km away (Garbett's wood).

Figure 3.1 Locations of experimental sites used to monitor *H. fraxineus* ascospore density during summer 2018 and/or 2019 (Table 3.1; Supplementary Table 3.1). Site locations are indicated by numbered red markers (1 = Devon; 2 = Hampshire; 3 = Wiltshire; 4 = Carmarthenshire; 5 = Shropshire; 6 = County Durham; 7 = Northumberland).

3.2.2 Site Measurements

Data loggers (Tinytag Plus 2, Gemini Data Loggers UK) were positioned 40 cm above ground level in two locations at each site. The loggers recorded temperature and relative humidity every 10 minutes. Dominant ground cover of the 15 m area surrounding spore traps was classified as either vegetation or litter. Areas classified as vegetation cover were dominated by a range of herbaceous plants (e.g. dog's mercury (*Mercurialis perennis*), grasses, nettles (*Urtica dioica*) and bracken (*Pteridium aquilinum*)) that shielded the litter layer below. Areas where ground cover was classified as litter cover had minimal plant growth and the ground was mainly covered in mixed broadleaf litter (except for Carmarthenshire D, which was also covered by bamboo (Bambusoideae) litter), consisting of decayed fallen leaves accumulated over 1-2 years.

3.2.3 Spore Traps

Aerial ascospore levels were monitored at three sites in 2018 using the rotating arm spore traps (ROTTRAP 120) described in detail by Dvorak et al. (2017). The trap consisted of two L shaped pieces of brass wire, with the vertical end of the wires 100 mm from the trap centre and covered with a 50 mm length strip of double-sided non-woven tape (Tesa, Norderstedt, Germany) to act as an adhesive agent for the ascospores (Figure 3.2). These wires were rotated by a motor set to run at 2400 rpm for 48 hours and powered by a 12 V battery.

Difficulties operating the ROTTRAP 120 led to development of a new rotating arm spore trap (FRAXTRAP) that was used on one site in 2018, and all six sites in 2019 (Figure 3.3). These traps rotated a piece of U-shaped steel spring wire, with the two vertical ends of the wire 97 mm from the trap centre and covered with a 50 mm length strip of double-sided non-woven tape (Tesa, Norderstedt, Germany) to act as an adhesive agent for the ascospores (Figure 3.3). Wires were rotated at 2400 rpm for 48 hours in 2018, however the speed was reduced to 1800 rpm in 2019 to prevent saturation of the adhesive tape. As before, all traps were powered by 12 V batteries.

After exposure, sample tapes were returned to the laboratory for processing. Following DNA extraction (Section 3.2.5), the width of the sample tapes were measured using digital calipers (± 0.03 mm) (RS PRO 150 mm Digital Caliper, RS Components, Corby, UK) at three points along each piece of tape (1 cm from each end, and then the centre of the tape) from which the average tape width for each sample was calculated. If tape was lost during DNA extraction, the tape width was estimated using the average width from the other samples collected on the site at the sampling date, and for the Hampshire site a single average width was used for all collected samples because tape was cut with high repeatability. These measurements allowed the *H. fraxineus* spore sampling efficiency and air volume sampled to be calculated using equations detailed by McCartney (1997) and Noll (1970) enabling corrected data to be expressed as ascospores m^{-3}.

3.2.4 Sample Collection

Spore sampling was conducted at least 20 m apart at four locations on each site, except for at Wiltshire, where logistical constraints meant three locations were sampled. Spore trap locations were chosen based on proximity to the quadrats used to monitor *H. fraxineus* apothecia development from April to September 2018 and 2019 (Chapter 2), and to minimise the risk of public interference. The traps were mounted at 1.4 m above the ground and operated at weekly intervals from June through until September

(Supplementary Table 3.1) in both sampling years. Additionally, at Hampshire, a pair of FRAXTRAPs were operated approximately 2 m apart on five separate dates at three separate locations (A, B, C) in 2019 to test the comparability of the traps.

Sampling was conducted by trained local volunteer groups who monitored the spore traps regularly and collected the sample tapes. Sample collection involved removal of the double sided non-woven tape and placing it in a sterile 2 ml Microtube. Samples arrived at the laboratory within 2 days of collection, where they were then stored at -20°C.

3.2.5 DNA Extraction

In the laboratory, sample tapes were placed in 2 ml microtubes and the ascospores removed by adding acid washed glass beads (0.3g of 0.150-0.212 mm and 0.1g of 0.425-600 mm), 220 ul 0.1% Nonidet P-40 Substitute BioXtra (Sigma-Aldrich, St. Louis, MO, USA) and then homogenising three times at 6 ms^{-1} for 40 seconds with 5 minute intervals (FastPrep 24, MP Biomedicals, Irvine, CA, USA). DNA extraction was then performed according to the MagMAX Plant DNA isolation kit using the KingFisher Flex system (Thermo Fisher Scientific, Waltham, MA, USA).

3.2.6 Real-Time PCR Quantification of ascospores

3.2.6.1 Multiplex detection of *H. fraxineus* and *H. albidus*

A multiplex real-time PCR reaction to detect *H. fraxineus* and *H. albidus*, a cryptic species which also infects ash leaves (Chapter 1), was explored. DNA was extracted from mycelial samples from *H. fraxineus* and *H. albidus* cultures (Section 3.2.5) and real-time PCR of serial dilutions from a mixture of DNA of both species was performed for both singleplex and multiplex reactions to examine specificity and reaction efficiency.

Singleplex *H. fraxineus* real-time PCR reaction consisted of Takyon No Rox Probe 2X MasterMix Blue dTTP (Eurogentec, Seraing, Belgium), Cfrax-F/-R/-P (Table 3.2), 1 µl sample and molecular grade water to make a final reaction volume of 20 µl. Singleplex *H. albidus* real-time PCR reaction used Halb-F/-R/-P (Table 3.2) rather than Cfrax-F/-R/-P and multiplex real-time PCR for *H. albidus* and *H. fraxineus* used both Cfrax-F/-R/-P and Halb-F/-R/-P primers.

All real-time PCR reactions were run on LightCycler 480 II (Roche Diagnostics, Basel, Switzerland) and cycling parameters were 95°C for 3 minutes followed by 45 cycles of 95°C for 10 seconds and 60°C for 60 seconds. Each real-time PCR reaction of spore trap samples was performed in multiplex and included an inter-plate calibrator sample from the multiplex standard curve to correct for differences between the real-time PCR

reactions (Roche Lightcycler 480 Software, Version 1.5). The second derivative maximum method was used to calculate cycle quantification cycle (Cq) (Roche Lightcycler 480 Software, Version 1.5).

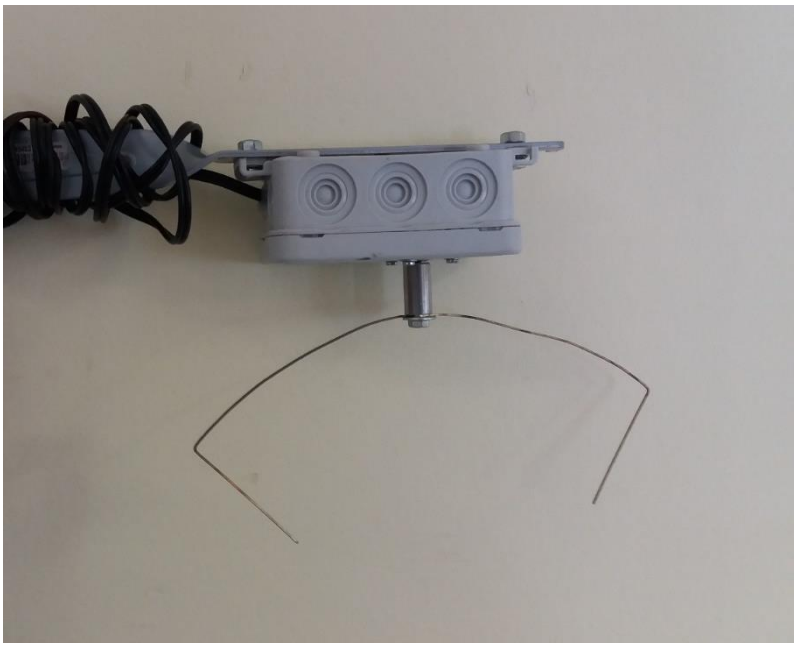

Figure 3.2 ROTTRAP 120 (Dvorak et al., 2017). AC motor within the grey box rotates the brass wire at 2400 rpm and raises the 50 mm ends of wire to a 90° vertical position 100 mm from centre of trap. The 50 mm wire ends are covered with double sided tape (Tesa, Norderstedt, Germany) to act as an adhesive agent for *H. fraxineus* ascospores. *H. fraxineus* ascospore quantities on samples can be estimated following DNA extraction and real-time PCR (Section 3.2.5; Section 3.2.6). Aerial ascospore densities are then estimated from the equations detailed by McCartney (1997) and Noll (1970).

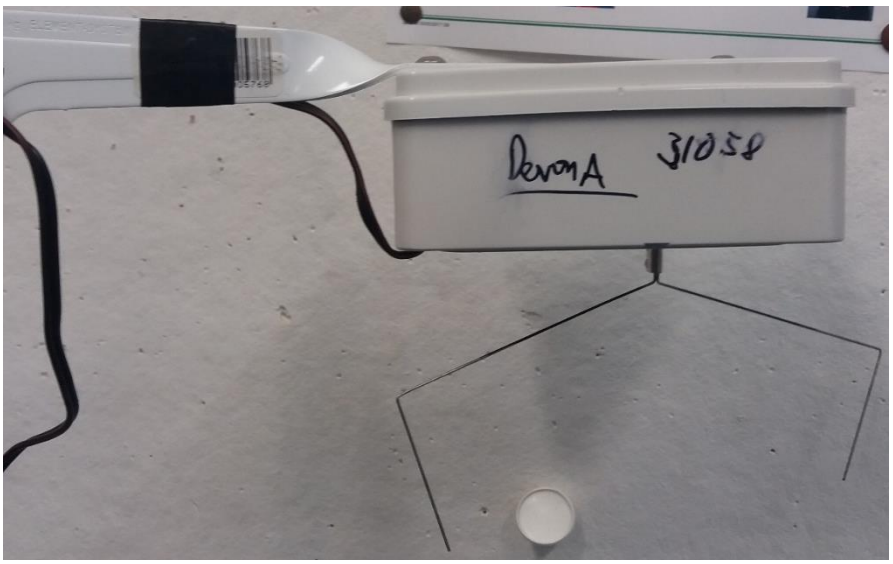

Figure 3.3 FRAXTRAP. DC motor in the grey box rotates the wire at either 2400 rpm (2018) or 1800 rpm (2019) and raises the 50 mm ends of steel spring wire to a 90° vertical position 97 mm from centre of trap. Wire ends are covered with double sided tape (Tesa, Norderstedt, Germany) to act as an adhesive agent for *H. fraxineus* ascospores. *H. fraxineus* ascospore quantities on samples can be estimated following DNA extraction and Real-Time PCR (Section 3.2.5; Section 3.2.6). Aerial ascospore densities can be estimated from the equations detailed by McCartney (1997) and Noll (1970).

Table 3.2 Primers/ Probes, their sequences and reaction concentration used in the multiplex real-time PCR reaction for detection of *H. fraxineus*, with a DNA extraction control to detect the presence of plant/ fungal DNA. Primers/probes have already been developed and tested for specificity ([a]Ioos, Kowalski et al., 2009; [b]Husson et al., 2011).

Primer/ Probe	Sequence (5'-3')	Reaction concentration (μM)	Species target
Cfrax-F	ATTATATTGTTGCTTTAGCAGGTC	0.5	*H. fraxineus*[a]
Cfrax-R	TCCTCTAGCAGGCACAGTC	0.5	
Cfrax-P	6FAM- CTCTGGGCGTCGGCCTCG-BHQ1	0.05	
Halb-F	TATATTGTTGCTTTAGCAGGTCGC	0.5	*H. albidus*[b]
Halb-R	ATCCTCTAGCAGGCACGGTC	0.5	
Halb-P	YY-CCGGGGCGTTGGCCTCG-BHQ2	0.05	

3.2.6.2 *H. fraxineus* ascospore standard curve

To quantify spore numbers from the real-time PCR of spore trap samples a *H. fraxineus* ascospore standard curve was generated from apothecia produced in the laboratory from naturally infected *F. excelsior* rachises. Clear plastic sandwich boxes were lined with two pieces of tissue paper, followed by a layer of soil, and then moss. *Fraxinus excelsior* rachises with pseudosclerotial plates, indicative of *H. fraxineus* colonisation, were collected from woodland in Hampshire in February 2021 and then placed on top of the moss layer in the boxes. Water was poured over the rachises, each box enclosed in a clear plastic bag and placed on the laboratory windowsill. Approximately 2 months later mature apothecia were collected from the incubated rachises and the hymenium dipped in 0.1% Nonidet P-40 Substitute BioXtra (Sigma-Aldrich, St. Louis, MO, USA) to collect the ascospores (Chandelier et al., 2014).

Concentrations of spore suspensions were determined using a haemocytometer. Serial dilutions of the collected ascospore suspension were performed over six $\log_{10}$ orders of magnitude and spores were added to 2 ml microtubes lined with two thin strips of 50 mm length of adhesive tape as used on both spore traps (Section 3.2.3). DNA was extracted (Section 3.2.5) and multiplex real-time PCR reaction performed for *H. albidus* and *H. fraxineus* (Section 3.2.6.1). This reaction also included inter-plate calibrator samples (Section 3.2.6.1) that were included in all real-time PCR reactions of spore trap samples, therefore enabling the quantification of *H. fraxineus* ascospores from these samples.

DNA of eight spore trap ascospore samples were serially diluted across three $\log_{10}$ orders of magnitude and multiplex qPCR reaction was performed to examine qPCR reaction efficiency of field collected samples (Table 3.3).

3.2.7 Statistical Analysis

Data were analysed using R software version 4.1.1 stats (R Core Team, 2021), lme4 (Bates et al., 2015), lmerTest (Kuznetsova et al., 2017), MuMIn (Barton, 2020), qpcR (Spiess et al., 2018), car (Fox and Weisburg, 2019), emmeans (Length, 2021), merTools (Knowles and Frederick, 2020), DHARMa (Hartig, 2021), ggplot2 (Wickham, 2016) packages. Nested linear mixed effects models specified that spore trap locations were nested within sites; site, trap location and sampling year were all defined as random effects. This allowed examination of both inter-site and intra-site level variables, whilst controlling for unaccounted variation between sites, trap locations and sampling years. The $\log_{10}$ of ascospores m^{-3} was used as the response variable and zero values were removed to meet model assumptions of a normal distribution of residuals. Only data collected using FRAXTRAPs were analysed due to the difficulties with the ROTTRAP 120 traps (Supplementary Table 3.1).

Maximal nested linear mixed effects models were constructed for mean temperature interacting with mean relative humidity and ground cover. Mean relative humidity and temperature were examined in models over 3 days and 5 days prior to sample collection. The effect of apothecia development on *H. fraxineus* ascospore density was controlled for in models by including the variable as a fixed effect. Apothecia development was estimated separately using both Apothecia Model 1 and Apothecia Model 3 developed in Chapter 2 (Section 2.3.2.1; Section 2.3.2.3).

All continuous explanatory variables were scaled by subtracting the mean and dividing the standard deviation from a given value, which allowed the modelling of variables on different scales.

Model selection and description was performed as detailed in Section 2.2.6. The maximal nested linear mixed effects models, fitted using REML (restricted/ residual maximum likelihood), were subject to stepwise model reduction of non-significant effects using Kenward-Roger approximation for denominator degrees of freedom (Luke, 2017), and 0.01 as a threshold value for significance. The reduced models containing significant variables were then fitted with ML (maximum likelihood), and AICc (Section 2.2.6) values calculated. Models were compared using ΔAICc, with ΔAICc values of less than 7 considered plausible (Burnham et al., 2011) (Section 2.2.6).

Most supported models (ΔAICc values less than 7) were fitted using REML to describe model features. The effect of significant terms in models was examined by calculated by estimating marginal mean of the $\log_{10}$(ascospore density (m^{-3})) within measured ranges of the explanatory variables, using Kenward-Roger approximation for denominator degrees of freedom. The variance explained by fixed effects in these models was represented using marginal R^2 values, and the variance explained by both fixed effects and random effects was represented using conditional R^2 values (Nakagawa and Schielzeith, 2013).

Spearman rank correlation analysis of ascospore density (m^{-3}) was performed on pairs of FRAXTRAPs that operated approximately 2 m apart on five separate dates at three separate locations (A, B, C) in Hampshire in 2019 (Section 3.2.4).

The standard curves from relevant real-time PCR reactions were calculated using regression analysis with Cq value as the response variable, and either $\log_{10}$(ascospore quantity), or $\log_{10}$(DNA quantity) as the explanatory variable (Section 3.2.6). The reaction efficiency can be calculated from the slope of the regression analysis (Efficiency = 10^(-1/slope) – 1).

3.3 Results

3.3.1 Detection and Quantification

3.3.1.1 Mutliplex reaction to detect *H. fraxineus* and *H. albidus*

Multiplex qPCR of *H. fraxineus* and *H. albidus* mycelium used for inter-plate calibrators had a reaction efficiency of 89.2% for *H. fraxineus* (y = -3.6175x + 34.35, R^2 = 0.9997) and 93.5% for *H. albidus* (y = -3.4888x + 36.91, R^2 = 0.9901). Low fluorescence amplification of *H. fraxineus* DNA by *H. albidus* primers/probes was detected whereas no amplification of *H. albidus* by *H. fraxineus* primers/probe was detected. Comparisons between *H. fraxineus* Cq detection values in singleplex and multiplex with *H. albidus* DNA across a range of concentrations showed that Cq values were 0.13 higher in singleplex compared to multiplex reaction (se = 0.04, $p < 0.01$). However, the difference in Cq values was not affected by the dilution series and singleplex reaction had a comparable reaction efficiency of 88.2% (y = -3.64067x + 34.53, R^2 = 0.9994).

3.3.1.2 Ascospore quantification for *H. fraxineus*

Ascospores were collected from apothecia to a maximum concentration of 345750 ascospores μl^{-1}. The standard curve generated from the spore suspensions detected spores down to a quantity of 8.64 spores with a 94.2% amplification efficiency (y = -

3.4688x + 40.673, R^2 = 0.995) (Figure 3.4). Using the standard curve, it was then possible to make accurate estimates of the number of spores collected on the sample tapes from the FRAXTRAP spore traps and test the effects of various environmental and developmental factors on the number of ascospores released into the environment between June and September 2018 and 2019.

3.3.1.3 Spore trap ascospore detection

H. fraxineus was detected by spore traps on all sites at all examined dates (Supplementary Table 3.1), however samples which had suboptimal amplification curves, indicating a suboptimal reaction efficiency were excluded from the analysis. Real-time PCR reaction efficiency was tested for a small subset of the field samples (Section 3.2.6.2) and ranged between 79.6% (which increased to 85.3% if one outlier dilution for this sample was removed) and 97.8%, averaging 93.2% (Table 3.3).

The pairs of FRAXTRAPs that were tested for comparability at three separate locations in Hampshire (A, B, C) (Section 3.2.4) collected spores at densities that were significantly correlated (r_s = 0.961, p < 0.001) (Figure 3.5) thus allowing data to be reliably compared across the trap network.

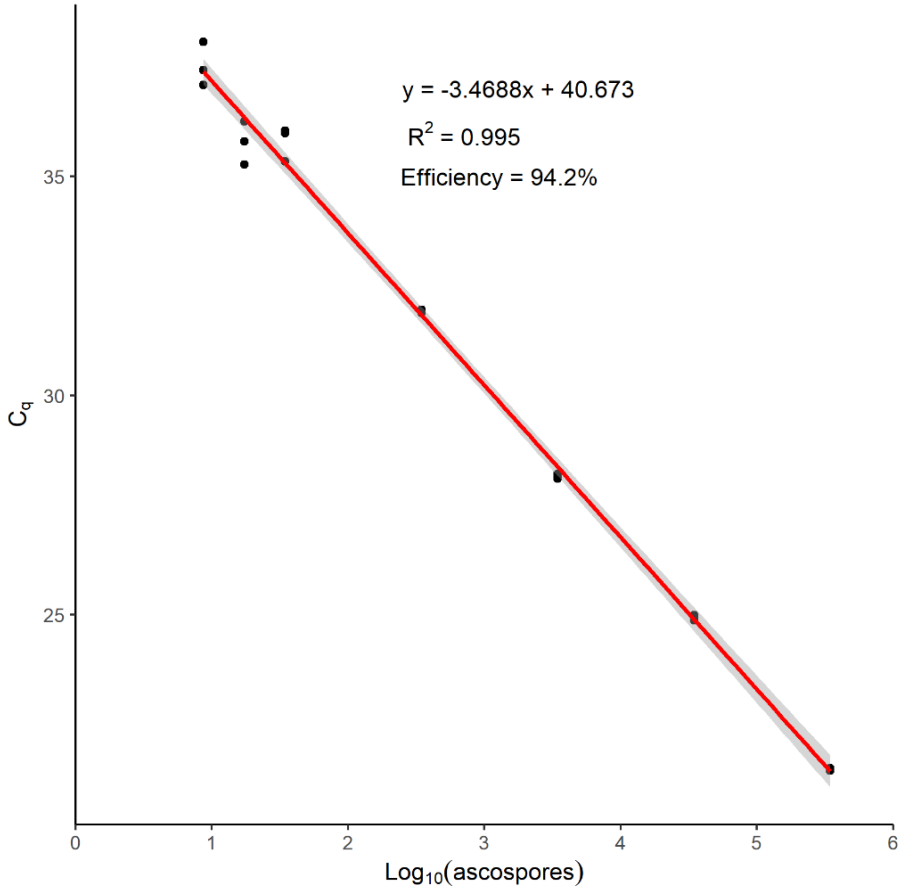

Figure 3.4 Standard curve to estimate the *H. fraxineus* ascospore quantities via multiplex real-time PCR (Cfrax-F/-R/-P, Halb-F/-R/-P; Section 3.2.6) Cq values. Ascospore suspensions ranged over six log_{10} orders of magnitude.

Table 3.3 Multiplex real-time PCR (Cfrax-F/-R/-P, Halb-F/-R/-P; 3.2.6) reaction efficiency estimates for detection of *H. fraxineus* from field samples collected using FRAXTRAPs (Section 3.2.3). Eight samples were diluted over four log_{10} orders of magnitude and reaction efficiency estimated from the regression equation (efficiency = 10^(-1/slope) – 1).

Site	Trap Location	Sample Collection Date	Regression Equation (R^2)	Reaction Efficiency (%)
Wiltshire	A	21/07/19	y = -3.38x + 30.82 (1.00)	97.8
Wiltshire	A	28/07/19	y = -3.39 + 30.25 (1.00)	97.1
Wiltshire	A	04/08/19	y = -3.93 + 30.64 (0.96)	79.6
Wiltshire	A	18/08/19	y = -3.54 + 29.97 (1.00)	91.5
Wiltshire	B	21/07/19	y = -3.41 + 31.27 (1.00)	96.6
Hampshire	D	25/07/19	y = -3.59 + 32.27 (1.00)	89.8
Hampshire	D	09/08/19	y = -3.42 + 31.87 (1.00)	96.1
Hampshire	D	17/08/19	y = -3.40 + 31.31 (1.00)	96.8

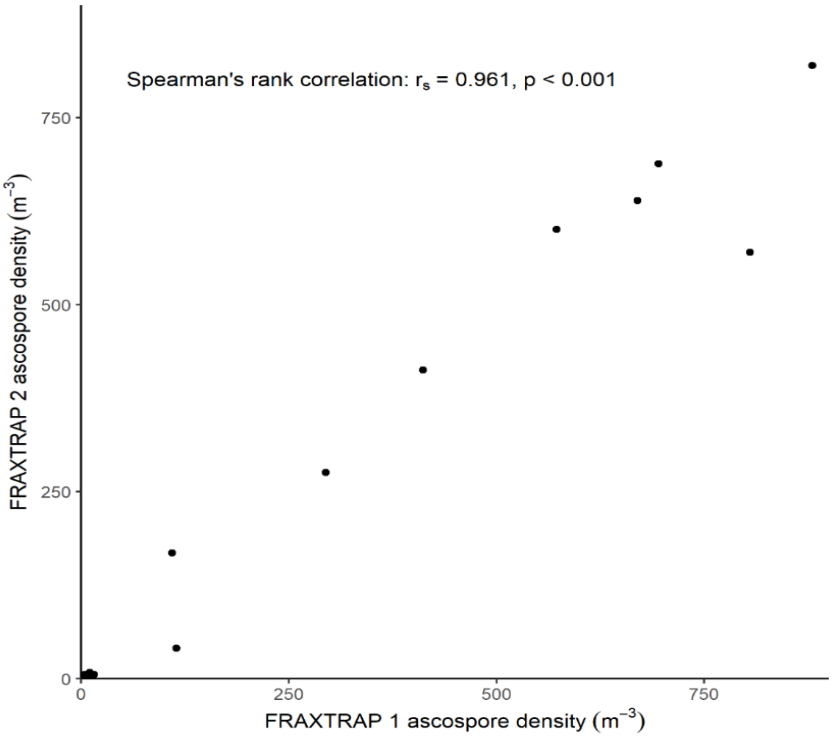

Figure 3.5 Comparison of *H. fraxineus* ascospore density (m^{-3}) between two FRAXTRAPs approximately 2 m apart. Ascospores were quantified via multiplex real-time PCR (Cfrax-F/-R/-P, Halb-F/-R/-P, Section 3.2.6) and the equations detailed by McCartney (1997) and Noll (1970) were used to express data as ascospore density (m^{-3}) via calculation of volume of air sampled and the sampling efficiency. Data were collected for trap comparisons on five separate dates at three locations within the Hampshire site (Supplementary Table 3.1). Spore densities were significantly correlated (r_s = 0.961, p < 0.001).

3.3.2 Site measurements

Site temperature and relative humidity data (Section 2.3.1) and apothecia development models (Section 2.3.2) are described in Chapter 2. The maximum *H. fraxineus* ascospore density varied both within and between sites (Figure 3.6), and the differences present within sites do not correspond to differences in ground cover type. The timing of maximum spore density ranged from the end of July to mid-August, and was typically much lower outside this period, although relatively high spore density was recorded in mid-June 2019 in Devon (trap location A) and late June 2019 in Carmarthenshire (trap location A). In 2019, the date of peak spore density varied between sites, within sites and among ground cover types within a site. Data for 2018 was only from the Shropshire site, but spore density at trap locations peaked on the same date (17/08/2019 – 19/08/2019). The date of maximum spore density was similar in 2019 at locations A, C, D (11/08/2019 – 13/08/2019), however comparisons could not be made for location B due to limited sampling dates in 2018. Inter-site interpretations from the raw data are difficult because of high intra-site variation

(a)

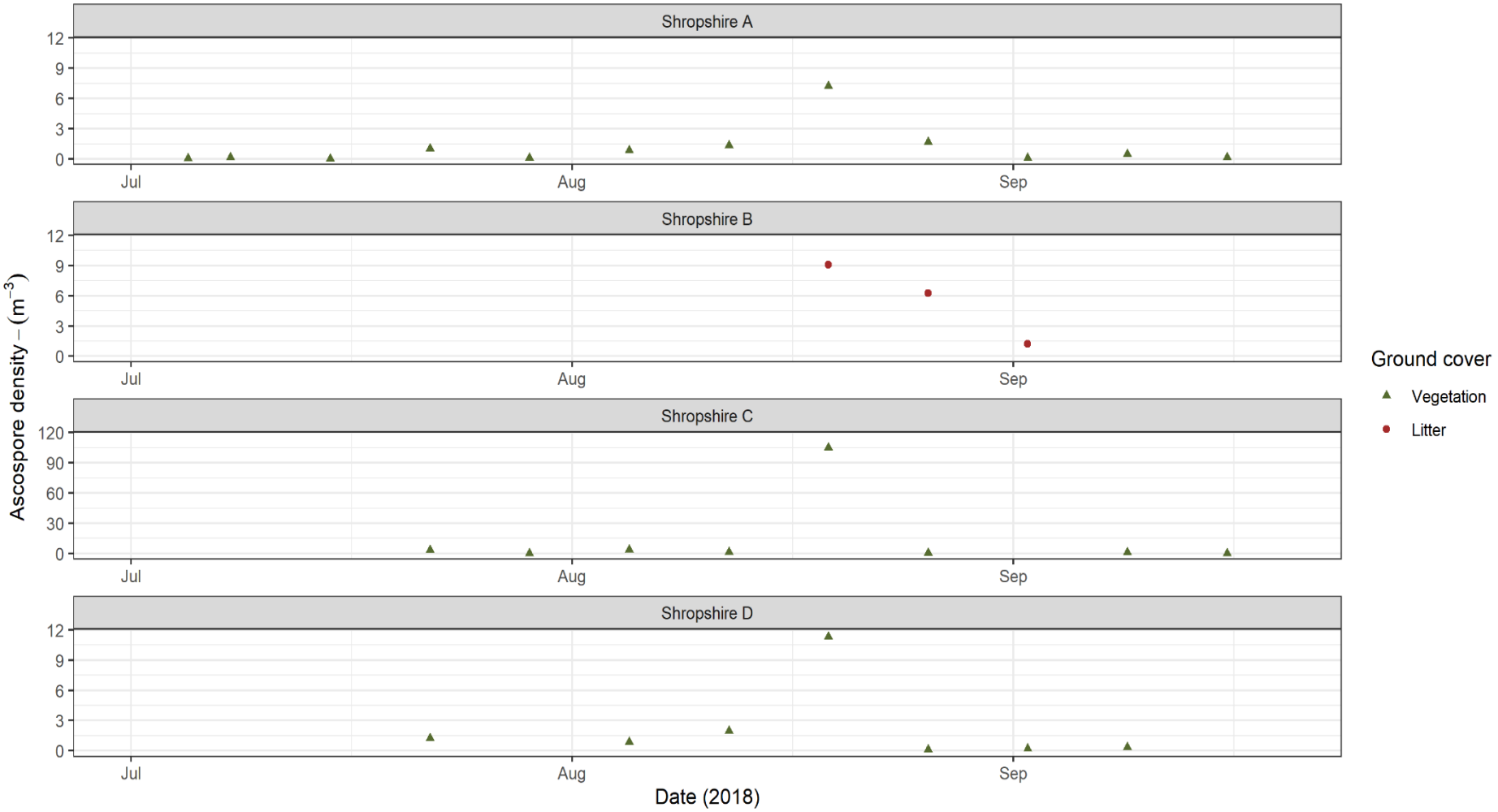
Shropshire A
Shropshire B
Shropshire C
Shropshire D
Ascospore density – (m^{-3})
Date (2018)
Jul
Aug
Sep
Ground cover
Vegetation
Litter

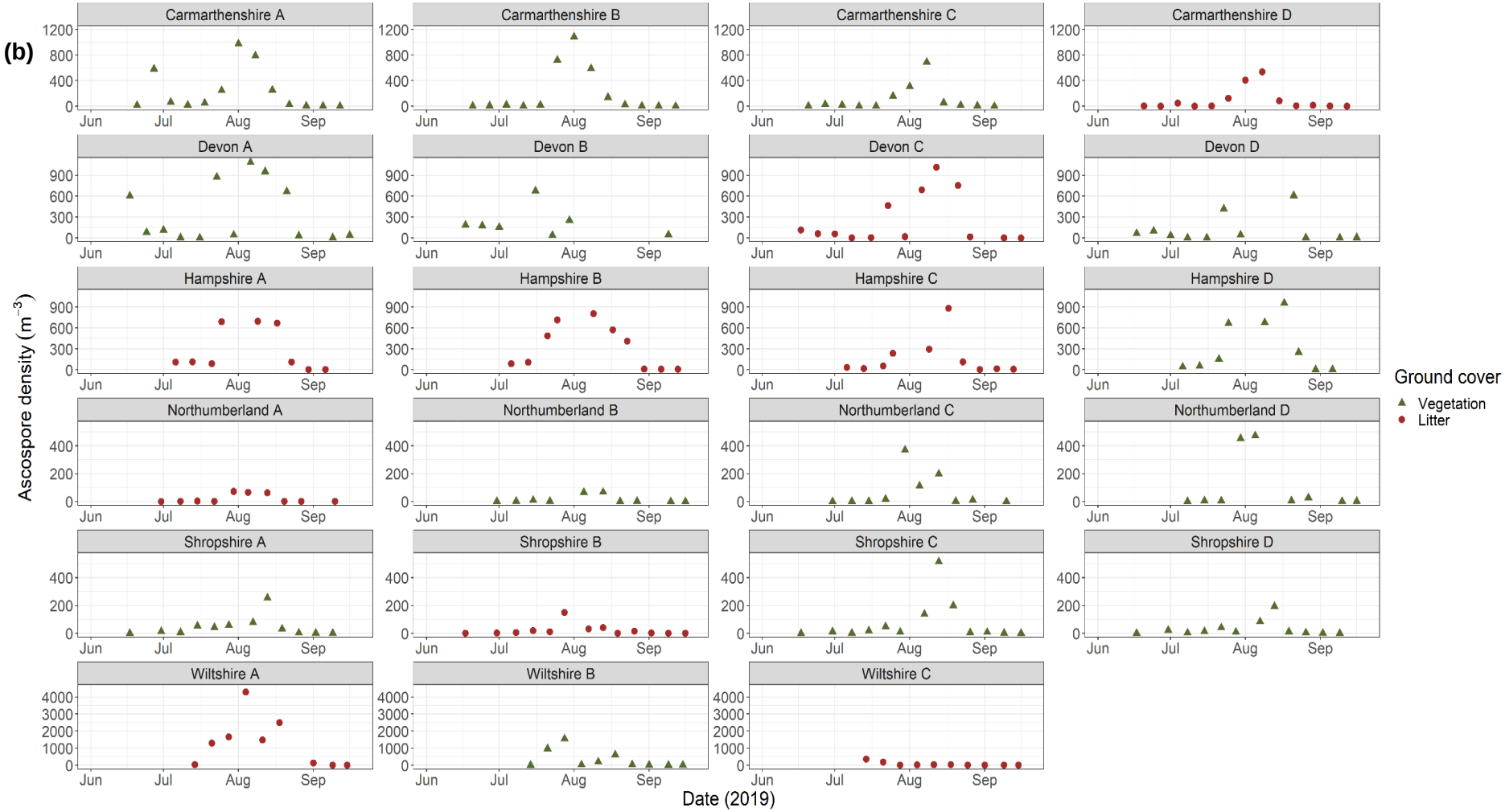

Figure 3.6 **(a)** *H. fraxineus* ascospore density (m^{-3}) from locations (A, B, C, D) in the Shropshire site from July – September 2018 **(b)** and from locations (A, B, C, D) at six sites (Carmarthenshire, Devon, Hampshire, Northumberland, Shropshire, Wiltshire) from June – September 2019 (Section 3.2). Ascospore samples were collected using FRAXTRAPs (Section 3.2.3), quantified via real-time PCR (Section 3.2.6) and ascospore density (m^{-3}) calculated using the equations detailed by McCartney (1997) and Noll (1970) for the calculation of the volume of air sampled and the sampling efficiency. Dominant ground cover in the 15 m surrounding spore trapping locations is indicated (Section 3.2.2).

3.3.3 Model construction and ranking

Several models were run to explore the effects of apothecia development, temperature, relative humidity and ground cover on ascospore release in *H. fraxineus.* One model (Spore density model 1) was identified with ΔAICc value of less than 7, indicating this was the best supported and plausible model (Table 3.4; Figure 3.7). Spore density model 1 found that apothecia development (estimated using apothecia model 3) (ddf = 263.8, $p < 0.001$) and mean relatively humidity during the 5 days prior to the collection of spore trap samples (ddf = 259.4, $p < 0.001$) positively affect the spore density. Each unit increase of apothecia development ($\log_{10}[\sqrt{\text{apothecia area [mm}^2]}]$) resulted in 2.06 unit (se = 0.33, df = 264) increase in the estimated marginal mean of $\log_{10}$(ascospore density [m^{-3}]) but each unit increase of relative humidity (%) over the 5 days preceding collection of spore trap samples only resulted in 0.10 unit (se = 0.01, df = 259) increase in the estimated marginal mean of $\log_{10}$(ascospore density [m^{-3}]). Ground cover and mean temperature in the 5 days prior to the collection of spore trap samples also interacted significantly to affect spore density (ddf = 268.0, $p < 0.01$) (Figure 3.8). The increase in estimated marginal mean of $\log_{10}$(ascospore density [m^{-3}]) per unit temperature was greater in areas with predominantly litter cover (0.22, se = 0.05, df = 267.0), compared to areas where vegetation cover dominated (0.06, se = 0.05, df = 260.0). When a warmer mean temperature (17°C) in the 5 days prior to the collection of traps was selected (with apothecia development set at 1.4 and relative humidity over the 5 days prior to collection at 90%), the estimated marginal mean of $\log_{10}$(ascospore density [m^{-3}]) was greater in areas with litter cover (1.26, se = 0.41, df = 1.65) compared to those with vegetation cover (0.72, se = 0.42, df = 1.84). However, when the mean temperature in the 5 days prior to the collection of traps was reduced to 13˚C, the estimated marginal mean of spore density in areas with vegetation cover (0.50, se = 0.40, df = 1.49) was similar to areas with litter cover (0.40, se = 0.41, df = 1.75).

(a)

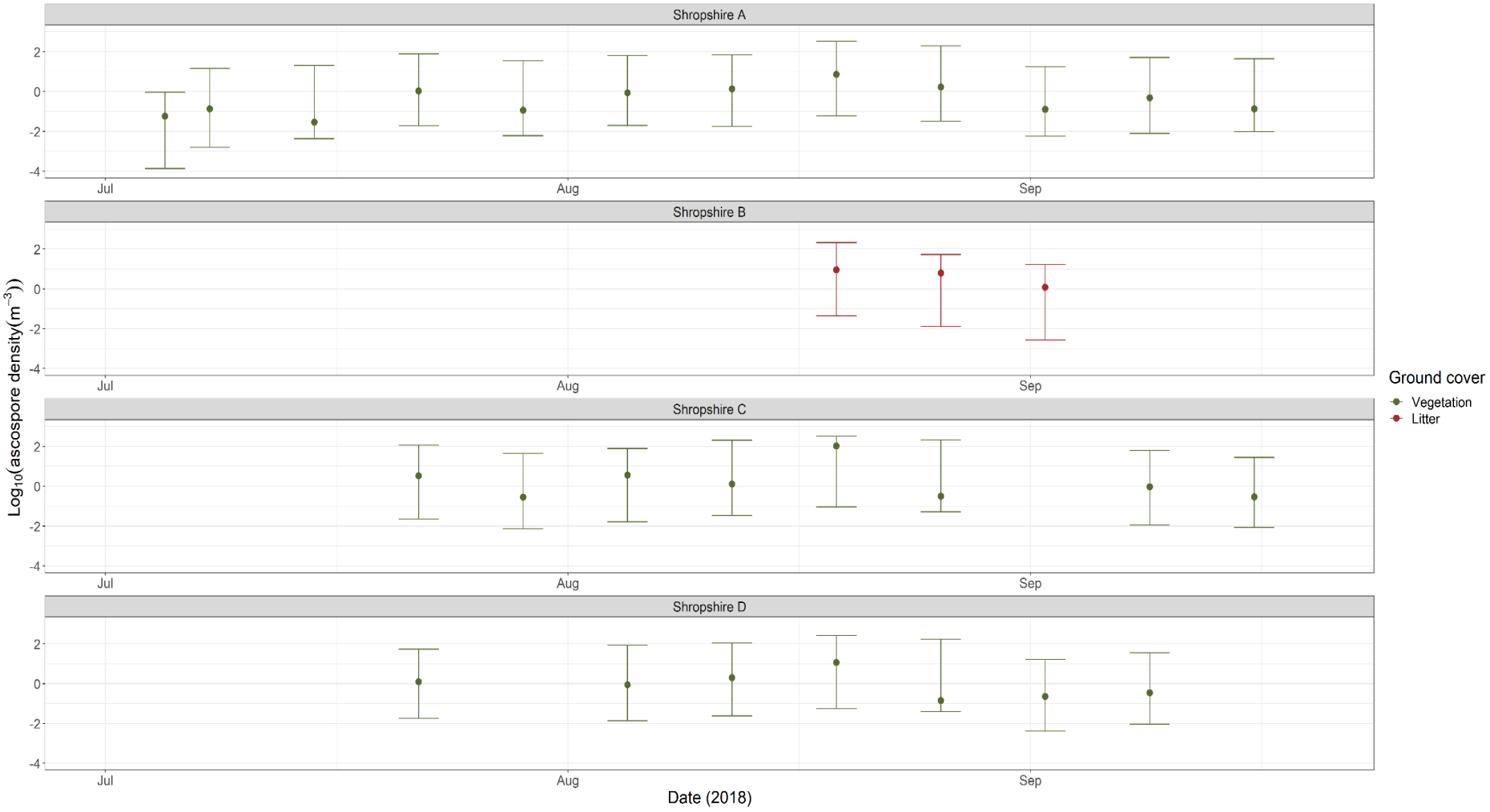
Shropshire A
Shropshire B
Shropshire C
Shropshire D
2
0
-2
-4
Jul
Aug
Sep
Log10(ascospore density(m−3))
Date (2018)
Ground cover
Vegetation
Litter

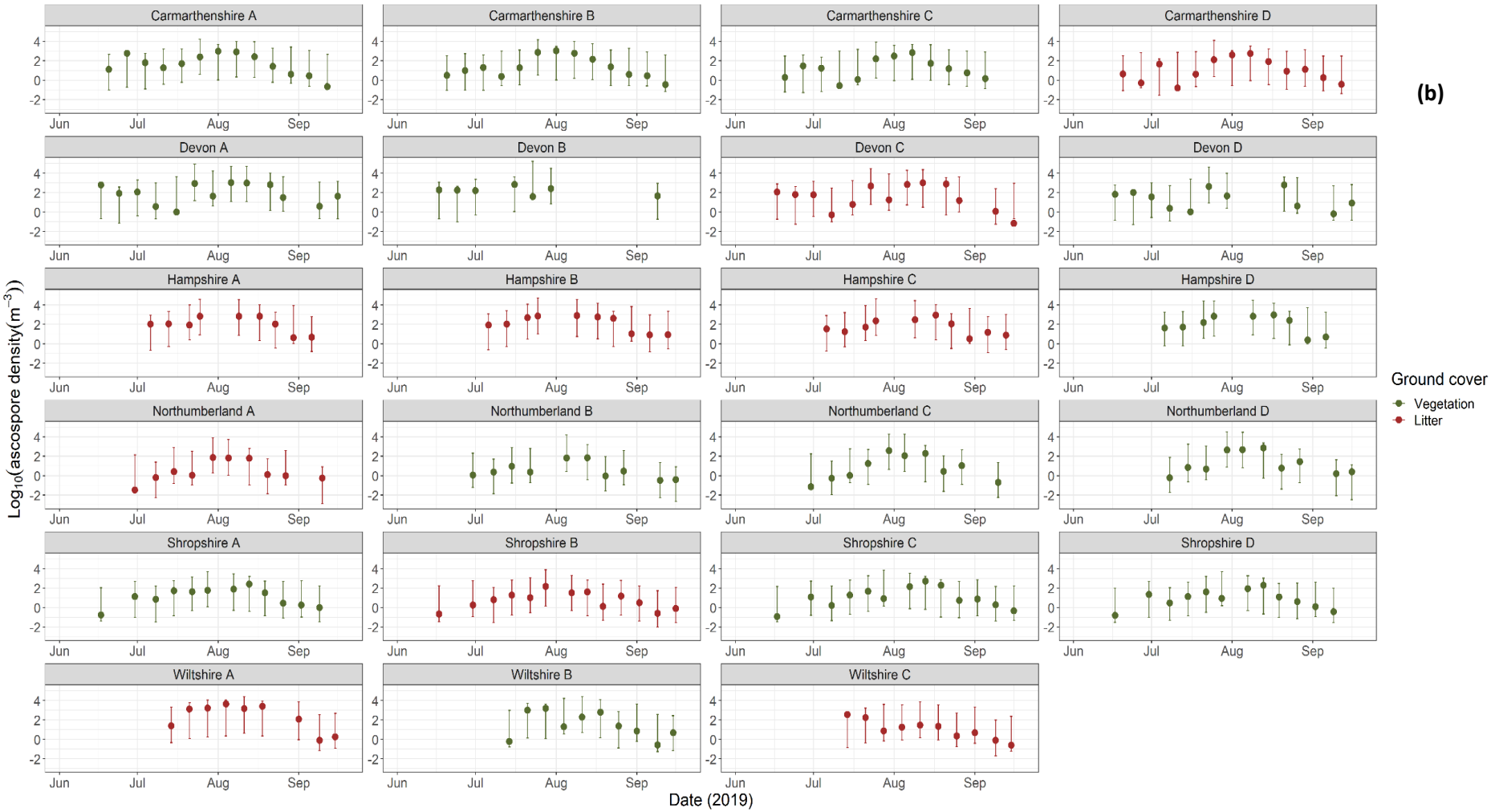

Figure 3.7 (a) Log_{10}(*H. fraxineus* ascospore density (m^{-3})) from locations (A, B, C, D) within the Shropshire site from July – September 2018 **(b)** and from locations (A, B, C, D) across six sites (Carmarthenshire, Devon, Hampshire, Northumberland, Shropshire, Wiltshire) from June – September 2019 (Section 3.2) with the most supported linear mixed effects model (Spore density model 1; ΔAICc = 0; marginal R^2 = 0.30; conditional R^2 = 0.58) fitted to the datapoints with corresponding 95% confidence intervals. The model accounted for unexplained variation between sites, trapping locations and sampling years by specifying these variables as random effects and that trapping locations were nested within sites. Fixed effects (explanatory variables) included in the model were apothecia development (log_{10}[√apothecia area[mm^2]]) (estimated using apothecia model 3; Section 2.3.2.3), mean temperature (°C) over the 5 days

prior to sample collection, mean relative humidity (%) over the 5 days prior to sample collection and dominant ground cover (vegetation or litter) in the surrounding 15 m. An interaction was present between mean temperature (°C) over the 5 days prior to sample collection and ground cover. Continuous explanatory variables were brought onto comparable scales by subtracting the mean and dividing by the standard deviation. Dominant ground cover in the 15 m surrounding spore trapping locations is indicated (Section 3.2.7; Section 3.3.3).

(a)

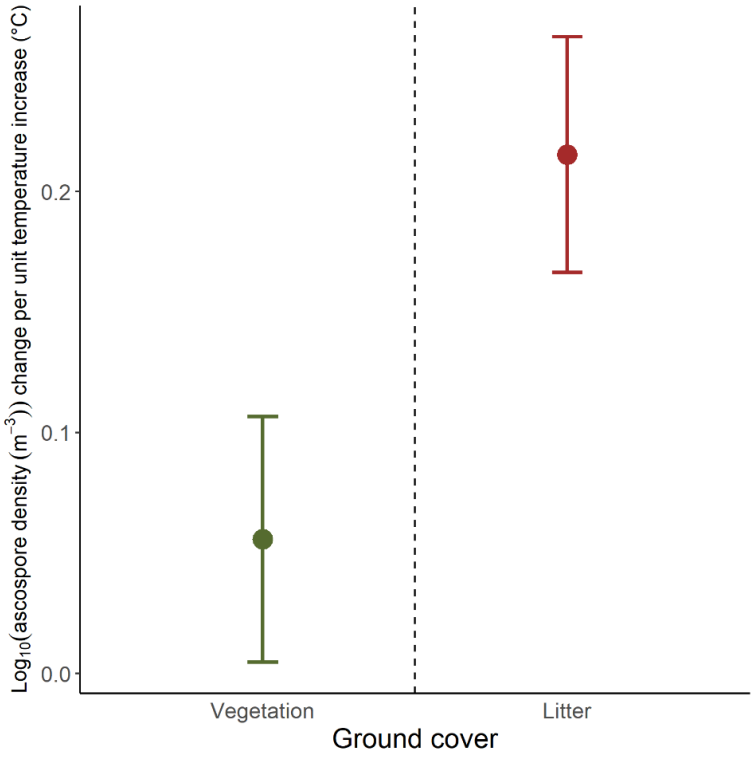

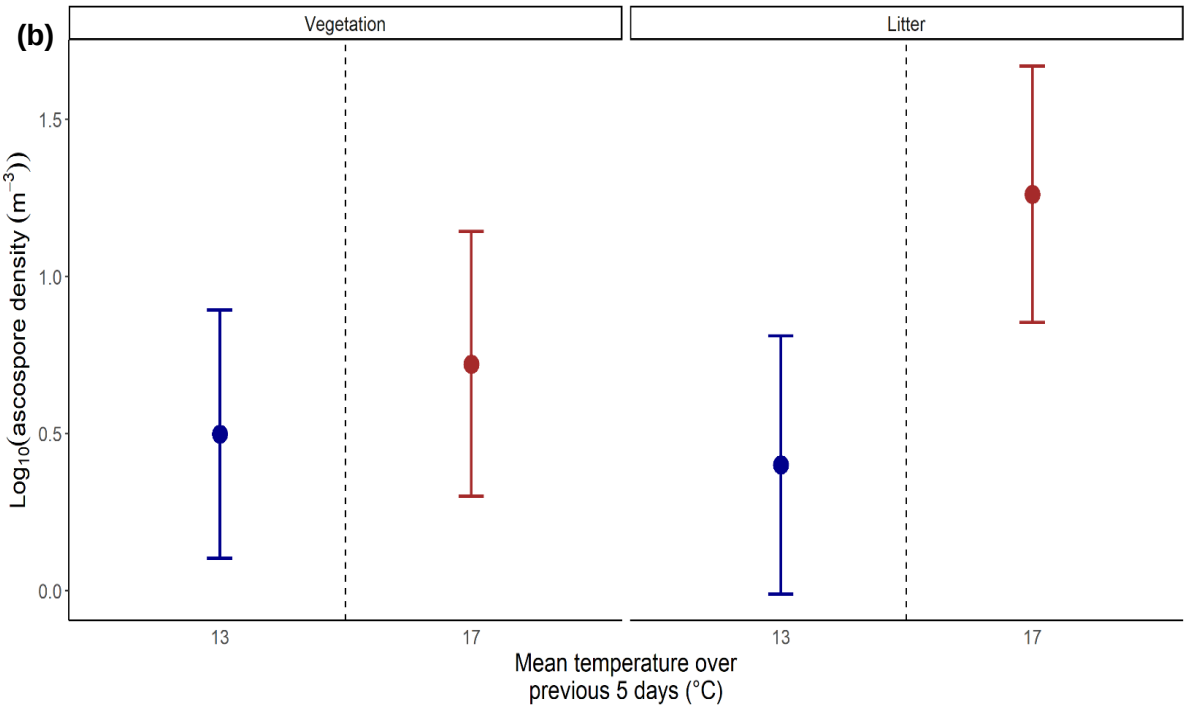

Figure 3.8 The significant interactive effect on $\log_{10}$(*H. fraxineus* ascospore density (m^{-3})) in spore density model 1 (Section 3.3.3) between mean temperature (°C) over the 5 days prior to sample collection and the dominant ground cover (vegetation or litter) in the 15 m surrounding the spore trapping location (ddf = 268.0, $p < 0.01$). (a) The change in the estimated marginal mean (from spore density model 1) of $\log_{10}$(ascospore density (m^{-3})) and standard error per unit increase of the mean temperature (°C) over the 5 days prior to sample collection in areas with predominantly vegetation or litter ground cover. (b) The estimated marginal mean (from spore density model 1) of $\log_{10}$(ascospore density (m^{-3})) and standard error in areas with predominantly vegetation or litter ground cover at a lower (13°C) and higher (17°C) mean temperature over the previous 5 days. Other explanatory variables in the model did not affect the trend of the interaction and were set at arbitrary values (mean relative humidity (%) over the 5 days prior to sample collection was specified as 90 and the apothecia development ($\log_{10}$[√apothecia area [mm^2]]) was specified as 1.4).

Table 3.4 Plausible linear mixed effects model (Spore density model 1; Section 3.3.3) for log_{10} (*H. fraxineus* ascospore density (m^{-3})) that had ΔAICc (Δ second-order Akaike Information Criterion) < 7. Fixed effects are listed at their highest interaction (An interaction is denoted by the symbol ':') and p values were calculated using Kenward-Roger approximation for denominator degrees of freedom (ddf). The variance of random effects denotes the variability in site, trap location and sampling year in the model. AICc and ΔAICc values were calculated not including site as a random effect to allow comparison of fixed effects of models. The full model is presented above the table.

Spore Density Model 1 <- Log_{10}(H. fraxineus ascospore density[m^{-3}]) ~ scale(apothecia development (apothecia model 3)) + scale(mean temperature previous 5 days) + scale(mean relative humidity previous 5 days) + Ground Cover + (1 | Site/Trap Location)+(1|Year) + scale(mean temperature previous 5 days):Ground Cover

Fixed Effects	p (ddf)		Random Effects	Variance (Std. Dev)	AICc	ΔAICc	Marginal R^2/ Conditional R^2
Apothecia development (Square root(log_{10}(apothecia area (mm^2))	< 0.001		Site	0.1259 (0.3548)	705.67	0	0.30/ 0.58
5 day mean humidity	< 0.001		Trap Location	0.0468 (0.2163)			
5 day mean temperature: Ground cover	<0.01		Year	0.2305 (0.4801)			

3.4 Discussion

Through the development of reliable rotating arm spore traps and an effective real-time PCR assay for quantifying *H. fraxineus* ascospores, this research demonstrated that various developmental and environmental factors could influence ascospore release by *H. fraxineus.* Apothecia development, temperature, relative humidity, and ground cover all had a significant effect on aerial ascospore density. Importantly, the inclusion in the model of data on apothecia development, from models developed in Chapter 2, allowed the environmental effects on ascospore release in *H. fraxineus* to be examined independently of apothecia development.

The present study showed that relative humidity was positively related to *H. fraxineus* aerial ascospore density. Interestingly, the model selection found the mean relative humidity 5 days prior to sample collection better explained ascospore density than the mean relative humidity 3 days prior to sample collection. Indeed, spore dispersal distances have been estimated which suggest that *H. fraxineus* can remain in the air for prolonged periods (Grosdidier, Ioos, Husson et al., 2018), thereby explaining that the

effect of relative humidity on ascospore density is more supported 5 days prior to sample collection. Alternatively, the results suggest a prolonged period of moisture is required to prime the ascospores for ejection. Water is essential for ascospore release in some ascomycetes because increases in hydrostatic pressure of the asci are required for the powerful ejection of ascospores (Trail, 2007). Although this process has not been studied in *H. fraxineus*, moisture uptake over several days likely maximises hydrostatic pressure thus leading to more readily, or to more powerfully, ejected ascospores that are more likely to be detected at the height of the spore traps.

Concurring with my findings, higher *H. fraxineus* ascospore density has previously been related to higher moisture. Ascospore density was found to be mainly influenced by relative humidity during sampling, and approximately 12 days prior to sampling (Čermáková et al., 2017), and a separate study correlated ascospore density the greatest with daily minimal relative humidity one day prior to sampling and daily minimal leaf wetness 13 days prior to sampling (Dvorak et al., 2015). A more recent study found that average leaf moisture 5 days prior to sampling had a greater positive effect on ascospore quantity compared to leaf moisture at earlier investigated intervals (within 2 hours and 2-24 hours prior to daily spore peak) (Burns et al., 2022). Furthermore, more ascospores were detected on sites classified as wet (Čermáková et al., 2017) and no spores were detected in the 2 days following a large drop in relative humidity (Dvorak et al., 2015). Aerial ascospore density in other ascomycetes has also been positively related to moisture, such as rainfall and relative humidity (Mondal et al., 2003; Rossi et al., 2010; Manstretta and Rossi, 2015).

Relative humidity may also affect spore release through its influence on air pressure. Humidity is negatively related to air pressure, and air will move from areas of high to low pressure. Presumably, as humidity in the woodland increases and pressure decreases, the potential for pressure differences increases. Pressure changes have been suggested to trigger ascospore release in ascomycetes (Roper et al., 2010). Indeed, it has been observed that most spore ejection occurs between 04h30 and 08h30 (Hietala et al., 2013), which is when humidity typically declines and therefore leads to changes in air pressure. Furthermore, ascospores are almost immediately ejected from apothecia incubated in sealed humid boxes in the laboratory when these boxes are opened, and the apothecia exposed to lower humidity laboratory conditions (Chapter 4).

Ascospore density of *H. fraxineus* (Chandelier et al., 2014; Čermáková et al., 2017) and other ascomycetes (Clarkson et al., 2003; Manstretta and Rossi, 2015; Imre and Füzi, 2015) has also been related to temperature. The current study provides support for the role of temperature in influencing ascospore release. In studied ascomycetes, an osmotic gradient leads to water influx into the asci, which then creates the hydrostatic

pressures required for spore release (Trail, 2007). Importantly, according to van't Hoff theory, as temperature decreases, the osmotic potential becomes less negative, thereby decreasing the osmotic gradient and negatively affecting the hydrostatic pressure generated in the asci. This would decrease the ability of asci to eject ascospores or the force with which they are ejected, meaning it is less likely they will reach heights to be detected by spore traps. Interestingly, as with the effect of relative humidity, my research found that mean temperature better explained ascospore density during the 5 days prior to sample collection, rather than during the 3 days prior to sample collection.

The present study also showed that ascospore release was dependent on the ground cover. Warmer temperatures (e.g. 17˚C) were associated with greater ascospore release in areas where the ground cover only consisted of litter. Importantly, the litter environment is exposed to greater solar radiation compared with ground overtopped with vegetation, which likely leads to higher temperatures for apothecia on rachises mixed with an exposed litter layer, rather than those under vegetation. In contrast, ascospore release at lower temperatures (e.g. 13˚C) differed little between areas dominated by vegetation compared to areas dominated by litter cover on the ground. However, greater spore ejection for apothecia mixed with an exposed litter layer in comparison to those under vegetation may not translate to differences in infection pressure because apothecia development on rachises under vegetation is greater than on rachises mixed with the litter layer (Chapter 2). Furthermore, exposed areas without vegetation cover are likely to have a lower humidity which could decrease both apothecia development (Chapter 2) and spore ejection. Additionally, no clear pattern in the maximum ascospore density was present within sites between areas dominated by vegetation and areas dominated by exposed litter, although this could be due to differences in the density of *H. fraxineus* infected *F. excelsior* rachises in the litter layer.

Surprisingly, ground cover did not interact with relative humidity to influence ascospore density. Ground cover will affect the microclimate surrounding the apothecia as evidenced by the significant interaction of ground cover with both temperature and relative humidity to influence apothecia development (Chapter 2). Humidity can be expected to be higher surrounding apothecia on rachises sheltered under vegetation compared to those mixed with an exposed litter layer. Despite this, the positive effect the sheltered vegetation environment has on humidity could be offset by the protection provided against potential triggers of spore ejection, such as changes in air pressure. Indeed, greater net radiation within 2 hours of the daily spore peak strongly delays the timing of the spore peak, and results in a lower daily spore quantity (Burns et al., 2022). Increased net radiation is associated with cloudier conditions, which, as with conditions under vegetation cover compared to an exposed litter layer, will lead to decreased fluctuations in temperature, and thus air pressure.

Vegetation could also provide a barrier to spore dispersal, although the behaviour of simultaneous mass spore ejection in *H. fraxineus* suggests that spores can readily pass obstacles that are encountered when they are part of a collective jet (Roper et al., 2010). Properties of *H. fraxineus* spore jets and the conditions that influence ejection would provide valuable information on how height or layering of obstacles affects dispersal of *H. fraxineus* ascospores. One laboratory investigation found that *H. fraxineus* ascospores have difficulty ejecting above 0.5 cm (Mansfield et al., 2018), but this contradicts personal observations where clouds of ascospores are readily visible at heights much greater than this when humid boxes containing apothecia are opened in the laboratory. Moreover, the buffered and sheltered environment surrounding apothecia on rachises under vegetation, which may limit the number of triggers for spore ejection and provide physical barriers to spore dispersal, could also explain the reduced sensitivity of ascospore ejection to changes in temperature in these environments.

As anticipated, unexplained variation in the model remained both within sites and between sites and sampling years. This is exemplified by differences in the quantity of maximum aerial ascospore density within sites in areas with the same dominant ground cover classification. It is expected this variation can largely be explained by microclimatic effects (as discussed in Chapter 2) and differences in the density of *H. fraxineus* infected *F. excelsior* rachises in the litter layer. Importantly, the period of peak aerial ascospore density occurred within a conserved timeframe from the end of July to mid-August, and corresponded to the period of maximum apothecia development and maximum mean daily temperature on experimental sites (Chapter 2). Notably, combined with my results from Chapter 2, this study suggests the timing and quantity of ascospore density will differ with projected future climatic changes.

3.5 Conclusions

Aerially dispersed ascospores of *H. fraxineus* were precisely quantified using the FRAXTRAP spore traps developed during this study with subsequent real-time PCR quantification of ascospores. Trained volunteers were essential in undertaking this work to monitor *H. fraxineus* ascospore release at multiple remote locations at weekly intervals.

Models of the factors affecting aerial ascospore density were produced, and when apothecia development was controlled using a model tested in Chapter 2, this allowed the environmental controls of spore ejection in *H. fraxineus* to be examined.

Mean temperature and relative humidity during the 5 days prior to spore sampling and also apothecia development had a significant positive effect on ascospore release by

H. fraxineus. Temperature significantly interacted with ground cover, and temperature had a greater positive effect in areas mainly covered by litter compared to vegetation.

At warmer temperatures (e.g. 17°C), areas with litter cover had greater ascospore ejection than areas with vegetation cover. However, the effect of this on disease progression may be unimportant because both ground cover types display high aerial spore density and areas of vegetation cover can be expected to have higher levels of apothecia development (Chapter 2). The relationship between spore density on disease progression is explored in Chapter 4.

Chapter 4: Laboratory and field experiments into the effects of moisture, temperature and *H. fraxineus* ascospore density on *F. excelsior* foliar colonisation and crown dieback

4.1 Introduction

Current evidence indicates that ash dieback disease has been in the UK since the 1990s (Wylder et al., 2018), despite only first being detected in the UK in 2012 (Sansford, 2013). Not all trees or woodlands are equally affected by the disease. Numerous environmental conditions such as altitude, precipitation, temperature, soil type, vertical terrain heterogeneity and species admixture, as well as *F. excelsior* genetics are known to affect the rate of disease progression (Havrdová et al., 2017; Stocks et al., 2019; Turczański et al., 2020; Klesse, Abegg et al., 2021). Elucidation of the processes responsible for differences in disease progression are important to develop effective disease management practices, thus, as mentioned in previous chapters, it is vital to understand the sexual reproduction of *H. fraxineus* since host infection and disease spread is via sexual spores (Timmerman et al., 2011; Cleary et al., 2013). Accordingly, Chapter 2 examined the conditions which affect the formation of the apothecia and Chapter 3 examined the conditions which affect ascospore ejection from the apothecia. Both Chapters found significant effects of temperature and humidity, and involved interactions with the ground cover (Chapter 2; Chapter 3) and the canopy closure (Chapter 2), presumably due to their influence on the litter layer microclimate. Therefore, intra- and inter-site, as well as intra- and inter-annual variations in temperature and humidity at the litter layer lead to variations of *H. fraxineus* inoculum quantity. However, it is not known whether differences in inoculum quantity affect disease progression.

Increased disease severity is associated with higher *F. excelsior* density in a woodland (Grosdidier et al., 2020; Klesse, Abegg et al., 2021). This suggests that the density of ascospores infecting *F. excelsior* foliage is important for disease outcome, because greater *F. excelsior* density in a stand will be associated with more *F. excelsior* litter on the forest floor, thus providing *H. fraxineus* with a greater density of material from which to produce a higher aerial ascospore density. Disease severity has also been found to decrease with increasing *F. excelsior* height (Havrdová et al., 2017; Erfmeier et al., 2019). Taller trees will presumably be exposed to fewer *H. fraxineus* ascospores because ascospore density decreases with height (Chandelier et al., 2014). Additionally, temperature (below 35°C) and moisture are positively related to disease progression in a

woodland (Marçais et al., 2016; Havrdová et al., 2017), and Chapters 2 and 3 demonstrate that both environmental variables affect inoculum production by regulating *H. fraxineus* apothecia production and ascospore ejection.

The conditions which affect *H. fraxineus* foliar colonisation are unknown, although both temperature and moisture are known to affect symptom progression following inoculation in multiple host-pathogen interactions (Arny and Rowe, 1991; Guzman-Plazola et al., 2003; Trapero-Casas and Kaiser 2007). Indeed, models incorporating this information have been produced for *Venturia inaequalis* and *Erysiphe necator* to guide disease management of Apple Scab and powdery mildew of grapevine respectively (Rossi et al., 2007; Caffi et al., 2011). It is important to understand factors affecting germination of *H. fraxineus* ascospores, in combination with the knowledge of conditions affecting inoculum production (Chapter 2; Chapter 3), so that woodland managers can spatially and temporally target disease surveys and applications of future disease treatments.

The goal of this chapter was to understand factors affecting *H. fraxineus* foliar colonisation of *F. excelsior*, and whether the degree of colonisation is related to crown dieback. To achieve this, foliar colonisation was estimated by measuring the proportion of previous seasons' rachis length in the litter layer colonised by *H. fraxineus* under *F. excelsior* trees in 2020 at locations where *H. fraxineus* ascospore density was recorded in 2019 (Chapter 3), and the crown dieback of trees was assessed. From these data, combined with the estimated time of disease arrival on a site, the tree dbh, and the total ash tree dbh in the surrounding 100 m^2, models were constructed to assess the relationship between *H. fraxineus* spore density in 2019 and colonisation of *F. excelsior* rachises in the litter layer in 2020, and the relationship between the colonisation of these rachises and *F. excelsior* crown dieback severity. Additionally, laboratory experiments using water agar examined the effects of water availability (solute potential) and temperature on *H. fraxineus* ascospore germination. It was hypothesised that *F. excelsior* crown dieback would be positively related to *H. fraxineus* rachis colonisation in the litter layer, and that higher *H. fraxineus* spore density in 2019 (Chapter 3) would be associated with a greater colonisation of rachises by *H. fraxineus* in the litter layer in 2020. *H. fraxineus* ascospore germination was expected to occur across a wide range of temperatures, but to be sensitive to changes in solute potential of media, as is true for other ascomycete foliar pathogens (Kettlewell et al., 2000; Huang et al., 2003; Trapero-Casas and Kaiser, 2007).

4.2 Methods

4.2.1 Factors affecting *F. excelsior* crown dieback and estimated leaf infection

4.2.1.1 Field sites

The proportion of previous seasons' rachis length in the litter layer colonised by *H. fraxineus* was measured on 6 of 7 sites (Table 4.1) that were used to quantify *H. fraxineus* ascospore density in summer 2018 and 2019 (Chapter 3; Figure 3.1), and the percentage *F. excelsior* crown dieback was examined on all 7 sites (Table 4.1).

4.2.1.2 *F. excelsior* crown dieback assessment

The percentage of crown dieback was estimated for the closest 12 *F. excelsior* trees (or 13 at County Durham location B and Shropshire location C) to spore traps that had canopy within at least approximately 25 m of the spore trap, and had diameter at breast height (dbh) greater than 10 cm. Trees were classified as having either minimal (0-4% crown dieback), low (5-24% crown dieback), medium (25-49% crown dieback), high (50-74% crown dieback), or very high crown dieback (75-100% crown dieback) (Supplementary Figure 4.1). This was conducted at each of the 4 spore trap locations within Carmarthenshire, Devon, Hampshire, Northumberland and Shropshire sites, at each of the 3 spore trap locations within Wiltshire site as well as at quadrat location B used to monitor apothecia development in Chapter 2, but only at 2 locations at the site in County Durham because *F. excelsior* at locations C and D were dominated by juvenile trees with dbh < 10 cm. Assessments were conducted at all sites in summer 2020, except for location A at Hampshire site which was assessed during summer 2019 (Table 4.1) because of tree felling at this location after spore trapping in 2019.

Table 4.1 Details of locations and dates where *F. excelsior* crown dieback was assessed (Section 4.2.1.2) and *H. fraxineus* foliar colonisation was estimated from the litter layer (Section 4.2.1.3).

Site	Grid ref.	*Estimated year of disease arrival	Woodland classification	*F. excelsior* litter collection and crown dieback assessment
County Durham (Hedley Hall Woods)	NZ218559	2014	*F. excelsior* plantation	A**, B** (05/08/20 [CL])
Shropshire (The Highfields)	SJ688275	2015	*F. excelsior* plantation	A, B, C, D (25/07/20 [CL])
Devon (Penstave Copse)	SX691611	2016	*F. excelsior* plantation	A, B**, C, D** (31/07/20 [CL])
Wiltshire (Colerne Park and Monks Wood)	ST837723	2014	Natural mixed broadleaved woodland	A, B, C, QB** (09/07/20 [CL])
Hampshire (Alice Holt Forest)	SU802401	2014	*Quercus* spp./ *F. excelsior* plantation	A (15/08/19[C]; 10/07/20[L]) B, C, D (10/07/20 [CL])
Carmarthenshire (National Botanic Gardens of Wales)	SN518179	2013	Natural mixed broadleaved woodland	A, B, C, D (12/08/20[C]; 05/09/20[L])
Northumberland (Nunsbrough Wood)	NY950595	2014	Natural mixed broadleaved woodland	A, B**, C, D (04/08/20 [CL])

*The estimated year of disease arrival is calculated from the first year *H. fraxineus* was recorded within 50 km of the site (Fera, 2021; Section 4.2.1.4).**Maximum *H. fraxineus* ascospore density in summer 2019 (Chapter 3) could not be estimated due to missing data (Section 4.2.1.4; Section 4.2.1.5).[C] date of crown dieback assessment and [L] date of litter collection for foliar colonisation estimate.

4.2.1.3 *F. excelsior* foliar colonisation estimates

F. excelsior foliar colonisation was estimated by measuring the proportion of the previous seasons' rachis length in the litter layer that was colonised by *H. fraxineus*. All rachises, or rachis segments were collected from a 20 x 20 cm area under the canopy of the closest eight *F. excelsior* trees that were within at least 20 m of each spore trap location. Wiltshire location quadrat B was also sampled, with the quadrat where apothecia development was monitored in 2018 and 2019 (Chapter 2) as the focal point for sampling, rather than a spore trap location. As trees were felled at Hampshire location A following spore trapping in 2019, sampling occurred at nine separate locations within 20 m of the spore trap location. If 30 rachis segments were not collected from a 20 x 20 cm area under a given tree, the sampling area was extended until this was achieved. Litter collections occurred at all sites during summer 2020 (Table 4.1), and rachises were stored at 4°C until assessment. Thirty rachis segments were randomly selected from the collected litter for measurement of the total length of rachis, and the length covered by a black pseudosclerotial plate, which is characteristic of *H. fraxineus* colonisation of *F. excelsior* rachises (Section 2.3.1; Kowalski and Bilański 2021).

4.2.1.4 Environmental variables

(1) The dbh of assessed tree, (2) the maximum ascospore density in 2019, (3) the density of *F. excelsior* trees and (4) the estimated time of disease arrival were recorded at *F. excelsior* foliar colonisation and crown dieback assessment locations.

(1) The dbh was recorded for each tree assessed for crown dieback and for estimated foliar colonisation. (2) The ascospore density was estimated throughout summer 2019 (June or July – September 2019; Chapter 3) via operation of FRAXTRAPs and subsequent real-time PCR quantification of *H. fraxineus* ascospores (Section 3.2). This was not conducted at the County Durham site and Wiltshire location quadrat B due to lack of volunteer availability. (3) At each location where ascospore density was monitored throughout summer 2019, the total dbh of *F. excelsior* trees within a 100 m^2 area surrounding spore trap location were measured. (4) The time of disease arrival on sites was estimated from data on the year of the first official *H. fraxineus* record on a 10 x 10 km grid resolution (Fera, 2021). However, the date of determination of arrival of *H. fraxineus* is dependent on the intensity of sampling in a 10 x 10 km grid square. To reduce this error, the disease arrival at a site was estimated by using the earliest arrival date less than 50 km from the site because the disease has been estimated to spread at a rate of approximately 30-70 km per year (Enderle et al., 2019).

4.2.1.5 Statistical analyses

All data were analysed using R software version 4.1.1 stats (R Core Team, 2021), lme4 (Bates et al., 2015), glmmTMB (Brooks et al., 2017), qpcR (Spiess et al., 2018), car (Fox and Weisburg, 2019), emmeans (Length, 2021), merTools (Knowles and Frederick, 2020), DHARMa (Hartig, 2021), ggplot2 (Wickham, 2016) packages. Generalised linear mixed models with binomial distribution and logit function were used to assess the variables affecting crown dieback. Separate models were constructed with four response variables; (1) probability of crown dieback 5-100% (≥ 5%), (2) probability crown dieback 25-100% (≥ 25%), (3) probability crown dieback 50-100% (≥ 50%) and (4) probability crown dieback 75-100% (≥ 75%). Models were constructed using assessment location within a site and the site as random effects to account for unexplained inter- and intra-site variation. Assessment location was specified as being nested within respective sites, thereby allowing the assessment of variables at the inter- and intra-site scale. Maximal models were constructed using the total proportion of previous seasons' rachis length in the litter layer that were colonised by *H. fraxineus* in 2020 at a sampling location, the dbh of assessed trees, the total dbh of *F. excelsior* trees within 100 m^2 of a spore trap, and the estimated time of disease arrival as explanatory variables (Section 4.2.1.4). Continuous explanatory variables were scaled by subtracting the mean and dividing by the standard deviation from a given value, which allowed the modelling of variables on different scales. Removal of non-significant effects from models was conducted, using type II Wald chisquare tests and $p < 0.05$ as a threshold for significance. Variables with the highest p value were removed in a stepwise approach. The variance explained by fixed effects in the final model containing only significant variables was represented using marginal R^2 values, and the variance explained by both fixed effects and random effects was represented using conditional R^2 values (Nakagawa and Schielzeith, 2013)

Generalised linear mixed effects models with beta distribution and logit function were used to assess conditions affecting the proportion of previous seasons' rachis length in the litter layer colonised by *H. fraxineus*. As described above, assessment location and site were specified as random effects to account for unexplained intra- and inter-site variation, and the assessment location was specified as nested within the respective site so the effect of explanatory variables could be examined at the intra- and inter-site scale. Maximal models were constructed using the maximum ascospore density recorded at a sampling location in 2019, the dbh of assessed trees, the total dbh of *F. excelsior* within 100 m^2 of a spore trap, and the estimated time of disease arrival as explanatory variables (Section 4.2.1.4). Continuous explanatory variables were scaled by subtracting the mean and dividing by the standard deviation from a given value, which allowed the modelling of variables on different scales. Removal of non-significant effects from models was conducted using type II Wald chisquare tests and $p < 0.05$ as a threshold for significance.

Data at Northumberland location B and Devon locations B and D were removed from analysis as ascospore density was not monitored weekly from mid-July to mid-August 2019, therefore the maximum ascospore density in 2019 could not be reliably determined.

AICc (Section 2.2.6) values of the final and null generalised linear mixed effects models were calculated, and likelihood ratio test used to assess whether the final model fitted the data significantly better the model containing only the random effects (Lewis et al., 2011).

The effect size of significant variables in models was examined by estimating the marginal mean from the fitted models of the response variable on the response scale at values of recorded explanatory variables.

4.2.2 Factors affecting *H. fraxineus* ascospore germination

4.2.2.1 Effect of temperature on ascospore germination

F. excelsior rachises with a black pseudosclerotial plate, which is characteristic of *H. fraxineus* colonisation (Section 2.3.1; Kowalski and Bilański 2021), were collected from Alice Holt Forest in September 2020. These were dipped in distilled water, then placed in clear plastic containers lined with wet paper towels sealed within clear plastic sampling bags next to the window, to create humid conditions in the presence of light, which are conducive for *H. fraxineus* apothecia formation.

Approximately 10 weeks after incubation of *H. fraxineus* colonised rachises, portions of rachis containing mature apothecia were placed in glass Petri dishes lined with wet filter paper to create humid conditions conducive for ascospore release. Sterile glass coverslips were balanced on paperclips no more than 0.5 cm above apothecia and left overnight, so that ejected spores would stick to the underside of glass coverslips. Glass coverslips with spores attached were then transferred onto 1.5 ml water agar (WA) (Supplementary Table 4.1), on sterile glass microscope slides, and incubated at either 5°C (n = 12), 10°C (n = 12), 15°C (n = 12), 20°C (n= 12), 25°C (n = 12), 30°C (n=12) or 35°C (n = 12). The 1.5 ml water agar slides were kept within Petri dishes sealed with parafilm to minimise moisture loss, and were incubated for 3 days at respective experimental temperatures prior to the transfer of spores.

Germination was assessed either daily, or on alternate days, to enable sufficient time for maximum ascospore germination, whilst ensuring that germ tubes did not overgrow spores, which would compromise the accuracy of germination assessments. Ascospore germination was assessed using Olympus BX53 microscope (Olympus, Tokyo, Japan) for a total of 100 spores per spore print, with 50 spores assessed along two

separate linear planes at two locations on the slide to prevent duplicate counts. If 100 spores could not be counted, counts were used from one linear plane with 50 spores. Spores were classified as germinated if they possessed a germ tube which was longer than the width of the spore.

4.2.2.2 Effect of solute potential on ascospore germination

H. fraxineus colonised *F. excelsior* rachises were collected from Alice Holt Forest in January 2021, and incubated in the laboratory under humid conditions in the presence of light to produce apothecia (Section 4.2.2.1). Approximately 10 weeks after incubation of *H. fraxineus* colonised rachises, ascospores were collected under humid conditions on sterile glass coverslips (Section 4.2.2.1) for 4 hours in the morning. Glass coverslips were then transferred to approximately 10 ml of WA that had been amended with 22.37, 44.73, 67.10, 89.46, or 119.28 g KCl L^{-1} prior to autoclaving to produce respective solute potentials of -1.35 MPa (n = 12), -2.68 MPa (n = 11), -4.01 MPa (n = 12), -5.36 MPa (n = 12) and -7.01 MPa (n = 12) at 25°C (Robinson and Stokes, 1959). Glass coverslips were also transferred to 10 ml WA unamended with KCl (n = 12). Petri dishes were sealed with parafilm to minimise moisture loss and were incubated for 3 days at 25°C prior to the transfer of spores. Ascospore germination was assessed (Section 4.2.2.1) 5, 12 and 27 days after the start of incubation (dasi). Spores on WA unamended with KCl were also assessed 6 dasi for comparison with Section 4.2.2.1 (see Section 4.2.2.4 and Section 4.2.2.5).

4.2.2.3 Effect of assessment approach on ascospore germination

H. fraxineus colonised rachises that had apothecia were collected from Alice Holt Forest in August 2021 and incubated in the laboratory under humid conditions in the presence of light (Section 4.2.2.1), to ensure apothecia were sufficiently mature to eject ascospores. Approximately 2 weeks after incubation, ascospores were collected overnight on glass coverslips under humid conditions (Section 4.2.2.1) and transferred onto approximately 10 ml WA in Petri dishes (n = 9) (Section 4.2.2.2) or 1.5 ml WA on sterile glass microscope slides (n = 7) (section 4.2.2.1) and incubated at 30°C. Germination was assessed (Section 4.2.2.1) 6 dasi.

4.2.2.4 Germination of ascospores from apothecia produced under different conditions

Germination success 6 dasi was compared at 30°C between ascospores that were collected from laboratory produced apothecia in Section 4.2.2.1 and field produced apothecia in Section 4.2.2.3. Germination success 6 dasi also was compared at 25°C between ascospores that were collected from laboratory produced apothecia in Section 4.2.2.1 (incubated October – December 2020) and Section 4.2.2.2 (incubated January – March 2021).

4.2.2.5 Statistical analyses

All data were analysed using R software version 4.1.1 stats (R Core Team, 2021), emmeans (Length, 2021), car (Fox and Weisburg, 2019), DHARMa (Hartig, 2021), ggplot2 (Wickham, 2016) packages. The conditions affecting the probability of *H. fraxineus* ascospore germination were assessed using generalised linear models with a quasibinomial distribution and logit function. Treatments with no ascospore germination were removed from analysis and germination 6 dasi was used as the dependent variable for the temperature effect experiment (Section 4.2.2.1) because this was the last day that ascospore germination could reliably be determined at 20°C and 25°C due to density of hyphae. Significance of variables was assessed using type II Wald chisquare tests and $p < 0.05$ as a threshold for significance. *Post hoc* analysis of significant variables with more than 2 treatments were conducted on the estimated marginal means of treatments on the log odds ratio scale, and using Tukey's method for calculation of p values, with $p < 0.05$ as a threshold for significance.

4.3 Results

4.3.1 Factors affecting *F. excelsior* crown dieback

F. excelsior crown dieback varied considerably both within and between sites (Figure 4.1). For example, 0/45 trees at Shropshire site had crown dieback ≥ 75%, and 5/45 had crown dieback ≥ 50%. In contrast, 8/33 trees at Hampshire site had crown dieback ≥ 75% and 17/33 had crown dieback ≥ 50%. Of the latter, 7 out of 7 were at location A, 6 out of 9 were at location D, 4 out of 8 were at location B, and 0 out of 9 were at location C.

Binomial general linear mixed models could only be fitted with the dependent variable as (1) the probability of *F. excelsior* crown dieback ≥ 5%, or (2) the probability of *F. excelsior* crown dieback ≥ 25%, but models would not converge with the dependent

variable as (3) probability of crown dieback ≥ 50% or (4) probability of crown dieback ≥ 75%. Stepwise deletion of non-significant effects from models that were constructed with (1) the probability crown dieback 5% as the dependent variable removed all explanatory variables. However, models constructed with (2) the probability of crown dieback ≥ 25% as the dependent variable revealed that the tree dbh (Chisq = 5.61, df = 1, $p < 0.05$) and the proportion of *H. fraxineus* colonised rachis material in an assessment area (Chisq = 11.17, df = 1, $p < 0.001$) significantly affected the probability of crown damage ≥ 25% (Table 4.2; Figure 4.2). Decreasing tree dbh and increasing the proportion of *H. fraxineus* colonised rachis material both increased the probability of crown dieback ≥ 25%. Indeed, at 55 cm dbh the estimated marginal mean of the probability of crown dieback ≥ 25% increased from 0.147 (df = ∞, se = 0.067) at 0.6 proportion of rachis colonised by *H. fraxineus* to 0.529 (df = ∞, se = 0.120) at 0.9 proportion of rachis colonised by *H. fraxineus*. At 25 cm dbh the estimated marginal mean of the probability of crown dieback ≥ 25% increased from 0.300 (df = ∞, se = 0.089) at 0.6 proportion of rachis colonised by *H. fraxineus* to 0.736 (df = ∞, se = 0.066) at 0.9 proportion of rachis colonised by *H. fraxineus* (Figure 4.3).

4.3.2 Factors affecting *F. excelsior* rachis colonisation by *H. fraxineus*

H. fraxineus colonisation of rachis material was very high, with 89% of the rachises sampled (5898 of 6597) showing evidence of *H. fraxineus* colonisation. Of these, 40% of rachises (2359) were completely colonised, 70% (4130) had a colonised proportion greater than 0.90, 83% (4874) had a colonised proportion greater than 0.75, and 93% (5484) had a colonised proportion greater than 0.50. *H. fraxineus* colonisation was always detected on at least one of the rachises sampled under every *F. excelsior* tree. The summed proportion of *H. fraxineus* colonisation for the rachises sampled under a given tree was greater than 0.90 for 78/221 sampled trees, greater than 0.75 for 158/221, greater than 0.50 on 210/221, with a minimum value of 0.22 for tree 3 at Shropshire location B. *H. fraxineus* colonisation of rachis material varied both within and between sites (Figure 4.4). For example, the overall proportion of *H. fraxineus* colonisation at Northumberland site ranged from 0.85 at location D, to 0.62 at location B, and at the Wiltshire site, from 0.94 at location A to 0.78 at location C.

Stepwise reduction of non-significant effects from beta regression mixed models revealed that the dbh of a sampled tree (Chisq = 6.79, df = 1, $p < 0.01$) and the maximum ascospore density recorded in 2019 (Chisq = 8.27, df = 1, $p < 0.01$) was significantly related to the proportion of *F. excelsior* rachises colonised by *H. fraxineus* (Table 4.3; Figure 4.4). Decreasing dbh of a tree and increasing maximum ascospore density in 2019 was associated with increased *F. excelsior* rachis colonisation in the litter layer in 2020. At

55 cm dbh the proportion of *H. fraxineus* colonisation of rachises increased from 0.687 (df = 151, se = 0.048) at 200 *H. fraxineus* ascospores m^{-3} to 0.774 (df = 151, se = 0.035) at 1200 *H. fraxineus* ascospores m^{-3}. At 25 cm dbh the estimated marginal mean of the proportion of *H. fraxineus* colonisation of rachises increased from 0.759 (df = 151, se= 0.035) at 200 *H. fraxineus* ascospores m^{-3} to 0.830 (df = 151, se = 0.024) at 1200 *H. fraxineus* ascospores m^{-3} (Figure 4.5).

Table 4.2 The generalised linear mixed effects model of the probability of *F. excelsior* crown dieback in 2020 ≥ 25% fitted with binomial distribution and logit function and containing only significant explanatory variables (Section 4.2.1; Section 4.3.1. The variance of random effects denotes the intra- and inter-site variability in the model. P values of the fixed effects were calculated using type II Wald chisquare tests, AICc value (Section 2.2.6) for the Final crown dieback model is presented with the AICc value of the model containing only random effects, a likelihood ratio test is used to compared the goodness of fit between these models, and R^2 values are provided as a measure of the variance explained by the final model (Section 4.2.1.5). The full model is presented above the table.

Final crown dieback model <- Probability of crown dieback ≥ 25% ~ scale(the proportion of rachis length in the litter layer colonised by H. fraxineus in 2020) + scale(diameter at breast height of assessed tree) + (1 | Site/Assessment Location)

Fixed Effects	**Type II Wald chisquare test**	**Random Effects**	**Variance (Std. Dev)**	**AICc (random effects model AICc)**	**Likelihood ratio test**	**Marginal R^2/ Conditional R^2**
Proportion of rachis length in the litter layer colonised by *H. fraxineus* in 2020	p < 0.001 (Chisq = 11.2, df = 1)	Site	0.1696 (0.4118)	345.7 (358.4)	p < 0.001 (Chisq = 16.7, df = 2)	0.18/ 0.31
Diameter at breast height of assessed tree	p < 0.05 (Chisq = 5.61, df = 1)	Assessment location	0.4606 (0.6787)			

Table 4.3 The generalised linear mixed effects model of the proportion of previous seasons' rachis length in the litter layer colonised by *H. fraxineus* in 2020 fitted with binomial distribution and logit function and containing only significant explanatory variables (Section 4.2.1; Section 4.3.2). The variance of random effects denotes the intra- and inter-site variability in the model. P values of the fixed effects were calculated using type II Wald chisquare tests, AICc value (Section 2.2.6) for the Final crown dieback model is presented with the AICc value of the model containing only random effects, and a likelihood ratio test is used to compared the goodness of fit between these models (Section 4.2.1.5). The full model is presented above the table.

Final rachis colonisation model <- Proportion of H. fraxineus rachis colonisation ~ scale(maximum ascospore density in 2019) + scale(diameter at breast height of assessed tree) + (1 | Site/Assessment Location)

Fixed effects	Type II Wald Chisquare Test	Random effects	Variance (Std. Dev)	AICc (random effects model AICc)	Likelihood ratio test
Maximum ascospore density in 2019	p < 0.01 (Chisq = 8.3, df = 1)	Site	0.0790 (0.2810)	-251.4 (-242.7)	p < 0.01 (Chisq = 12.7, df = 2)
Diameter at breast height of assessed tree	P < 0.01 (Chisq = 6.8, df = 1)	Assessment location	0.1857 (0.4309)		

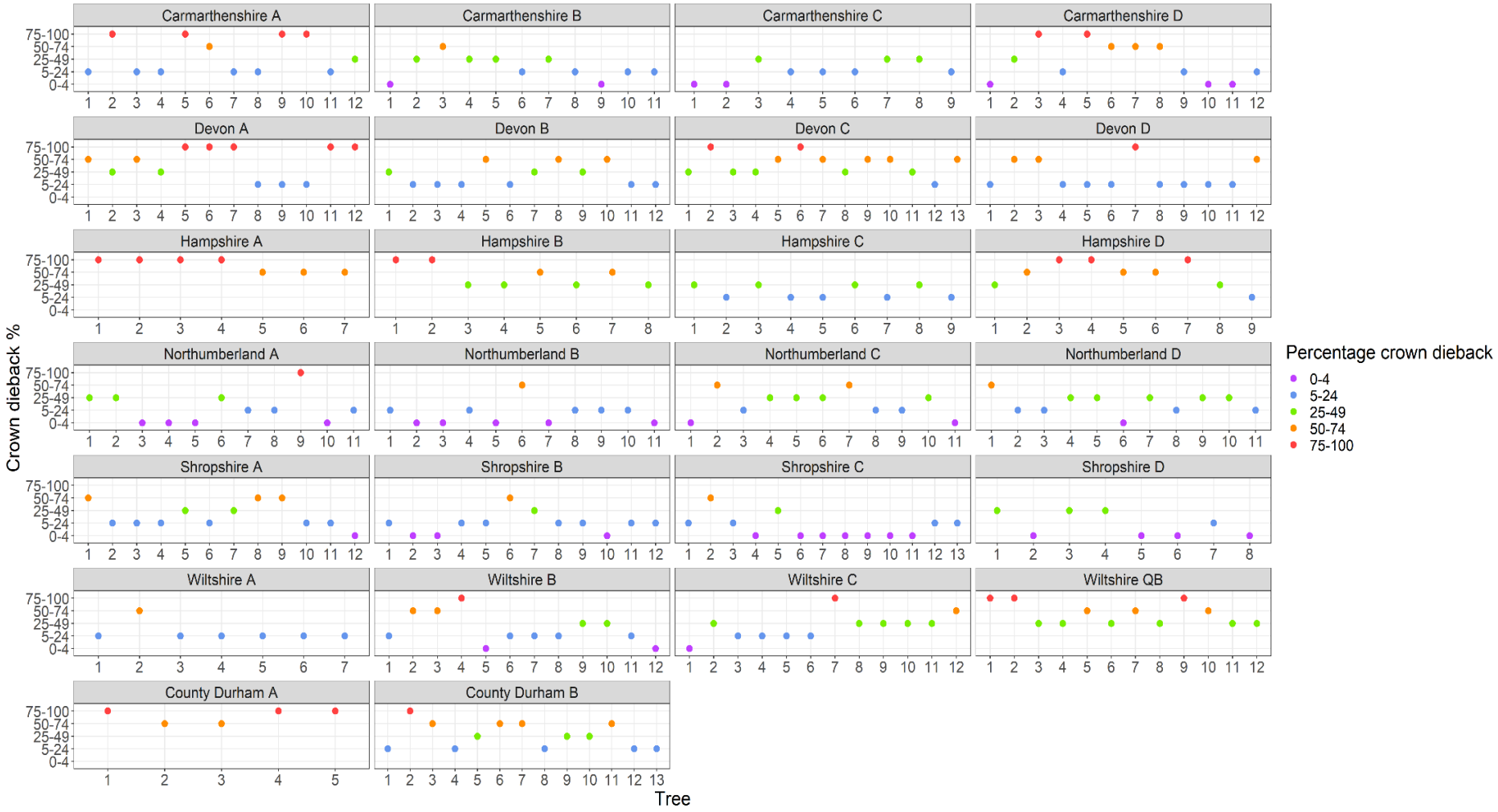

Figure 4.1 *F. excelsior* (dbh > 10 cm) crown dieback for trees (closest 12 trees (or 13 at Shropshire C and County Durham C) to spore trap) with canopy within 25 m of different locations (A, B, C, D, QB) at 7 sites (Carmarthenshire, Devon, Hampshire, Northumberland, Shropshire, Wiltshire and County Durham) assessed in July-August 2020 (Section 4.2.1.2; Table 4.1). The colour of each datapoint represents the classification of crown dieback; 0-4%, 5-24%; 25-49%; 50-74%; 75-100%.

(a)

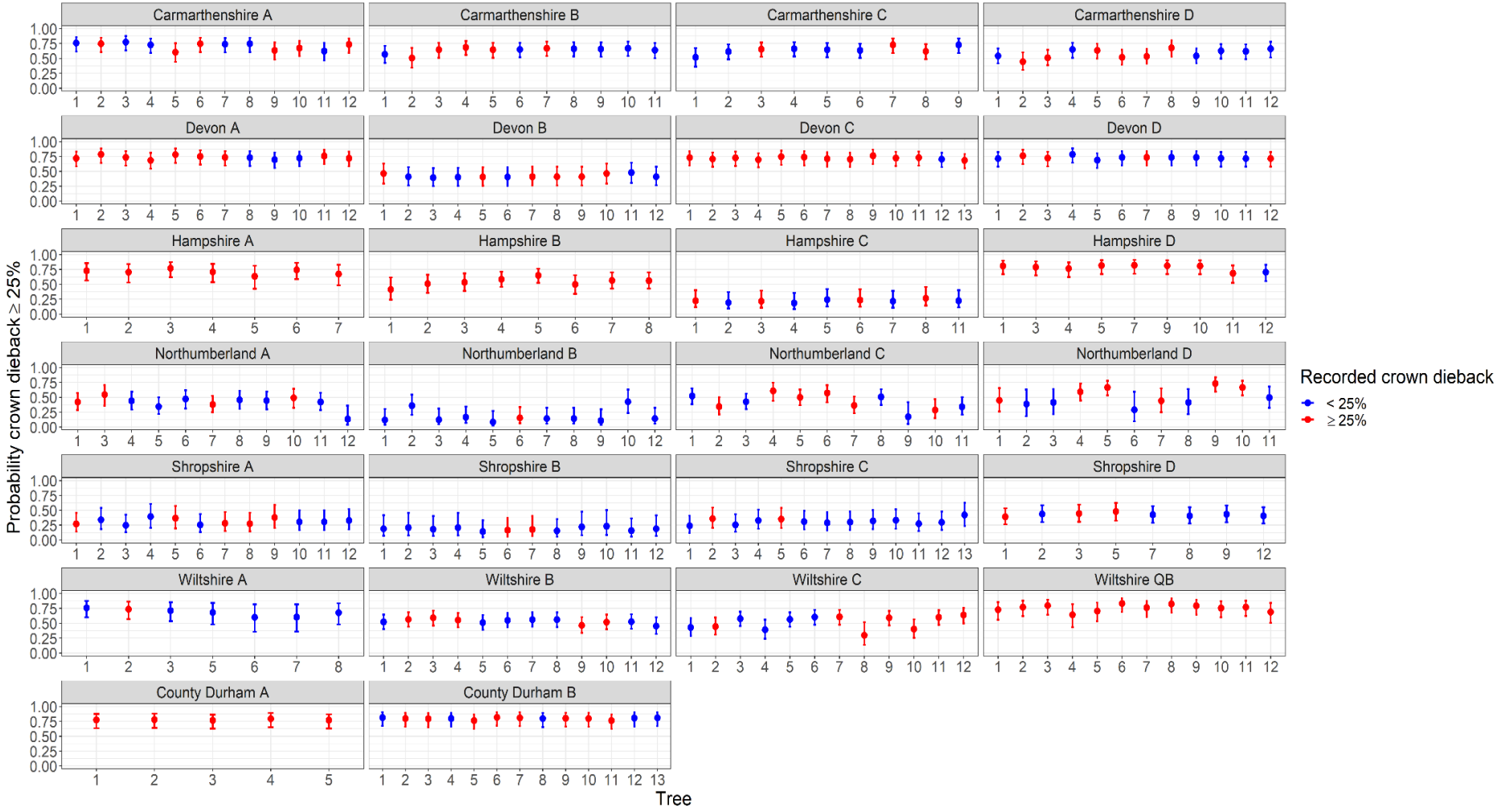
Carmarthenshire A
Carmarthenshire B
Carmarthenshire C
Carmarthenshire D
Devon A
Devon B
Devon C
Devon D
Hampshire A
Hampshire B
Hampshire C
Hampshire D
Northumberland A
Northumberland B
Northumberland C
Northumberland D
Shropshire A
Shropshire B
Shropshire C
Shropshire D
Wiltshire A
Wiltshire B
Wiltshire C
Wiltshire QB
County Durham A
County Durham B
Probability crown dieback ≥ 25%
Tree
Recorded crown dieback
< 25%
≥ 25%

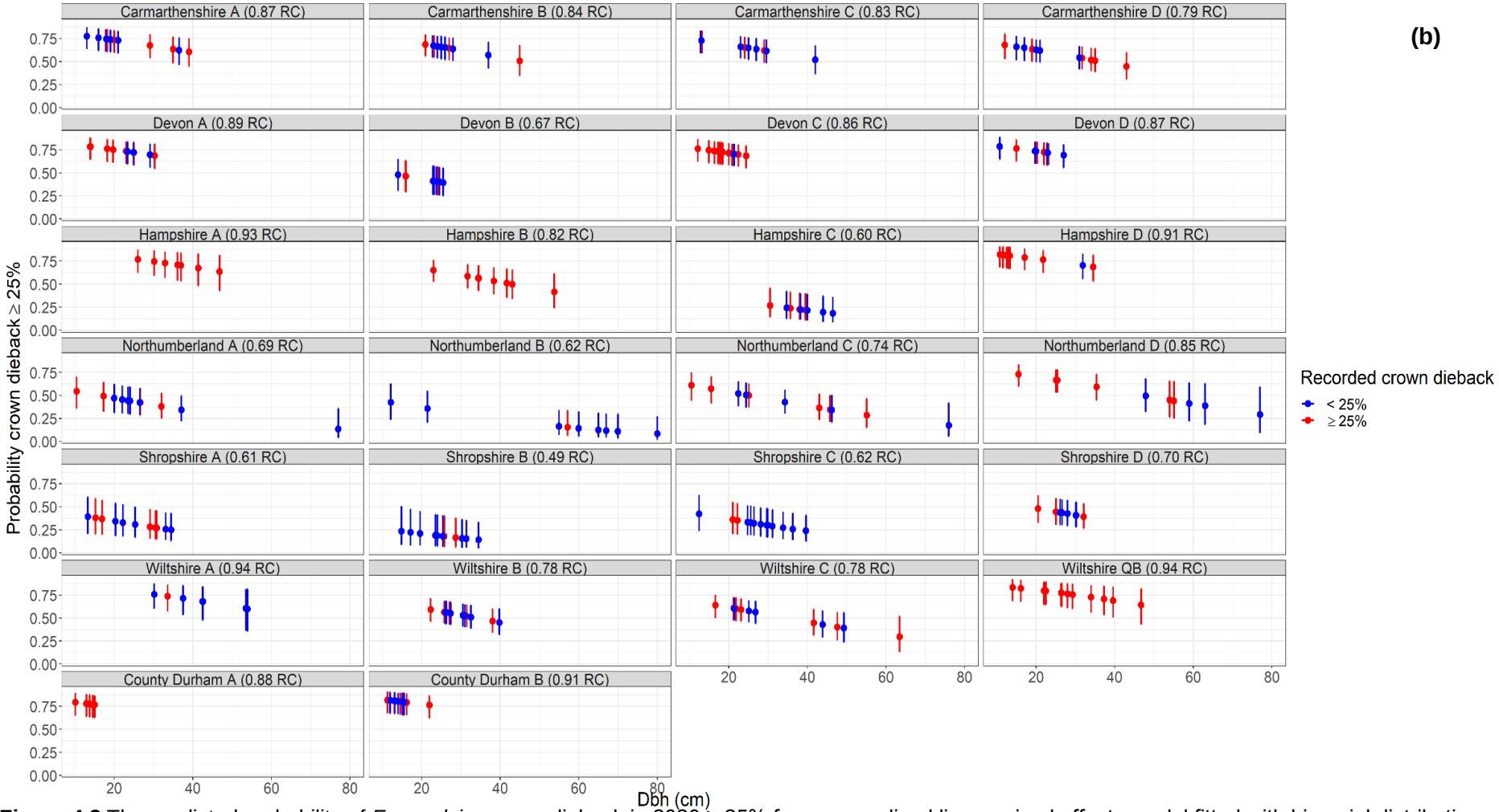

Figure 4.2 The predicted probability of *F. excelsior* crown dieback in 2020 ≥ 25% from generalised linear mixed effects model fitted with binomial distribution and logit function containing only significant explanatory variables (the dbh of an assessed tree (Chisq = 5.61, df = 1, $p < 0.05$); the proportion of previous seasons' rachis length in the litter layer that was colonised by *H. fraxineus* in 2020 (Chisq = 11.17, df = 1, $p < 0.001$)) (Section 4.2.1; Section 4.3.1; Table 4.2). The sites (Carmarthenshire, Devon, Hampshire, Northumberland, Shropshire, Wiltshire or County Durham) and assessment locations (A, B, C, D or QB) were included in models as random effects to account for unexplained intra- and inter-site variation. The assessment location was specified as nested within a site to allow the analysis of variables at the intra- and inter-site scale (Section 4.2.1.5). **(a)** The predicted probability (with 95% confidence intervals) of *F. excelsior*

crown dieback ≥ 25% for each assessed tree, with the colour indicating the recorded crown dieback. **(b)** with the dbh of each assessed tree and the proportion of previous seasons' rachis length in the litter layer that was colonised by *H. fraxineus* in 2020 displayed for each location (RC) (A, B, C, D, QB).

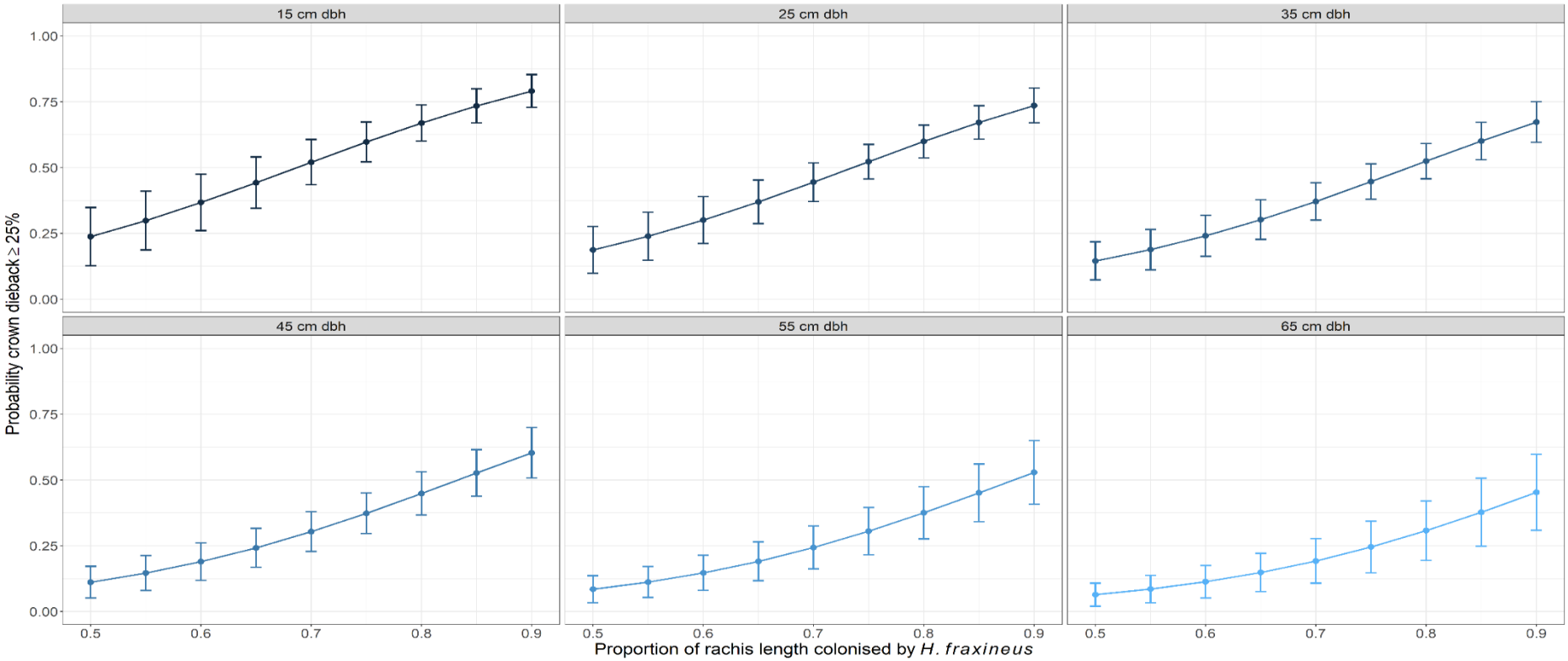

Figure 4.3 The estimated marginal mean (with standard error bars) across a measured range of the explanatory variables, from generalised linear mixed effects model fitted with binomial distribution and logit function of the probability of *F. excelsior* crown dieback in 2020 ≥ 25%. The model contains only significant explanatory variables (the dbh of an assessed tree (Chisq = 5.61, df = 1, $p < 0.05$); the proportion of previous seasons' rachis length in the litter layer that was colonised by *H. fraxineus* in 2020 (Chisq = 11.17, df = 1, $p < 0.001$)) (Section 4.2.1; Section 4.3.1; Table 4.2).

(a)

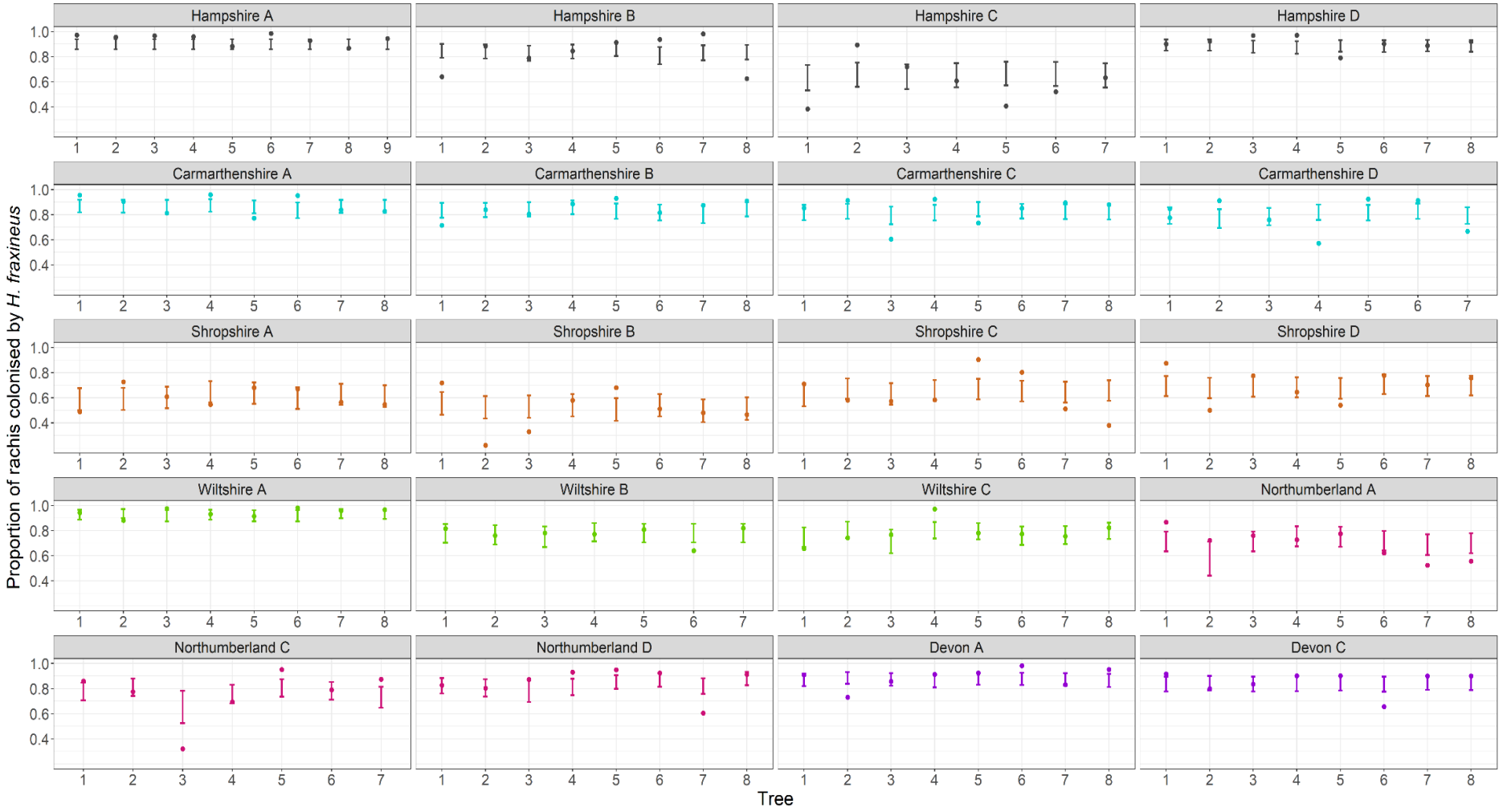
Hampshire A
Hampshire B
Hampshire C
Hampshire D
Carmarthenshire A
Carmarthenshire B
Carmarthenshire C
Carmarthenshire D
Shropshire A
Shropshire B
Shropshire C
Shropshire D
Wiltshire A
Wiltshire B
Wiltshire C
Northumberland A
Northumberland C
Northumberland D
Devon A
Devon C
Proportion of rachis colonised by H. fraxineus
Tree

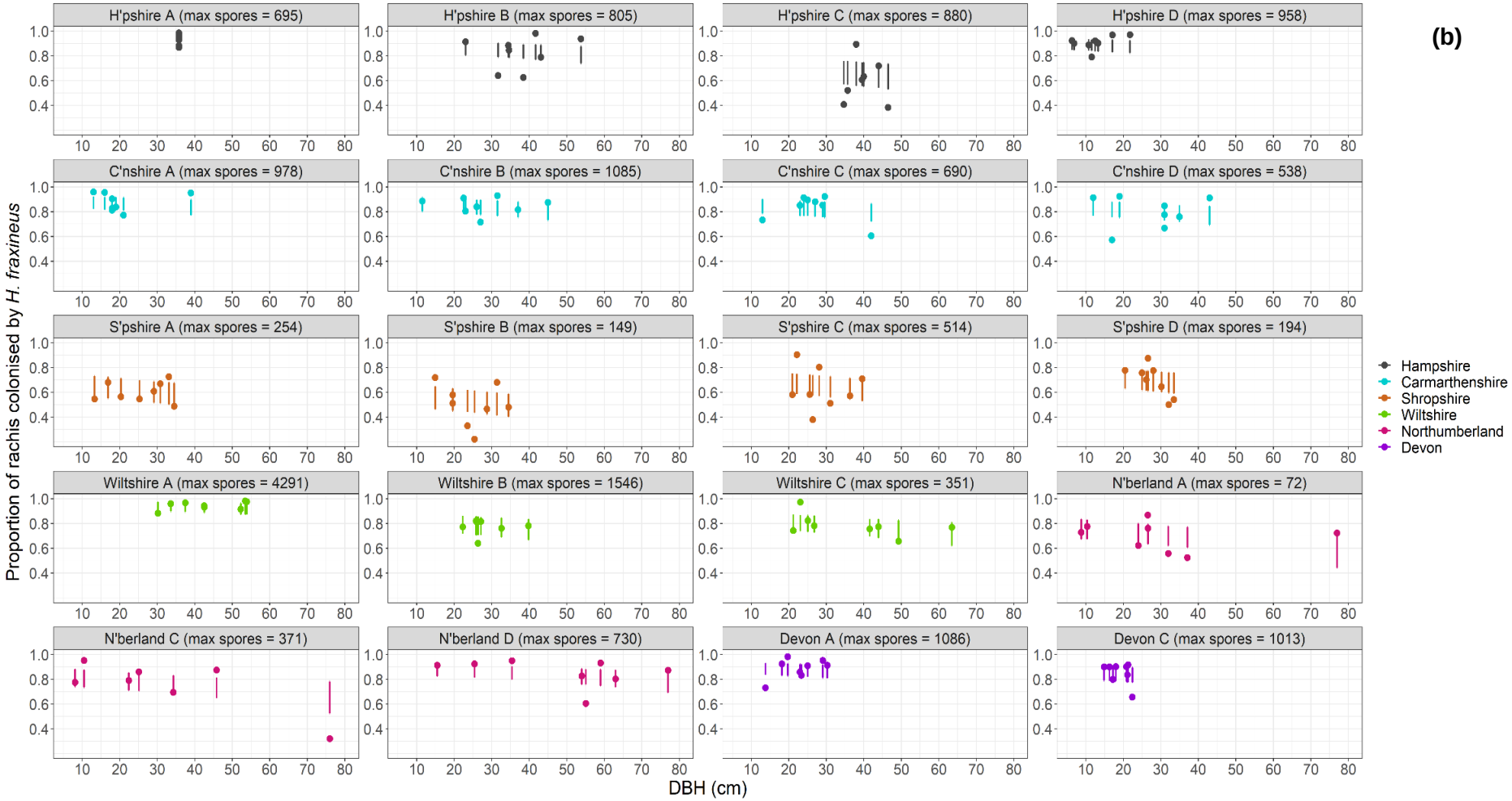

Figure 4.4 The predicted proportion of previous seasons' rachis length in the litter layer colonised by *H. fraxineus* in 2020 from generalised linear mixed effects model fitted with binomial distribution and logit function containing only significant explanatory variables (the dbh of an assessed tree (Chisq = 6.79, df = 1, $p < 0.01$); the maximum ascospore density recorded at a location in 2019 (Chisq = 8.27, df = 1, $p < 0.01$)) (Section 4.2.1; Section 4.3.2; Table 4.3). The sites (Carmarthenshire, Devon, Hampshire, Northumberland, Shropshire, Wiltshire) and assessment location (A, B, C, D) were included in models as random effects to account for unexplained intra- and inter-site variation. The assessment location was specified as nested within a site to allow the analysis of variables at the intra- and inter-site scale (Section 4.2.1.5). **(a)** The recorded proportion of previous seasons' rachis length in the litter layer colonised by *H.*

fraxineus in 2020 is plotted with 95% confidence intervals from model predictions displayed. **(b)** with the dbh of each assessed tree and the maximum *H. fraxineus* ascospore density in 2019 displayed for each location (max spores) (A, B, C, D).

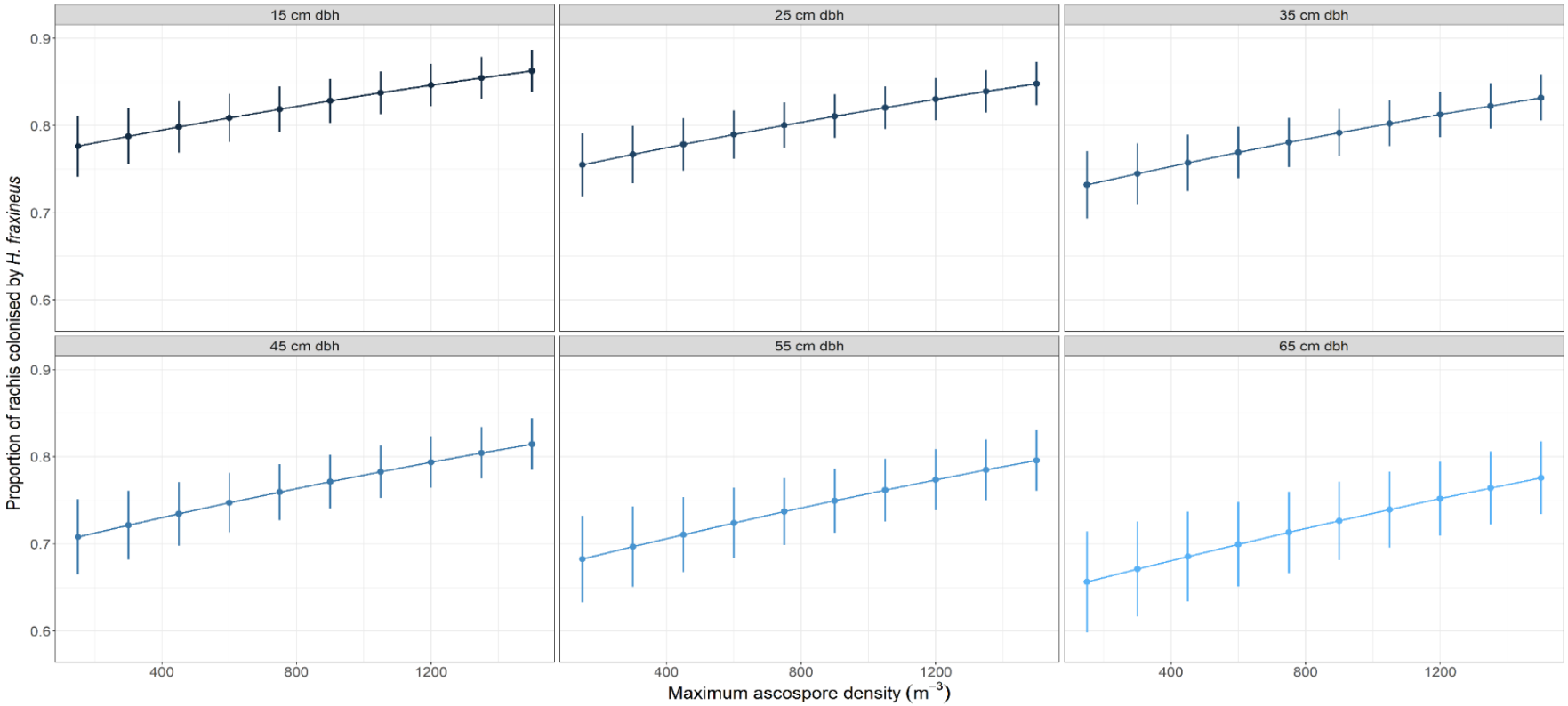

Figure 4.5 The estimated marginal mean (with standard error bars) across a measured range of the explanatory variables, from generalised linear mixed effects model fitted with binomial distribution and logit function of the proportion of previous seasons' rachis length in the litter layer colonised by *H. fraxineus* in 2020. The model contains only significant explanatory variables (the dbh of an assessed tree (Chisq = 6.79, df = 1, $p < 0.01$); the maximum ascospore density recorded at a location in 2019 (Chisq = 8.27, df = 1, $p < 0.01$)) (Section 4.2.1; Section 4.3.2; Table 4.3).

4.3.3 Temperature effects on ascospore germination

Temperature significantly affected ascospore germination (Chisq = 159.66, df = 5, $p < 0.001$), although there was large variation between spores from different apothecia (Figure 4.6). The probability of ascospore germination was greatest between 15°C and 25°C (0.704(±0.040) – 0.724(±0.044)) and no spore germination occurred at 35°C, other than on a very localised patch on one slide.

4.3.4 Solute potential effects on ascospore germination

There was large variation in germination between replicates from different apothecia, however the solute potential significantly affected ascospore germination (Chisq = 182.45, df= 2, $p < 0.001$). Maximum mean germination probability (5 dasi) of 0.453 (±0.057) was on medium whose solute potential had not been adjusted. There was a considerable decrease at -1.35 MPa (mean = 0.046, ±0.021), with no germination at or below -4.01 MPa (Figure 4.7).

4.3.5 Effect of assessment approach on ascospore germination

Ascospore germination was significantly greater (Chisq = 8.58, df = 1, $p < 0.01$) on approximately 10 ml of water agar in Petri dishes (0.975, se = 0.065), than in 1.5 ml of water agar on glass microscope slides (0.783, se = 0.062) (Figure 4.8).

4.3.6 Germination of ascospores from apothecia produced under different conditions

Germination success 6 dasi on 1.5 ml water agar slides at 30°C was significantly greater (Chisq = 29.94, df = 1, $p < 0.001$) for ascospores that were collected from field produced apothecia (0.783, ±0.062) rather than laboratory produced apothecia (0.397, ±0.034) (Figure 4.9).

Germination 6 dasi at 25°C was significantly greater (Chisq = 7.79, df = 1, $p < 0.01$) for laboratory produced apothecia used to investigate the effect of temperature (0.704, ±0.040) (Section 4.2.2.1; Section 4.3.1) compared to laboratory produced apothecia used to investigate the effect of solute potential (0.477, ±0.054) (Section 4.2.2.2; Section 4.3.2) (Figure 4.10).

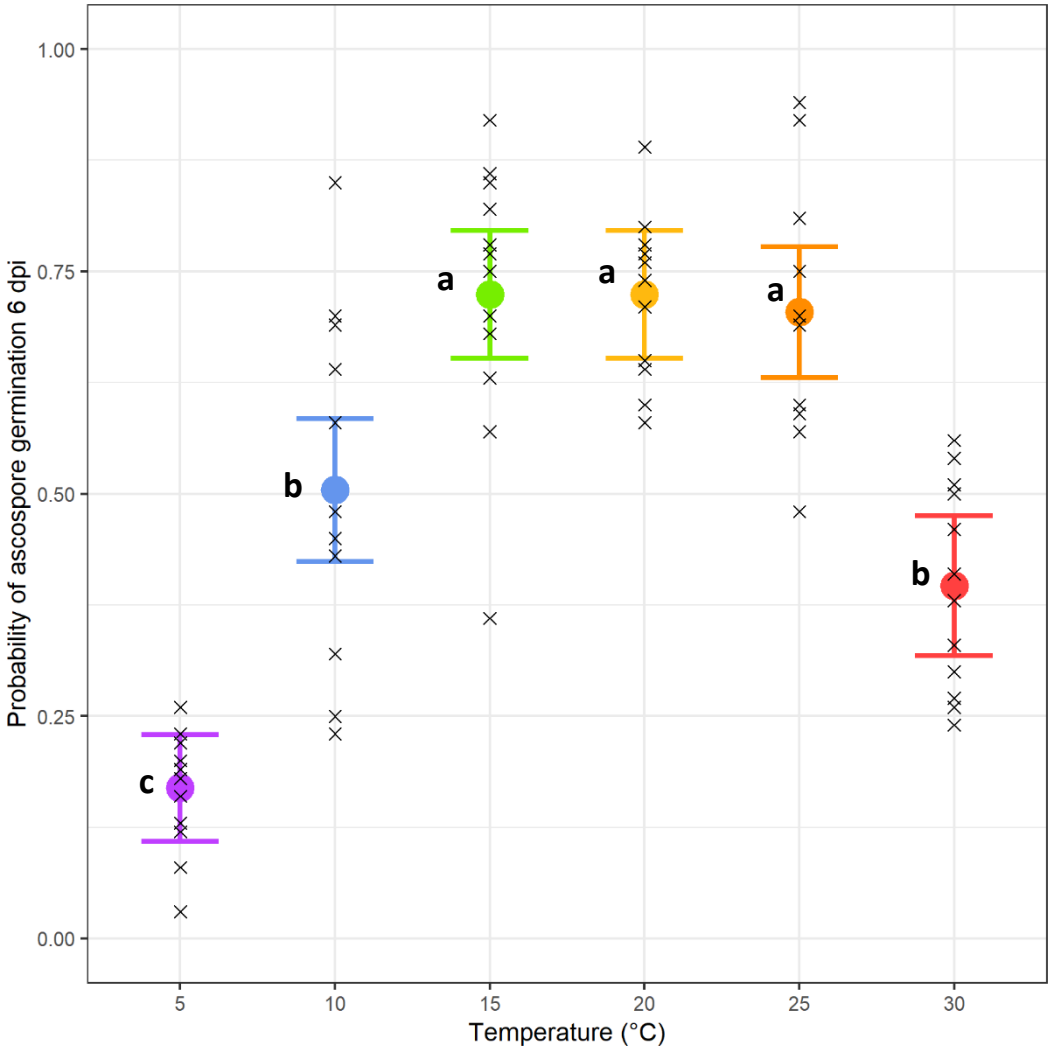

Figure 4.6 The significant effect (Chisq = 159.66, df = 5, p < 0.001) of temperature on *H. fraxineus* ascospore germination 6 days after the start of incubation (dasi) (Section 4.2.2.1; Section 4.3.3). A generalised linear model was fitted with quasibinomial distribution and logit function. Black crosses represent recorded data, the coloured points represent the model prediction, and the 95% confidence intervals are indicated. Significant differences between estimated marginal means of treatments are represented by different letters (Section 4.2.2.5).

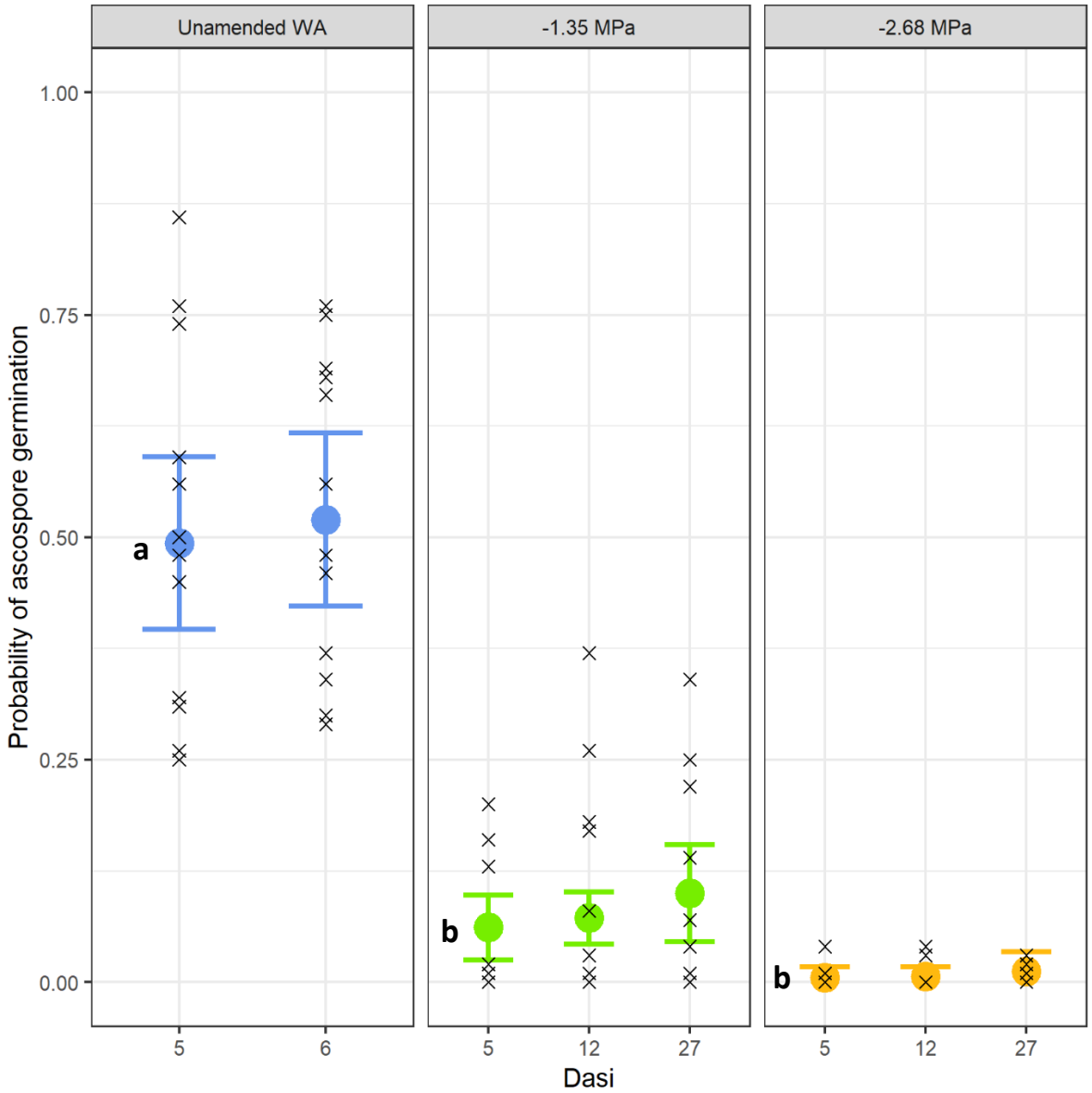

Figure 4.7 The significant effect (Chisq = 182.45, df= 2, p < 0.001) of solute potential on *H. fraxineus* ascospore germination 5, 6, 12, 27 days after the start of incubation at 25°C (dasi) on WA amended with KCl (Section 4.2.2.2; Section 4.3.4). A generalised linear model was fitted with quasibinomial distribution and logit function. Black crosses represent recorded data, the coloured points represent the model prediction, and the 95% confidence intervals are indicated. Significant differences between estimated marginal means of treatments 5 dasi are represented by different letters (Section 4.2.2.5).

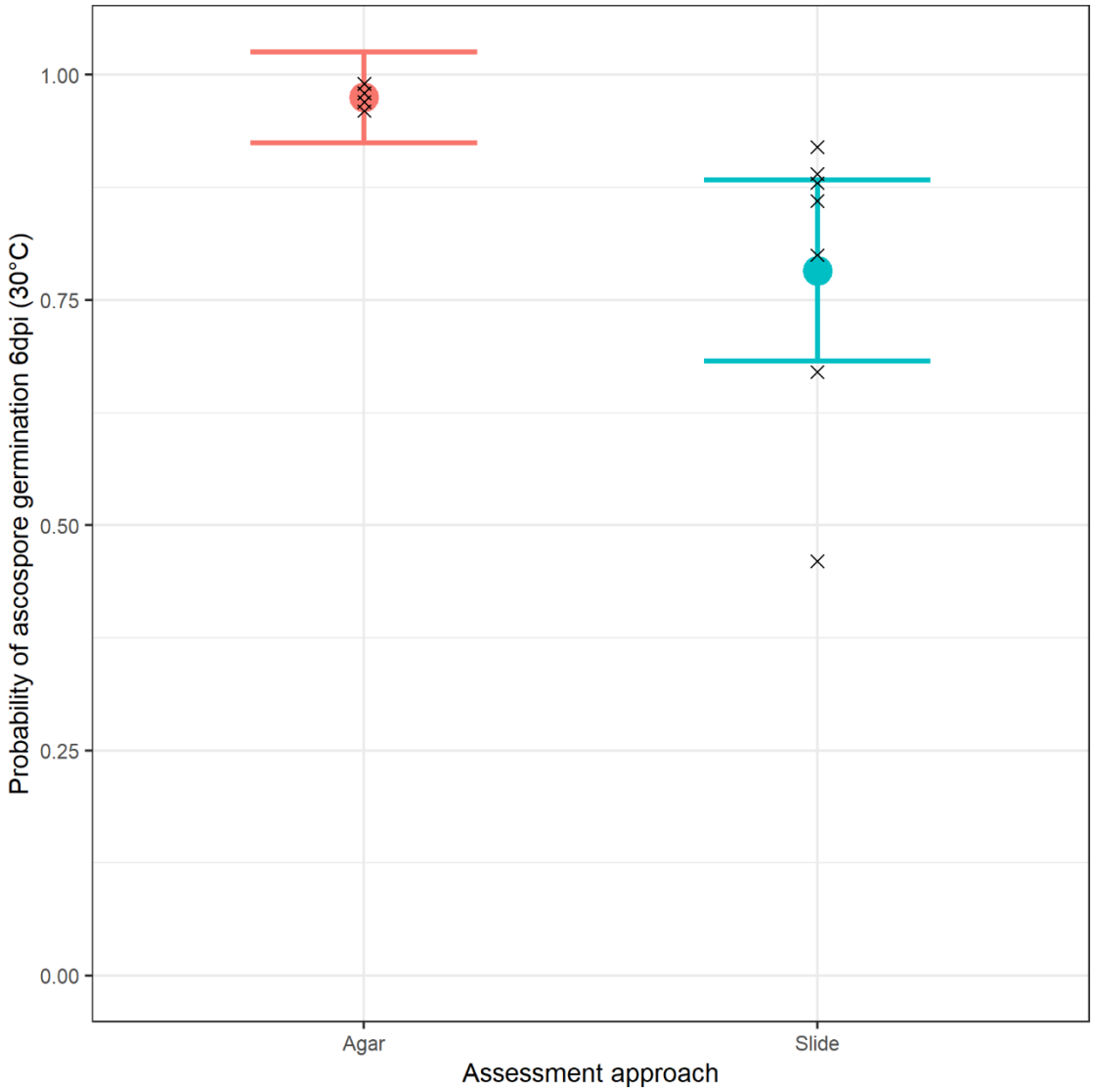

Figure 4.8 The significant effect (Chisq = 8.58, df = 1, p < 0.01) of assessment approach on *H. fraxineus* ascospore germination 6 days after the start of incubation (dasi) at 30°C (Section 4.2.2.3; Section 4.3.5). A generalised linear model was fitted to the data with quasibinomial distribution and logit function (section 4.2.2.5). Black crosses represent recorded data, the coloured points represent the model prediction, and the 95% confidence intervals are indicated.

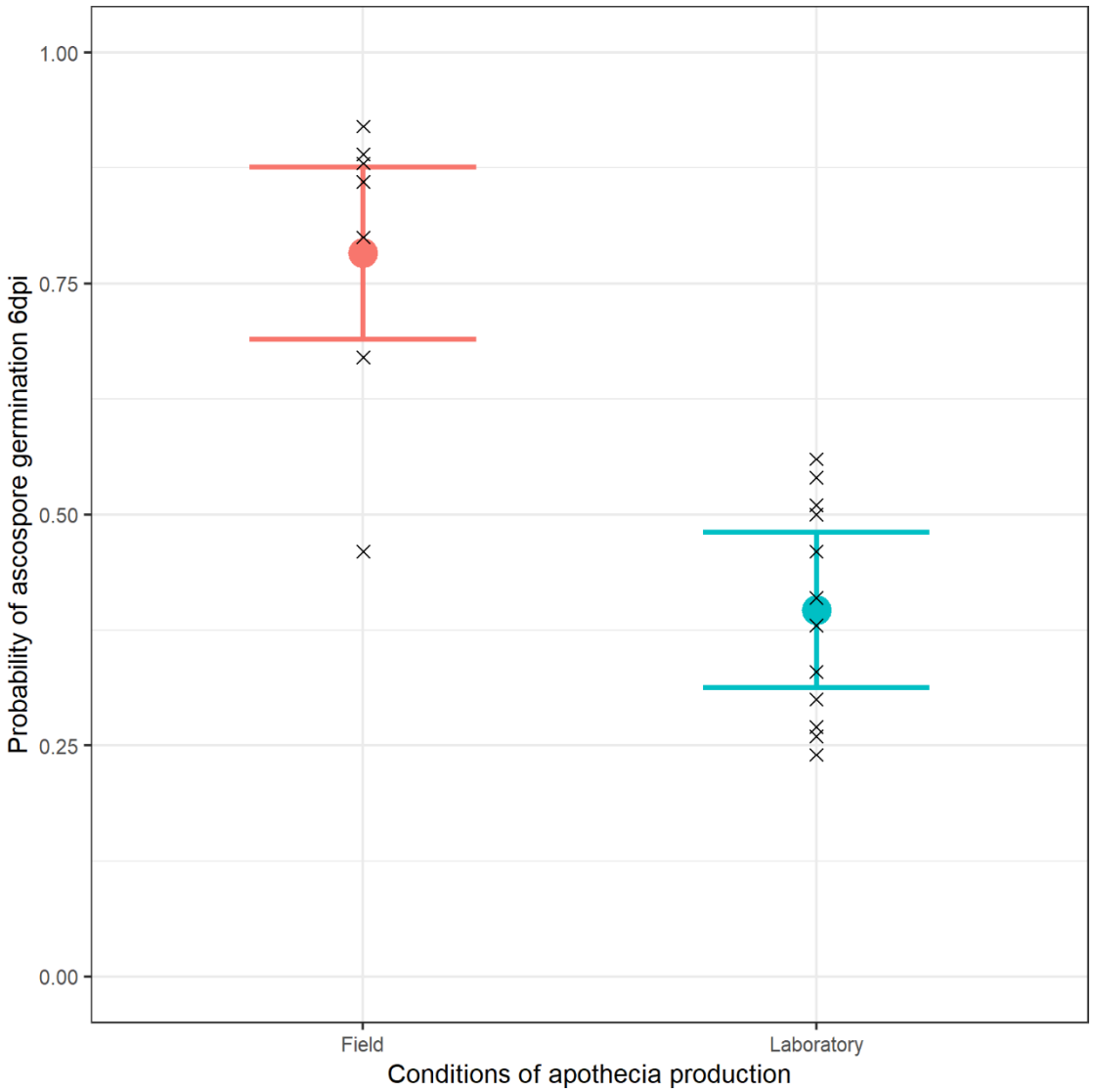

Figure 4.9 The significant effect (Chisq = 29.94, df = 1, $p < 0.001$) of the conditions of apothecia production on *H. fraxineus* ascospore germination 6 days after the start of incubation (dasi) at 30°C (Section 4.2.2.4; Section 4.3.6). A generalised linear model was fitted with quasibinomial distribution and logit function (Section 4.2.2.5). Black crosses represent recorded data, the coloured points represent the model prediction, and the 95% confidence intervals are indicated.

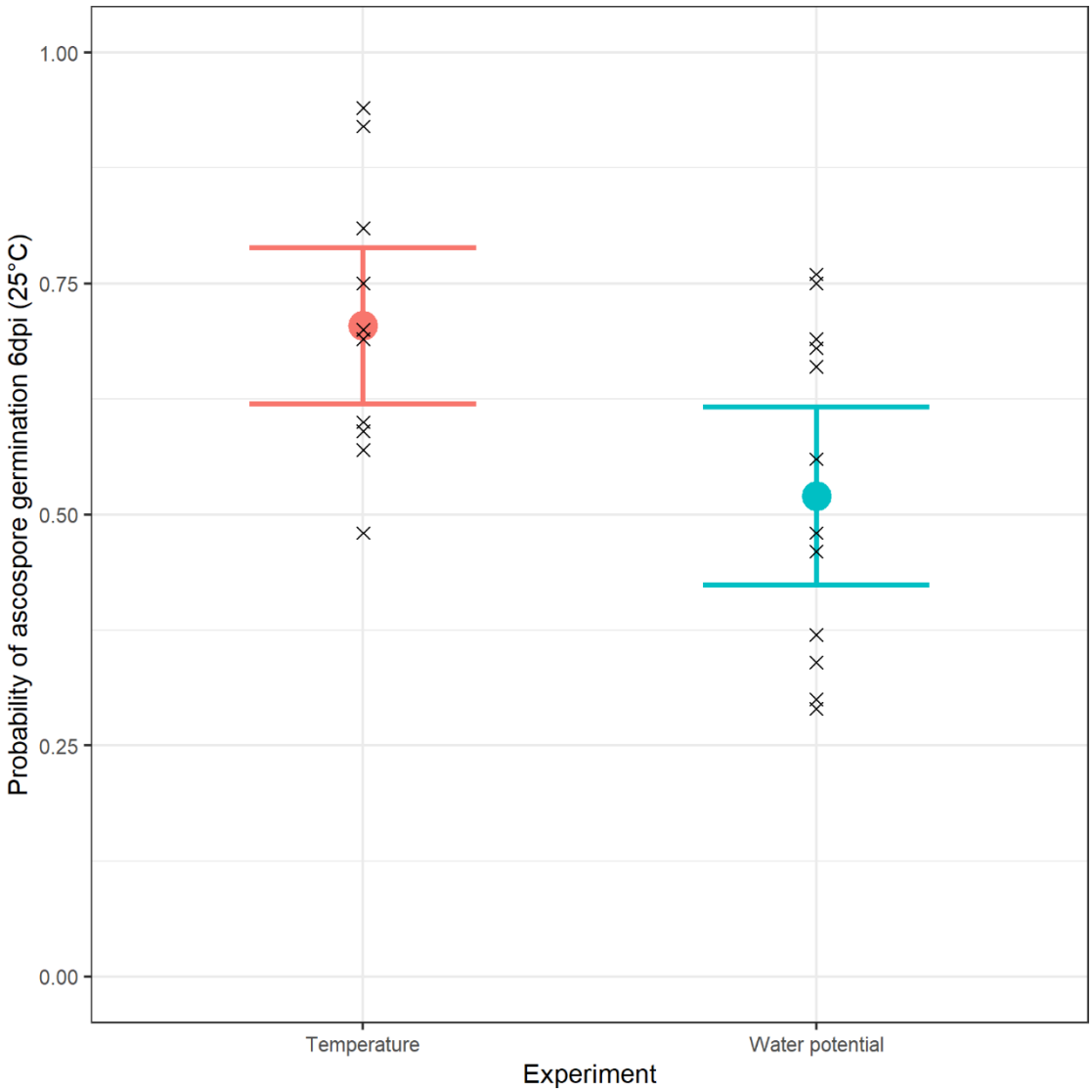

Figure 4.10 The significant difference (Chisq = 7.79, df = 1, p < 0.01) of *H. fraxineus* ascospore germination 6 days after the start of incubation (dasi) at 25°C between laboratory produced apothecia for the temperature effect experiment (Section 4.2.2.1) and for the solute potential effect experiment (Section 4.2.2.2) (Section 4.2.2.4; Section 4.3.6). A generalised linear model was fitted with quasibinomial distribution and logit function (Section 4.2.2.5). Black crosses represent recorded data, the coloured points represent the model prediction, and the 95% confidence intervals are indicated.

4.4 Discussion

This study demonstrated that *F. excelsior* crown dieback in 2020 was significantly positively related to the proportion of previous seasons' rachis length colonised by *H. fraxineus*, and the size (dbh) of tree. Furthermore, the proportion of previous seasons' rachis length in the litter layer colonised by *H. fraxineus* in 2020 was significantly positively related to the dbh of the assessed tree and the maximum ascospore density recorded at a location in 2019. Unsurprisingly, considering the large number of variables known to affect disease progression, large amounts of unexplained variation remained in models. It was shown that *H. fraxineus* ascospores germinate over a wide range of temperatures (5°C to 30°C), but were sensitive to reduced solute potential, germinating with low success at -1.35 MPa and -2.68 MPa, and not germinating below -4.01 MPa.

4.4.1 *F. excelsior* crown dieback and rachis colonisation by *H. fraxineus*

Previous work has associated the proportion of rachis colonised by *H. fraxineus* in the litter layer with the crown dieback severity (Grosdidier, Ioos, Marçais et al., 2018), and larger size of *F. excelsior* trees has been repeatedly associated with better disease outcome (Havrdová et al., 2017; Erfmeier et al., 2019; Klesse, Abegg et al., 2021). However, leaflets of *F. excelsior* taken from symptomatic and 'healthy' trees prior to abscission did not display significant differences in *H. fraxineus* DNA quantity in September, at the end of the field infection period, indicating that *H. fraxineus* leaf colonisation is not related to the presence of *F. excelsior* crown dieback (Agan et al., 2020). Although apparently contradictory, these findings are supported by my research, which found that the proportion of rachis length in the litter layer colonised by *H. fraxineus* was significantly related to the probability of crown dieback ≥ 25% (i.e. the presence of considerable crown dieback), but not to the probability crown dieback ≥ 5% (i.e. the presence of noticeable crown dieback). Furthermore, my work found that the maximum ascospore density recorded at locations in 2019 (Chapter 3) was significantly related to the proportion of previous seasons' rachis length in the litter layer colonised by *H. fraxineus* in 2020, with higher *H. fraxineus* ascospore density in 2019 associated with greater rachis colonisation in the litter layer in 2020.

Greater ascospore density will increase the probability of *H. fraxineus* infection of *F. excelsior* leaves. The pathogen reaches the stem via the petiole-shoot junction (Haňáčková et al., 2017), which leads to shoot death and crown dieback. Therefore, a greater colonisation of leaves due to increased probability of infection by *H. fraxineus* can be expected to increase the probability the pathogen crosses the petiole-shoot junction. As mentioned in Chapter 1, *H. fraxineus* is a hemi-biotroph that does not extensively colonise foliage as a biotroph (Mansfield et al., 2018), and field studies demonstrated low

H. fraxineus DNA quantities in asymptomatic leaves, but high *H. fraxineus* DNA quantity and a change in fungal community structure upon the development of necrosis (Cross et al., 2017). Together, this indicates that *H. fraxineus* remains quiescent on leaves until a threshold density is reached, which triggers a switch to necrotrophy (Cross et al., 2017) that is an important determinant of disease outcome.

It is likely that the models did not find an association between any investigated variables and the probability of crown dieback ≥ 5% because of the genetic component of *F. excelsior* disease resistance (Stocks et al., 2019). Indeed, as *H. fraxineus* causes crown dieback by killing shoots after crossing via the petiole-shoot junction (Haňáčková et al., 2017), it is probable that leaves of trees with crown dieback < 5% and ≥ 5% are similarly infected by *H. fraxineus* under field conditions, but in negligibly damaged trees (crown dieback < 5%) *H. fraxineus* did not cross into shoots.

The negative relationship between *F. excelsior* dbh and the proportion of rachis length in the litter layer colonised by *H. fraxineus* reflects the fact that spore density decreases with height above ground (Chandelier et al., 2014), and therefore trees with a larger dbh typically having a higher canopy, should have a lower probability of leaf infection. However, tree height is not linearly related to dbh, so other factors such as age-related resistance (Develey-Rivière and Galiana, 2007) could also be responsible.

Importantly, my results measured the proportion of previous seasons' rachis length in the litter layer colonised by *H. fraxineus* in 2020. Therefore, this is not a direct representation of the *H. fraxineus* colonisation of leaves in the canopy, as shed leaves will continue to be colonised by *H. fraxineus* in the litter layer. Strikingly, 89.4% of rachises in the litter layer showed colonisation by *H. fraxineus*, which is higher than the estimate of 33.7% from Poland (Kowalski and Bilański, 2021), although it is consistent with quantities seen at some sites in France (Grosdidier, Ioos, Marçais et al., 2018). Of the 89.4% of leaves displaying *H. fraxineus* infection in my study, only 40% were completely colonised by *H. fraxineus*, i.e. in 60% of rachises colonised by *H. fraxineus*, other fungi were likely to have established. Indeed, fruiting of other fungi has been reported on 87.6% of rachises colonised by *H. fraxineus* (Kowalski and Bilański, 2021). Multiple studies have also identified endophytes that are antagonistic to *H. fraxineus* (Schlegel et al., 2016; Kosawang et al 2018; Becker et al., 2020; Ulrich et al., 2020; Kowalski and Bilański, 2021). Together, this indicates that the inability of *H. fraxineus* to completely colonise rachises is due to the presence of antagonistic species. Thus, the positive relationship between crown dieback and the proportion of previous seasons' rachis length in the litter layer colonised by *H. fraxineus* suggests a reduction in the presence of antagonists to *H. fraxineus*, which have likely been prevented from establishing in fallen rachises due to the dominance of *H. fraxineus* ascospores in the air (Cross et al., 2017).

Although higher ascospore density in 2019 was associated with a greater proportion of previous seasons' rachis length in the litter layer colonised by *H. fraxineus* in 2020, it is likely that, as with other foliar pathogens (Canihos et al., 1999; Trapero-Casas and Kaiser 2007; Uysal and Kurt, 2017), the environmental conditions also affect the infection success and subsequent symptom progression. Indeed, *H. fraxineus* DNA quantity was lower in washed leaves at the end of the infection season in September, than in unwashed leaves (Agan et al., 2020). This indicates that ungerminated *H. fraxineus* ascospores may have been residing on leaf surfaces.

4.4.2 *H. fraxineus* ascospore germination

As with other ascomycete foliar pathogens present in temperate regions (MacHardy and Gadoury, 1989; Huang et al., 2003; Trapero-Casas and Kaiser, 2007), *H. fraxineus* ascospores were able to germinate at a wide range of temperatures on water agar (5°C to 30°C). Germination was likely inhibited at 35°C, but this may have been partly due to drying of water agar.

Ascospore germination was very sensitive to reduced solute potential with a reduced percentage of germination at -1.35 MPa, little germination at -2.68 MPa and none at or below -4.01 MPa. This is in marked contrast with most ascomycetes, including other pathogens such as *Didymella rabiei* and *Fusarium graminearum*, which could germinate respectively at -6 MPa and -8.4 MPa on media amended with NaCl (Trapero-Casas and Kaiser 2007; Ramirez et al., 2004). Additionally, the reduced germination of ascospores at 30°C 6 dasi on 1.5 ml water agar slides compared to approximately 10 ml water agar in Petri dishes demonstrates the sensitivity of ascospore germination to moisture, because in theory, the only difference between the two methods will be a decrease in water potential due to greater evaporation from the agar on the slides compared to in Petri dishes. Moreover, ascospore germination decreased from 84-93% to 5.7-11.7% after 7 days of air drying in the laboratory followed by addition of water (Mansfield et al., 2018). Together with increased apothecia production (Chapter 2) and increased ascospore ejection (Chapter 3) at higher humidity, increased infection success of the host via increased ascospore germination may also be responsible for the repeated association between ash dieback disease severity on sites with apparently greater moisture (Havrdová et al., 2017; Grosdidier et al., 2020; Klesse, Abegg et al., 2021). This also indicates that trees with more open canopies, that experience greater air flow, and have a lower air humidity, may experience reduced infection success of *H. fraxineus* ascospores.

Isolated trees in agricultural settings have been associated with less crown dieback, and although not significant, the proportion of infected rachises was slightly higher in a woodland setting (Grosdidier et al., 2020). In fact, high temperatures lethal to

H. fraxineus may also have limited host disease progression, due to high exposure to solar radiation in leaves of isolated trees (Grosdidier et al., 2020). My research indicates that for germination to be inhibited, temperatures may need to reach 35°C, which is consistent with experiments examining temperature limits on *H. fraxineus* hyphal extension (Hauptman et al., 2013). Further investigation is required to determine whether these temperatures are lethal for *H. fraxineus*, or whether ascospores can remain dormant and germinate when the temperature drops below 35°C. In summary, my results indicate that *H. fraxineus* ascospore germination is unlikely to be prevented by air temperatures in the UK, however measurement of leaf temperature is required to understand the frequency that leaves exposed to high levels of solar radiation exceed 35°C.

Although probability of *H. fraxineus* ascospore germination differed between the temperature treatments, with ascospore germination significantly greater between 15°C and 25°C than below 10°C or above 30°C, there were also significant differences between ascospore germination between the three separately conducted experiments, as well as between field collected apothecia and laboratory produced apothecia. The differences in germination between experiments reflects differences in the development of apothecia and ascospores. I hypothesise that these differences in apothecia and ascospore development are associated with differences in concentrations of organic compounds that are essential for metabolic pathways involved in spore germination. Alternatively, there could be differences in accumulation of compatible solutes that enable fungi to tolerate unfavourable conditions such as water stress, and temperature stress (Dijksterhuis and de Vries, 2006), and may also explain why little germination occurred below -2.68 MPa. The low oxygen concentrations in sealed boxes in the laboratory, potentially causing anaerobic stress, could lead to the metabolism of available compatible solutes, which would be required to tolerate stress in the ejected ascospores. Moreover, different light intensity, wavelengths and durations, which will be present between a laboratory and field environment, can affect fungal development (Thind and Schilder, 2018), and its importance to *H. fraxineus* is evidenced by the importance of near UV light in the successful development of mature apothecia (Gross, Zaffarano et al., 2012; Chapter 5). Differences in light conditions could explain why apothecia produced by incubating infected rachises between October-December had higher germination success than those produced on rachises incubated between January-March. Overall, my findings demonstrate, particularly as the experiment was conducted *in vitro*, that the probability of ascospore germination under different conditions in this Chapter does not represent absolute values that are directly transferable to field conditions. However, the variation present between the germination of ascospores from separate apothecia does suggest that ejected ascospores are not equally capable of host infection. It is beneficial for apothecia to eject all ascospores synchronously upon suitable triggers for ejection to limit

the effect of drag and successfully bypass obstacles (Roper et al., 2010). Therefore, without simultaneous ejection of immature ascospores, the transport of mature ascospores to the *F. excelsior* canopy would be compromised. Notably, the probability of ascospore germination on approximately 10 ml of water agar at 30°C is very high and with little variation, which is consistent with findings from other studies (Schlegel et al., 2016; Mansfield et al., 2018).

4.5 Conclusions

There was considerable colonisation of rachises (89.4% of rachises had some colonisation, and a summed colonisation proportion of 0.79) by *H. fraxineus* but there was large variation within (from 0.60 to 0.93) and between sites (from 0.61 to 0.90). Likewise, there was large variation in crown dieback.

Larger tree dbh was associated with lower colonisation of the previous seasons' rachises in the litter layer, corresponding with a lower probability of crown dieback ≥ 25%. Higher maximum ascospore density at locations in 2019 was associated with a higher rachis colonisation in the litter layer, which was in turn associated with a greater probability of crown dieback ≥ 25%. Large variation remained in models, although this is unsurprising given the array of factors known to affect disease progression.

H. fraxineus ascospore germination occurred at temperatures ranging from 5°C to 30°C, but was inhibited at temperatures ≥ 35°C. Ascospore germination was extremely sensitive to reduced water potential. For example, ascospore germination was significantly greater on media incubated to limit water loss via evaporation, but little germination occurred on media amended with KCl to a solute potential of -2.68 MPa, and no germination occurred at -4.01 MPa or below. The use of laboratory produced apothecia in experiments could have affected the development of ascospores and their tolerance of unfavourable conditions likely due to decreased accumulation of compatible solutes (Dijksterhuis and de Vries, 2006).

My findings indicate that greater foliar colonisation is associated with increased crown dieback, and the density of ascospores is related to foliar colonisation. The temperature and moisture, in addition to affecting apothecia formation (Chapter 2) and ascospore release (Chapter 3), can affect the infection success of host leaf tissue by ascospores. Further investigation is required to establish how often leaf temperatures exceed 35°C in the UK, and thus present lethal conditions for *H. fraxineus* hyphae (Hauptman et al., 2013), and likely inhibit ascospore germination. Actions to reduce apothecia production, ascospore ejection and crown humidity, through methods such as

selective thinning, may be effective measures to reduce infection success of *H. fraxineus* ascospores.

Chapter 5: Laboratory investigation of temperature and light effects on *H. fraxineus* apothecia development

5.1 Introduction

By their very nature ecological studies conducted in the field are not under controlled conditions, and the results are dependent on the prevailing conditions which are likely to vary between seasons; collinearity is also often present between some of the variables (Freckleton, 2011). In addition, prior knowledge of the system under study is required to ensure that the experimental design is meaningful and statistical analysis can be robust (Burnham and Anderson, 2001). All these complexities mean that it is difficult accurately to determine the impact of one variable in a multipart environmental study (Freckleton, 2011).

Indeed, from the field studies of the environmental effects on apothecia development in Chapter 2 it was not possible to examine threshold temperature value for apothecia formation, despite its importance for understanding the timing of *H. fraxineus* inoculum production. Furthermore, as discussed in Chapter 2, unexplained variation remained in the mixed effects models. Growing degree days (GDD), which are based on the principle of accumulated heat degrees over a threshold temperature (Zhou and Wang, 2018), are positively correlated with *H. fraxineus* ascospore levels (Hietala et al., 2018). Therefore, as *H. fraxineus* apothecia development and ascospore quantity are linked (Chapter 3), it was hypothesised in Chapter 2 that overwintering conditions accounted for some of the unexplained variation in apothecia development. Additionally, it was not possible to investigate the effects of light on apothecia development in the field, despite its known effects on developmental processes in other fungi (Thind and Schilder, 2018).

Therefore, the goals of the current Chapter were to examine the threshold temperature for *H. fraxineus* apothecia development, the effect of light on this process, and the effect of overwinter temperature on the apothecia formation through the use of controlled laboratory experiments. This was done by regularly monitoring apothecia development on *H. fraxineus* infected *F. excelsior* rachises incubated at 4°C, 10°C, 15°C and 20°C over 17 weeks, and then continuing regularly to monitor subsequent apothecia development when rachises were moved to laboratory conditions (18°C). Infected rachises were also incubated at 10°C and 20°C, either in the presence or absence of light. It was hypothesised that apothecia development would require mean temperature of at least 10°C regardless of light regime, because of their absence during winter (Timmermann et al., 2011), but concurring with previous findings (Gross, Zaffarano et al., 2012), mature apothecia development would only occur in the presence of light. Furthermore, due to decreasing growth rates of *H. fraxineus* at temperatures below 20°C

(Hauptman et al., 2013), it was expected that slower apothecia development would occur on rachises which were previously incubated at lower temperatures.

5.2 Methods

5.2.1 The effect of incubation temperature on laboratory apothecia development

F. excelsior rachises with a black pseudosclerotial plate, which is characteristic of *H. fraxineus* colonisation of rachises (Section 2.3.1; Kowalski and Bilański 2021), were collected from Queen Elizabeth Country Park, Hampshire in March 2018, placed individually in sealed plastic bags, and then stored at 4°C for 3 days prior to the start of experiments.

Using *H. fraxineus* infected individual rachises, a 4 cm segment taken 1 cm above the rachis base, was cut from each one and submerged in water for 2 seconds and then placed in sealed plastic boxes (17 cm length x 10 cm width x 4.5 cm height), the bases of which had been lined with 2 wet paper towels to maintain high humidity. Each box contained 13 - 16, 4 cm infected rachis segments, and were incubated at 4, 10, 15 or 20°C (7 replicate boxes), in darkness.

Visual assessment of each rachis segment was conducted at 1 to 2 week intervals for 12 weeks, beginning 5 weeks after the start of incubation. The number of rachis segments that developed immature apothecia (structure which consisted of only a stipe) and mature apothecia (stipe and spore bearing cup; Figure 5.1) were recorded for each box. Stipes and mature apothecia were only recorded if they were white, as darker coloured structures were probably non-viable.

The experiment was stopped 17 weeks after the start, when the majority of white stipes on individual rachises had turned black, and those which still had white stipes were showing signs of blackening.

5.2.2 The effect of earlier rachis incubation temperature on laboratory apothecia development

After 17 weeks, the boxes from Section 5.2.1 were removed from the dark incubators (4°C (n = 6), 10°C (n = 6), 15°C (n = 15) and 20°C (n = 6)), opened briefly to reoxygenate boxes and moved into the laboratory (18°C) in the presence of light. Assessment of apothecia development (Section 5.2.1) began 3 weeks after removal from incubators, and continued at 1 to 2 week intervals for a further 19 weeks**.** However, sample numbers were reduced as some rachis segments were taken from boxes to test

material for the presence of *H. fraxineus* material via Real-Time PCR (Section 5.2.4), and some samples became desiccated during photography.

5.2.3 The effect of daylight on apothecia development

F. excelsior rachises colonised by *H. fraxineus* were collected from Alice Holt Forest in February 2021 and stored at 4°C until further use (Section 5.2.1). Six months later, 4 cm rachis segments were dipped in water, placed in humid sealed containers (Section 5.2.1), and incubated at either 20°C, or 10°C under a 16h/8h (day/night) cycle (20,000 lx; MLR-351, Sanyo, Japan). To investigate the effect of daylight on apothecia development, 7 of the 14 boxes at each temperature were wrapped in foil to ensure these rachises were kept in the dark. Apothecia development was assessed (Section 5.2.1) on all incubated rachises 9 weeks after the start of incubation, and again 19 weeks after the start of incubation for boxes that had been incubated in the dark at 10°C. Apothecia development was not assessed for other treatments 19 weeks after the start of incubation because incomplete sealing of boxes used in the experiment resulted in the drying of material under all treatments except in boxes incubated in the dark at 10°C. The temperature of boxes in each treatment (20°C foil wrapped, 20°C non-foil wrapped, 10°C foil wrapped, 10°C non-foil wrapped) were measured using data loggers (Tinytag Plus 2, Gemini Data Loggers UK) to record temperature every 10 minutes over a 72 h period.

5.2.4 Apothecia identification

F. excelsior rachises with a black pseudosclerotial plate are characteristic of *H. fraxineus* colonisation (Section 2.3.1; Kowalski and Bilański 2021). Their apothecia are distinct from other species in this niche, except for *Hymenoscyphus albidus,* which occurs at sufficiently low frequency in ash dieback affected stands (Koukol et al., 2016; Hietala et al., 2018) that it has previously been assumed extinct (McKinney et al., 2012). The identity of four apothecia produced on rachises from Queen Elizabeth Country Park (Section 5.2.1; Section 5.2.2) were checked via Real-Time PCR of extracted DNA (Section 2.2.4). The identity of apothecia produced on rachises from Alice Holt Forest were checked via DNA extraction and Real-Time PCR of ascospores (Section 3.3.1.2).

5.2.5 Statistical Analyses

The data were analysed using R software version 4.1.1 stats (R Core Team, 2021), DHARMa (Hartig, 2021), car (Fox and Weisberg, 2021), emmeans (length, 2021), ggplot2 (Wickham, 2016) packages. Generalised linear models with a binomial distribution

and logit function were fitted to examine: (1) the effect of temperature (Section 5.2.1) on the probability of apothecia development on a rachis (based on stipe development, because mature apothecia were extremely rare; Section 5.3.1); (2) the effect of earlier rachis incubation temperature (Section 5.2.2); (3) the effect of light and temperature (Section 5.2.3) on the probability of stipe development on a rachis. Treatments with negligible apothecia development were removed from analysis to avoid zero inflation of models, and because the information acquired would not be beneficial. Boxes in 10°C incubators with light (Section 5.2.3) where rachises had become dry were also removed from analysis. Significance of variables from these models was assessed using type II Wald Chisquare tests and $p < 0.05$ as a threshold for significance. *Post hoc* analysis on the models produced for (2) and (3) (Sections 5.2.2 and 5.2.3) were conducted on the estimated marginal means of treatments on the log odds ratio scale, using Tukey's method for calculation of p values, with $p < 0.05$ as a threshold for significance. *Post hoc* analysis was not required for the model produced to analyse data from (1) (Section 5.2.1) because apothecia development only occurred in two treatments.

The effect of temperature on the timing of the maximum proportion of rachises with stipes in a box (Section 5.2.1) was examined using the Wilcoxon rank sum test with continuity correction. The effect of earlier rachis incubation temperature on the timing of the maximum proportion of rachises with apothecia in a box (Section 5.2.2) was examined using a Kruskal-Wallis rank sum test, with a Wilcoxon rank sum test with continuity and Bonferroni correction for *post hoc* pairwise comparisons between treatments.

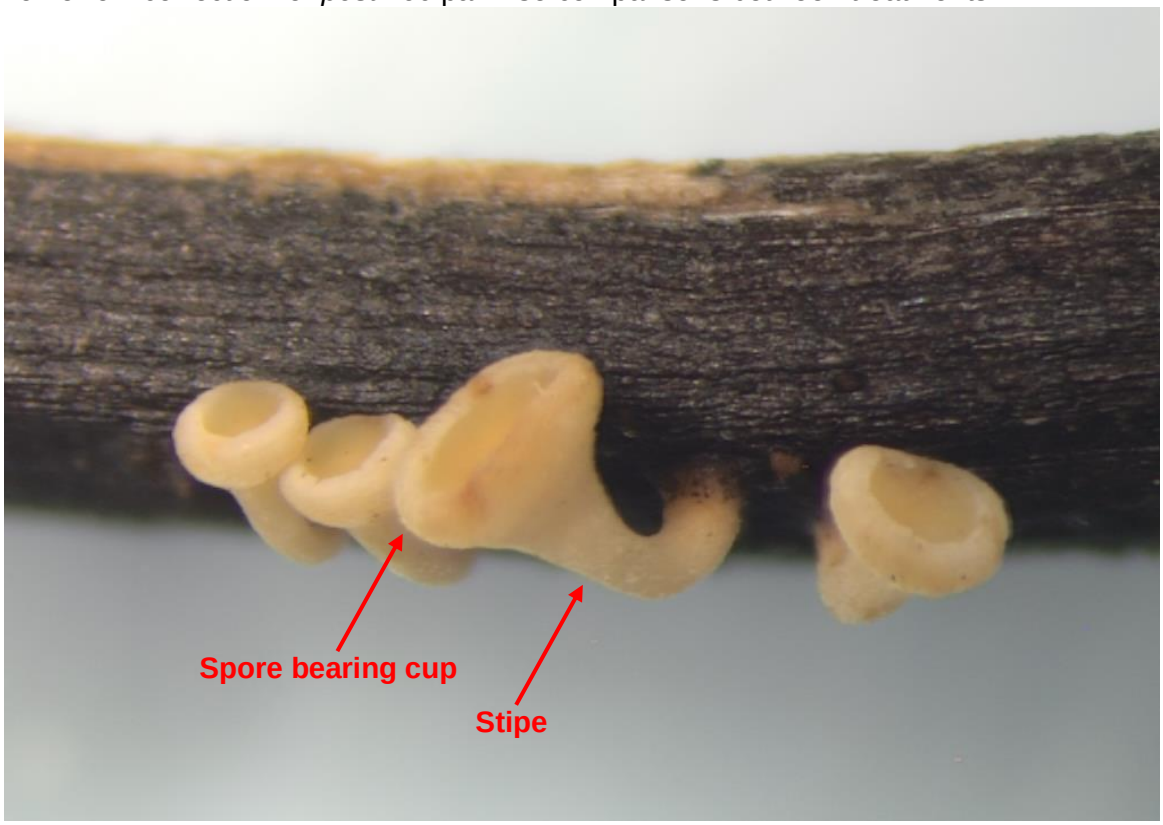

Figure 5.1 Mature apothecia (approximately 300 µm diameter) of *H. fraxineus* on an infected *F. excelsior* rachis.

5.3 Results

5.3.1 The effect of incubation temperature on laboratory apothecia development

Stipe formation was prolific on rachises at 15°C and 20°C, but not present on rachises incubated at either 4°C or 10°C. No mature apothecia developed in the dark at 4°C or 10°C, but one rachis (out of 106) developed mature apothecia at 15°C, and 16 (out of 102) developed mature apothecia at 20°C.

The proportion of rachises that developed stipes was not only significantly greater at 20°C (0.960, ± 0.020) than at 15°C (0.651, ± 0.082) (Chisq = 35.61, df = 1, p < 0.001) (Figure 5.2), but was also significantly quicker to reach the maximum for boxes (20°C median = 53 days, IQR = 7 days; 15°C median = 74 days, IQR = 7 days) (W = 47.5, p < 0.01) (Figure 5.3).

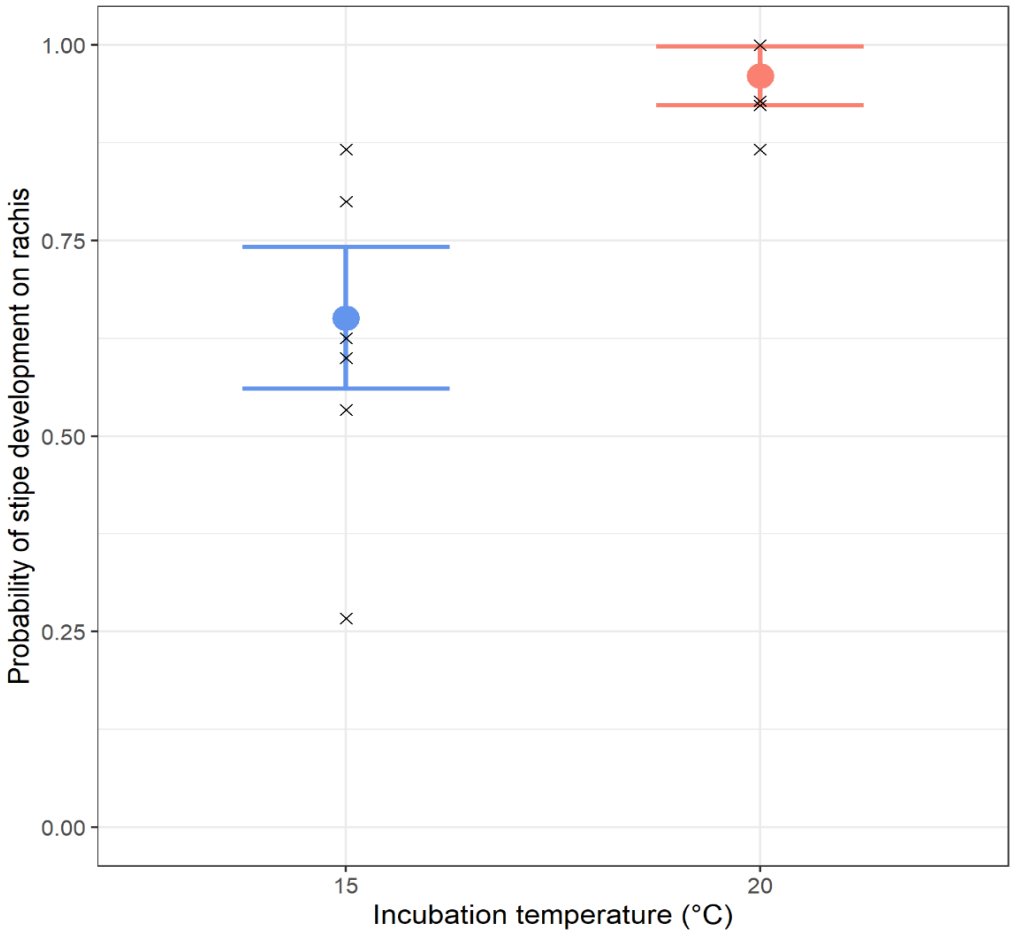

Figure 5.2 Probability of *H. fraxineus* stipe development on rachises that were incubated at 15°C (n = 7) and 20°C (n = 7) under high humidity in the dark for 17 weeks (Chisq = 35.61, df = 1, p < 0.001) (Section 5.2.1). Generalised linear model with binomial distribution and logit function was fitted to the data (Section 5.2.5); model predictions with associated 95% confidence intervals are displayed in colour, and recorded data is marked by back crosses.

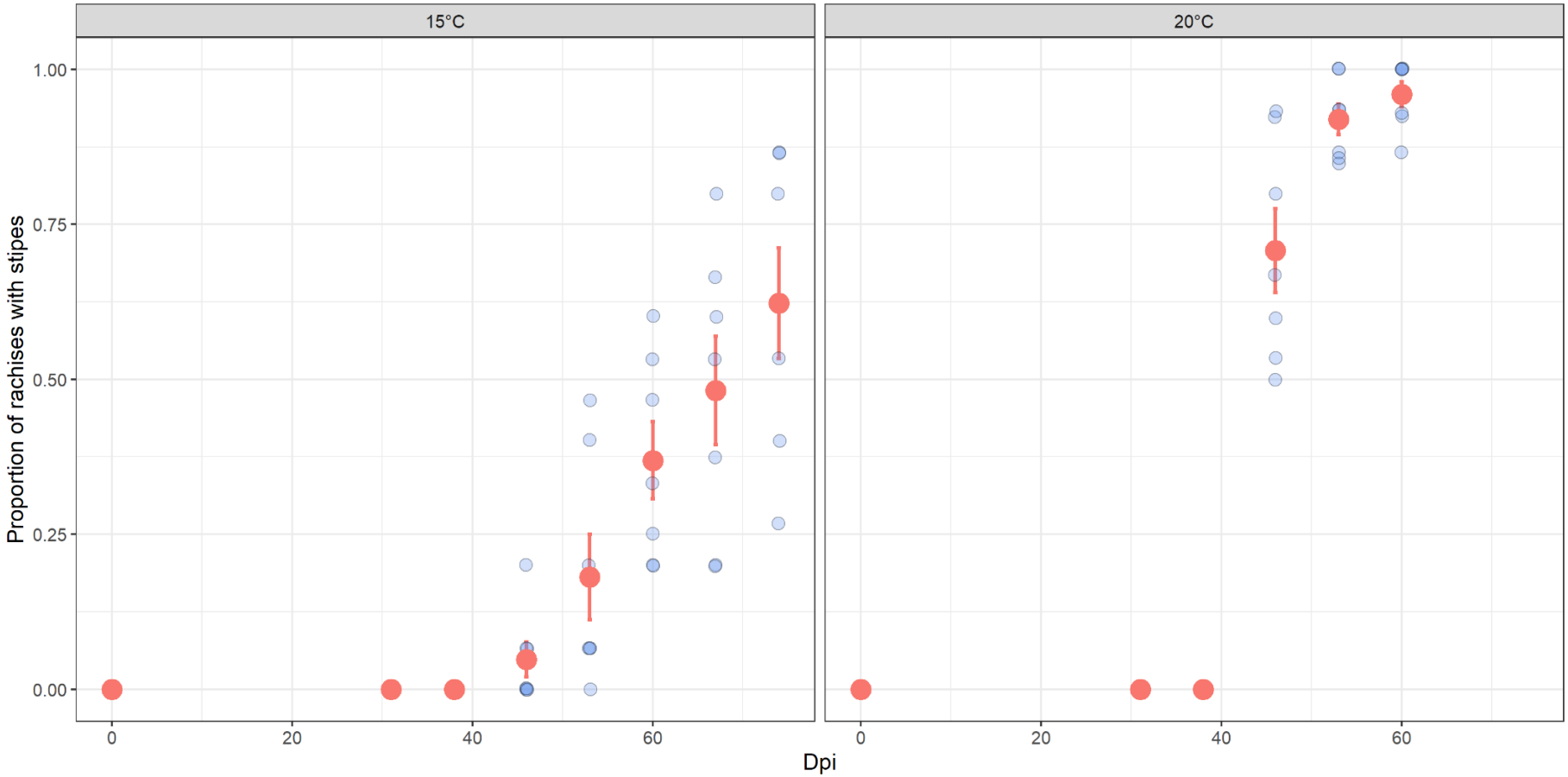

Figure 5.3 Proportion of rachises with *H. fraxineus* stipe development by the days after the start of incubation at 15°C (n = 7) and 20°C (n = 7) under high humidity in the dark for 17 weeks (Section 5.2.1). Treatments significantly differed in the timing of maximum rachises with stipe development ($W = 47.5$, $p < 0.01$) (Section 5.2.5). Data from individual replicate boxes are marked by blue dots, with darker points representing multiple overlapping data, and the mean (with standard error) are represented by the red points. Data is presented until all boxes at a respective temperature reach the maximum proportion of rachises with stipes.

5.3.2 The effect of earlier rachis incubation temperature on laboratory apothecia development

New mature apothecia formed abundantly at 18°C in the presence of light on rachises previously incubated at either 4°C, 10°C, 15°C or 20°C (Section 5.3.1). The temperature at which rachises were initially incubated (Section 5.3.1) significantly affected the proportion of rachises that developed mature apothecia (Chisq = 18.43, df = 3, $p < 0.001$), with rachises previously incubated at 4°C (Section 5.3.1) most likely to develop apothecia (0.935, ± 0.034) (Figure 5.4). The time taken for the maximum proportion of rachises to develop apothecia significantly differed between treatments (Chisq = 16.56, df = 3, $p < 0.001$), and was most rapid for rachises that had previously been incubated at 4°C (median = 66 days, IQR = 18 days) (Figure 5.5).

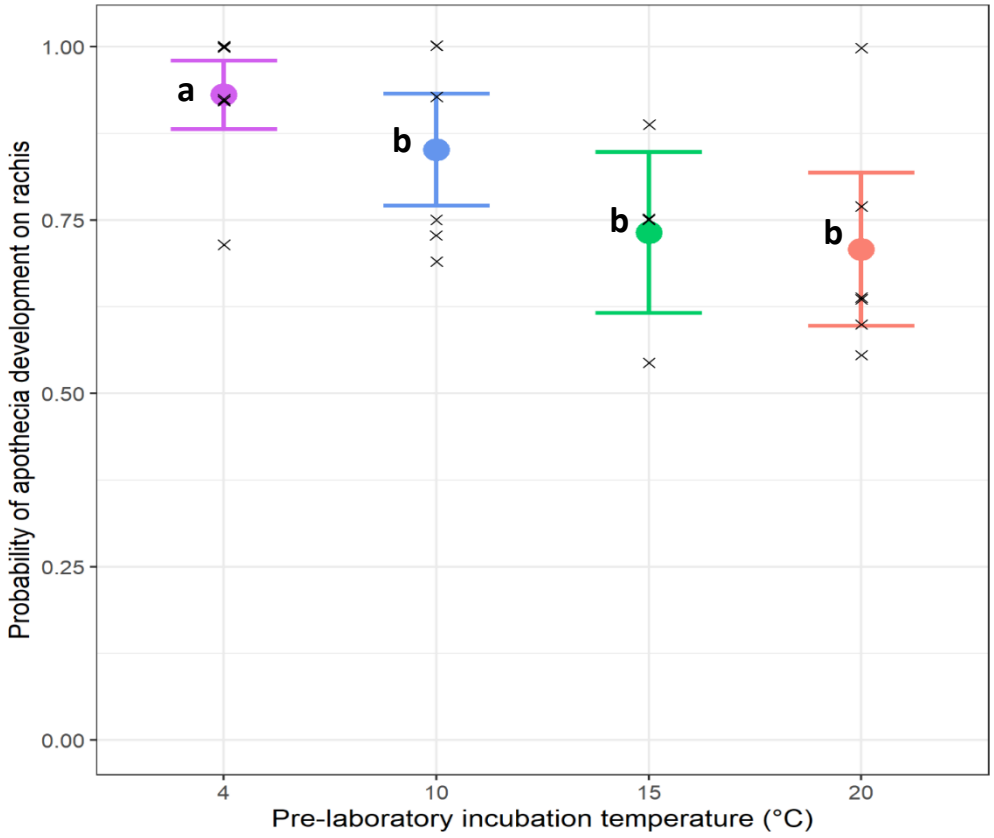

Figure 5.4 Probability of *H. fraxineus* mature apothecia development on rachises that were pre-incubated at 4°C (n = 6), 10°C (n = 6), 15°C (n = 5) and 20°C (n = 6) under high humidity in the dark (Section 5.2.1), prior to their movement to laboratory conditions (18°C) under the presence of light and high humidity (Section 5.2.2). Generalised linear model with binomial distribution and logit function was fitted to the data (Chisq = 18.43, df = 3, $p < 0.001$), and model predictions with associated 95% confidence intervals are displayed in colour, and recorded data is marked by back crosses. Significant differences between treatments are represented by different letters (Section 5.2.5).

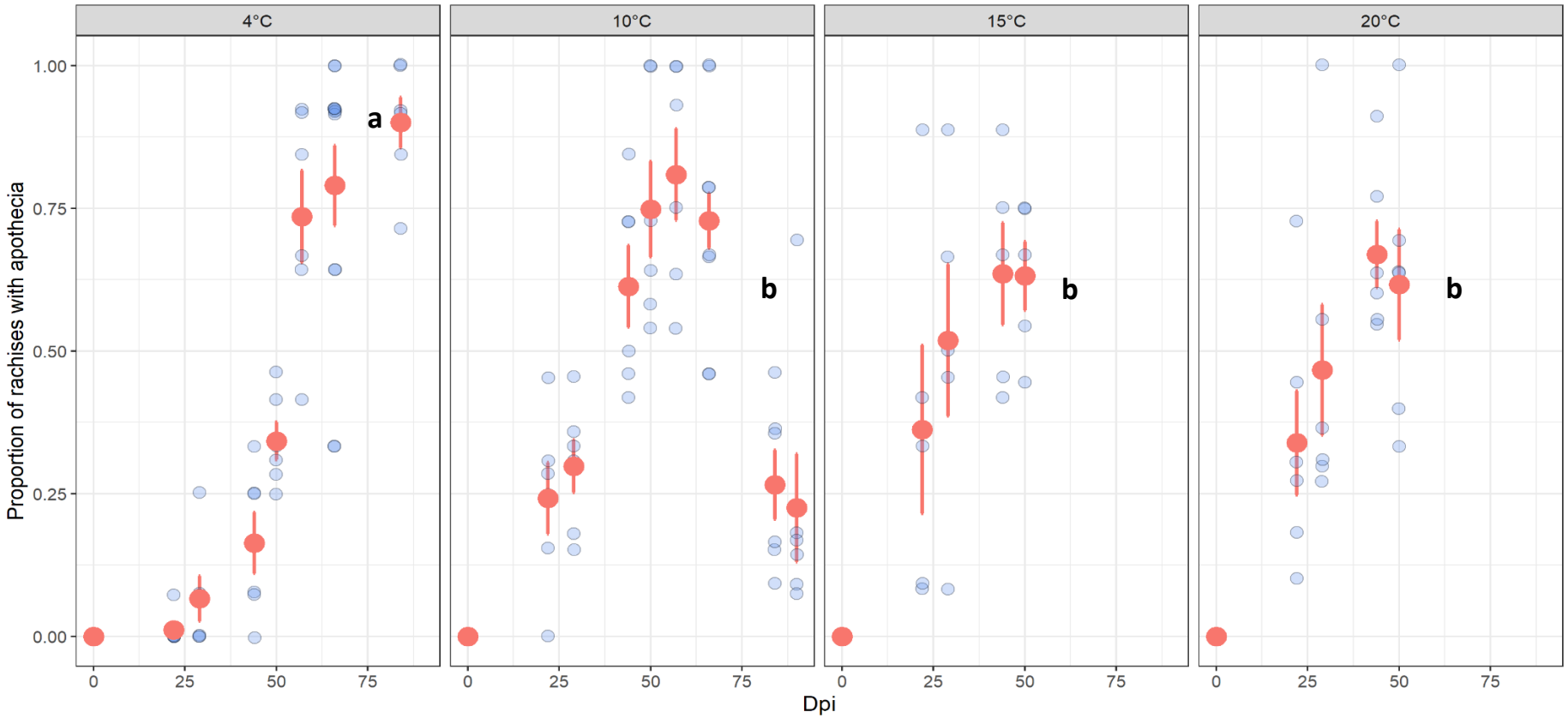

Figure 5.5 Proportion of rachises with *H. fraxineus* apothecia development by the days after movement to laboratory conditions. Rachises were pre-incubated at 4°C (n = 6), 10°C (n = 6), 15°C (n = 5) and 20°C (n = 6) under high humidity in the dark (Section 5.2.1) for 17 weeks, prior to their movement to laboratory conditions (18°C) under the presence of light and high humidity (Section 5.2.2). Data from individual replicate boxes are marked by blue dots, with darker points representing multiple overlapping data, and the mean (with standard error) are represented by the red points. Data is presented until all boxes at a temperature reach the maximum proportion of rachises with mature apothecia. Significant differences between treatments in the timing of maximum rachises with apothecia development (Chisq = 16.56, df = 3, $p < 0.001$) are represented by different letters (Section 5.2.5).

5.3.3 The effect of daylight on apothecia development

Mature apothecia were present 9 weeks after the start of incubation on approximately half of the rachises at 20°C in the presence of light (48 of 105), on only 3 of 105 rachises at 20°C in the dark, and on no rachises at 10°C. Dried material was present in all treatments except rachises kept at 10°C in the dark. Stipe development was present 9 weeks after the start of incubation on all rachises at 20°C in the presence of light, 103 of 105 at 20°C in the dark, 75 of 105 at 10°C in the light (56 of 60 when including only non-dried boxes) (Figure 5.6), and 3 of 105 incubated at 10°C in the dark. The presence of stipes was apparent 19 weeks after the start of incubation on 11 of 90 rachises (across 4 of 6 examined boxes) at 10°C in the dark. Only one of these boxes contained more than one rachis with stipe development, and this was also the only box in this treatment with more than 5 stipes per rachis.

The temperature within boxes of treatments that were wrapped in foil were consistent with incubation temperatures (10°C = 9.6°C; 20°C = 19.6°C), however the temperature of boxes that were not wrapped in foil were higher when incubators were illuminated (10°C = 14.2°C; 20°C = 22.2°C), leading to an elevated mean temperature over each 24h period (10°C = 13.1°C; 20°C = 21.4°C).

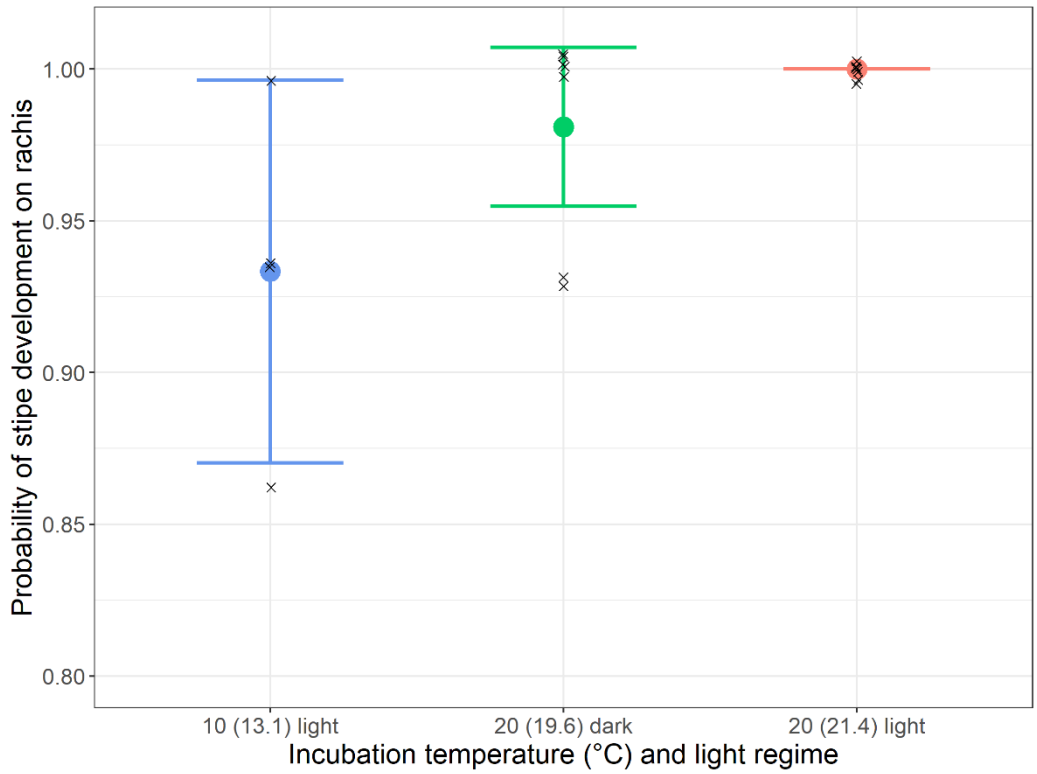

Figure 5.6 Probability of *H. fraxineus* stipe development on rachises that were incubated at 10°C in the light (n = 4), 20°C in the light (n = 7), and 20°C in the dark (n = 7). The recorded mean daily temperature within incubated boxes is indicated in brackets (Section 5.2.3). Generalised linear model with binomial distribution and logit function was fitted to the data (Chisq = 8.35, df = 2, $p < 0.05$) (Section 5.2.5); model predictions with associated 95% confidence intervals are displayed in colour, and recorded data is marked by back crosses. Post hoc analysis (Section 5.2.5) did not find significant differences between treatments.

5.4 Discussion

The research has revealed that the incubation temperature of *H. fraxineus* colonised rachises positively affects the rate of apothecia development, and that apothecia development is extremely limited at mean temperatures of 10°C or lower. However, this is based solely on stipe development rather than mature apothecia formation, because mature apothecia rarely formed in the dark, which is consistent with earlier findings demonstrating the necessity of near-UV light for mature apothecia formation of *H. fraxineus* (Gross, Zaffarano et al., 2012). Furthermore, the pre-incubation temperature of rachises positively affected the subsequent rate of apothecia development in the presence of light.

The positive effect of temperature on the rate of apothecia development is consistent with the growth rate of *H. fraxineus in vitro*, which is at a maximum around 20°C (Hauptman et al., 2013). The lower limit for growth in culture was between 0.5°C and 4°C (Bengtsson et al., 2014), and ascospore germination occurs at 5°C (Chapter 4), however my findings indicate that apothecia development at or below 10°C is extremely limited. No apothecia developed in rachises incubated at 10°C (Section 5.3.1), although there was also extremely limited stipe formation 19 weeks after the start of incubation (Section 5.3.3). The difference between experiments could be explained by minor differences in the duration that boxes were removed from incubators for assessment of apothecia development, a process which exposed rachises to light and elevated temperature.

Additionally, the difference between experiments could be explained by differences in the rachis moisture content. Rachises were dipped in water prior to incubation in boxes that were lined with wet paper towels to create a humid environment (Section 5.2.1; Section 5.2.3), but the moisture content of the rachises was not quantified. Furthermore, in Section 5.3.3 the boxes did not seal correctly leading to the drying of material within incubated boxes. Excessive moisture in the boxes in Section 5.3.1 could lead to anaerobic conditions for *H. fraxineus* in the rachises incubated at cooler temperatures due to less evaporation from these rachises. This would explain why the proportion of rachises exhibiting apothecia development were lower in 15°C in comparison to 20°C in Section 5.3.1, but not in Section 5.3.3 between boxes with mean daily temperature 14.2°C and 19.6/ 21.4°C. However, rachises in Section 5.3.3 were incubated in light, and light intensity has been shown to interact with environmental regulators of apothecia development in *Sclerotinia sclerotiorum* (Sun and Yang, 2000).

The occurrence of few stipes on an individual rachis in a box at 9.6°C (Section 5.3.3) could also represent genetic variation in the threshold temperature for apothecia formation between individuals. *H. fraxineus* demonstrates high genotypic and phenotypic

diversity (Kowalski and Bartnik, 2010; Gross, Grünig et al., 2012), exemplified via growth rate and pathogenicity differences between isolates, as well as the extent of vegetative compatibility groups (Brasier and Webber, 2013; Orton et al., 2019). The environmental conditions required for apothecia development should be under strong selection because production of apothecia at temperatures much lower than 10°C, prior to host flushing, would not allow *H. fraxineus* to successfully infect host foliage and continue its life-cycle, thereby wasting finite nutrient resources in the rachis, although a high temperature threshold for apothecia development may not be favourable due to competition to establish on host foliage. Concurring with results in this Chapter, apothecia of diameter > 200 µm (smaller apothecia could not be sampled reliably) were only recorded in woodlands from Chapter 2 when the mean temperature over the previous week was at least 12.2°C.

Interestingly, the pre-incubation temperature of *F. excelsior* rachises significantly affected the timing of maximum apothecia development, thereby indicating that a warmer overwinter temperature affects the rate at which *H. fraxineus* apothecia form when suitable conditions arise. Indeed, as mentioned in Section 5.1, growing degree days have been significantly correlated with *H. fraxineus* ascospore quantities (Hietala et al., 2018). In agreement with my findings, this indicates a cumulative effect of environmental conditions on mycelial development in rachises that can affect the timing of apothecia development.

Moreover, rachises can continue to produce new apothecia without an overwintering period, as evidenced by those incubated in the dark at 15°C and 20°C that were able to initiate new apothecia formation when moved to the laboratory in the presence of light. This also indicates that a change in the environment (e.g. a change in light levels) is required to retrigger apothecia development. Indeed, field observations (Chapter 2) of variation in apothecia size on a single rachis supports the continual development of new apothecia in the field under suitable conditions, thus indicating that diurnal temperature and humidity fluctuations may be sufficient to retrigger apothecia development. However, my results could also be due to the reoxygenation of boxes, that could have become anaerobic after a long period of apothecia development (17 weeks) without aeration. Intriguingly, rachises at pre-incubation temperatures (15°C and 20°C) least likely to develop apothecia had already developed apothecia in Section 5.3.1. This can be explained by the energy expenditure required to initiate apothecia development on a finite nutritional resource (the rachis), and is in accordance with previous findings that apothecia development reduced in quantity over the number of seasons that *H. fraxineus* developed apothecia (Kirisits, 2015). However, rachises pre-incubated at 15°C and 20°C did not significantly differ from those that were incubated at 10°C and did not initiate apothecia development in Section 5.3.1**,** although based on *H. fraxineus in vitro* growth

rates, the metabolic activity of *H. fraxineus* between 10°C and 20°C will be greater than at 4°C, and therefore may have utilised more of the finite nutritional resources on the rachis.

The eventual browning and death of apothecia in my experiments suggest that the development of an apothecium is a time limited event, but it is possible that this was due to poor ventilation in boxes that created an anaerobic environment. However, laboratory observations from the incubation of rachises with apothecia at the end of the field season (September 2020) revealed that field apothecia senesced a few weeks later, although new apothecia formation was subsequently initiated. The reasons for this are not known, but suggest that apothecia longevity is biologically constrained, and once initiated, apothecia senescence is not a reversible process. However, the conditions affecting the senescence of *H. fraxineus* apothecia have not previously been investigated despite its significance in the disease epidemiology, although findings from Chapter 2 indicate that cool temperatures and high humidity negatively affect apothecia. Indeed, apothecia longevity of another ascomycete, *Monilinia vaccinii-corymbosi,* is also affected by temperature (Wharton and Schilder, 2005).

5.5 Conclusions

Under controlled conditions, the threshold temperature for the initiation of *H. fraxineus* apothecia development appears to be around 10°C, which coincides with the timing of the first apothecia in late spring/ early summer (Chapter 2; Dvorak et al., 2015; Mansfield et al., 2018) when accounting for the rate of apothecia development.

The extended duration required for apothecia development is beneficial for *H. fraxineus* because it should prevent apothecia development outside of the spring/ summer season, which would lead to unnecessary energy expenditure. However, further research is required to understand the events that trigger apothecia development in the field, and the conditions which lead to *H. fraxineus* apothecia senescence.

Results also demonstrate a positive relationship between the ‘overwintering temperature’ and the rate of subsequent apothecia development, but a negative relationship with the probability of apothecia development. This supports the hypothesis in Chapter 2 that some of the unexplained variation in models of apothecia development in the field was due to conditions prior to the monitored spring/ summer field season, and suggests the importance of *F. excelsior* rachis nutrients on limiting the life-cycle of *H. fraxineus*.

Chapter 6 Preliminary study: Identification of *Armillaria* spp. associated with basal lesions in the UK

6.1 Introduction

In addition to symptoms in the crown, trees affected by ash dieback disease display necrosis at the base of the trunks and in the roots (Husson et al., 2012), with *H. fraxineus* infection presumably occurring via lenticels (Husson et al., 2012; Chandelier et al., 2016; Meyn et al., 2019; Nemesio-Gorriz et al., 2019). *Armillaria* spp. have also been detected in the necrosis. *A. gallica* is the most dominant *Armillaria* spp. in surveys in Germany, France and Belgium (Enderle et al., 2013; Marçais et al., 2016; Chandelier et al., 2016), although *A. cepistipes* was most common in surveys in Lithuania (Lygis et al., 2005; Bakys et al., 2011). These species can behave as secondary pathogens (Prospero et al., 2004; Marçais and Breda, 2006), although they behave as saprotrophs in undisturbed woodlands (Tsykun et al., 2012). Indeed, the absence of *Armillaria* spp. affecting *H. fraxineus* from *H. fraxineus* free plots in France (Husson et al., 2012) suggests their role as secondary pathogens of *F. excelsior*. The presence of *Armillaria* spp. is associated with more developed basal lesions, and present a health hazard to the public (Enderle et al., 2017).

Throughout Europe, five *Armillaria* spp. (excluding the two species from closely related *Desarmillaria* genus) have been identified which differ in their ecology and pathogenicity (Guillaumin et al., 1993; Heinzelmann et al., 2018). Therefore, identifying the role of *Armillaria* species in basal lesions of *F. excelsior* in UK woodlands is important for disease prognosis and to effectively respond to ash dieback disease in the UK. To achieve this, the presence of basal lesions, and their association with *Armillaria* spp., and symptoms at both the base and in the crown of trees were surveyed. Additionally, species present in basal lesions were isolated onto nutrient media. However, time limitations owing to Coronavirus related disruption resulted in only one woodland survey and the molecular identification of only *Armillaria* spp. isolates. Three *Armillaria* spp. were also molecularly identified from *F. excelsior* basal lesions at two additional woodlands.

6.2 Methods

6.2.1 Site survey

Sleaford wood was surveyed for the presence of basal lesions. This was conducted by walking through the woodland along two parallel transects approximately 25 m apart and assessing the closest *F. excelsior* to the transect approximately every 15 m.

The presence of basal necrosis was assessed by removing a 5 x 5 cm piece of bark at North, South, East and West. Visible symptoms of basal lesions prior to bark removal were recorded, and the presence of epicormic shoots on the main stem and branches were used to estimate tree health. The proportion of crown dieback could not be estimated as the woodland was sampled in February 2020. This systematic transect was conducted for 15 *F. excelsior* trees.

Table 6.1 Details of woodlands and the surveying/ sampling conducted to examine the frequency of basal lesions and the associated fungal/ oomycete species (Section 6.2). The limitation in sites and surveying/ sampling was due to Coronavirus related disruptions.

Site	Grid Reference	Woodland classification	Dominant species in sampling locations	Survey/ Sampling
Sleaford (Lincolnshire County)	TF070469	Secondary woodland (18th century plantation)	*Fraxinus excelsior, Quercus* spp., *Acer pseudoplatanus*	Survey: Frequency of basal lesions and relationship to presence of epicormics in crown/ on stem, visibility of basal lesions without removing bark Sampling: species present in lesions
Watersend (Kent County)		Semi-natural woodland	*Fraxinus excelsior*	Sampling: *Armillaria* spp. identification from one basal lesion
Backhouse (Kent County)		Semi-natural woodland	*Fraxinus excelsior*	Sampling: *Armillaria* spp. identification from one basal lesion

6.2.2 Lesion Sampling

When a lesion was present, a 5 x 5 cm section of wood, comprising the sapwood, was removed with a sterile chisel at the lesion centre and the lesion edge. A section of bark material was also removed which contained mycelial fans of *Armillaria* spp. when present. Mycelial fan samples were taken from two additional trees on Sleaford, two trees at Watersend wood and one tree at Backhouse wood to maximise sample size. Samples were stored for a maximum of one week at 4°C in sealed plastic bags until laboratory isolations.

6.2.3 Isolations

Each sample was surface sterilised by placing in 0.5% sodium hypochlorite (NaOCl) for 1 minute and then rinsing in 70% methylated spirit. Subsequently, 15 pieces (approximately 2 mm x 2 mm) of inner bark tissue were plated on malt agar (2%) and streptomycin (MA+S) (Supplementary Table 4.1) to grow the fungal species present in the sampled lesions. Another 10 pieces were plated on synthetic mucor agar (SMA) (Supplementary Table 4.1) to isolate any *Phytophthora* spp. present. Bark samples containing mycelial fans were not surface sterilised, and the mycelial fans were cultured directly on MA+S after removing the outer bark. Cultures were incubated in the laboratory at approximately 20°C and were checked every few days for growth. Isolates growing were subcultured onto identical media and incubated at 20°C in the dark ahead of molecular identification.

6.2.4 Molecular identification

Due to time limitations from Coronavirus related disruptions, only *Armillaria* species isolated from mycelial fans were subject to molecular identification. DNA was extracted from mycelial samples using DNeasy Plant Pro kit (Qiagen, Hilden, Germany) according to manufacturer's instructions. PCR amplification was performed by amplifying elongation factor-1 alpha (EF-1 α) region using 0.5 µM Arm EF1-α-FOR (5'-GGA ACT GGT GAG TTC GAA GCC-3') and 0.5 µM EF1-α-REV primers (5'-AGA CGG AGA GGC TTG TCG GAG-3') (Mullholland et al., 2012), 10 µL Quick-Load Taq 2X Master Mix (New England Biolabs, MA, USA), and 1 µL DNA, with reaction volume of 20 µL. Reaction was performed using ProFlex PCR system (Applied Biosystems, Waltham, MA, USA). Following initial denaturation at 95°C for 2 minutes, reaction conditions involved 30 cycles of 95°C denaturation for 35 seconds, 55 seconds annealing at 55°C and 45 second extension at 72°C, followed by a 10 minute final extension at 72°C. PCR products were purified using DNA clean and concentrator kit (Zymo Research, Irvine, CA, USA) according to manufacturer's instructions and were then sequenced by Source Bioscience (Cambridge, UK) using EF1-α-FOR and EF1-α-REV primers. Sequence data was processed using MEGA11 software (Tamura et al., 2021) and species were identified by using BLAST against sequences in the National Centre for Biotechnology Information (NCBI) GenBank database (Altschul et al., 1990). The percent identity greater than 97% of a published sequence was used for species identification.

6.3 Results

From the transect survey at Sleaford wood, 3/15 trees had basal lesions at the root collar. Of these three lesions, two were visible without removing the bark and mycelial fans were present in two lesions. All trees with basal lesions in this woodland had epicormic growth on main branches, or on the stem. However, trees without lesions present at the root collar also had epicormic shoots on the main stem and branches. At Backhouse wood, a mature tree was identified without crown symptoms, but displayed large visible necrosis at the base. Across all sites, of the 10 trees with basal lesions, mycelial fans indicative of *Armillaria* spp. were present in nine trees. The mycelial fans for two trees were old, and could not be cultured on media.

In total, of seven mycelial fans cultured and sequenced, five were identified as *A. gallica*, and two as *A. mellea* (Table 6.2). The sequences from two trees at Sleaford wood shared 98% query cover and 100% percent identity. The presence of species other than *Armillaria* spp. in basal lesions were only examined at Sleaford wood (Section 6.2). At this site, *Phytophthora* spp. were not isolated onto *Phytophthora* selective media from any of the seven trees sampled. A fruit body belonging to *Ganoderma* spp. was morphologically identified at the base of two trees. Although not sequenced, eight fungal morphotypes were isolated from seven basal lesions.

Table 6.2 Species from mycelial fan isolates (Section 6.2) identified via Sanger sequencing and BLAST of NCBI Genbank database (Altschul et al., 1990) (Section 6.2.4).

Woodland	Dbh (cm)	Species present	GenBank accession	Visible Basal symptoms	Epicormics
Backhouse		*Armillaria gallica*	KT822414[1] (QC = 100%, PI = 99.87%)		
Watersend		*Armillaria gallica*	KT822414[1] (QC = 100%, PI = 98.92%)		
Watersend		*Armillaria gallica*	KT822414[1] (QC = 100%, PI = 98.9%)		
Sleaford*	19.1	*Armillaria gallica*	KT822414[1] (QC = 100%, PI = 99.78%)	Lesion, but smooth bark	Stem epicormics
Sleaford*	40.9	*Armillaria gallica*	KT822414[1] (QC = 100%, PI = 99.78%)	No	Main branch epicormics
Sleaford	23	*Armillaria mellea*	MN580161[2] (QC = 100%, PI = 100%)	Bleed and bark peeling	Main branch epicormics
Sleaford	54.4	*Armillaria mellea*	MN580161[2] (QC = 100%, PI = 100%)	Bleed and bark peeling	Main branch epicormics

* denotes sequences which were identified with 100% percent identity using BLAST tool (Altschul et al., 1990). [1]Guo et al., 2016; [2]Chen et al., 2019.

6.4 Discussion

The detection of *Armillaria* spp. mycelial fans on 9 of 10 basal lesions in this study concurs with the role of *Armillaria* spp. in the aetiology of basal lesion development. The primary detection of *A. gallica* supports evidence from Europe that *Armillaria* spp. are secondary colonisers of *H. fraxineus* induced basal lesions (Husson et al., 2012; Chandelier et al., 2016). *A. gallica* has an extensive network of rhizomorphs throughout woodlands, which will reside on the exterior of potential hosts, and colonise upon death or weakening of the tree (Guillaumin et al., 1993; Tsykun et al., 2012). Accordingly, the 100% percent identity between two sequences in Sleaford wood from different trees indicates these samples may be the same individual. *A. cepistipes* also produces an extensive network of rhizomorphs and has a similar ecological role as a decomposer in natural woodlands (Tsykun et al., 2012). However, *A. cepistipes* occurs at greater frequency in colder climates (Guillaumin et al., 1993). Indeed, surveys from Serbia and Albania found *A. cepistipes* was more common at higher altitudes than *A. gallica* (Keca et al., 2009; Lushaj et al., 2010). Together, this suggests *A. gallica* is likely dominant over *A. cepistipes* in southern UK.

The absence of *Phytophthora* spp. is in agreement with findings from previous studies (Schumacher, 2011; Husson et al., 2012) and suggests an insignificant role in the aetiology of *F. excelsior* basal lesion development associated with ash dieback. However, this does not mean that *Phytophthora* spp. are insignificant on *F. excelsior* in general. For example, the presence of *Phytophthora* spp. in *F. excelsior* basal or root lesions has been reported from woodlands in Germany, Denmark and Poland (Orlikowski et al., 2011; Langer et al., 2017). The large number of fungal morphotypes isolated from a small number of basal lesions in this study also highlights the potential role of species other than *Armillaria* spp. or *H. fraxineus* in basal lesion development. Notably, my study also found two trees with fruit bodies of wood decay *Ganoderma* spp. (Schwarze and Ferner, 2003). Indeed, a recent study in Germany isolated 16 taxa other than *H. fraxineus* and *Armillaria* spp. from four *F. excelsior* bases and rootstocks (Meyn et al., 2019). The species composition is likely to affect the progression of root and basal rot in *F. excelsior* through the presence of endophytic, pathogenic, or decay species.

The presence of *A. mellea* from two of four cultured mycelial fans at Sleaford wood contradicts findings from continental Europe, which suggest *A. gallica* is the primary species involved in *F. excelsior* basal lesion development. However, *A. mellea* has been detected in a minority of *F. excelsior* basal lesions from studies in France (4 of 45 identified *Armillaria* spp. (Husson et al., 2012), and on 6 of 42 plots investigated (Marçais et al., 2016)) and Belgium (1 of 45 identified *Armillaria* spp. (Chandelier et al., 2016)). *A. mellea* does not tolerate cold temperatures, thus is suited to the mild Atlantic climate in England (Guillaumin et al., 1993). *A. mellea* appears to have greater pathogenicity than *A.*

gallica (Rishbeth, 1982), so could contribute to more extensive *F. excelsior* decline in comparison to *A. gallica*. Importantly, unlike *A. gallica*, *A. mellea* does not produce extensive rhizomorph networks throughout woodlands (Guillaimin et al., 1993). Indeed, land history is an important determinant of *Armillaria* spp. presence (Labbé et al., 2015), and *A. mellea* was the most common *Armillaria* spp. from plantations in Serbia (Keca et al., 2009). Accordingly, Sleaford wood, the woodland from which *A. mellea* was detected in this study, was a plantation from the mid-18th century. In fact, in France the majority of plots with absence of *Armillaria* spp. in stands were from formerly agricultural sites (Marçais et al., 2016).

Surveys were not performed on hedgerow trees, but the prevalence of *Armillaria* spp. will be determined by the history of the hedgerow and the surrounding land. Collar cankers are less prevalent in areas with lower ash density and greater tree cover fragmentation (Grosdidier et al., 2020). However, this will be specific to the individual tree and factors which may increase the ascospore density or infection potential at the base of the tree (Chapter 2 and Chapter 3) will be important. Accordingly, basal lesion development is positively associated with indicators of elevated moisture (Marçais et al., 2016).

My research also found that crown condition was not noticeably worse in trees with basal lesions, although all trees with basal lesions were visibly stressed as exemplified by the presence of epicormic shoots. A tree at Backhouse also had an externally visible advanced basal necrosis, yet crown symptoms were negligible. This concurs with previous findings of a significant, but weak (Muñoz et al., 2016) or moderate correlation between crown and basal condition (Madsen et al., 2021). Additionally, a survey from Germany found that although collar rots were more likely on trees with greater disease intensity, they were still present on 15% of trees that were otherwise asymptomatic (Enderle et al., 2013).

6.5 Conclusions

Only one site was extensively surveyed for the presence of basal lesions and species present in the lesions due to Coronavirus related disruptions. On this site eight fungal morphotypes were isolated from seven basal lesions and *Ganoderma* spp. were morphologically identified on two trees. *Phytophthora* spp. were not isolated. Epicormic shoots were always present on trees with basal lesions in the present study, although this was not an indicative factor of basal lesion presence, and lesions were not always visible without removing the bark.

Continuation of the research across more sites, and involving root material is required to identify the prevalence of root and basal lesions, and species present within both active and dormant lesions in woodlands in the UK. This will allow better disease prognosis and examination of species or species combinations that may inhibit or facilitate the development of basal and root lesions.

Chapter 7: Synthesis

Hymenoscyphus fraxineus, the causal agent of ash dieback, is dependent on the sexual cycle for reproduction, and subsequent infection of the host (Gross, Holdenrieder et al., 2014). Therefore, my thesis examined of the environmental regulators influencing different stages of the sexual cycle (Figure 7.1) to enable better understanding of current and future disease impacts, as well as the development of management practices to limit the impact of *H. fraxineus*.

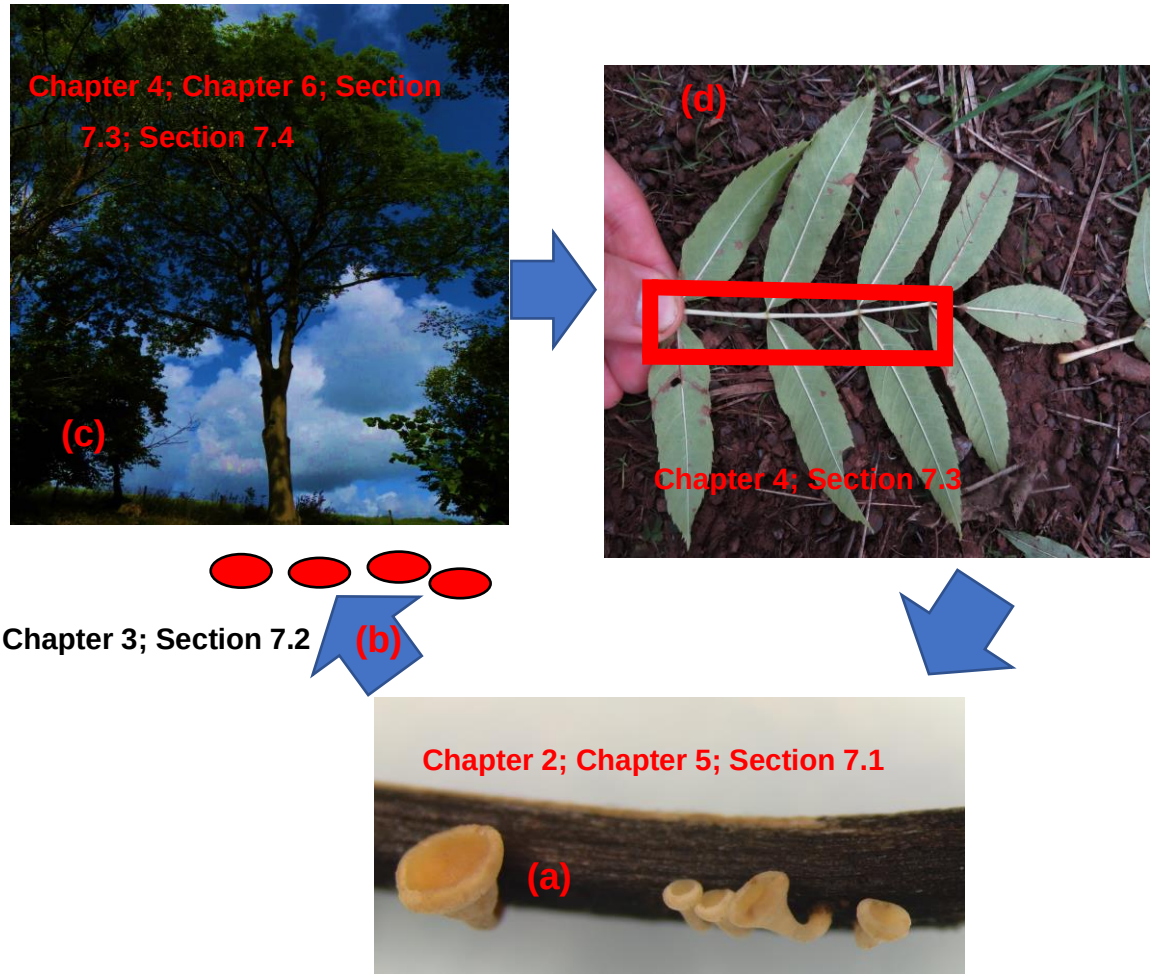

Figure 7.1 Outline of *H. fraxineus* sexual lifecycle and the chapters in this thesis that stages were investigated. **(a)** Environmental conditions affecting the development of apothecia in the field and laboratory (Chapter 2; Chapter 5; Section 7.1) **(b)** Environmental conditions affecting ascospore ejection in the field (Chapter 3; Section 7.2) **(c)** The effect of temperature and solute potential on ascospore germination (Chapter 4) and the species associated with basal necrosis of *F. excelsior* (Chapter 6; Section 7.3; Section 7.4) **(d)** The relationship between spore density, rachis (highlighted in the red box) colonisation by *H. fraxineus* and disease progression in the field (Chapter 4; Section 7.3).

7.1 Environmental regulation of *H. fraxineus* sexual cycle: Apothecia development

A combination of field (Chapter 2) and laboratory (Chapter 5) experiments revealed the positive effect of temperature (between approximately 10°C, the threshold temperature for apothecia development, and 22°C, the maximum mean daily temperature in this study) and relative humidity on *H. fraxineus* apothecia development. However, the relationship between humidity and apothecia development was negative at cooler temperatures (14°C). Laboratory experiments (Chapter 5) also demonstrated the importance of light for mature apothecia development. Field experiments (Chapter 2) determined the importance of ground cover and the degree of canopy closure on the development of apothecia, which likely influences apothecia development via effects on the microclimate at the litter layer. Previous work had noted that greater apothecia development of *H. fraxineus* (Mansfield et al., 2018), and other pathogens such as *Sclerotinia sclerotiorum* (Kora et al., 2005) occurs under vegetation than on exposed litter and management of the latter can limit apothecia development in crop fields (Kora et al., 2005). My thesis furthers this previous research by uncovering significant interactive effects between the ground cover and the temperature and relative humidity. Greater apothecia development under vegetation cover at warmer (16.5°C) temperatures is presumably due to greater moisture retention in the litter layer (Chapter 2). Canopy closure influences the microclimate of the litter layer directly via shading, but an open canopy has a greater opposite impact by allowing greater growth of ground vegetation (Chapter 2). More open canopies in *F. excelsior* woodlands due to dieback from disease progression could therefore act as a positive feedback loop for infection pressure.

7.1.1 Effect of ground vegetation

The significant influence of microclimate on the development of apothecia provides management options to reduce *H. fraxineus* apothecia development. For example, clearing of the understorey to reduce moisture in the litter layer, or choosing species admixtures in future *F. excelsior* woodlands that will minimise moisture retention in the litter layer. The restricted apothecia development in areas with an exposed litter layer highlights the sensitivity of *H. fraxineus* to moisture limitations that can occur through evaporation from an exposed litter layer. The negative impact of low moisture on *H. fraxineus* apothecia development in exposed litter layers via increased evaporation from exposure to solar radiation (Chapter 2) can be expected to increase with an increased frequency of heatwaves with climate change.

My results provide hope for *F. excelsior* in urban areas as low humidity on the ground should limit *H. fraxineus* apothecia production. However, urban environments pose their own challenges for the host with regards to root compression and less nutrient

availability (Jim, 2019). My results are also of relevance to prioritising woodland surveys. If a site has a drier soil and limited understorey, *H. fraxineus* apothecia development will be compromised. This is exemplified by the reduced disease severity in ash-beech woodlands, in comparison to ash-alder woodlands (Erfmeier et al., 2019). The use of 'indicator' species and soil type may be a particularly useful tool for land managers to estimate moisture in the litter layer as a proxy for the fruiting potential of *H. fraxineus*. The possible utility of this method can be highlighted by the association between the number of apothecia and the flood-risk index of a site (Grosdidier, Ioos, Marçais et al., 2018), as well as the higher density of ascospores present on sites described as wet (Čermáková et al., 2017). However, other factors such as the density of *F. excelsior* in a woodland (Klesse, Abegg et al., 2021) and the presence of *F. excelsior* nearby (Grosdidier et al., 2020), will both affect the total *H. fraxineus* apothecia development in an area that can affect a host tree. Most spores are dispersed within 50 m of a stand (Chandelier et al., 2014; Grosdidier, Ioos, Husson et al., 2018), however *H. fraxineus* inoculum dispersal has been estimated as 1.4 to 2.6 km (Grosdidier Ioos, Husson et al., 2018), and the effects of the *F. excelsior* abundance are significant up to 300 m (Grosdidier et al., 2020). Therefore, management of *H. fraxineus* will require cooperation and communication between different individuals and organisations.

Although it is anticipated that ground cover and canopy closure affect *H. fraxineus* apothecia development primarily via microclimatic effects, the effect of light may also be important. In accordance with previous work on *H. fraxineus* (Gross, Zaffarano et al., 2012) and other ascomycetes (Raynal et al., 1987), my research demonstrated light is required for production of the apothecium cup (Chapter 5). Fungi have photoreceptors, and developmental processes are regulated by light intensity, wavelength, and duration (Thind and Schilder, 2018). Indeed, light has even been shown to affect the virulence of *Botrytis cinerea* (Canessa et al., 2013). Future research into the importance of light in *H. fraxineus* developmental processes is essential to guide disease management.

7.1.2 Effect of 'overwintering' environment

My research also demonstrated that environmental conditions over winter affect the subsequent development of apothecia in the summer (Chapter 5). This had previously been inferred by the effect of growing degree days (a measure of accumulated temperature) on the maximum quantity of *H. fraxineus* ascospores produced in a season (Hietala et al., 2018). My results indicate that *H. fraxineus* on rachises which overwintered at warmer temperatures (up to 20°C) produce apothecia quicker when apothecia development is triggered, although the probability of producing apothecia is lower. This could be because better growth conditions for *H. fraxineus* on the rachis meant the

pathogen had greater energy expenditure and utilised more resources from the rachis, which increased the rate of apothecia development, but decreased the probability of apothecia developing on a rachis. Previous research highlighting a negative relationship between the quantity of *H. fraxineus* apothecia production and the number of seasons apothecia have developed on a rachis further indicates that energy expenditure and rachis resources are important for apothecia development (Kirisits, 2015). Indeed, *in vitro* importance of nutrient affects sexual reproduction in *Orbilia spp.*, another ascomycete (Guo et al., 2009). Furthermore, under field conditions the co-occurrence of other species are known to affect the ability to produce apothecia (Gourbière and Debouzie, 2003). Future research should focus on understanding the effects of rachis moisture, nutrient content and species composition on *H. fraxineus* growth rate, mating success and apothecia production. Indeed, accelerating rachis degradation has recently been explored as a tool to control *H. fraxineus* (Bartha et al., 2017; Noble et al., 2019). The efficacy of the pseudosclerotial plates to restrict biotic degradation is demonstrated by the detection fruit bodies from only one other species (*Cyathicula coronata*) on the *H. fraxineus* pseudosclerotised region from one of 202 rachises (Kowalski and Bilański 2021).

7.1.3 Triggers for apothecia development

My research revealed that under high humidity, an average temperature of approximately 10°C is the threshold temperature to trigger apothecia development (Chapter 5), which is in accordance with aerial ascospore trapping records (Chapter 3; Chandelier et al., 2014). Further laboratory studies should be conducted to determine thresholds for the temperature, moisture, nutrient content of rachises, and light intensity, wavelength and duration. These conditions should then be measured across time in the litter layer within woodlands, and the timing of first *H. fraxineus* stipe emergence recorded to accurately model variations in the emergence of apothecia. The initiation of apothecia development is important to understand because earlier flushing in *F. excelsior* is associated with increased resistance to the disease (Bakys et al., 2013). Therefore, projecting future impacts of climate change on *H. fraxineus* apothecia emergence will allow for more accurate projections of the future impacts of ash dieback.

7.1.4 Senescence of apothecia

The conditions and mechanisms involved in the senescence of apothecia need to be investigated. Thus far there is no information in the literature, however my research uncovered a negative effect of high humidity on apothecia development at cooler temperatures (14°C), thereby indicating these conditions could accelerate the senescence of apothecia (Chapter 2). Therefore, sites with high moisture in the litter layer may be prone to earlier senescence of apothecia as the season progresses and temperatures drop, although apothecia development at warmer temperatures (i.e. during the main summer fruiting period) will be greater. However, as previously mentioned, the impact of infection of *F. excelsior* later in the season is probably less than infection earlier in the season. Indeed, the association between sites with indicators of high moisture and increased disease severity (Havrdová et al., 2017; Grosdidier et al., 2020; Klesse, Abegg et al., 2021) indicate that the effect of earlier senescence of *H. fraxineus* apothecia is outweighed by the positive effects of moisture on apothecia development prior to senescence, or on other aspects of *F. excelsior* infection. Laboratory observations indicate that apothecia senescence is an irreversible process (Chapter 5), and additional research should manipulate temperature, moisture and light conditions to determine the thresholds that can trigger apothecia senescence. The role of other species in this process should also be investigated. Boxes that were incubated in the laboratory under high humidity over extended periods were observed to have nematodes inhabiting apothecia, and *Bacillus thuringiensis* isolates have been shown to negatively affect *Ciboria shiraiana* apothecia (Sultana and Kim, 2016).

7.2 Environmental regulation of ascospore ejection

My research examined the conditions affecting ascospore ejection in the field by incorporating apothecia development (Chapter 2) into models of aerial ascospore density from six woodlands from June to September 2019, and one woodland from June to September 2018 (Chapter 3). Temperature and relative humidity were positively related to ascospore ejection, however the effect of temperature depended on the ground cover type. Indeed, although not directly relevant to ascospore ejection, previous studies have determined positive effects of temperature and moisture indicators on aerial ascospore density (Chandelier et al., 2014; Dvorak et al., 2015; Hietala et al., 2018; Burns et al., 2022). In my study, the positive effect of temperature on ascospore ejection was weaker when ground was covered by vegetation compared to exposed litter. This resulted in increased ascospore ejection in areas of litter cover compared to areas of vegetation cover at warmer temperatures (17°C). The interaction provides insight into potential triggers for ascospore ejection. Ascospore ejection in other ascomycetes involves the

increase of asci hydrostatic pressure until asci rupture, release their spores and trigger ejection of ascospores from neighbouring asci in the apothecium (Trail, 2007; Roper et al., 2010).

Laboratory experiments have previously revealed that the quantity of ascospores ejected varies diurnally, with greatest ascospore ejection between 06:00-12:00 (Mansfield et al., 2018). However, the laboratory conditions were not specified, so variations in temperature, humidity or generation of air flow by opening doors could have interfered with the experiment and triggered ejection. Furthermore, as mentioned in Section 7.1, light is important for the regulation of developmental processes in fungi (Thind and Schilder, 2018), therefore the daily light regime could be sufficient to affect ascospore release. Indeed, early morning ejection is beneficial for *H. fraxineus* because humidity in a woodland is comparatively high, which is beneficial for ascospore germination (Section 7.3). This concurs with observations of an early morning peak in ascospore density from a woodland in Norway (Hietala et al., 2013). Therefore, a diurnal clock in *H. fraxineus* that regulates the ejection of ascospores would be extremely adaptive. The position of *H. fraxineus* apothecia under vegetation cover, or mixed in an exposed litter layer will affect the light regime that the rachises are exposed to and could potentially affect ascospore release.

Temperature and humidity will affect ascospore ejection both directly and indirectly. An increase in temperature (up to around 20°C) will increase the growth rate of *H. fraxineus*, and therefore will presumably increase the rate that ascospores develop and are subsequently ejected, whilst also increasing the hydrostatic pressure within asci via affects on the water potential (Chapter 3). Similarly, increased humidity can be expected to be associated with increased water availability for *H. fraxineus*, which will increase the water that can be transported into asci to maximise the hydrostatic pressure (Chapter 3). Both variables likely indirectly influence ascospore ejection via their effects on air pressure, which can affect air currents that are capable of triggering ascospore ejection (Roper et al., 2010). The ejection of ascospores when humid boxes are opened in the laboratory, and when humidity typically decreases in the early hours of the morning are indicative that pressure changes that result in air currents are sufficient to trigger the ejection of ascospores. I hypothesise that apothecia in areas of exposed litter cover are more frequently exposed to air flow that can trigger ascospore release. Furthermore, increases in temperature have a greater effect in areas of bare litter cover because the litter layer is exposed to more solar radiation and therefore heats up more, which will lead to greater changes in pressure and thus greater air flow that can trigger ascospore ejection (Chapter 3). Indeed, of a range of environmental variables considered, net radiation, a measure of energy going into the earth, had the strongest influence on the timing of the daily spore peak (Burns et al., 2022). However, net radiation, soil

temperature and leaf moisture all influenced the quantity of spores (Burns et al., 2022). This concurs with my findings (Chapter 3), which suggest that the process of *H. fraxineus* ascospore ejection can be divided into two separate processes: (1) the conditions that optimise asci maturation and priming for ascospore release, and (2) the conditions that trigger the release of ascospores.

Further research is required in both the laboratory and field to understand environmental conditions and associated mechanisms that trigger ascospore release and affect the rate of asci maturation. Indeed, ascospore ejection in *Gibberella zeae* can be suppressed by inhibitors of potassium and calcium ion channels (Trail et al., 2002). The limitation of *H. fraxineus* ascospore development and release would restrict colonisation of *F. excelsior* foliage (Section 7.3) and limit the pathogen lifecycle. Importantly, the reduced ascospore ejection in areas of vegetation cover could indicate limitation of ascospores to disperse beyond vegetation cover. This suggests that physical barriers may be able to prevent ascospores infecting host foliage. However, if ascospores are ejected, but prevented from dispersing beyond the vegetation cover then extremely high spore density may be present at the ground level under the vegetation and could increase the likelihood of basal infection of *F. excelsior.* The possibility of a high ascospore density trapped at the litter layer that can be washed into the soil to infect roots of *F. excelsior* should be explored. This is of particular importance because *H. fraxineus* root and collar colonisation (Chapter 6) ultimately leads to accelerated tree decline and a public safety hazard following secondary colonisation by *Armillaria* spp. (Enderle et al., 2017).

Therefore, the removal of understorey vegetation around the base of *F. excelsior* could reduce the risk of collar infection. Importantly, my research only monitored ascospore density at weekly intervals and it is likely that if vegetation cover prevents ascospores dispersing, or ejection is less likely to be triggered because the litter layer is sheltered from air flow, on days with high wind, ejection from the comparatively large quantity of apothecia under vegetation cover could lead to an extremely high spore density. This requires investigation by more frequent sampling within a site with measures of local wind speed. The absence of local wind speed measurements has prevented the accurate examination of its effect on ascospore density in this study and in previous research (Chapter 3; Hietala et al., 2018; Burns et al., 2022). This is of particular importance on railways and roads, because they will be frequently exposed to greater disturbance from air flow. Furthermore, the frequency of ejection and the overall number of ascospores that apothecia can eject and how this is influenced by the environment should be investigated. Indeed, in *Monilinia vaccinii-corymbosi*, apothecia ejected fewer ascospores at 10°C and 15°C in comparison to 20°C and 25°C, yet due to enhanced longevity, the overall number of ascospores ejected were greater (Wharton and Schilder,

2005). Further research of these unknows will allow a better understanding of the risk from *H. fraxineus* infection.

7.3 Environmental regulation of ascospore germination and host colonisation

Ejection of ascospores and transport to the foliage of *F. excelsior* does not equate to successful infection and host colonisation. For foliar infection, *H. fraxineus* ascospores germinate and form appressoria which enzymatically degrade the cuticle and mechanically penetrate epidermal cells (Cleary et al., 2013). My research revealed a large variation in the probability of ascospore germination not reported in previous studies of *H. fraxineus* (Schlegel et al., 2016; Mansfield et al., 2018). Additionally, ascospores collected from apothecia that were produced by incubating rachises in the laboratory between January and March were less likely to germinate than those produced by incubating between October and December, although the probability of germination was greatest for field collected apothecia (Chapter 4). Together, this highlights variable maturation of *H. fraxineus* ascospores, likely due to different environmental conditions during apothecia development that lead to differences in the accumulation of organic compounds important for metabolic pathways in ascospore germination. Additionally, the sensitivity of *H. fraxineus* ascospore germination to water potential in comparison to other ascomycetes (Trapero-Casas and Kaiser 2007; Ramirez et al., 2004) could be indicative that ascospores produced in the laboratory had lower concentrations of compatible solutes. Compatible solutes are important for fungi to manage stress (Dijksterhuis and de Vries, 2006) and the incubation of apothecia in sealed boxes in the laboratory for prolonged periods could have led to anaerobic stress and utilisation of compatible solutes prior to ascospore development. Further research should investigate the possibility of variation in ascospore germination across a season due to environmental conditions, and across time for an individual apothecium.

Importantly, my research revealed that *H. fraxineus* ascospores were not sensitive to temperature changes, but were very sensitive to changes in solute potential in comparison to other ascomycetes (Chapter 4). However, this experiment was conducted with laboratory produced apothecia, and as discussed above, likely had poor resilience to stressful conditions. Nonetheless, my research identifies decreasing solute potential as a stressful state for *H. fraxineus*, and suggests that, as with other foliar pathogens (Trapero-Casas and Kaiser 2007), high moisture and high humidity are conducive for successful host colonisation. Therefore, although open canopies may increase apothecia development via indirectly increasing moisture retention in the litter layer (Section 7.1.1), the reduction of humidity in the canopy could limit *H. fraxineus* infection success. The overall aim of management should be to reduce moisture at the litter layer and increase

aeration in the canopy. Importantly, my results suggest that the infection capability of ascospores on *F. excelsior* along roads or railways will be lower than in woodland environments. Accordingly, previous work found that trees which were more isolated in an agricultural setting, compared to a woodland setting, had reduced disease severity. Although the proportion of *H. fraxineus* infected rachises did not significantly differ, it was slightly higher in a woodland setting (Grosdidier et al., 2020).

My research found germination in ascospores from laboratory produced apothecia were inhibited at 35°C (Chapter 4). Previous work demonstrated that *H. fraxineus* hyphal survivability is compromised by temperatures in excess of 36°C (Hauptman et al., 2013), and such temperatures in the field have been associated with reduced disease severity (Davydenko et al., 2013; Grosdidier, Ioos, Marçais et al., 2018; Grosdidier et al., 2020). However, further research is required to determine whether findings are consistent with field produced apothecia and whether such temperatures kill spores. Extreme temperatures may induce a period of dormancy in ascospores to circumvent exposure of subsequent hyphae to lethal temperatures. Additionally, although a temperature range between 5°C to 30°C does not prevent the germination of ascospores, the effect of temperature on the growth rate of *H. fraxineus*, which peaks at approximately 20°C (Kowalski and Bartnik, 2010; Hauptman et al., 2013), will likely impact the colonisation of host foliage colonisation. My experiments (Chapter 4) need to be repeated with field collected apothecia, and using ascospore suspension inoculations of *F. excelsior* foliage. The relative humidity and temperature in the crowns of trees should also be recorded to investigate how laboratory experiments relate to the field. Indeed, in *Sclerotinia sclerotiorum*, microenvironment at the stem base was sufficient to enable ascospore germination, even when experimental conditions were suboptimal (Clarkson et al., 2014).

H. fraxineus ascospore and mycelial density could also stimulate or inhibit germination and host colonisation. Following an extended quiescent phase on *F. excelsior* leaves, a rapid increase in *H. fraxineus* DNA is associated with the presence of necrosis. This indicates that at a threshold density *H. fraxineus* switches to a more aggressive necrotrophic behaviour (Cross et al., 2017). Interestingly, in the native range of *H. fraxineus* in Japan, *H. fraxineus* DNA increases in *F. mandshurica* foliage with the onset of senescence (Inoue et al., 2019). The presence of other species on host foliage can also affect ascospore germination, and is exemplified by the *in vitro* inhibition of *H. fraxineus* ascospore germination by a number of *Fraxinus* spp. endophytes (Schlegel et al., 2016).

My research revealed that the maximum ascospore density recorded within approximately 25 m of an *F. excelsior* canopy was associated with greater *H. fraxineus* colonisation of the rachises in the litter layer the following season, which was associated with poorer crown condition (Chapter 4). However, this may not be a causal relationship

because the results are based on field data. Rather, my results could indicate that a higher spore density results in greater disease progression which could occur through both an earlier switch to a more aggressive necrotrophic lifestyle, and through increased probability of ascospore infection of foliage (Chapter 4). Incomplete colonisation of 60% of *H. fraxineus* infected rachises in the litter layer demonstrates that once the leaves are infected and subsequently shed, the pathogen colonisation of the whole rachis is not guaranteed. This could be due to environmental conditions that induce the formation of pseudosclerotia and lead to a 'dormant' state that prevents further *H. fraxineus* colonisation of the rachis in the litter layer.

However, numerous other fungi inhabit the uncolonised regions of the rachis, some of which are antagonistic towards *H. fraxineus* (Kowalski and Bilański, 2021). Therefore, it is likely that interactions with particular species, or combinations of species, on the rachis limit the growth of *H. fraxineus* and induce pseudosclerotial formation. Importantly, the high density and earlier timing of *H. fraxineus* spore release relative to competitors has been hypothesised to lead to the dominance of *H. fraxineus* (Cross et al., 2017). Therefore, identification of antagonists that occupy uncolonised regions of *F. excelsior* rachises, and their early application to *F. excelsior* foliage would likely be effective at disrupting the sexual reproduction in *H. fraxineus* and therefore limiting infection of *F. excelsior*. Identification of compounds, from these interactions or environmental conditions, that restrict *H. fraxineus* colonisation of rachises will lead to effective management of the disease. Fungal culture collections should be gathered from sites that are earlier in the process of disease establishment because *H. fraxineus* eventually could lead to the displacement of species on *F. excelsior* rachises antagonistic towards *H. fraxineus* but are outcompeted on foliage due to a much lower spore density or later fructification in comparison to *H. fraxineus*.

7.4 *F. excelsior* basal lesion development

H. fraxineus also infects the collar and roots of *F. excelsior*, presumably via lenticels leading to basal and root lesions (Husson et al., 2012; Chandelier et al., 2016; Meyn et al., 2019; Nemesio-Gorriz et al., 2019). Current evidence indicates that these lesions are subsequently colonised by *Armillaria* spp. acting as secondary pathogens (Bakys et al., 2011). The presence of *Armillaria* spp. is associated with more developed lesions that can be hazardous to the public (Enderle et al., 2017). *Armillaria* spp. have also been detected in a minority of lesions without *H. fraxineus* (Chandelier et al., 2016; Madsen et al., 2021), although the absence of *Armillaria* spp. associated with basal lesions from *H. fraxineus* free sites in France (Husson et al., 2012) suggests that even in the absence of *H. fraxineus* in lesions, the stress associated with *H. fraxineus* exposure is

important for *Armillaria* spp. colonisation. Effective management of the sexual cycle of *H. fraxineus* will reduce host stress, reduce the probability of root or collar infection by *H. fraxineus* and thus limit the likelihood of associated hazardous tree decline.

A. gallica was the primary *Armillaria* spp. identified in lesions from Germany, France and Belgium (Enderle et al., 2013; Marcais et al., 2016; Chandelier et al., 2016), but *A. cepistipes* was primarily detected in Lithuania (Lygis et al., 2005; Bakys et al., 2011). My preliminary study (Chapter 6) found that *A. gallica* on 5/7 lesions, although *A. mellea* was present on 2/4 lesions from one woodland. Additional to *Armillaria* spp., eight fungal morphotypes were isolated from seven lesions and *Ganoderma* spp. were fruiting on two trees. My preliminary findings highlight the necessity of further surveys to understand the aetiology of basal and root lesion development in *F. excelsior* in the UK to provide more accurate prognosis for disease management, and to identify species which may inhibit or exacerbate lesion development.

Previous studies have weakly (Muñoz et al., 2016) or moderately (Madsen et al,. 2021) correlated crown dieback with the presence of basal lesions. My study found that epicormics shoots, which are indicative of stress, were present on trees with lesions. However, the crown condition of trees with basal lesions were not noticeably worse (Chapter 6). Crown symptoms are currently the best way to estimate hazardous basal lesion development on mature *F. excelsior* because deeply fissured bark hides the presence of basal lesions. As mentioned above, the prioritisation of surveys in areas with indicators of high moisture at the litter layer which is conducive for both apothecia development, ascospore release, and likely host infection (Chapter 2; Chapter 3; Chapter 4), along with the clearing of vegetation from the basal area of trees to prevent the build up of a high spore density and thus reduce the likelihood of root or basal infection. Accurate modelling of the disease risk on a particular site, incorporating the regulators of *H. fraxineus* sexual cycle and its effects on disease progression will enable land managers to prioritise surveys and application of treatments, thereby minimising risk to the public from root and trunk basal rot.

7.5 Methodological considerations

My thesis utilised a combination of field and laboratory experiments to examine the environmental conditions affecting the sexual cycle of *H. fraxineus* and its effect on host colonisation and disease progression (Section 7.1). Laboratory experiments can manipulate specific conditions such as light, temperature or humidity to examine their effects on biological processes, determine causal relationships, and precisely quantify the effect of an individual variable. However, because environmental factors often interact to affect biotic processes, the results cannot be directly translated to field scenarios. It is not

possible to replicate field conditions in the laboratory for example, experiments examining the effect of temperature on apothecia development in the laboratory could only be conducted in the dark under four constant temperatures (5°C, 10°C, 15°C, 20°C), whereas temperatures and light fluctuate in the field (Chapter 5). Further, spore germination experiments were conducted using apothecia that were produced in the laboratory because access to the building was limited during the main period of apothecia production in 2020 due to Coronavirus restrictions. Subsequently, my thesis revealed the probability of ascospore germination was much smaller in laboratory produced apothecia compared to field collected apothecia (Chapter 4). However, the major utility of laboratory experiments is the ability to determine causal relationships via manipulation experiments. For example, statistical analysis of field data revealed that the maximum *H. fraxineus* spore density in 2019 was related to the proportion of *F. excelsior* rachises in the litter colonised by *H. fraxineus* in 2020, which was related to the severity of crown dieback (Chapter 4). However, laboratory experiments inoculating *F. excelsior* with different ascospore densities are needed to establish whether relationships are causal (Section 7.3).

Alternatively, field experiments quantify the effect of environmental variables using statistical models and are required to understand whether results from laboratory experiments transfer into the field setting. However, the information provided by the model is dependent on the model fit and only provides relationships between variables over the time frame of the study. This is exemplified by the presence of annual variation, and intra- and inter-site variation in models in this thesis (Chapter 2; Chapter 3; Chapter 4).

The heterogenous woodland environment is a particular challenge for field studies, and particularly for *H. fraxineus* apothecia production and ascospore release, which occurs on the forest floor. As highlighted in my thesis, ground cover type and canopy closure both affect *H. fraxineus* sexual cycle, presumably via effects on the microclimate. On top of this, differences in soil properties, air flow, site slope and aspect can all influence the environmental conditions, and these will vary within sites. Indeed incline, edaphic series, vertical terrain heterogeneity and tree cover fragmentation all affect disease progression (Havrdová et al., 2017; Enderle et al., 2018; Grosdidier et al., 2020). The use of random effects within mixed effects models aims to control for systematic differences between the specified random effects (e.g. inter- or intra-site variation). This also highlights the importance for replication in studies to ensure the accuracy of results. I achieved this by working in conjunction with volunteer groups to assist sample collection (Chapter 2; Chapter 3), which wouldn't have been possible individually, particularly given the wide geographic distribution of sites with a gradient of long-term meteorological variables. My thesis demonstrates the important role of the public in managing threats to UK woodlands, and continued communication of this role is essential for future

collaboration. Additionally, the use of home-made spore traps maximised replication by reducing costs by approximately twenty fold. Innovative solutions are required to maximise available resources and to accelerate the rate pertinent research questions can be answered. For example, the measurement of *H. fraxineus* colonisation of rachises in the litter layer was used to estimate *H. fraxineus* foliar colonisation (Grosdidier, Ioos, Marçais et al., 2018; Grosdidier et al., 2020; Chapter 5).

Future research to understand the mechanisms responsible for *H. fraxineus* sexual cycle could also involve induced mutagenesis, as has been utilised in *Sordaria macrospora* (Teichert et al., 2017). This could provide an additional avenue for disease management of *H. fraxineus* and other fungal pathogens. If *H. fraxineus* individuals are uncovered that have an incomplete sexual cycle, an early spray treatment of shed ash foliage on the forest floor could allow the domination of the litter layer by an individual that cannot complete the reproductive life cycle and therefore cannot infect *F. excelsior* in the following seasons.

7.6 Conclusions

My thesis has uncovered environmental regulation of the sexual cycle of *H. fraxineus*, which likely has consequences for disease progression. My research has highlighted the complexity of the sexual cycle and infection process, whilst identifying nascent possibilities for management practices. In combination with research on antagonists, potential disease treatments, and *F. excelsior* resistance, future areas of research indicated above could significantly impact on management of the disease through both the development of a model assessing the risk of ash dieback, and the development of novel treatments and management practices. With the increasing occurrence of invasive forest pathogens (Santini et al., 2013), my thesis highlights the importance of mycology and public engagement to combat this threat.

References

Agan, A. Drenkhan R., Adamson K., Tedersoo L., Solheim H., Børja I., Matsiakh I., Timmermann V., Nagy N.E., Hietala A.M. 2020. The relationship between fungal diversity and invasibility of a foliar niche—The case of ash dieback. *Journal of Fungi* 6, 150. doi: 10.3390/jof6030150.

Altschul, S.F., Gish, W., Miller, W., Myers, E.W. and Lipman, D.J. 1990. Basic local alignment search tool. *Journal of Molecular Biology* 215, 403–410. doi: 10.1016/S0022-2836(05)80360-2.

Arny, C.J. and Rowe, R.C. 1991. Effects of temperature and duration of surface wetness on spore production and infection of cucumbers by *Didymella bryoniae*. *Phytopathology* 81, 206. doi: 10.1094/Phyto-81-206.

Bakys, R., Vasiliauskas, A., Ihrmark, K., Stenlid, J., Menkis, A. and Vasaitis, R. 2011. Root rot, associated fungi and their impact on health condition of declining *Fraxinus excelsior* stands in Lithuania. *Scandinavian Journal of Forest Research* 26, 128–135. doi: 10.1080/02827581.2010.536569.

Bakys, R., Vasaitis, R. and Skovsgaard, J.P. 2013. Patterns and severity of crown dieback in young even-aged stands of European ash (*Fraxinus excelsior* L.) in relation to stand density, bud flushing phenotype, and season. *Plant Protection Science* 49, 120–126. doi: 10.17221/70/2012-PPS.

Bates, D., Maechler, M., Bolker, B., Walker, S. (2015). Fitting linear mixed-effects models using lme4. *Journal of Statistical Software*, 67, 1-48. doi:10.18637/jss.v067.i01.

Baral, H.-O. and Bemmann, M. 2014. *Hymenoscyphus fraxineus* vs. *Hymenoscyphus albidus* - A comparative light microscopic study on the causal agent of European ash dieback and related foliicolous, stroma-forming species. *Mycology* 5, 228–290. doi: 10.1080/21501203.2014.963720.

Baral, H.O., Queloz, V., Hosoya, T. 2014. *Hymenoscyphus fraxineus*, the correct scientific name for the fungus causing ash dieback in Europe. *IMA Fungus* 5, 79–80. doi: 10.5598/imafungus.2014.05.01.09.

Bartha, B., Mayer, A. and Lenz, H.D. 2017. Acceleration of ash petiole decomposition to reduce *Hymenoscyphus fraxineus* apothecia growth - a feasible method for the deprivation of fungal substrate. *Baltic Forestry* 23, 82–88.

Barton, K.. 2020. MuMIn: Multi-Model Inference. R package version 1.43.17. https://CRAN.R-project.org/package=MuMIn.

Becker, R., Ulrich, K., Behrendt, U., Kube, M. and Ulrich, A. 2020. Analyzing ash leaf-colonizing fungal communities for their biological control of *Hymenoscyphus fraxineus*. *Frontiers in Microbiology* 11. Available at: https://www.frontiersin.org/article/10.3389/fmicb.2020.590944.

Bengtsson, S.B.K., Barklund, P., Brömssen, C. von and Stenlid, J. 2014. Seasonal pattern of lesion development in diseased *Fraxinus excelsior* infected by *Hymenoscyphus pseudoalbidus*. *PLOS ONE* 9, e76429. doi: 10.1371/journal.pone.0076429.

Burnham, K.P., Anderson, D.R. and Huyvaert, K.P. 2011. AIC model selection and multimodel inference in behavioral ecology: some background, observations, and comparisons. *Behavioral Ecology and Sociobiology* 65, 23–35. doi: 10.1007/s00265-010-1029-6.

Burns, P., Timmermann, V. and Yearsley, J.M. 2022. Meteorological factors associated with the timing and abundance of *Hymenoscyphus fraxineus* spore release. *International Journal of Biometeorology* 66, pp. 493–506. doi: 10.1007/s00484-021-02211-z.

Burokiene, D., Prospero, S., Jung, E., Marčiulynienė, D., Moosbrugger, K., Norkute, G., Rigling, D., Lygis, V. and Schoebel, C. 2015. Genetic population structure of the invasive ash dieback pathogen *Hymenoscyphus fraxineus* in its expanding range. *Biological Invasions* 17, 2743–2756. doi: 10.1007/s10530-015-0911-6.

Brasier, C. and Webber, J. 2013. Vegetative incompatibility in the ash dieback pathogen *Hymenoscyphus pseudoalbidus* and its ecological implications. *Fungal Ecology* 6, 501–512. doi: 10.1016/j.funeco.2013.09.006.

Brooks, M.E., Kristensen, K., van Benthem, K.J., Magnusson, A., Berg, C.W., Nielsen, A., Skaug, H.J, Maechler, M., and Bolker, B.M. 2017. glmmTMB balances speed and flexibility among packages for zero-inflated generalized linear mixed modeling. *The R Journal*, 9, 378-400.

Brühwiler, V. and Sieber, T. 2020. Aqueous leaf extract of *Ligustrum vulgare* inhibits ascospore germination and mycelial growth of *Hymenoscyphus fraxineus*. *Forest Pathology* 51. doi: 10.1111/efp.12657.

Burnham, K.P. and Anderson, B.D.O. 2001. Kullback-Leibler information as a basis for strong inference in ecological studies. doi: 10.1071/wr99107.

Caffi, T., Rossi, V., Legler, S.E. and Bugiani, R. 2011. A mechanistic model simulating ascosporic infections by *Erysiphe necator*, the powdery mildew fungus of grapevine. *Plant Pathology* 60, 522–531. doi: 10.1111/j.1365-3059.2010.02395.x.

Canihos, Y., Peever, T.L. and Timmer, L.W. 1999. Temperature, leaf wetness, and isolate effects on infection of *Minneola Tangelo* leaves by *Alternaria* sp. *Plant Disease* 83, 429–433. doi: 10.1094/PDIS.1999.83.5.429.

Canessa, P., Schumacher, J., Hevia, M.A., Tudzynski, P. and Larrondo, L.F. 2013. Assessing the effects of light on differentiation and virulence of the plant pathogen *Botrytis cinerea*: Characterization of the white collar complex. *PLOS ONE* 8, e84223. doi: 10.1371/journal.pone.0084223.

Čermáková, V., Kudláček, T., Rotková, G., Rozsypálek, J. and Botella, L. 2017. *Hymenoscyphus fraxineus* mitovirus 1 naturally disperses through the airborne inoculum of its host, *Hymenoscyphus fraxineus*, in the Czech Republic. *Biocontrol Science and Technology* 27, 992–1008. doi: 10.1080/09583157.2017.1368455.

Chandelier, A., Helson, M., Dvorak, M. and Gischer, F. 2014. Detection and quantification of airborne inoculum of *Hymenoscyphus pseudoalbidus* using real-time PCR assays. *Plant Pathology* 63, 1296–1305. doi: 10.1111/ppa.12218.

Chandelier, A., Gerarts, F., San Martin, G., Herman, M. and Delahaye, L. 2016. Temporal evolution of collar lesions associated with ash dieback and the occurrence of *Armillaria* in Belgian forests. *Forest Pathology* 46, pp. 289–297. doi: 10.1111/efp.12258.

Chaudhary, R., Rönneburg, T., Stein Åslund, M., Lundén, K., Durling, M., Ihrmark, K., Menkis, A., Stener, L.-G., Elfstrand, M., Cleary, M., Stenlid, J. 2020. Marker-trait associations for tolerance to ash dieback in common ash (*Fraxinus excelsior* L.). *Forests* 11, 1083. doi: 10.3390/f11101083.

Chen, L. Bóka B., Kedves, O., Nagy, V.D., Szűcs, A., Champramary, S., Roszik, R., Patocskai, Z., Münsterkötter, M., Huynh, T., Indic, B., Vágvölgyi, C., Sipos, G., Kredics, L. 2019. Towards the biological control of devastating forest pathogens from the genus *Armillaria*. *Forests* 10, 1013. doi: 10.3390/f10111013.

Chira, D., Chira, F., Tăut, I., Popovici, O., Blada, I., Doniță, N., Bândiu, C., Gancz, V., Biriș, I. A., Popescu, F., Tănasie, Ș., Dinu, C. 2017. Evolution of ash dieback in Romania. *Dieback of European ash (Fraxinus spp.) – Consequences and Guidelines for Sustainable Management*. Uppsala, Sweden: Swedish University of Agricultural Sciences. 185–194.

Chumanová, E., Romportl, D., Havrdová, L., Zahradník, D., Pešková, V. and Černý, K. 2019. Predicting ash dieback severity and environmental suitability for the disease in forest stands. *Scandinavian Journal of Forest Research* 34, 254–266. doi: 10.1080/02827581.2019.1584638.

Clarkson, J.P., Staveley, J., Phelps, K., Young, C.S. and Whipps, J.M. 2003. Ascospore release and survival in *Sclerotinia sclerotiorum*. *Mycological Research* 107, 213–222. doi: 10.1017/s0953756203007159.

Clarkson, J.P., Fawcett, L., Anthony, S.G. and Young, C. 2014. A Model for *Sclerotinia sclerotiorum* infection and disease development in lettuce, based on the effects of temperature, relative humidity and ascospore density. *PLOS ONE* 9, e94049. doi: 10.1371/journal.pone.0094049.

Cleary, M.R., Daniel, G. and Stenlid, J. 2013. Light and scanning electron microscopy studies of the early infection stages of *Hymenoscyphus pseudoalbidus* on *Fraxinus excelsior*. *Plant Pathology* 62, 1294–1301. doi: 10.1111/ppa.12048.

Cleary, M., Nguyen, D., Marčiulynienė, D., Berlin, A., Vasaitis, R. and Stenlid, J. 2016. Friend or foe? Biological and ecological traits of the European ash dieback pathogen *Hymenoscyphus fraxineus* in its native environment. *Scientific Reports* 6. Available at: http://www.nature.com/articles/srep21895.

Coker, T.L.R., Rozsypálek, J., Edwards, A., Harwood, T.P., Butfoy, L. and Buggs, R.J.A. 2019. Estimating mortality rates of European ash (*Fraxinus excelsior*) under the ash dieback (*Hymenoscyphus fraxineus*) epidemic. *PLANTS, PEOPLE, PLANET* 1, 48–58. doi: 10.1002/ppp3.11.

Cross, H., Sønstebø, J.H., Nagy, N., Timmermann, V., Solheim, H., Børja, I., Kauserud, H., Carlsen, T., Rzepka, Ba., Wasak, K., Vivian-Smith, A., Hietala, A. 2017. Fungal diversity and seasonal succession in ash leaves infected by the invasive ascomycete *Hymenoscyphus fraxineus*. *New Phytologist* 213, 1405–1417. doi: 10.1111/nph.14204.

Davydenko, K., Vasaitis, R., Stenlid, J. and Menkis, A. 2013. Fungi in foliage and shoots of *Fraxinus excelsior* in eastern Ukraine: a first report on *Hymenoscyphus pseudoalbidus*. *Forest Pathology* 43, pp. 462–467. doi: 10.1111/efp.12055.

Develey-Rivière, M.-P. and Galiana, E. 2007. Resistance to pathogens and host developmental stage: a multifaceted relationship within the plant kingdom. *The New Phytologist* 175, 405–416. doi: 10.1111/j.1469-8137.2007.02130.x.

Dijksterhuis, J. and de Vries, R.P. 2006. Compatible solutes and fungal development. *Biochemical Journal* 399, e3. doi: 10.1042/BJ20061229.

Dobrowolska, D., Sebastian, H., Oosterbaan, A., Wagner, S., Clark, J. and Skovsgaard, J.P. 2011. A review of European ash (*Fraxinus excelsior* L.): Implications for silviculture. *Forestry*. doi: 10.1093/forestry/cpr001.

Drenkhan, R., Riit, T., Adamson, K. and Hanso, M. 2016. The earliest samples of *Hymenoscyphus albidus* vs. *H. fraxineus* in Estonian mycological herbaria. *Mycological Progress* . doi: 10.1007/s11557-016-1209-5.

Drenkhan, R., Sander, H. and Hanso, M. 2014. Introduction of Mandshurian ash (*Fraxinus mandshurica* Rupr.) to Estonia: Is it related to the current epidemic on European ash (*F. excelsior* L.)? *European Journal of Forest Research* 133, pp. 769–781. doi: 10.1007/s10342-014-0811-9.

Dvorak, M., Rotkova, G. and Botella, L. 2015. Detection of airborne inoculum of *Hymenoscyphus fraxineus* and *H. albidus* during seasonal fluctuations associated with absence of apothecia. *Forests* 7, 1.

Dvorak, M., Janoš, P., Botella, L., Rotková, G. and Zas, R. 2017. Spore dispersal patterns of *Fusarium circinatum* on an infested Monterey pine forest in North-Western Spain. *Forests* 8, 432. doi: 10.3390/f8110432.

Elfstrand, M., Chen, J., Cleary, M., Halecker, S., Ihrmark, K., Karlsson, M., Davydenko, K., Stenlid, J., Stadler, M. and Durling, M. 2021. Comparative analyses of the *Hymenoscyphus fraxineus* and *Hymenoscyphus albidus* genomes reveals potentially adaptive differences in secondary metabolite and transposable element repertoires. *BMC genomics* 22, 503. doi: 10.1186/s12864-021-07837-2.

Enderle, R., Peters, F., Nakou, A. and Metzler, B. 2013. Temporal development of ash dieback symptoms and spatial distribution of collar rots in a provenance trial of *Fraxinus excelsior*. *European Journal of Forest Research* 132, 865–876. doi: 10.1007/s10342-013-0717-y.

Enderle, R., Nakou, A., Thomas, K. and Metzler, B. 2014. Susceptibility of autochthonous German Fraxinus excelsior clones to *Hymenoscyphus pseudoalbidus* is genetically determined. *Annals of Forest Science* 72. doi: 10.1007/s13595-014-0413-1.

Enderle, R., Sander, F. and Metzler, B. 2017. Temporal development of collar necroses and butt rot in association with ash dieback. *iForest - Biogeosciences and Forestry* 10, 529–536. doi: 10.3832/ifor2407-010.

Enderle, R., Metzler, B., Riemer, U. and Kändler, G. 2018. Ash dieback on sample points of the national forest inventory in South-Western Germany. *Forests* 9, 25. doi: 10.3390/f9010025.

Enderle, R., Stenlid, J. and Vasaitis, R. 2019. An overview of ash (*Fraxinus* spp.) and the ash dieback disease in Europe. *CAB Reviews* 14(no. 025), 1–12.

Erfmeier, A., Haldan, K.L., Beckmann, L.-M., Behrens, M., Rotert, J. and Schrautzer, J. 2019. Ash dieback and its impact in near-natural forest remnants – A plant community-based inventory. *Frontiers in Plant Science*. Available at: https://www.frontiersin.org/article/10.3389/fpls.2019.00658.

FERA, B. 2021. *Chalara (Hymenoscyphus fraxineus) - infections confirmed in the Wider Environment*. Available at: https://chalaramap.fera.co.uk/ [Accessed: September 2021].

Fones, H.N., Mardon, C. and Gurr, S.J. 2016. A role for the asexual spores in infection of *Fraxinus excelsior* by the ash-dieback fungus *Hymenoscyphus fraxineus*. *Scientific Reports* 6, srep34638. doi: 10.1038/srep34638.

Fox, J., Weisberg, S. 2019. *An {R} Companion to Applied Regression*, Third Edition. Thousand Oaks CA: Sage. URL:https://socialsciences.mcmaster.ca/jfox/Books/Companion/

Frąckowiak, P., Pospieszny, H., Smiglak, M. and Obrępalska-Stęplowska, A. 2019. Assessment of the efficacy and mode of action of Benzo(1,2,3)-Thiadiazole-7-Carbothioic Acid S-Methyl Ester (BTH) and Its derivatives in plant protection against viral disease. *International Journal of Molecular Sciences* 20, 1598. doi: 10.3390/ijms20071598

FRAXIGEN. 2005. *Ash species in Europe: biological characteristics and practical guidelines for sustainable use*. Oxford Forestry Institute, University of Oxford, UK.

Freckleton, R.P. 2011. Dealing with collinearity in behavioural and ecological data: model averaging and the problems of measurement error. *Behavioral Ecology and Sociobiology* 65, 91–101. doi: 10.1007/s00265-010-1045-6.

Goberville, E., Hautekeete, N., Kirby, R., Piquot, Y., Luczak, C. and Beaugrand, G. 2016. Climate change and the ash dieback crisis. *Scientific Reports* 6. doi: 10.1038/srep35303.

Gourbière, F. and Debouzie, D. 2003. Local variations in microfungal populations on *Pinus sylvestris* needles. *Mycological research* 107, 1221–1230. doi: 10.1017/s0953756203008451.

Griffiths, S., Galambao, M., Rowntree, J., Goodhead, I., Hall, J., O'Brien, D., Atkinson, N., Antwis, R. 2019. Complex associations between cross-kingdom microbial endophytes and host genotype in ash dieback disease dynamics. *Journal of Ecology* 108. doi: 10.1111/1365-2745.13302.

Grosdidier, M., Ioos, R., Husson, C., Cael, O., Scordia, T. and Marçais, B. 2018. Tracking the invasion: dispersal of *Hymenoscyphus fraxineus* airborne inoculum at different scales. *FEMS Microbiology Ecology* 94, fiy049. doi: 10.1093/femsec/fiy049.

Grosdidier, M., Ioos, R. and Marçais, B. 2018. Do higher summer temperatures restrict the dissemination of *Hymenoscyphus fraxineus* in France? *Forest Pathology* 48, e12426. doi: 10.1111/efp.12426.

Grosdidier, M., Scordia, T., Ioos, R. and Marçais, B. 2020. Landscape epidemiology of ash dieback. *Journal of Ecology* 108, 1789–1799. doi: 10.1111/1365-2745.13383.

Gross, A., Grünig, C.R., Queloz, V. and Holdenrieder, O. 2012. A molecular toolkit for population genetic investigations of the ash dieback pathogen *Hymenoscyphus pseudoalbidus*. *Forest Pathology* 42, 252–264. doi: 10.1111/j.1439-0329.2011.00751.x.

Gross, A., Zaffarano, P.L., Duo, A. and Grünig, C.R. 2012. Reproductive mode and life cycle of the ash dieback pathogen *Hymenoscyphus pseudoalbidus*. *Fungal Genetics and Biology* 49, 977–986. doi: 10.1016/j.fgb.2012.08.008.

Gross, A. and Holdenrieder, O. 2013. On the longevity of *Hymenoscyphus pseudoalbidus* in petioles of *Fraxinus excelsior*. *Forest Pathology* 43, 168–170. doi: 10.1111/efp.12022.

Gross, A., Holdenrieder, O., Pautasso, M., Queloz, V. and Sieber, T.N. 2014. *Hymenoscyphus pseudoalbidus*, the causal agent of European ash dieback: *H. pseudoalbidus*, the causal agent of ash dieback. *Molecular Plant Pathology* 15, 5–21. doi: 10.1111/mpp.12073.

Gross, A., Hosoya, T. and Queloz, V. 2014. Population structure of the invasive forest pathogen *Hymenoscyphus pseudoalbidus*. *Molecular Ecology* 23, 2943–2960. doi: 10.1111/mec.12792.

Gross, A. and Holdenrieder, O. 2015. Pathogenicity of *Hymenoscyphus fraxineus* and *Hymenoscyphus albidus* towards *Fraxinus mandshurica* var. japonica. *Forest Pathology* 45, 172–174. doi: 10.1111/efp.12182.

Gross, A. and Sieber, T.N. 2015. Virulence of *Hymenoscyphus albidus* and native and introduced *Hymenoscyphus fraxineus* on *Fraxinus excelsior* and *Fraxinus pennsylvanica*. *Plant Pathology* 65, 655–663. doi: 10.1111/ppa.12450.

Guillaumin, J.-J. Mohammed, C., Anselmi, N., Courtecuisse, R., Gregory, S.C., Holdenrieder, O., Intini, I., Lung, B., Marxmüller, H., Morrison, D. 1993. Geographical

distribution and ecology of the *Armillaria* species in western Europe. *European Journal of Forest Pathology* 23, 321–341. doi: 10.1111/j.1439-0329.1993.tb00814.x.

Guo, J., Yu, Z., Qiao, M. and Zhang, K. 2009. Effects of carbon and nitrogen sources on sexual reproduction of five strains from the ascomycete *Orbilia*. *Annals of Microbiology* 59, 51–55. doi: 10.1007/BF03175598.

Guo, T., Wang, H.C., Xue, W.Q., Zhao, J. and Yang, Z.L. 2016. Phylogenetic analyses of *Armillaria* reveal at least 15 phylogenetic lineages in China, seven of which are associated with cultivated *Gastrodia elata*. *PloS One* 11, e0154794. doi: 10.1371/journal.pone.0154794.

Guzman-Plazola, R.A., Davis, R.M. and Marois, J.J. 2003. Effects of relative humidity and high temperature on spore germination and development of tomato powdery mildew (*Leveillula taurica*). *Crop Protection* 22, 1157–1168. doi: 10.1016/S0261-2194(03)00157-1.

Han, J.-G., Shrestha, B., Hosoya, T., Lee, K.-H., Sung, G.-H. and Shin, H.-D. 2014. First report of the ash dieback pathogen *Hymenoscyphus fraxineus* in Korea. *Mycobiology* 42, 391–396. doi: 10.5941/MYCO.2014.42.4.391.

Haňáčková, Z., Koukol, O., Čmoková, A., Zahradník, D. and Havrdová, L. 2017. Direct evidence of *Hymenoscyphus fraxineus* infection pathway through the petiole-shoot junction. *Forest Pathology* 47, p. e12370. doi: 10.1111/efp.12370.

Harper, A.L. McKinney, L.V., Nielsen, L.R., Havlickova, L., Li, Y., Trick, M., Fraser, F., Wang, L., Fellgett, A., Sollars, E.S.A., Janacek, S.H., Downie, J.A., Buggs, R.J.A., Kjær, E.D. and Bancroft, I. 2016. Molecular markers for tolerance of European ash (*Fraxinus excelsior*) to dieback disease identified using associative transcriptomics. *Scientific Reports* 6, 19335.

Hartig, F. 2021. DHARMa: Residual diagnostics for hierarchical (multi-level / mixed) regression models. R package version 0.4.4. https://CRAN.R-project.org/package=DHARMa

Hauptman, T., Piškur, B., Groot, M. de, Ogris, N., Ferlan, M. and Jurc, D. 2013. Temperature effect on *Chalara fraxinea*: heat treatment of saplings as a possible disease control method. *Forest Pathology* 43, 360–370. doi: 10.1111/efp.12038.

Havrdová, L., Novotná, K., Zahradník, D., Buriánek, V., Pešková, V., Šrůtka, P. and Černý, K. 2016. Differences in susceptibility to ash dieback in Czech provenances of *Fraxinus excelsior*. *Forest Pathology* 46, 281–288. doi: 10.1111/efp.12265.

Havrdová, L., Zahradník, D., Romportl, D., Pešková, V. and Černỳ, K. 2017. Environmental and silvicultural characteristics influencing the extent of ash dieback in forest stands. *Baltic Forestry* 23, 168–182.

Heinzelmann, R., Dutech, C., Tsykun, T., Labbé, F., Soularue, J.-P. and Prospero, S. 2018. Latest advances and future perspectives in *Armillaria* research. *Canadian Journal of Plant Pathology* 41. doi: 10.1080/07060661.2018.1558284.

Hill, L., Hemery, G., Hector, A. and Brown, N. 2019. Maintaining ecosystem properties after loss of ash in Great Britain. *Journal of Applied Ecology* 56, 282–293. doi: 10.1111/1365-2664.13255.

Hietala, A.M., Timmermann, V., BØrja, I. and Solheim, H. 2013. The invasive ash dieback pathogen *Hymenoscyphus pseudoalbidus* exerts maximal infection pressure prior to the onset of host leaf senescence. *Fungal Ecology* 6, 302–308. doi: 10.1016/j.funeco.2013.03.008.

Hietala, A.M., Børja, I., Solheim, H., Nagy, N.E. and Timmermann, V. 2018. Propagule pressure build-up by the invasive *Hymenoscyphus fraxineus* following its introduction to an ash forest inhabited by the native *Hymenoscyphus albidus*. *Frontiers in Plant Science* 9. Available at: https://www.frontiersin.org/articles/10.3389/fpls.2018.01087/full.

Hinsinger, D.D., Basak, J., Gaudeul, M., Cruaud, C., Bertolino, P., Frascaria-Lacoste, N. and Bousquet, J. 2013. The phylogeny and biogeographic history of ashes (*Fraxinus*, Oleaceae) highlight the roles of migration and vicariance in the diversification of temperate trees. *PLOS ONE* 8, e80431. doi: 10.1371/journal.pone.0080431.

Huang, Y.J., Toscano-Underwood, C., Fitt, B.D.L., Hu, X.J. and Hall, A.M. 2003. Effects of temperature on ascospore germination and penetration of oilseed rape (*Brassica napus*) leaves by A- or B-group *Leptosphaeria maculans* (phoma stem canker). *Plant Pathology* 52, 245–255. doi: 10.1046/j.1365-3059.2003.00813.x.

Hultberg, T., Sandström, J., Felton, A., Öhman, K., Rönnberg, J., Witzell, J. and Cleary, M. 2020. Ash dieback risks an extinction cascade. *Biological Conservation* 244, 108516. doi: 10.1016/j.biocon.2020.108516

Hurvich, C.M. and Tsai, C.-L. 1989. Regression and time series model selection in small samples. *Biometrika* 76, 297–307. doi: 10.1093/biomet/76.2.297.

Husson, C., Caël, O., Grandjean, J.P., Nageleisen, L.M. and Marçais, B. 2012. Occurrence of *Hymenoscyphus pseudoalbidus* on infected ash logs. *Plant Pathology* 61, 889–895. doi: 10.1111/j.1365-3059.2011.02578.x.

Husson, C., Scala, B., Caël, O., Frey, P., Feau, N., Ioos, R. and Marçais, B. 2011. *Chalara fraxinea* is an invasive pathogen in France. *European Journal of Plant Pathology* 130, 311–324. doi: 10.1007/s10658-011-9755-9.

Hu, L. and Yang, L. 2019. Time to fight: molecular mechanisms of age-related resistance. *Phytopathology* 109, 1500–1508. doi: 10.1094/PHYTO-11-18-0443-RVW.

Imre, H. and Füzi, I. 2015. Monitoring of ascospore density of *Erysiphe necator* in the air in relation to weather factors and powdery mildew development. *European Journal of Plant Pathology* 144. doi: 10.1007/s10658-015-0823-4

Inoue, T., Okane, I., Ishiga, Y., Degawa, Y., Hosoya, T. and Yamaoka, Y. 2019. The life cycle of *Hymenoscyphus fraxineus* on Manchurian ash, *Fraxinus mandshurica*, in Japan. *Mycoscience* 60, 89–94. doi: 10.1016/j.myc.2018.12.003.

Ioos, R., Fourrier, C., Iancu, G. and Gordon, T. 2009. Sensitive detection of *Fusarium circinatum* in pine seed by combining an enrichment procedure with a real-time polymerase chain reaction using dual-labeled probe chemistry. *Phytopathology* 99, 582–90. doi: 10.1094/PHYTO-99-5-0582.

Ioos, R., Kowalski, T., Husson, C. and Holdenrieder, O. 2009. Rapid in planta detection of *Chalara fraxinea* by a real-time PCR assay using a dual-labelled probe. *European Journal of Plant Pathology* 125, 329–335. doi: 10.1007/s10658-009-9471-x.

Jim, C.Y. 2019. Resolving intractable soil constraints in urban forestry through research–practice synergy. *Socio-Ecological Practice Research* 1, 41–53. doi: 10.1007/s42532-018-00005-z.

Keca, N., Karadžić, D. and Woodward, S. 2009. Ecology of *Armillaria* species in managed forests and plantations in Serbia. *Forest Pathology* 39. doi: 10.1111/j.1439-0329.2008.00578.x.

Keča, N., Tkaczyk, M., Żółciak, A., Stocki, M., Kalaji, H.M., Nowakowska, J.A. and Oszako, T. 2018. Survival of European ash seedlings treated with phosphite after infection with the *Hymenoscyphus fraxineus* and *Phytophthora* species. *Forests* 9, 442. doi: 10.3390/f9080442.

Kettlewell, P.S., Cook, J.W. and Parry, D.W. 2000. Evidence for an osmotic mechanism in the control of powdery mildew disease of wheat by foliar-applied potassium chloride. European Journal of *Plant Pathology* 106, 297–300. doi: 10.1023/A:1008761202455.

Kirisits, T. 2015. Ascocarp formation of *Hymenoscyphus fraxineus* on several-year-old pseudosclerotial leaf rachises of *Fraxinus excelsior*. *Forest Pathology* 45, 254–257. doi: 10.1111/efp.12183.

Kirisits, T., Dämpfle, L. and Kräutler, K. 2013. *Hymenoscyphus albidus* is not associated with an anamorphic stage and displays slower growth than *Hymenoscyphus pseudoalbidus* on agar media. *Forest Pathology* 43, 386–389. doi: 10.1111/efp.12042.

Klesse, S., Abegg, M., Hopf, S.E., Gossner, M.M., Rigling, A. and Queloz, V. 2021. Spread and severity of ash dieback in Switzerland – Tree characteristics and landscape features explain varying mortality probability. *Frontiers in Forests and Global Change*. Available at: https://www.frontiersin.org/article/10.3389/ffgc.2021.645920

Klesse, S., von Arx, G., Gossner, M.M., Hug, C., Rigling, A. and Queloz, V. 2021. Amplifying feedback loop between growth and wood anatomical characteristics of *Fraxinus excelsior* explains size-related susceptibility to ash dieback. *Tree Physiology* 41, 683–696. doi: 10.1093/treephys/tpaa091.

Knowles, J.E., Frederick, C. 2020. merTools: Tools for analyzing mixed effect regression models. R package version 0.5.2. https://CRAN.R-project.org/package=merTools

Kora, C., McDonald, M.R. and Boland, G.J. 2005. Lateral clipping of canopy influences the microclimate and development of apothecia of *Sclerotinia sclerotiorum* in carrots. *Plant Disease* 89, 549–557. doi: 10.1094/PD-89-0549.

Kosawang, C., Amby, D.B., Bussaban, B., McKinney, L.V., Xu, J., Kjær, E.D., Collinge, D.B., Nielsen, L.R. 2018. Fungal communities associated with species of *Fraxinus* tolerant to ash dieback, and their potential for biological control. *Fungal Biology* 122, 110–120. doi: 10.1016/j.funbio.2017.11.002.

Kosawang, C., McKinney, L.V., Nielsen, L.R. and Kjær, E.D. 2020. Variation in aggressiveness of *Hymenoscyphus fraxineus* genotypes amid the ash dieback epidemic. *Plant Pathology* 69, 677–684. doi: 10.1111/ppa.13158.

Koukol, O., Haňáčková, Z., Dvořák, M. and Havrdová, L. 2016. Unseen, but still present in Czechia: *Hymenoscyphus albidus* detected by real-time PCR, but not by intensive sampling. *Mycological Progress* 15. doi: 10.1007/s11557-015-1149-5.

Kowalski, T. (2006). *Chalara fraxinea* sp. nov. associated with dieback of ash (*Fraxinus excelsior*) in Poland. *Forest Pathology* 36, 264–270. doi: 10.1111/j.1439-0329.2006.00453.x.

Kowalski, T. and Holdenrieder, O. 2009. The teleomorph of *Chalara fraxinea*, the causal agent of ash dieback. *Forest Pathology* 39, 304–308. doi: 10.1111/j.1439-0329.2008.00589.x.

Kowalski, T. and Bartnik, C. 2010. Morphologial variation in colonies of *Chalara fraxinea* isolated from ash (*Fraxinus excelsior* L.) stems with symptoms of dieback and effects of temperature on colony growth and structure. *Acta Agrobotanica* 63, 99–106.

Kowalski, T., Białobrzeski, M. and Ostafińska, A. 2013. The occurrence of *Hymenoscyphus pseudoalbidus* apothecia in the leaf litter of *Fraxinus excelsior* stands with ash dieback symptoms in southern Poland. *Acta Mycologica* 48, 135–146. doi: 10.5586/am.2013.031.

Kowalski, T., Kraj, W. and Bednarz, B. 2016. Fungi on stems and twigs in initial and advanced stages of dieback of European ash (*Fraxinus excelsior*) in Poland. *European Journal of Forest Research* 135, 565–579. doi: 10.1007/s10342-016-0955-x.

Kowalski, T., Bilański, P. and Kraj, W. 2017. Pathogenicity of fungi associated with ash dieback towards *Fraxinus excelsior*. *Plant Pathology* 66, 1228–1238. doi: 10.1111/ppa.12667.

Kowalski, T. and Bartnik, C. 2010. Morphologial variation in colonies of *Chalara fraxinea* isolated from ash (*Fraxinus excelsior* L.) stems with symptoms of dieback and effects of temperature on colony growth and structure. *Acta Agrobotanica* 63, 99–106.

Kowalski, T. and Bilański, P. 2021. Fungi Detected in the Previous Year's Leaf Petioles of *Fraxinus excelsior* and Their Antagonistic Potential against *Hymenoscyphus fraxineus*. *Forests* 12, 1412. doi: 10.3390/f12101412.

Kraj, W., Zarek, M. and Kowalski, T. 2012. Genetic variability of *Chalara fraxinea*, dieback cause of European ash (*Fraxinus excelsior* L.). *Mycological Progress* 11, pp. 37–45. doi: 10.1007/s11557-010-0724-z.

Kuznetsova A., Brockhoff P.B., Christensen R.H.B. 2017. lmerTest package: tests in linear mixed effects models. *Journal of Statistical Software*, 82, 1-26. doi: 10.18637/jss.v082.i13 (URL: https://doi.org/10.18637/jss.v082.i13).

Labbé, F. et al. 2015. Pre-existing forests as sources of pathogens? The emergence of *Armillaria ostoyae* in a recently planted pine forest. *Forest Ecology and Management* 357, 248. doi: 10.1016/j.foreco.2015.08.028.

Langer, G. 2017. Collar rots in forests of Northwest Germany affected by ash dieback. *Baltic Forestry* 23, 4–19.

Length, R., V. 2021. emmeans: estimated marginal means, aka least-squares means. R package version 1.7.0. https://CRAN.R-project.org/package=emmeans

Lewis, F., Butler, A. and Gilbert, L. 2011. A unified approach to model selection using the likelihood ratio test. *Methods in Ecology and Evolution* 2, 155–162. doi: 10.1111/j.2041-210X.2010.00063.x.

Lobo, A., McKinney, L.V., Hansen, J.K., Kjær, E.D. and Nielsen, L.R. 2015. Genetic variation in dieback resistance in Fraxinus excelsior confirmed by progeny inoculation assay. *Forest Pathology* 45, 379–387. doi: 10.1111/efp.12179.

Luke, S.G. 2017. Evaluating significance in linear mixed-effects models in R. *Behavior Research Methods* 49, 1494–1502. doi: 10.3758/s13428-016-0809-y.

Lushaj, B.M., Woodward, S., Keča, N. and Intini, M. 2010. Distribution, ecology and host range of *Armillaria* species in Albania. *Forest Pathology* 40, 485–499. doi: 10.1111/j.1439-0329.2009.00624.x.

Lygis, V., Vasiliauskas, R., Larsson, K.-H. and Stenlid, J. 2005. Wood-inhabiting fungi in stems of *Fraxinus excelsior* in declining ash stands of northern Lithuania, with particular reference to *Armillaria cepistipes*. *Scandinavian Journal of Forest Research* 20, 337–346. doi: 10.1080/02827580510036238.

Lygis, V., Prospero, S., Burokienė, D., Schoebel, C., Marčiulynienė, D., Norkute, G. and Rigling, D. 2016. Virulence of the invasive ash pathogen *Hymenoscyphus fraxineus* in old and recently established populations. *Plant Pathology* 66. doi: 10.1111/ppa.12635

MacHardy, W.E., Gadoury, D. 1989. A revision of Mills' criteria for predicting apple scab infection periods. *Phytopathology* 79, 304–310.

Madsen, C.L., Kosawang, C., Thomsen, I.M., Hansen, L.N., Nielsen, L.R. and Kjær, E.D. 2021. Combined progress in symptoms caused by *Hymenoscyphus fraxineus* and *Armillaria* species, and corresponding mortality in young and old ash trees. *Forest Ecology and Management* 491, 119177. doi: 10.1016/j.foreco.2021.119177.

Mansfield, J., Brown, I. and Papp-Rupar, M. 2019. Life at the edge – the cytology and physiology of the biotroph to necrotroph transition in *Hymenoscyphus fraxineus* during lesion formation in ash. *Plant Pathology* 68, 908–920. doi: 10.1111/ppa.13014.

Mansfield, J.W., Galambos, N. and Saville, R. 2018. The use of ascospores of the dieback fungus *Hymenoscyphus fraxineus* for infection assays reveals a significant period of biotrophic interaction in penetrated ash cells. *Plant Pathology* 67, 1354–1361. doi: 10.1111/ppa.12844.

Manstretta, V. and Rossi, V. 2015. Effects of weather variables on ascospore discharge from *Fusarium graminearum* perithecia. *PLOS ONE* 10, e0138860. doi: 10.1371/journal.pone.0138860.

Marçais, B. and Breda, N. 2006. Role of an opportunistic pathogen in the decline of stressed oak trees. *Journal of Ecology* 94,1214–1223. doi: 10.1111/j.1365-2745.2006.01173.x.

Marçais, B., Husson, C., Godart, L. and Caël, O. 2016. Influence of site and stand factors on *Hymenoscyphus fraxineus* -induced basal lesions. *Plant Pathology* 65, 1452–1461. doi: 10.1111/ppa.12542.

Marçais, B. Husson, C., Caël, O., Collet, C., Dowkiw, A., Saintonge, F.-X., Delahaye, L., and Chandelier, A. 2017. Estimation of ash mortality induced by *Hymenoscyphus fraxineus* in France and Belgium. *Baltic Forestry* 23

Matsiakh, I., Solheim, H., Nagy, N., Hietala, A. and Kramarets, V. 2015. Tissue-specific DNA levels and hyphal growth patterns of *Hymenoscyphus fraxineus* in stems of naturally infected *Fraxinus excelsior* saplings. *Forest Pathology* 46, p. n/a-n/a. doi: 10.1111/efp.12245.

McCartney, H.A., Fitt, B.D.L. and Schmechel, D. 1997. Sampling bioaerosols in plant pathology. *Journal of Aerosol Science* 28, 349–364. doi: 10.1016/S0021-8502(96)00438-7.

McCracken A.R., Douglas G.C., Ryan C., Destefanis M, Cooke L.R. 2017. Ash dieback on the island of Ireland. *Dieback of European ash (Fraxinus spp.) – Consequences and Guidelines for Sustainable Management*. Uppsala, Sweden: Swedish University of Agricultural Sciences. 125–39.

McKinney, L.V., Nielsen, L.R., Hansen, J.K. and Kjær, E.D. 2011. Presence of natural genetic resistance in *Fraxinus excelsior* (Oleraceae) to *Chalara fraxinea* (Ascomycota): an emerging infectious disease. *Heredity* 106, 788–797. doi: 10.1038/hdy.2010.119.

McKinney, L.V., Thomsen, I.M., Kjær, E.D., Bengtsson, S.B.K. and Nielsen, L.R. 2012. Rapid invasion by an aggressive pathogenic fungus (*Hymenoscyphus pseudoalbidus*) replaces a native decomposer (*Hymenoscyphus albidus*): a case of local cryptic extinction? *Fungal Ecology* 5, 663–669. doi: 10.1016/j.funeco.2012.05.004.

McKinney, L.V., Nielsen, L.R., Collinge, D.B., Thomsen, I.M., Hansen, J.K. and Kjær, E.D. 2014. The ash dieback crisis: genetic variation in resistance can prove a long-term solution. *Plant Pathology* 63, 485–499. doi: 10.1111/ppa.12196.

McMullan, M., Rafiqi, M., Kaithakottil, G., Clavijo, B.J.,Bilham, L., Orton, E., Percival-Alwyn, L., Ward, B.J., Edwards, A., Saunders, D.G.O, Accinelli, G.G., Wright, J., Verweij, W., Koutsovoulos, G., Yoshida, K., Hosoya, T., Williamson, L., Jennings, P., Ioos, R., Husson, C., Hietala, A.M., Vivian-Smith, A., Solheim, H., MaClean, D., Fosker, C., Hall, N., Brown, J.K.M, Swarbreck, D., Blaxter, M., Downie, J.A. and Clark, M.D. 2018. The ash dieback invasion of Europe was founded by two genetically divergent individuals. *Nature Ecology & Evolution* 2, 1000–1008. doi: 10.1038/s41559-018-0548-9.

Met Office (2017): UKCP09: Met Office gridded land surface climate observations - daily temperature and precipitation at 5km resolution. *Centre for Environmental Data Analysis*, 10/06/18.

Meyn, R., Langer, G.J., Gross, A. and Langer, E.J. 2019. Fungal colonization patterns in necrotic rootstocks and stem bases of dieback-affected *Fraxinus excelsior* L. *Forest Pathology* 49, e12520. doi: 10.1111/efp.12520.

Michalko, R., Košulič, O., Martinek, P. and Birkhofer, K. 2021. Disturbance by invasive pathogenic fungus alters arthropod predator-prey food-webs in ash plantations. *The Journal of Animal Ecology* 90, 2213–2226. doi: 10.1111/1365-2656.13537.

Milenković, I., Jung, T., Stanivuković, Z. and Karadžić, D. 2017. First report of *Hymenoscyphus fraxineus* on *Fraxinus excelsior* in Montenegro. *Forest Pathology* 47, e12359. https://doi.org/10.1111/efp.12359

Mitchell, R.J., J.K. Beaton, P.E. Bellamy, A. Broome, J. Chetcuti, S. Eaton, C.J. Ellis, A. Gimona, R. and Harmer, A.J. 2014. Ash dieback in the UK: A review of the ecological and conservation implications and potential management options. *Biological Conservation* 175, 95–109. doi: 10.1016/j.biocon.2014.04.019

Mitchell, R.J., Pakeman, R., Broome, A., Beaton, J., Bellamy, P., Brooker, R., Ellis, C., Hester, A., Hodgetts, N., Iason, G., Littlewood, N., Pozsgai, G., Ramsay, S., Riach, D., Stockan, J., Taylor, A. and Woodward, S.. 2016. How to replicate the functions and biodiversity of a threatened tree species?: The case of *Fraxinus excelsior* in Britain. *Ecosystems* 19, 573–586. doi: 10.1007/s10021-015-9953-y

Mondal, S.N., Gottwald, T.R. and Timmer, L.W. 2003. Environmental factors affecting the release and dispersal of ascospores of *Mycosphaerella citri*. *Phytopathology* 93, 1031–1036. doi: 10.1094/PHYTO.2003.93.8.1031.

Montecchio, L., Dal Maso, E., Fanchin, G., Accordi, S. and Scattolin, L. 2012. Ultrastructural modifications in Common ash tissues colonised by *Chalara fraxinea*. *Phytopathologia Mediterranea* 51, 599–606. doi: 10.14601/Phytopathol_Mediterr-11132.

Mulholland, V., MacAskill, G., Laue, B., Steele, H., Kenyon, D. and Green, S. 2012. Development and verification of a diagnostic assay based on *EF-1 α* for the identification of *Armillaria* species in Northern Europe. *Forest Pathology* 42. doi: 10.1111/j.1439-0329.2011.00747.x.

Muñoz, F., Marçais, B., Dufour, J. and Dowkiw, A. 2016. Rising out of the ashes: Additive genetic variation for crown and collar resistance to *Hymenoscyphus fraxineus* in *Fraxinus excelsior*. *Phytopathology* 106, 1535–1543. doi: 10.1094/PHYTO-11-15-0284-R.

Musolin, D., Selikhovkin, A., Shabunin, D., Viacheslav, Z. and Baranchikov, Y. 2017. Between ash dieback and Emerald Ash Borer: Two Asian invaders in Russia and the future of ash in Europe. *Baltic Forestry* 23, 316–333.

Nakagawa, S. and Schielzeth, H. 2013. A general and simple method for obtaining R^2 from generalized linear mixed-effects models. *Methods in Ecology and Evolution* 4, 133–142. doi: 10.1111/j.2041-210x.2012.00261.x.

Nave, C., de Vries, J., Eickhorst, C. and Schulz, B. 2017. Each isolate of *Hymenoscyphus fraxineus* is unique as shown by exoenzyme and growth rate profiles. *Baltic Forestry* 23, 25–40.

Nemesio-Gorriz, M., McGuinness, B., Grant, J., Dowd, L. and Douglas, G.C. 2019. Lenticel infection in *Fraxinus excelsior* shoots in the context of ash dieback. *iForest - Biogeosciences and Forestry* 12, 160. doi: 10.3832/ifor2897-012.

Nemesio-Gorriz, M., Menezes R.C., Paetz, C., Hammerbacher, A., Steenackers, M., Schamp, K., Höfte, M., Svatoš, A., Gershenzon, J., Douglas, G.C.. 2020. Canditate metabolites for ash dieback tolerance in Fraxinus excelsior. *Journal of Experimental Botany* 71, 6074–6083. doi: 10.1093/jxb/eraa306.

Nielsen, L.R., McKinney, L.V., Hietala, A.M. and Kjær, E.D. 2017. The susceptibility of Asian, European and North American *Fraxinus* species to the ash dieback pathogen *Hymenoscyphus fraxineus* reflects their phylogenetic history. *European Journal of Forest Research* 136, 59–73. doi: 10.1007/s10342-016-1009-0.

Nielsen, L., Mckinney, L. and Kjaer, E. 2017. Host phenological stage potentially affects dieback severity after *Hymenoscyphus fraxineus* infection in *Fraxinus excelsior* seedlings. *Baltic Forestry* 23, 229–232.

Noble, R. Woodhall, J., Dobrovin-Pennington, A., Perkins, K., Somoza-Valdeolmillos, E., Lekuona Gomez, H., Lu, Y., Macarthur, R., Henry, C. 2019. Control of *Hymenoscyphus fraxineus*, the causal agent of ash dieback, using composting. *Forest Pathology* 49, p. e12568. doi: 10.1111/efp.12568.

Noll, K.E. 1970. A rotary inertial impactor for sampling giant particles in the atmosphere. *Atmospheric Environment* 4, 9–19. doi: 10.1016/0004-6981(70)90050-8.

Orlova-Bienkowskaja, M. Drogvalenko, A.N., Zabaluev, I., Sazhnev, A., Peregudova, E., Mazurov, S., Комаров, E., Struchaev, V., Martynov, V., Nikulina, T., Bieńkowski, A. 2020. Current range of *Agrilus planipennis Fairmaire*, an alien pest of ash trees, in European Russia and Ukraine. *Annals of Forest Science* 77. doi: 10.1007/s13595-020-0930-z.

Orlikowski, Ptaszek, Rodziewicz, Nechwatal, J., Thinggaard and Jung, T. 2011. *Phytophthora* root and collar rot of mature *Fraxinus excelsior* in forest stands in Poland and Denmark. *Forest Pathology* 41, pp. 510–519. doi: 10.1111/j.1439-0329.2011.00714.x.

Orton, E.S., Brasier, C.M., Bilham, L.J., Bansal, A., Webber, J.F. and Brown, J.K.M. 2017. Population structure of the ash dieback pathogen, *Hymenoscyphus fraxineus*, in relation to its mode of arrival in the UK. *Plant Pathology*. Available at: http://doi.wiley.com/10.1111/ppa.12762.

Orton, E.S., Clarke, M., Brasier, C.M., Webber, J.F. and Brown, J.K.M. 2019. A versatile method for assessing pathogenicity of *Hymenoscyphus fraxineus* to ash foliage. *Forest Pathology* 49, e12484. doi: 10.1111/efp.12484.

Pliura, A., Lygis, V., Marčiulyniene, D., Suchockas, V. and Bakys, R. 2015. Genetic variation of *Fraxinus excelsior* half-sib families in response to ash dieback disease following simulated spring frost and summer drought treatments. *iForest - Biogeosciences and Forestry* 9, 12. doi: 10.3832/ifor1514-008.

Power, M., Hopkins, A., Chen, J., Bengtsson, S.B.K., Vasaitis, R. and Cleary, M. 2017. European *Fraxinus* species introduced into New Zealand retain many of their native endophytic fungi. *Baltic Forestry* 23, 74–81.

Pratt, J. 2017. Management and use of Ash in Britain from the prehistoric to the present: some implications for its preservation. *Dieback of European ash (Fraxinus spp.) – Consequences and Guidelines for Sustainable Management*. Uppsala, Sweden: Swedish University of Agricultural Sciences. 1–15.

Prospero, S., Holdenrieder, O. and Rigling, D. 2004. Comparison of the virulence of *Armillaria cepistipes* and *Armillaria ostoyae* on four Norway spruce provenances. *Forest Pathology* 34, 1–14. doi: 10.1046/j.1437-4781.2003.00339.x.

Queloz, V., Grünig, C.R., Berndt, R., Kowalski, T., Sieber, T.N. and Holdenrieder, O. 2011. Cryptic speciation in *Hymenoscyphus albidus*. *Forest Pathology* 41, 133–142. doi: 10.1111/j.1439-0329.2010.00645.x.

R Core Team (2021). R: A language and environment for statistical computing. R Foundation for Statistical Computing, Vienna, Austria. URL https://www.R-project.org/.

Ramirez, M.L., Chulze, S.N. and Magan, N. 2004. Impact of osmotic and matric water stress on germination, growth, mycelial water potentials and endogenous accumulation of sugars and sugar alcohols in *Fusarium graminearum*. *Mycologia* 96, pp. 470–478. doi: 10.1080/15572536.2005.11832946.

Raynal, G., Ferrari, F. and Mouret, M. 1987. Facteurs agissant sur la formation des apothécies de Sclerotinia trifoliorum Eriks. en conditions contrôlées. *Agronomie* 7, 715–725. doi: 10.1051/agro:19870909.

Rishbeth, J. 1982. Species of *Armillaria* in southern England. *Plant Pathology* 31, 9–17. doi: 10.1111/j.1365-3059.1982.tb02806.x.

Robinson, R.A., Stokes, R.H. 1959. *Electrolyte Solutions*. 2nd Revised Edition. London. Butterworth and Co. (Publishers) Ltd.

Roper, M., Seminara, A., Bandi, M.M., Cobb, A., Dillard, H.R. and Pringle, A. 2010. Dispersal of fungal spores on a cooperatively generated wind. *Proceedings of the National Academy of Sciences* 107, 17474–17479. doi: 10.1073/pnas.1003577107.

Rossi, V., Giosuè, S. and Bugiani, R. 2007. A-scab (Apple-scab), a simulation model for estimating risk of *Venturia inaequalis* primary infections*. *EPPO Bulletin* 37, 300–308. doi: 10.1111/j.1365-2338.2007.01125.x.

Rossi, V., Caffi, T. and Legler, S.E. 2010. Dynamics of ascospore maturation and discharge in *Erysiphe necator*, the causal agent of grape powdery mildew. *Phytopathology* 100, 1321–1329. doi: 10.1094/PHYTO-05-10-0149.

Rytkönen, A., Lilja, A., Drenkhan, R., Gaitnieks, T. and Hantula, J. 2011. First record of *Chalara fraxinea* in Finland and genetic variation among isolates sampled from Åland, mainland Finland, Estonia and Latvia. *Forest Pathology* 41, 169–174. doi: 10.1111/j.1439-0329.2010.00647.x.

Sahraei, S.E., Cleary, M., Stenlid, J., Brandström Durling, M. and Elfstrand, M. 2020. Transcriptional responses in developing lesions of European common ash (*Fraxinus excelsior*) reveal genes responding to infection by *Hymenoscyphus fraxineus*. *BMC Plant Biology* 20, 455. doi: 10.1186/s12870-020-02656-1.

Sansford, C.E. 2013 Pest risk analysis for *Hymenoscyphus pseudoalbidus* (anamorph *Chalara fraxinea*) for the UK and the Republic of Ireland. https://webarchive.nationalarchives.gov.uk/ukgwa/20140904082245/http://www.fera.defra.

gov.uk/plants/plantHealth/pestsDiseases/documents/hymenoscyphusPseudoalbidusPRA.pdf (archived: accessed on 05/04/2022).

Santini, A. et al. 2013. Biogeographical patterns and determinants of invasion by forest pathogens in Europe. *New Phytologist* 197, 238–250. doi: 10.1111/j.1469-8137.2012.04364.x.

Schlegel, M., Dubach, V., von Buol, L. and Sieber, T.N. 2016. Effects of endophytic fungi on the ash dieback pathogen. *FEMS microbiology ecology* 92, fiw142. doi: 10.1093/femsec/fiw142.

Schlegel, M., Queloz, V. and Sieber, T.N. 2018. The endophytic mycobiome of European ash and sycamore maple leaves – Geographic patterns, host specificity and influence of ash dieback. *Frontiers in Microbiology* 9. Available at: https://www.frontiersin.org/article/10.3389/fmicb.2018.02345.

Schneider, C.A., Rasband, W.S. and Eliceiri, K.W. 2012. NIH Image to ImageJ: 25 years of image analysis. *Nature Methods* 9, 671–675. doi: 10.1038/nmeth.2089.

Schumacher, J., Kehr, R. and Leonhard, S. 2010. Mycological and histological investigations of *Fraxinus excelsior* nursery saplings naturally infected by *Chalara fraxinea*. *Forest Pathology* 40, 419–429. doi: 10.1111/j.1439-0329.2009.00615.x.

Schumacher, J. 2011. The general situation regarding ash dieback in Germany and investigations concerning the invasion and distribution strategies of *Chalara fraxinea* in woody tissue. *EPPO Bulletin* 41. doi: 10.1111/j.1365-2338.2010.02427.x.

Schwarze, F.W.M.R. and Ferner, D. 2003. *Ganoderma* on trees—Differentiation of species and studies of invasiveness. *Arboricultural Journal* 27, 59–77. doi: 10.1080/03071375.2003.9747362.

Semizer-Cuming, D., Finkeldey, R., Nielsen, L.R. and Kjær, E.D. 2019. Negative correlation between ash dieback susceptibility and reproductive success: good news for European ash forests. *Annals of Forest Science* 76, 16. doi: 10.1007/s13595-019-0799-x.

Semizer-Cuming, D., Chybicki, I.J., Finkeldey, R. and Kjær, E.D. 2021. Gene flow and reproductive success in ash (*Fraxinus excelsior* L.) in the face of ash dieback: restoration and conservation. *Annals of Forest Science* 78, 1–15. doi: 10.1007/s13595-020-01025-0.

Sollars, E.S.A., Kelly, L.J., Sambles, C.M., Ramirez-Gonzalez, R.H., Swarbreck, D., Kaithakottil, G., Cooper, E.D., Uauy, C., Havlickova, L., Worswick, G., Studholme, D.J., Zohren, J., Salmon, D.L., Clavijo, B.J., Li, Y., He, Z., Fellgett, A., McKinney, L.V., Nielsen, L.R., Douglas, G.C., Kjær, E.D., Downie, J.A., Boshier, D., Lee, S., Clark, J.,

Grant, M., Bancroft, I., Caccamo, M. and Richard J.A. 2016. Genome sequence and genetic diversity of European ash trees. Nature 541, 212.

Sollars, E.S.A. and Buggs, R.J.A. 2018. Genome-wide epigenetic variation among ash trees differing in susceptibility to a fungal disease. *BMC Genomics* 19, 502. doi: 10.1186/s12864-018-4874-8.

Spiess, A.-N. 2018. qpcR: Modelling and Analysis of Real-Time PCR Data. R package version 1.4-1. https://CRAN.R-project.org/package=qpcR

Stener, L.-G. 2013. Clonal differences in susceptibility to the dieback of *Fraxinus excelsior* in southern Sweden. *Scandinavian Journal of Forest Research* 28, 205–216. doi: 10.1080/02827581.2012.735699.

Stocks, J.J., Buggs, R.J.A. and Lee, S.J. 2017. A first assessment of *Fraxinus excelsior* (common ash) susceptibility to *Hymenoscyphus fraxineus* (ash dieback) throughout the British Isles. *Scientific Reports* 7. Available at: http://www.nature.com/articles/s41598-017-16706-6

Stocks, J.J., Metheringham, C.L., Plumb, W.J., Lee, S.J., Kelly, L.J., Nichols, R.A. and Buggs, R.J.A. 2019. Genomic basis of European ash tree resistance to ash dieback fungus. *Nature Ecology & Evolution* 3, 1686–1696. doi: 10.1038/s41559-019-1036-6.

Sultana, R. and Kim, K. 2016. *Bacillus thuringiensis* C25 suppresses popcorn disease caused by *Ciboria shiraiana* in mulberry (*Morus australis* L.). *Biocontrol Science and Technology* 26, 145–162. doi: 10.1080/09583157.2015.1084999.

Sun, P. and Yang, X.B. 2000. Light, temperature, and moisture effects on apothecium production of *Sclerotinia sclerotiorum*. *Plant Disease* 84, 1287–1293. doi: 10.1094/PDIS.2000.84.12.1287.

Tamura, K., Stecher, G. and Kumar, S. 2021. MEGA11: Molecular Evolutionary Genetics Analysis Version 11. *Molecular Biology and Evolution* 38(7), pp. 3022–3027. doi: 10.1093/molbev/msab120.

Teichert, I., Lutomski, M., Märker, R., Nowrousian, M. and Kück, U. 2017. New insights from an old mutant: SPADIX4 governs fruiting body development but not hyphal fusion in *Sordaria macrospora*. *Molecular genetics and genomics: MGG* 292, 93–104. doi: 10.1007/s00438-016-1258-0.

Thind, T. and Schilder, A. 2018. Understanding photoreception in fungi and its role in fungal development with focus on phytopathogenic fungi. *Indian Phytopathology* 71, 169–182. doi: 10.1007/s42360-018-0025-z.

Timmermann, V., Børja, I., Hietala, A.M., Kirisits, T. and Solheim, H. 2011. Ash dieback: pathogen spread and diurnal patterns of ascospore dispersal, with special emphasis on Norway. *EPPO Bulletin* 41, 14–20.

Trail, F., Xu, H., Loranger, R. and Gadoury, D. 2002. Physiological and environmental aspects of ascospore discharge in *Gibberella zeae* (anamorph *Fusarium graminearum*). *Mycologia* 94, 181–189.

Trail, F. 2007. Fungal cannons: explosive spore discharge in the Ascomycota. *FEMS Microbiology Letters* 276, 12–18. doi: 10.1111/j.1574-6968.2007.00900.x

Trapero-Casas, A. and Kaiser, W.J. 2007. Differences between ascospores and conidia of *Didymella rabiei* in spore germination and infection of chickpea. *Phytopathology* 97, 1600–1607. doi: 10.1094/PHYTO-97-12-1600.

Tsykun, T., Rigling, D., Nikolaychuk, V. and Prospero, S. 2012. Diversity and ecology of *Armillaria* species in virgin forests in the Ukrainian Carpathians. *Mycological Progress* 11, 403–414. doi: 10.1007/s11557-011-0755-0.

Turczański, K., Rutkowski, P., Dyderski, M.K., Wrońska-Pilarek, D. and Nowiński, M. 2020. Soil pH and organic matter content affects European ash (*Fraxinus excelsior* L.) crown defoliation and its impact on understory vegetation. *Forests* 11, 22. doi: 10.3390/f11010022.

Turczański, K., Bełka, M., Kukawka, R., Spychalski, M. and Smiglak, M. 2021. A novel plant resistance inducer for the protection of European ash (*Fraxinus excelsior* L.) against *Hymenoscyphus fraxineus*—Preliminary Studies. Forests 12, 1072. doi: 10.3390/f12081072.

Ulrich, K., Becker, R., Behrendt, U., Kube, M. and Ulrich, A. 2020. A comparative analysis of ash leaf-colonizing bacterial communities identifies putative antagonists of *Hymenoscyphus fraxineus*. *Frontiers in Microbiology* 11. Available at: https://www.frontiersin.org/article/10.3389/fmicb.2020.00966.

Uysal, A. and Kurt, ş. 2017. Influence of inoculum density, temperature, wetness duration, and leaf age on infection and development of spinach anthracnose caused by the fungal pathogen *Colletotrichum spinaciae*. *European Journal of Plant Pathology* , 1–12. doi: 10.1007/s10658-017-1249-y.

van de Pol, M., Bailey, L.D., McLean, N., Rijsdijk, L., Lawson, C.R. and Brouwer, L. 2016. Identifying the best climatic predictors in ecology and evolution. *Methods in Ecology and Evolution* 7, 1246–1257. doi: 10.1111/2041-210X.12590

Villari, C. Dowkiw, A., Enderle, R., Ghasemkhani, M., Kirisits, T., Kjær, E.D., Marčiulynienė, D., McKinney, L.V., Metzler, B., Muñoz, F., Nielsen, L.R., Pliūra, A., Stener,L.-G., Suchockas, V., Rodriguez-Saona, L., Bonello, P. and Cleary, M. 2018. Advanced spectroscopy-based phenotyping offers a potential solution to the ash dieback epidemic. *Scientific Reports* 8, 17448. doi: 10.1038/s41598-018-35770-0.

Wallander, E. 2008. Systematics of *Fraxinus* (Oleaceae) and evolution of dioecy. *Plant Systematics and Evolution* 273, 25–49. doi: 10.1007/s00606-008-0005-3.

Wey, T., Schlegel, M., Stroheker, S. and Gross, A. 2016. MAT – gene structure and mating behavior of *Hymenoscyphus fraxineus* and *Hymenoscyphus albidus*. *Fungal Genetics and Biology* 87, 54–63. doi: 10.1016/j.fgb.2015.12.013.

Wharton, P.S. and Schilder, A.C. 2005. Effect of temperature on apothecial longevity and ascospore discharge by apothecia of *Monilinia vaccinii-corymbosi*. *Plant Disease* 89, 397–403. doi: 10.1094/PD-89-0397.

Wickham, H. 2016. *ggplot2: Elegant Graphics for Data Analysis*. Springer-Verlag New York.

Wohlmuth, A., Essl, F. and Heinze, B. 2018. Genetic analysis of inherited reduced susceptibility of *Fraxinus excelsior* L. seedlings in Austria to ash dieback. *Forestry: An International Journal of Forest Research* 91, 514–525. doi: 10.1093/forestry/cpy012.

Wylder, B., Biddle, M., King, K., Baden, R. and Webber, J. 2018. Evidence from mortality dating of Fraxinus excelsior indicates ash dieback (Hymenoscyphus fraxineus) was active in England in 2004–2005. *Forestry: An International Journal of Forest Research* 91, 434–443. doi: 10.1093/forestry/cpx059.

Zhao, Y., Hosoya, T., Baral, H.O., Hosaka, K. and Kakishima, M. 2012. *Hymenoscyphus pseudoalbidus*, the correct name for *Lambertella albida* reported from Japan. *Mycotaxon* 122, 25–41.

Zheng, H.-D. and Zhuang, W.-Y. 2014. *Hymenoscyphus albidoides* sp. nov. and *H. pseudoalbidus* from China. *Mycological Progress* 13, 625–638. doi: 10.1007/s11557-013-0945-z.

Zhou, G., Wang, Q. 2018. A new nonlinear method for calculating growing degree days. *Scientific reports* 8, 10149–10149. https://doi.org/10.1038/s41598-018-28392-z.

Appendix

Supplementary Table 2.1 (a) Sampling dates (2018) when rachises at each quadrat location (A, B, C, D) within each site (County Durham, Shropshire, Devon, Wiltshire, Hampshire, Carmarthenshire) were collected and sent to the laboratory **(b)** Sampling dates (2019) when rachises at each quadrat location (A, B, C, D) within each site (County Durham, Shropshire, Devon, Wiltshire, Hampshire, Carmarthenshire, Northumberland) were collected and sent to the laboratory to assess *H. fraxineus* apothecia development by measuring the apothecia area (mm^2) (Section 2.2). The 12 sampling weeks are indicated in first column of the table. Data was excluded from statistical analysis for a given quadrat location if the measured apothecia area was 0 mm^2, if data loggers had not been recording for at least 42 days, or if no sample was sent to the laboratory. Precise sample dates used in statistical analysis are listed in black for respective sites, and brackets with A, B, C or D indicate the quadrat location sampled. Data in red indicates that no data from the site was used in statistical analysis on this date ^{0} = Apothecia area was 0 mm^2 (i.e. no sampled apothecia with diameter > 200 µm), ^{DL} = Data loggers not recording for at least 42 days, ^{N} = No sample was sent to laboratory. Continued across pages.

(a)

Sample Date (Week Beginning)	County Durham (Hedley Hall Woods)	Shropshire (The Highfields)	Devon (Penstave Copse)	Wiltshire (Colerne Park and Monks Wood)	Hampshire (Alice Holt Forest)	Carmarthenshire (National Botanic Garden of Wales)
29/04/18	30/04/18 (A, B, C, D)^{0}	29/04/18 (A, B, C, D)^{0}	30/04/18 (A, B, C, D)^{0}	30/04/18 (A, B, C, D)^{0}	27/04/18 (A, B, C, D)^{0}	01/05/20 (A, B, C, D)^{0}
13/05/18	14/05/18 (A, B, C, D)^{0}	13/05/18 (A, B, C, D)^{0}	14/05/18 (A, B, C, D)^{0}	14/05/18 (A, B, C, D)^{0}	14/05/18 (A, B, C, D)^{0}	15/05/20 (A, B, C, D)^{0}

(a)

27/05/18	28/05/18 (A, B, C, D)^{0}	28/05/18 (A, B, C, D)^{0}	28/05/2018 (A^{0}, B^{0}, C, D^{0})	29/05/18 (A, B^{0}, C^{0}, D^{0})	31/05/18 (A^{0}, B^{DL}, C^{0}, D^{0})	29/05/20 (A, B, C, D)^{0}
10/06/18	11/06/18 (A, B, C, D)^{0}	10/06/18 (A, B, C^{0}, D)	11/06/18 (A, B, C^{0}, D)	11/06/18 (A, B, C^{0}, D)	14/06/18 (A, B, C, D)^{DL}	12/06/20 (A ^{DL}, B ^{DL}, C^{0}, D ^{DL})
24/06/18	25/06/18 (A, B^{0}, C, D)	24/06/18 (A^{0}, B, C, D)	25/06/18 (A, B, C, D)	25/06/18 (A, B, C^{0}, D)	26/06/18 (A, B, C^{0}, D)^{DL}	26/06/18 (A, B, C, D)
08/07/18	09/07/18 (A^{0}, B, C^{0}, D)	08/07/18 (A, B, C, D)	09/07/18 (A, B, C, D)	09/07/18 (A, B, C, D)	09/07/18 (A, B, C, D)	10/07/18 (A, B, C, D)
22/07/18	23/07/18 (A, B, D)	22/07/18 (A, B, C, D)	23/07/18 (A, B, C, D)	23/07/18 (A, B, C^{0}, D)	24/07/18 (A, B, C, D)	24/07/18 (A, B, C, D)
29/07/18	30/07/18 (A, B, C, D)	29/07/18 (A, B, C, D)	30/07/18 (A, B, C, D)	02/08/18 (A, B, C^{0}, D)	01/08/18 (A, B, C, D)	31/07/18 (A, B, C, D)
12/08/18	13/08/18 (A, B, C, D)	12/08/18 (A, B, C, D)	13/08/18 (A, B, C, D)	13/08/18 (A, B, C^{0}, D)	14/08/18 (A, B, C, D)	14/08/18 (A^{0}, B, C, D)
26/08/18	27/08/18 (A, B, C, D)	26/08/18 (A^{0}, B, C^{0}, D)	27/08/18 (A, B, C, D)	27/08/18 (A, B, C^{0}, D)	01/09/18 (A, B, C, D)	28/08/18 (A, B, C, D)
09/09/18	10/09/18 (A, B, C, D)	09/09/18 (A, B, C, D^{0})	10/09/18 (A, B, C, D)^{N}	10/09/18 (A^{0}, B, C^{0}, D)	12/09/18 (A, B, C, D)	11/09/18 (A, B, C, D^{0})
23/09/18	24/09/18 (A, B^{0}, C^{0}, D)	23/09/18 (A^{0}, B, C^{0}, D^{0})	24/09/18 (A^{0}, B^{0}, C^{0}, D)	24/09/18 (A^{0}, B, C, D^{0})	26/09/18 (A, B, C, D)^{0}	25/09/20 (A, B, C, D)^{0}

(b)

Sample Date (Week Beginning)	County Durham (Hedley Hall Woods)	Shropshire (The Highfields)	Devon (Penstave Copse)	Wiltshire (Colerne Park and Monks Wood)	Hampshire (Alice Holt Forest)	Carmarthenshire (National Botanic Garden of Wales)	Northumberland (Nunsbrough Wood)
28/04/19	28/04/19 (A, B, C, D)^{0}	29/04/19 (A, B, C, D)^{0}	29/04/19 (A, B, C, D)^{0}	29/04/19 (A, B, C, D)^{0}	27/04/19 (A, B, C, D)^{N}	30/04/19 (A, B, C, D)^{0}	28/04/19 (A, B, C, D)^{0}
12/05/19	12/05/19 (A, B, C, D)^{0}	13/05/19 (A, B, C, D)^{0}	13/05/19 (A, B, C, D)^{0}	13/05/19 (A, B, C, D)^{0}	14/05/19 (A, B, C, D)^{0}	14/05/19 (A, B, C, D)^{0}	12/05/19 (A, B, C, D)^{0}
26/05/19	26/05/19 (A, B, C, D)^{0}	27/05/19 (A, B, C, D)^{0}	27/05/19 (A, B, C, D)^{0}	27/05/19 (A, B, C, D)^{0}	03/06/19 (A, B, C, D)^{0}	28/05/19 (A, B, C, D)^{0}	23/05/19 (A, B, C, D)^{0}
09/06/19	09/06/19 (A, B, C, D)	10/06/19 (A^{0}, B, C^{0}, D^{0})	11/06/19 (A, B, C, D)	10/06/19 (A, B, C^{0}, D)	03/06/19 (A, B, C, D)^{N}	11/06/19 (A, B, C, D)	08/06/19 (A, B, C, D)^{0}
21/06/19	21/06/19 (A, B, C, D)	24/06/19 (A, B, C, D)	24/06/19 (A, B, C, D)	27/06/19 (A, B, C, D)	19/06/19 (A, B, C, D)	25/06/19 (A, B, C, D)	22/06/19 (A, B^{0}, C^{0}, D^{0})
06/07/19	06/07/19 (A, B, C, D)	08/07/19 (A, B, C, D) 15/07/19 (A, B, C, D)	01/07/19 (A, B, C, D) 09/07/19 (A, B, C, D)	08/07/19 (A, B, C, D) 15/07/19 (A, B, C, D)	01/07/19 (A, B, C, D)	09/07/19 (A^{N}, B, C, D^{0})	07/07/19 (A^{0}, B^{0}, C^{0}, D)
21/07/19	21/07/19 (A, B, C, D)	22/07/19 (A, B, C, D)	23/07/19 (A, B, C, D)	22/07/19 (A, B, C, D)	19/07/19 (A, B, C, D)	23/07/19 (A, B, C, D)	20/07/19 (A, B, C, D)
28/07/19	28/07/19 (A, B, C, D)	28/07/19 (A, B, C, D)	30/07/19 (A, B, C, D)	28/07/19 (A, B, C, D)	25/07/19 (A, B, C, D)	30/07/19 (A, B, C, D)	28/07/19 (A, B, C^{0}, D)
04/08/19	04/08/19 (A, B, C, D)	28/07/19 (A, B, C, D)^{N}	06/08/19 (A, B, C, D)	07/08/19 (A, B, C, D)	07/08/19 (A, B, C, D)	06/08/19 (A, B, C, D)	03/08/19 (A, B, C, D)
11/08/19	11/08/19 (A, B, C, D)	13/08/19 (A, B, C, D)	12/08/19 (A, B, C, D)	13/08/19 (A, B, C, D)	15/08/19 (A, B, C, D)	13/08/19 (A, B, C, D^{0})	11/08/19 (A, B, C, D)
25/08/19	25/08/19 (A, B, C, D)	26/08/19 (A, B, C, D)	21/08/19 (A, B, C, D) 26/08/19 (A, B, C, D)	28/08/19 (A, B, C, D^{0})	28/08/19 (A, B, C, D)	27/08/19 (A^{0}, B^{0}, C, D^{0})	25/08/19 (A, B, C, D)
08/09/19	08/09/19 (A, B, C, D)	09/09/19 (A, B, C, D)	09/09/19 (A, B, C, D)	11/09/19 (A^{0}, B, C^{0}, D^{0})	11/09/19 (A, B, C, D)	10/09/19 (A, B, C, D)^{0}	07/09/19 (A, B^{0}, C, D^{0})

(b)

22/09/19	22/09/19 (A, B, C^0, D)	25/09/19 (A, B^0, C^0, D^0)	23/09/19 (A, B^0, C, D^0)	23/09/19 (A^0, B, C^0, D^0)	25/09/19 (A^0, B^0, C, D)	24/09/19 (A, B, C, D)^0	21/09/19 (A^0, B^0, C, D^0)

Supplementary Table 3.1 (a) Sampling dates (2018) with reliable quantification of *H. fraxineus* ascospore samples collected using FRAXTRAP rotating arm spore trap over a 48 h period at each spore trap location (A, B, C, D) within the Shropshire site (Section 3.2). Samples were also taken from sites in County Durham, Carmarthenshire and Devon, however difficulties operating the ROTTRAP 120 meant that data was not sufficiently reliable to include in the analysis **(b)**. Sampling dates (2019) with reliable quantification of *H. fraxineus* ascospore samples collected using FRAXTRAP rotating arm spore trap over a 48 h period at each spore trap location (A, B, C, D) within each site (Shropshire, Devon, Wiltshire, Hampshire, Carmarthenshire, Northumberland) (Section 3.2). Sample collection date and spore trap location are indicated. Missing samples were attributable to either volunteer availability, suboptimal amplification curves, or DNA extraction error. Data in red indicates that no data from the site was used in statistical analysis on this date ^{S} = Suboptimal amplification, ^{D} = DNA extraction error. Trap locations at Hampshire between 09/08/19 – 06/09/19 with ^{x2} were used to test the reliability of FRAXTRAPs by running traps approximately 2 m apart and comparing real-time PCR quantified ascospore numbers (Section 3.2). *H. fraxineus* was detected via real-time PCR on all samples.

(a)

Sample Collection Date	Shropshire (The Highfields) Trap Location
05/07/18	A, B^{N}, C^{N}, D^{N}
08/07/18	A, B^{N}, C^{N}, D^{N}
15/07/18	A, B^{N}, C^{N}, D^{N}
22/07/18	A, B^{N}, C, D
29/07/18	A, B^{N}, C, D^{N}
05/08/18	A, B^{D}, C, D
12/08/18	A, B^{D}, C, D
19/08/18	A, B, C, D
26/08/18	A, B, C, D
02/09/18	A, B, C^{D}, D
09/09/18	A, B^{A}, C, D
16/09/18	A, B^{N}, C, D^{N}

(b)

Sample Collection Date (Week Beginning)	Shropshire (The Highfields)	Devon (Penstave Copse)	Wiltshire (Colerne Park and Monks Wood)	Hampshire (Alice Holt Forest)	Carmarthenshire (National Botanic Garden of Wales)	Northumberland (Nunsbrough Wood)
16/06/19	17/06/19 (A, B, C, D)	17/06/19 (A, B, C, D)	16/06/19 (A, B, C)^{N}	16/06/19 (A, B, C, D)^{N}	20/06/19 (A, B, C, D)	16/06/19 (A, B, C, D)^{N}
23/06/19	24/06/19 (A, B, C, D)^{N}	24/06/19 (A, B, C, D)	23/06/19 (A, B, C)^{N}	23/06/19 (A, B, C, D)^{N}	27/06/19 (A, B, C, D)	23/06/19 (A, B, C, D)^{N}
30/06/19	30/06/19 (A, B, C, D)	01/07/19 (A, B, C, D)	30/06/19 (A, B, C)^{N}	06/07/19 (A, B, C, D)	04/07/19 (A, B, C, D)	30/06/19 (A, B, C, D^{N})
07/07/19	08/07/19 (A, B, C, D)	08/07/19 (A, B^{N}, C, D)	07/07/19 (A, B, C)^{N}	13/07/19 (A, B, C, D)	11/07/19 (A, B, C, D)	08/07/19 (A, B, C, D)
14/07/19	15/07/19 (A, B, C, D)	16/07/19 (A, B, C, D)	14/07/19 (A, B, C)	14/07/19 (A, B, C, D)^{N}	18/07/19 (A, B, C, D)	15/07/19 (A, B, C, D)
21/07/19	22/07/19 (A, B, C, D)	23/07/19 (A, B, C, D)	21/07/19 (A, B, C)	21/07/19 (A, B, C, D) 25/07/19 (A, B, C, D)	25/07/19 (A, B, C, D)	22/07/19 (A, B, C, D)
28/07/19	28/07/19 (A, B, C, D)	30/07/19 (A, B, C, D)	28/07/19 (A, B, C)	28/07/19 (A, B, C, D)^{N}	01/08/19 (A, B, C, D)	30/07/19 (A, B^{D}, C, D)
04/08/19	07/08/19 (A, B, C, D)	06/08/19 (A, B^{D}, C, D^{N})	04/08/19 (A, B, C)	09/08/19 (A^{x2}, B^{x2}, C^{x2}, D)	08/08/19 (A, B, C, D)	05/08/19 (A, B, C, D)
11/08/19	13/08/19 (A, B, C, D)	12/08/19 (A, B^{D}, C, D^{N})	11/08/19 (A, B, C)	17/08/19 (A^{x2}, B^{x2}, C^{x2}, D)	15/08/19 (A, B, C, D)	13/08/19 (A, B, C, D)
18/08/19	19/08/19 (A, B, C, D)	21/08/19 (A, B^{D}, C, D)	18/08/19 (A, B, C)	23/08/19 (A^{x2}, B^{x2}, C^{x2}, D)	22/08/19 (A, B, C, D)	20/08/19 (A, B, C, D)
25/08/19	26/08/19 (A, B, C, D)	26/08/19 (A, B^{D}, C, D)	25/08/19 (A^{N}, B, C)	30/08/19 (A^{x2}, B^{x2}, C^{x2}, D)	29/08/19 (A, B, C, D)	27/08/19 (A, B, C, D)

(b)

01/09/19	02/09/19 (A, B, C, D)	01/09/19 (A, B, C, D)^{N}	01/09/19 (A, B, C)	06/09/19 (A ^{x2}, B ^{x2}, C ^{x2}, D)	05/09/19 (A, B, C, D)	01/09/19 (A, B, C, D)^{N}
08/09/19	09/09/19 (A, B, C, D)	09/09/19 (A, B, C, D)	09/09/19 (A, B, C)	13/09/19 (A, B, C, D)	12/09/19 (A, B, C^{A}, D)	10/09/19 (A, B, C, D)
15/09/19	16/09/19 (A^{A}, B, C, D^{A})	16/09/19 (A, B^{A}, C, D)	15/09/19 (A, B, C)	15/06/19 (A, B, C, D)^{N}	15/06/19 (A, B, C, D)^{N}	16/09/19 (A^{A}, B, C^{A}, D)


(a)


(b)


(c)


(d)

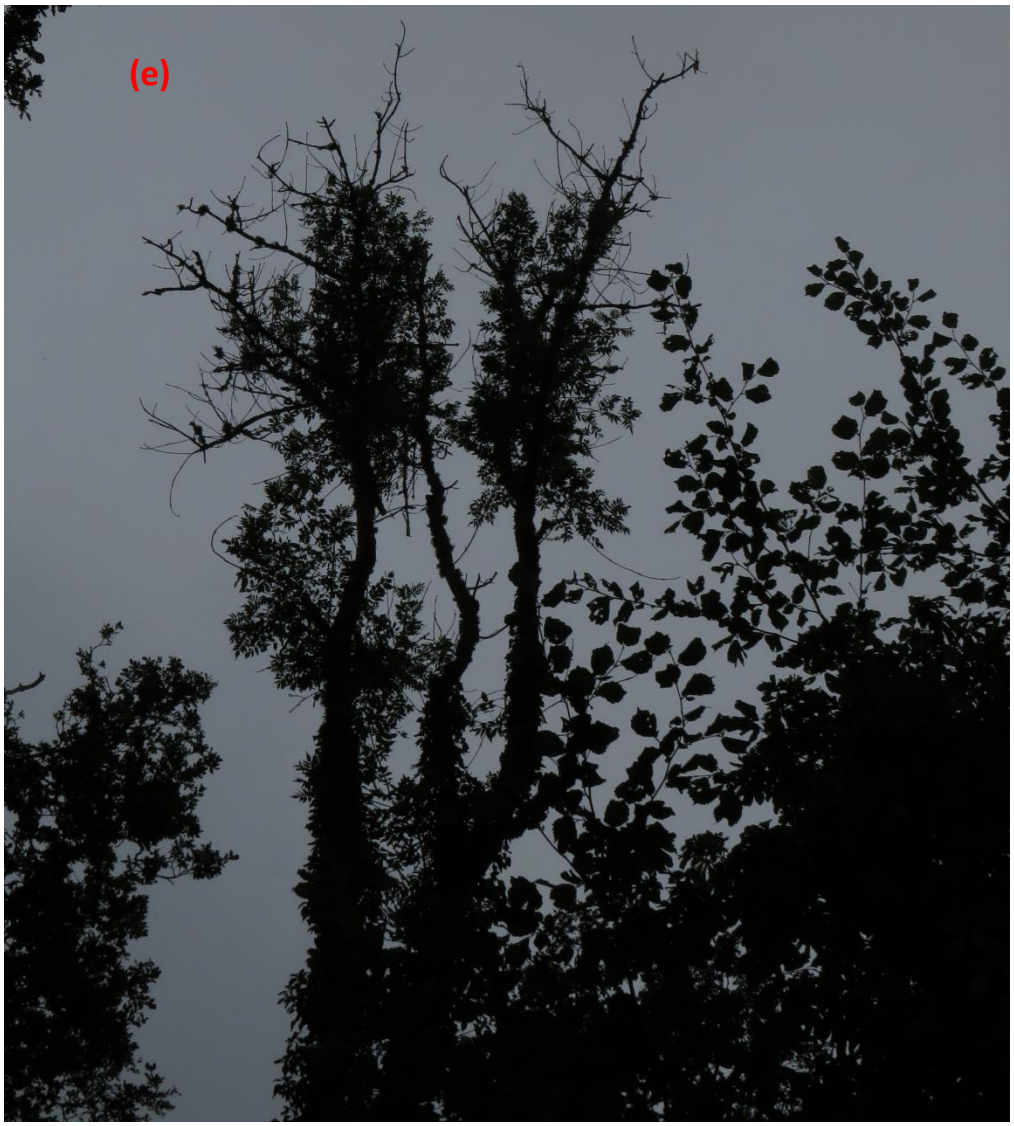

Supplementary Figure 4.1 Examples of classification of *F. excelsior* crown dieback severity (Section 4.2.1.2) **(a)** minimal (0-4% crown dieback); **(b)** low (5-24% crown dieback); **(c)** medium (25-49% crown dieback); **(d)** high (50-74% crown dieback); **(e)** very high (75-100% crown dieback).

Supplementary Table 4.1 Details of the ingredients and preparation of media used for *H. fraxineus* ascospore germination experiments (Section 4.2.2) or culturing of fungi and oomycetes from *F. excelsior* basal lesions (Section 6.2.3).

Media	Preparation
Water agar (WA)	14 g agar technical no. 2, 1000 ml distilled water, autoclave for 20 mins at 121°C/ 15lb psi
Malt agar (2%) and streptomycin (MA+S)	20 g malt extract, 15 g agar technical no. 2, 1 L distilled water; autoclave for 20 mins at 121°C/ 15lb psi; 1% Streptomycin solution added when cooled to 50°C
Synthetic mucor agar (SMA)	10 g sucrose, 1 g L-Asparagine, 0.25 g magnesium sulphate, 0.001 g Thiamine HCL, 1 ml trace element solution (0.088 g sodium tetraborate decahydrate, 1.007 g ferric sulphate, 0.393 g copper sulphate pentahydrate, 0.072 g manganese (II) chloride tetrahydrate, 0.05 g sodium molybdate dihydrate, 4.403 g zinc sulphate heptahydrate, 5 g ethylenediaminetetraacetic acid, 1000 ml distilled water), 15 g agar technical no. 2, 0.5 g potassium dihydrogen orthophosphate, 4% MBC solution (4 g carbendazim, 2.8 ml hydrochloric acid (37%), distilled water (47.2 ml), 1000 ml distilled water. Adjust pH to 6.5 with 1 M sodium hydroxide. Autoclave for 20 mins at 121°C/ 15lb psi